THE SYNTHESIS OF HYDRAZINE FROM AMMONIA IN A GLOW DISCHARGE.

Submitted in part fulfilment of degree of Doctor of Philosophy.

David Savage B.Sc.,

November 1970.

VOLUME CONTAINS CLEAR OVERLAYS

OVERLAYS HAVE BEEN SCANNED SEPERATELY AND THEN AGAIN OVER THE RELEVANT PAGE

ACKNOWLEDGEMENTS

Prof. J.D. Thornton for his support, guidance and encouragement in this work.

Prof. J.M. Coulson in whose laboratories the work was carried out.

Mr. C.A. Currie and technicians for their advice and assistance.

Mr. McColgan for translating some technical papers.

Friends and colleagues at Newcastle University for their helpful discussions.

Science Research Council for their financial support.

Summary

The glow discharge is one of the most economic methods of producing electrons as reaction promoters in gas phase chemical reactions. The reaction considered here is that between electrons and ammonia to produce hydrazine with nitrogen and hydrogen as by products.

A parallel flow cylindrical reactor with porous electrodes was operated at a pressure of 10 torr over a range of power levels from 1 to 10 watts input/cc of reactor volume. Continuous direct current and pulsed direct current power was supplied to the reactor.

Previous work has shown that high energy yields of hydrazine are obtained by using low discharge power levels and low residence times. This work compares the fast flow continuous d.c. system with the pulsed d.c. system of equivalent residence time. The results show that the pulsed discharge gives higher energy yields and conversions to hydrazine than the continuous d.c. discharge, energy yields of over 40 gms/kwh being recorded. The reason for the improved results in the pulsed discharge system is thought to be due to the lower overall hydrogen atom concentration present. The lower concentration reduces the degradation of hydrazine by hydrogen atoms.

The discharge pulse also gives higher energy electrons and hence a higher rate of primary reaction between the electrons and ammonia.

The relative effects of the different discharge zones, the addition of helium gas to the ammonia and the effects of wall reactions on the energy yield and conversions to hydrazine were determined for the continuous d.c. system. The current voltage characteristics of the continuous d.c. discharge were also measured.

A tentative kinetic model of the reacting system is proposed and recommendations are made for future studies in this field.

CONTENTS PAGE

CONTENTS

1.0 INTRODUCTION.

1.1 General Introduction.

The study of new methods of production of hydrazine is a particularly rewarding field of research. Hydrazine is an interesting and useful chemical, it is readily oxidised and as such is used as an anti oxidant[5] in the treatment of boiler waters and as a rocket and jet fuel[9,135] its' derivatives find use as blowing agents for rubber and plastics but its extensive use is limited by its high cost. If production costs are considerably reduced hydrazine could find application in fluxes, photographic developing agents, explosives, insecticides, dyes and pharmacuticals, etc.

Considerable development occurred as a result of the discovery by the Germans that hydrazine is an excellent rocket fuel, however, the Rashig process still remains the only commercial process. The process operating at the moment gives a product liquor containing only about 2% hydrazine, and it is the cost of separation of the hydrazine from the liquor which makes it so expensive.

One method of overcoming this separation problem is to use a gaseous system, where the hydrazine can then be frozen out from the product gases directly (although this presents handling

problems because of its explosive nature), or absorbed by a suitable medium.

Direct combination from nitrogen and hydrogen to form hydrazine has so far been rather unsuccessful.[81,28,134,49,105] The formation of hydrazine from the decomposition of ammonia has been more promising,[68] with pyrolysis, photolysis, radiolysis and electrical discharge methods all being investigated. The table below shows the cost of supplying power to the systems mentioned above.[52]

	Approximate Cost in Shillings/kWh
Glow or corona discharge	0.10
Microwave discharge	0.40
Photolysis	2.0
Electron accelerator	4.0 - 8.0
Cobalt 60	8.0 - 40.0

Although the electron accelerator and cobalt 60 sources can give electron sources of known energy range, their costs at 40 times greater than direct power input of a glow discharge make them uneconomic. Recent work by the Electricity Research Council[4] has shown areas of constant electron energy can be created in a glow discharge but the fraction of total power in these regions is only small so the use of these areas alone also becomes uneconomic. The level of energy input from light sources can also be controlled by

choosing the frequency but the efficiency of converting the electricity in the lamp into light of the required frequency is very low resulting in high costs. Similarly the frequency of microwave power can be varied to some extent to alter the effective field strength of the discharge but the power is four times more expensive than power to a glow discharge which means energy yields and conversions have to be substantially higher to offset this cost. The microwave discharge and the glow discharge are very similar and one would not expect a substantial difference in energy yield and conversion to occur. Clearly then the cheapest method of supplying power to the gas is by a glow or corona discharge and with the rapid development of nuclear reactors it may be expected that electrical power costs will become even cheaper.

Despite this, however, the use of electrical discharges for chemical processing has received little commercial application. Its use has been limited to the production of ozone and hydrogen peroxide and the electrocracking of hydrocarbons, to give olefins and acetylene. In more recent years it has found application in surface polymerisation techniques for the coating of metals and plastics.

The synthesis of silicon compounds in high temperature plasma jets may also soon become a commercially viable proposition.

Further commercial development is hindered by the lack of understanding of the complex nature of an electrical discharge viz.

(i) The electrical discharge is normally in a non equilibrium condition with electron temperatures very much higher than that of the surrounding molecular gas. This is an important condition in the synthesis of a thermally unstable gas, in that a molecule can be dissociated by electron impact without the need for the other molecules to exist at similar energy levels.

(ii) The electrical characteristics and chemical characteristics of the discharge are not independent. This makes it extremely difficult, if not impossible, to optimise all the process variables of flowrate, temperature, current, current density, voltage, wave form, frequency, reactor geometry etc. For example, changing the discharge tube diameter changes the surface to volume ratio in the discharge; this will in turn change the fraction of chemical reaction occurring on the walls to that occurring in the gas phase. Changing the tube diameter also alters the mean field strength in the discharge, which in turn changes

the mean electron energy, and this in turn could alter the reaction mechanism and rate of activation.

(iii) The reactions occurring are complex. Several different types of reaction can occur, some involving charged ions and electrons and others involving neutral molecules, free radicles and atoms. The nature and extent of these reactions depend on the electrical characteristics of the discharge, reactor geometry, pressure, wall surface, added gases, third bodies etc. The rates of the reactions can also vary by factors greater than 10^6 and rate constants of over 10^{14} lit/mole sec have been recorded. Kaufman The relative importance of many of these reactions has now been established and the reactions occurring in a d.c. glow discharge are described in that section on page 40.

(iv) "Basic" data is not available.

If the electron energy and electron density distribution were known for any given operating conditions, together with collision cross sections and all the reaction rates the effect of the electrical discharge could be predicted.

Very little of this information is known and only a small amount of the information can be applied to the conditions normally found in technological gas discharge work.

In developing an electrical discharge for chemical synthesis three characteristics must be optimised:

(i) a high energy yield (gms of product/kWh power input) is necessary to avoid high electrical running costs.

(ii) a high conversion to the desired product per pass is necessary to reduce pumping costs and plant size.

(iii) a highly specific reaction is necessary to avoid high separation costs and to reduce to a minimum the amount of reactant converted to an unwanted product.

Very little systematic work has been carried out on the optimisation of the above, but as the effect of different variables becomes known a little more clearly, more coherent studies should be possible. As a result of these studies it should be possible to improve the techniques of electrical discharge synthesis, and to reduce production costs by this method even further.

1.2 Gas discharges.

1.2.1 General Features.

Whenever a current flows in a gas, a gas discharge is formed. This current can be from less than 10^{-9} amps to over a million amps, depending on the type of discharge maintained. Three distinct types of discharge can be formed, (see fig. 1b). At currents up to approx. 1μA a Townsend or dark discharge exists. This relies partly on ultraviolet light, cosmic rays, etc. to provide the ionization necessary to maintain the current flow. If the voltage across the tube is increased still further, "breakdown" occurs and the current increases up to about 100mA, the discharge becomes self sustaining and a luminous glow is emitted from the gas. It is from this glow that the discharge derives its name. If the resistance of the external circuitry is low the current increases and the voltage falls giving rise to an arc discharge. The discharge is intensely luminous and is accompanied by comparatively large thermal effects.

These discharges exist in slightly different forms depending on the frequency of the applied voltage. A direct current discharge is said to exist where the polarity of the applied voltage remains unchanged. An a.c. discharge exists up to about 500HZ, high frequency from about

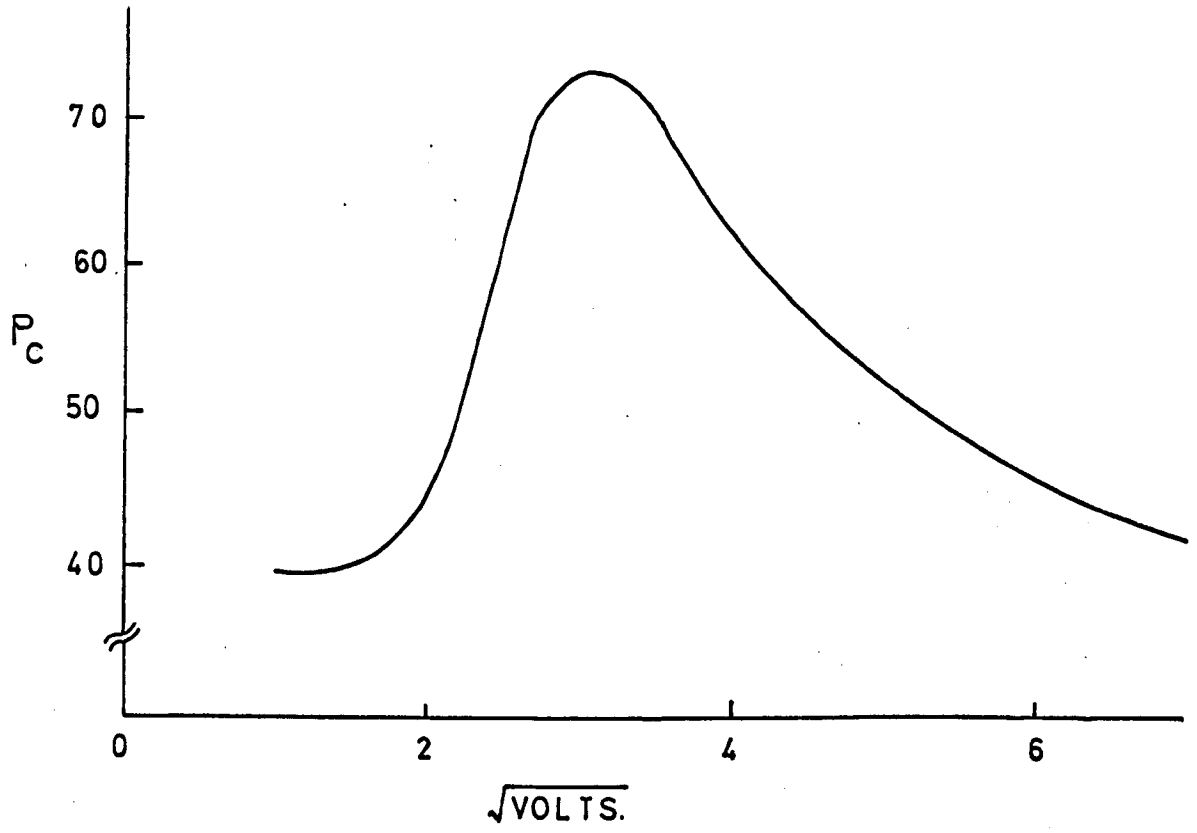

fig 1a. COLLISION PROBABILITY.

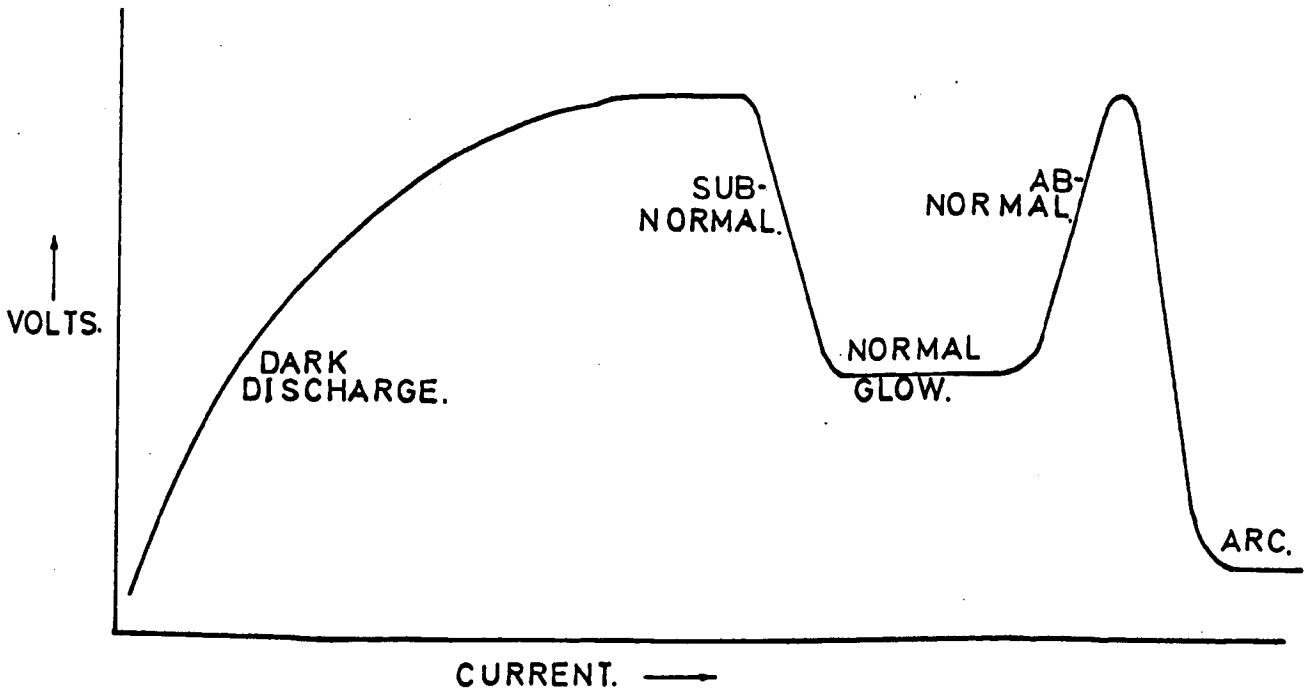

fig 1b. TYPES OF DISCHARGE.

500HZ-1500HZ, radio frequency from about 150 kHz to 100 MHz and microwave above 100 MHz. These frequencies are only given as a general guide since the type of discharge formed also depends upon the nature of the gas, gas pressure, electrode system employed, external electrical circuitry etc. The most important type of discharge for chemical synthesis is the glow discharge, so it is discussed in more detail below.

1.2.2 The d.c. glow discharge.

The glow discharge was ~~discovered~~ studied by Faraday in the course of his work at the Royal Institution between the years 1831 and 1835.[41] At low pressures (1 mmHg) he found that the discharge consisted of glowing areas separated by dark spaces of the form shown in fig. 2a.
These regions are formed by the different electron motions and electron collisions in each region.

(i) Electron motion and collision.

A certain number of electrons, positive and negative ions exist in the atmosphere due to the action of cosmic rays, ultraviolet light, and radioactivity. An electron finding itself in the discharge tube will come under the action of

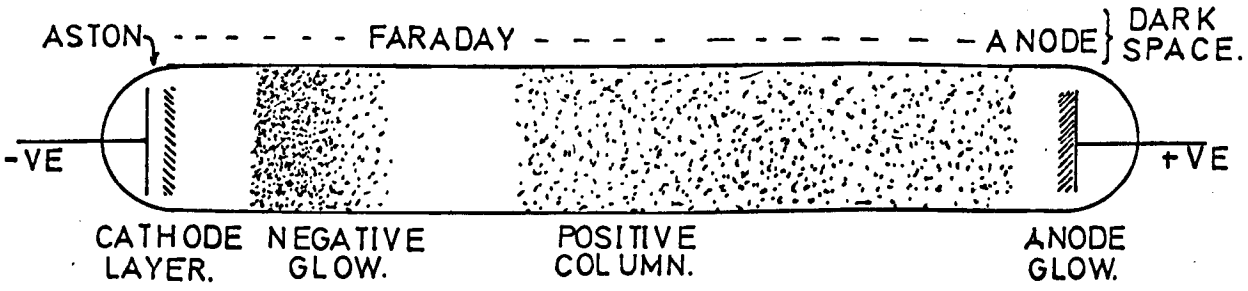

fig 2a. ZONES IN DISCHARGE.

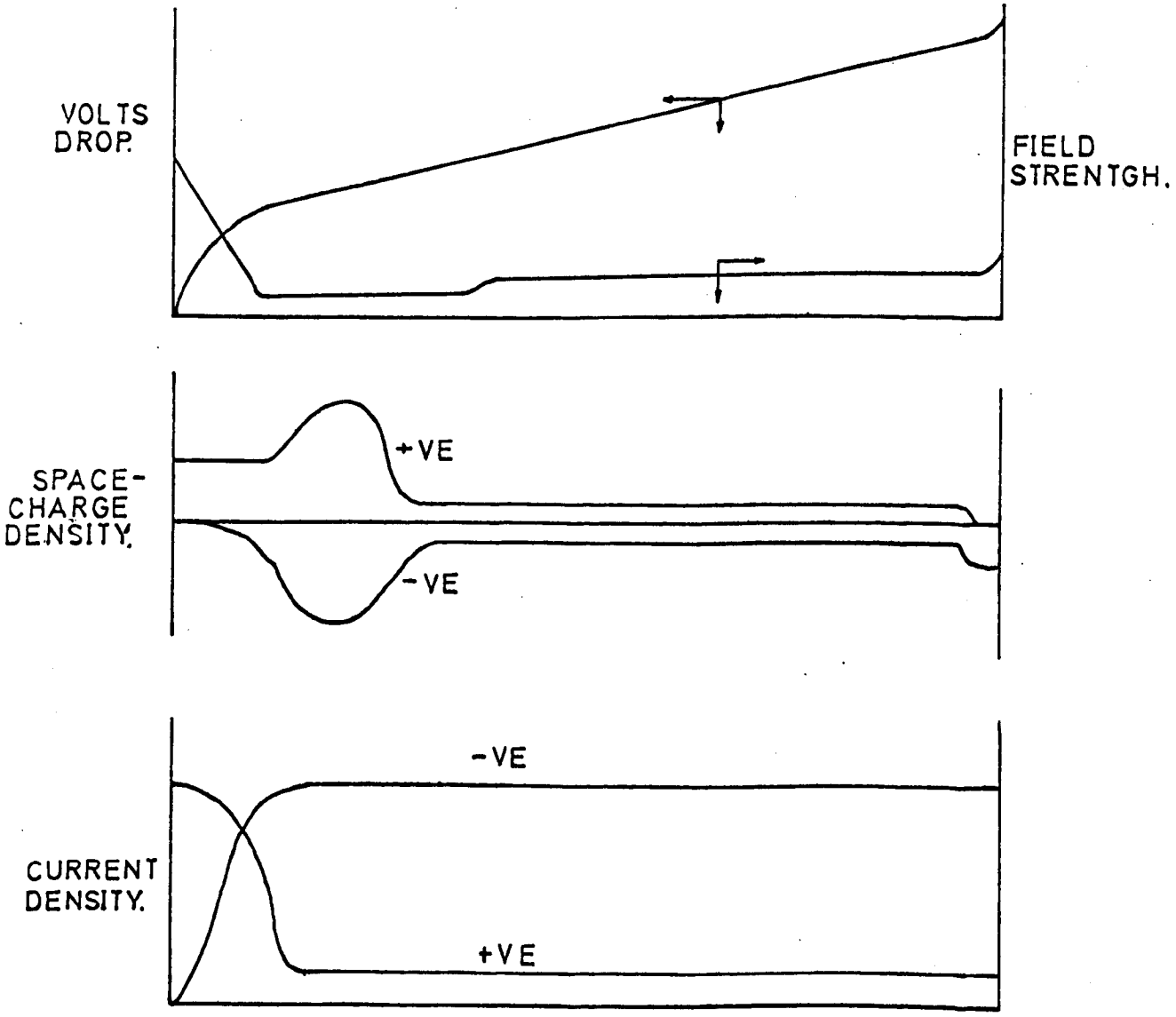

fig 2 b. VARIATION OF ELECTRICAL CHARACTERISTICS ALONG THE DISCHARGE TUBE.

the field created by the voltage applied between the electrodes, and as a result will accelerate in the direction of the field with an acceleration F.,

$$F = \frac{E\ e}{m}$$

where E is the field strength, m the mass of the electron, and e its charge. The electron will continue to increase its velocity (v) and kinetic energy ($\frac{1}{2}mv^2$) until such times as it is involved in a collision. The energy of the electron at this point will be proportional to the field (E) and the distance travelled (λ) since :-

$v^2 = V_o^2 + \frac{2Ee}{m}\lambda$ (Laws of motion).

Different types of collisions can occur with their probability depending on the electron energy. A typical graph of collision probability .v. electron energy is given in fig. 1a for ammonia [22].

This probability is often presented as a "collision cross section", (Q) cm^2/cm^3, which is the reciprocal of the mean free path (λ).

Essentially the electron can undergo two types of collisions, elastic and inelastic.

a) <u>elastic.</u>

If the electron has an energy less than that required by quantum mechanics for excitation or activation of a molecule, it will undergo an

elastic collision. Since electrons have much lower mass (m) than molecules (M) it can be shown that the fractional change in energy (ΔU) in an elastic collision is 2m/M. For ammonia $\Delta U = 11.3 \times 10^{-4}$.

This is extremely small and means that the electron retains practically all of its energy. It is in this way that high electron temperatures can be maintained in a gas of low molecular temperature. The very low energy change in an elastic collision also means that molecules cannot be easily activated by such collisions, but as the electron energy increases, inelastic collisions become more probable and these can cause excitation, dissociation and ionization.

(b) Inelastic collisions.

An inelastic collision results in a change in the internal energy of the molecule and alters the translational kinetic energy of the molecule. The change in the internal energy of the molecule can be in its rotational and vibrational energies as well as that associated with a change in the electron levels in the molecule, but the energy of the electron must be greater than that required by quantum mechanics for that change. The molecules can then lose this energy in several ways:

i) By collision with a wall or molecule

$$e + AB \longrightarrow AB^*$$

$$AB^* + M \longrightarrow AB$$

ii) By emission of light

$$e + AB \longrightarrow AB^* \longrightarrow AB + h\nu$$

iii) By dissociating into atoms and free radicales

$$e + AB \longrightarrow AB^* \longrightarrow A + B$$

iv) By losing an electron

$$e + AB \longrightarrow AB^* \longrightarrow AB^+ + e$$

This last process releases new electrons into the system which are subsequently accelerated and undergo further excitation collisions. The free radicales, atoms, ions, electrons and molecules react as described below.

c) Ion-molecule reactions

These can be simple charge transfer reactions of the form

$$A^+ + B \longrightarrow A + B^+$$

with little or no activation energy and high rate constants of the order of 10^{12} lit/mole sec[98]. Even when the threshold energy of a reaction is quite high, rate constants are high, e.g.

$$NH_3 + NH_3^+ \longrightarrow NH_4^+ + NH_2$$

at a threshold energy of 10.2e.v. has a rate constant of 9×10^{11} lit/mole sec.

Ions of course will react rapidly with low energy electrons and be neutralised.

d) Electron and Ion recombination reactions.

Electron Ion reactions can be strongly exothermic and coulombic attraction between the oppositely charged electrons and ions means the rate constants are again very large at 10^{13} - 10^{14} lit/mole sec. The reactions often result in dissociation of the form.

$$e + AB^{+} \longrightarrow A + B$$

Where both negative and positive ions exist these can react to give neutral species by mutual neutralisation as

$$A^{+} + B^{-} \longrightarrow A + B$$

or in the presence of a third body recombine as

$$A^{+} + B^{-} + M \longrightarrow AB + M$$

At a pressure of 10 torr the recombination is more likely with a rate constant of approximately 10^{13} lit/mole sec. The negative ions B^{-} are formed by electron attachment and detachment.

e) Electron attachment and detachment.

The rate at which an electron is attached to a radicle or molecule depends upon the electron energy and the nature of the radicle or molecule.

$$B + e \longrightarrow B^{-}$$

Negative ions can also be formed by dissociative

attachment of the form

$$AB + e \longrightarrow A + B^-$$

$$AB + e \longrightarrow A^+ + B^- + e$$

The rate of reaction again depends on the electron energy. At electron energies of 1-2ev rate constants will only be of the order of 10^8 lit/mole sec. which is considerably slower than the rate of recombination of negative ions with electrons of approx. 10^{13} - 10^{14} lit/mole sec. This means negative ion concentrations are very low in a discharge; for example in ammonia with 100ev electrons only 0.4% of the species produced are negative ions.

iv) Free radicle reactions.

Most of the reactions described above result in the formation of atoms or free radicles. Free radicle reactions of the form

$$A + B \longrightarrow C + D$$

have comparatively low rate constants of approximately 10^7 - 10^9 lit/mole sec. which means the rate controlling step in the production of neutral products from atoms and radicles is the rate of the free radicle reactions. The free radicle reactions of importance occurring in an ammonia glow discharge are described in more detail in section 2.4 page 40.

These collision processes occur to varying degrees along the discharge tube, and it is these which cause the different regions found by Faraday to appear.

(ii) Construction of a discharge.

The voltage, electric field, space charge and current density variations along the tube are shown in fig. 2. It can be seen from fig. 2 that most of the applied voltage falls in the cathode space or "cathode fall region" and then falls uniformly over the positive column. This means that electrons leaving the cathode are rapidly accelerated in the Aston dark space until they have acquired sufficient energy to make excitation collisions (cathode layer) and ionizing collisions (negative glow). These collisions slow the electrons down causing the Faraday Dark Space to be formed. The field strength, however, increases slightly so the electrons accelerate to the positive column. Here a low uniform field exists but the electrons acquire large random velocities by elastic collisions. It is these random velocities which give rise to the ionization and excitation found in the positive column, rather than their drift velocity, which is gained under the action of the field.

Electrons near the anode are attracted by it and accelerate through the anode dark space to excite the gas immediately in front of the electrode forming the anode glow.

Space charges (fig 2) are set up because electrons (-ve) and ions (+ve) diffuse at different rates. In the positive column the electric field is constant and the number of positive and negative charges per unit length are the same. If both were allowed to freely diffuse to the walls a positive space charge would result due to the higher diffusion rate of the lighter electrons. A negative space charge is therefore built up on the walls of the tube which repels the slower electrons and attracts the positive ions, until the rates of diffusion of the electrons and ions become the same. The phenomenon is known as ambipolar diffusion.

The discharge can exist without the positive column. If the electrodes are close together only the negative glow area exists. As the electrodes are moved apart the positive column length increases, but the cathode fall and negative glow regions remain unchanged. If the cathode is rotated the negative glow region rotates with it but the positive column simply fills the

remaining space. This feature has been used in certain types of reactor for the production of diffuse decaying discharges. The main discharge system employed in the research presented here is a pulsed d.c. system. Some aspects of this are discussed below.

1.2.3 Pulsed discharges.

In a pulsed discharge the gas is first broken down, a glow discharge then starts to form and finally, when the applied voltage is removed, the discharge decays back to its original condition.

The electrical breakdown of gases has been studied a great deal [115,85] but the processes occurring are so complex that a clear picture cannot be given. If the voltage between the electrodes in a low pressure gas is slowly increased we pass through the saturation and Townsend regions given in fig. 1b, until at some value of applied voltage, which depends on the electrode distance, pressure and the ability of the electrodes and walls to release ions, the current increases to a large finite value dependent upon the external circuitry. The breakdown voltage is reduced if a space charge is present in the tube, either from a previous discharge [21, 58] or created by the flow of electrons in the tube from an external electron source.

The time taken to break the gas down and build up a discharge is also reduced by the effect of space charges. This time lag is normally divided into two sections, a statistical time lag Ts, and a formative time lag T_f. In order to break down a gas, an electron has to be accelerated in the field, the statistical time lag is the time required for such an electron to appear in the tube. The formative time lag is the time required for the discharge to reach an equilibrium value after the appearance of an electron. Since it is difficult to estimate when a discharge has reached equilibrium, formative time lags cannot be given with any certainty. It was thought that the formative time lag was the transit time of a positive ion between the electrodes, but formative time lags much shorter than this have been reported which indicates that this cannot be completely correct.

Once the discharge has been formed it operates in the way described previously until the applied voltage is removed. The discharge then "decays" electrically and chemically. The current falls to zero and the ions and electrons diffuse away at a rate determined by the ambipolar diffusion and the free electron diffusion coefficients.

Free radicales, atoms, and ions react at a rate determined by the chemicals kinetics until reaction is complete or another discharge occurs. The process described above is then repeated.

Further details of the physics and chemistry of discharges can be found in the standard texts 40, 12, 78, 85, 110, 111.

2.0 LITERATURE SURVEY.

2.1 Formation of hydrazine from gaseous ammonia.

Glow discharges can be used to carry out a whole range of chemical reactions from the production of ozone to the synthesis of aminoacids. The survey presented here mainly covers the synthesis and decomposition of hydrazine in a glow discharge. Details of other reactions are given in reviews of Spedding,[132] Jolly,[75] Schenk,[123] Suzuki[136] and Dundas.[38]

The effect of a glow discharge on ammonia had been studied for several years[15, 31] but it was not until 1911 that Besson[14] showed that hydrazine could be formed as a product of the reaction. Using a flow system he had to pass the gas through the discharge continuously for a week in order to get a measurable amount of hydrazine.

Bredig, Keonig and Wagner[17] carried out the first really systematic study of hydrazine synthesis. Comparing the results an a.c. Siemens tube discharge apparatus and from a cooled arc discharge they found that the less intense Siemens discharge gave the better energy yields, up to 3.9gm/kwh, high yields being favoured by low current densities and high gas flowrates. The conversion of ammonia to hydrazine went through a maximum with flowrate but the

total conversion to hydrazine was low, at 0.016%, even though up to 80% of the ammonia used was converted to hydrazine. [152, 18] Westhavers work on the dissociation of ammonia in a normal glow discharge added to the understanding of hydrazine formation when he found that hydrazine could be frozen out of the positive column but not out of the negative glow. In the positive column approx. 10% of the ammonia decomposed formed hydrazine (cf 80% Bredig, Keonig and Wagner) but hydrazine was detected with up to 50% total decomposition of ammonia. This could correspond to a total conversion of upto 5% per pass but insufficient data is presented toform a definite conclusion.

Particular mention is given in Westhavers [152] paper to the "working in" of the cathode. Freshly machined cathodes gave significantly different results from those which had been "aged" by running them in a discharge for at least three hours. This ageing effect is thought to be due to the nitriding of the surface [65] which changes the work function of the metal and the ammonia absorption on the surface. The results given in the paper are for "aged" cathodes.

The rate of dissociation of ammonia was found to be proportional to the current and independent of pressure in the range 4 - 16 mm Hg which suggests that ammonia decomposition cannot be controlled by interaction of activated states. Most added gases (N_2, He, Ar, O_2) had no effect on the rate of dissociation of ammonia but hydrogen did retard the rate. The mechanism of decomposition Westhaver presented cannot be considered to be correct since it only considers ionic reactions.

Ouchi[108] also considered this to be a "biased view" and proposed a free radical reaction of the form $NH_3 + NH \rightarrow N_2H_4$. Ouchi's work, which took nearly ten years to complete, studied the discharge characteristics as well as the formation of hydrazine. He first repeated the work of Koenig and Wagner[79] with an a.c. discharge in a Seimens tube and found that the conversion to hydrazine went through a maximum with respect to power and increased with increasing flowrate, reaching 0.37% conversion. Although the power measurement was not very accurate in this case, energy yields were about 3 gm N_2H_4/kwh in agreement with the work of Koenig et al but the conversions obtained by Ouchi are over ten times as high.

In order to improve the power measurement and avoid dielectric losses in the glass walls of the reactor Ouchi used a Geissler tube (fig. 3) and compared a normal 50 cycle a.c. discharge with an intermittent discharge formed by the half wave rectification of a 50 cycle a.c. voltage. This gave discharges with an on time of 0.008 seconds and off times of 0.002 seconds and 0.012 seconds respectively. The energy yields and conversions to hydrazine with the intermittent discharges were both higher than with a normal 50 cycle a.c. discharge. These results were later confirmed by Jogaro and Sastri[73] using an ozonizer discharge and by Schuller[126] using a long Geisler tube. The reason given for the high yields and conversion was that in the intermittent discharge the residence time of the gas molecules in the reactor whilst the discharge was on was less than for the normal a.c. case. Since the yield is inversely proportional to residence time this would account for the difference.

Increasing the "off time" of the discharge would be expected to give even higher yields. To investigate this a high voltage rectangular wave generator was built giving pulses of 0.01 sec long and off times of 0.02 to 0.6 seconds.

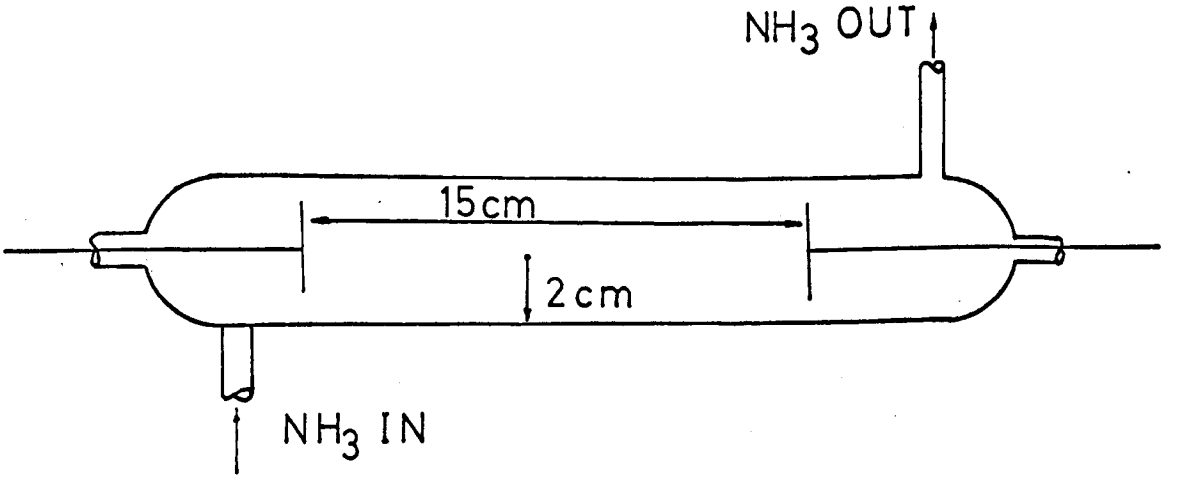

fig 3a. GEISLER DISCHARGE TUBE

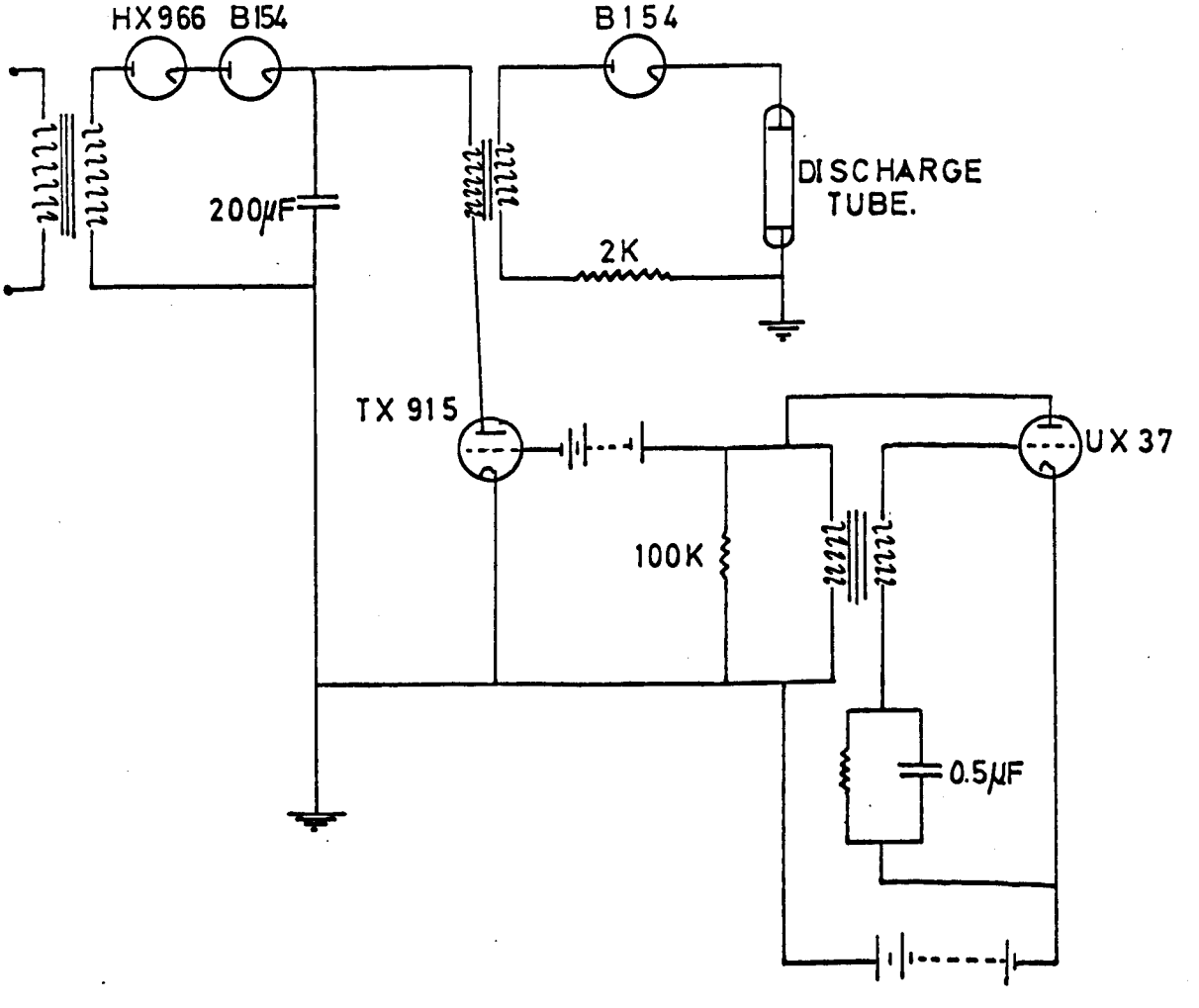

fig 3b. OUCHIS IMPULSE GENERATING CIRCUIT

The energy yields did increase upto 9.4 gm/kwh and conversions upto 0.42% were attained but, unfortunately, the high conversions occurred at low yields and vice versa. The low conversions to hydrazine are not really surprising when one considers the long off times used. If, as suggested by Ouchi, the actual waveform has little effect, an impulse discharge of very short duration would reduce the residence time of the molecule in the discharge without the need to increase the off time very much.
A generator was built giving short 2 milli second impulse discharges. The circuit is shown in fig. 3.
Yields of up to 47 gm/kwh were reported but conversions were very low at 0.01%. The energy yield could be correlated in terms of the parameter watt seconds where the seconds seem to refer to the mean residence time in the discharge, not the reactor.

The interpretation of the relationship between hydrazine produced and electrode spacing is incorrect because increasing the electrode spacing also increases the residence time. If

a correction is made for this it is found that the hydrazine formed increases linearly with electrode spacing, showing that hydrazine is produced uniformly throughout the positive column.

Amongst the other discharge characteristics investigated were the effect of pressure and current on the width of the cathode dark space and the cathode fall voltage.

The cathode fall region was also shown not to be responsible for the production of hydrazine, in agreement with the results of Westhaver, Devins and Burton.[34] In most of their conclusions Devins and Burton agreed with the results of Ouchi and Westhaver in that the hydrazine yield increased with increasing flowrate, increasing electrode distance and increasing pressure, up to 8 mmHg, but they found the yield reached a maximum with pressure somewhere between 8 and 10 mmHg. Since the reduced field strength (E/P) was shown to be one of the basic parameters describing a discharge[153, 86] Devins and Burton measured the influence of the discharge tube radius on X/p and found it agreed with the theoretical analysis of Engel and Steenbeck.[87] However, the hydrazine

yield was found to be not only a function of E/p but also of the tube radius. This strongly suggests that the wall influences the chemical reactions as well as the discharge characteristics
133
This possibility was also noted by Skrikantan in 1929 when he could not reproduce results in the h.f. decomposition of ammonia" due to some peculiar effect coming intc play between the gas and the walls of the vessel". In some of the experiments of Devins and Burton platinum probes were used in the discharge and these greatly increased the yield of hydrazine but when placed JUST outside the discharge they had no effect. By coating the discharge walls with platinum the yield of hydrazine increased from 10 to 43 gms/kwh, based on the positive column power input only. The platinum walls did not alter the yield of nitrogen, which is rather surprising when one considers that nitrogen is now considered to be a product of degradation of hydrazine. If, as proposed in the paper the platinum walls prevent the degradation of hydrazine it would be expected that the nitrogen yield would fall. The mechanism given to describe the results is of the form

$$NH_3 \rightarrow NH_3^* \longrightarrow NH_2 + H$$

$$\longrightarrow NH + H_2$$

$$2NH_2 + M \text{ or } W \longrightarrow N_2H_4$$

$$N_2H_4 + H \longrightarrow NH_2 + NH_3$$

nitrogen being formed by

$$NH + NH_3 \longrightarrow N_2 + 2H_2$$

and the platinum walls reducing the degradation by the reaction

$$H + H \xrightarrow{W} H_2$$

Patents based on the work of Devins and Burton were taken out by the Olin Mathieson Chemical Corporation.[34]

Rathsack[114] extended Devins and Burton's work and showed the effect wall surfaces and metals acting as catalysts had on the formation of hydrazine. It was known hydrogen atom recombination was retarded by coating the reaction vessel walls with phosphoric acid so experiments were carried out with and without this treatment. With the reactor treated to prevent hydrogen recombination yields and conversions to hydrazine were only one fifth of those from the untreated reactor, clearly showing hydrogen atoms either prevented the formation of hydrazine or degraded it. Rathsack also put forward the possibility that hydrazine was also formed on the reactor

walls explaining his theory in terms of Ouchi's reaction mechanism. viz

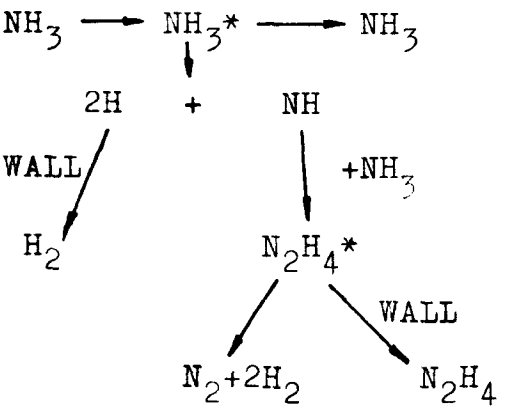

This reaction mechanism fitted his results and also explained why the yield of hydrazine fell when the reactor walls overheated.

By using electrodes made of different metals Rathsack also showed the increase in yield of hydrazine was not due to a change in the work function of the electrode or electrical characteristics of the discharge but was caused by the catalytic effect of the electrode material. Platinum was found to be the best electrode material in agreement with Devins and Burton's work.

An interesting calculation made by Rathsack was an estimate of the efficiency of production of hydrazine in the glow discharge. The calculation is only very approximate and it must be remembered Rathsack operated in the 'subnormal'

rather than the 'normal' or 'abnormal' glow discharge regions, but it does give us an order of magnitude guide. The fraction of electrons having sufficient energy to dissociate an ammonia molecule was calculated as one electron in every two thousand. It was assumed a molecule of hydrazine could be formed for every collision. The number of molecules formed per unit time and volume was then calculated as 0.8×10^{-9} molecules. This meant approximately one in every 400,000 collisions which could produce hydrazine did so, indicating theoretically at least that there was considerable room for improvement.

By this time a much greater understanding of chemical reactions in glow discharges existed. This was due not only to the work previously mentioned but also to the work of the photochemists, especially McDonald et al[90], and the radiolysis work. Over the next few years many patents were taken out relating to the methods of carrying out the reactions and to the reactor design needed to increase the energy yield and conversion to hydrazine[127,93,72,26,13,606] J.P. Manion[92], also of

Olin Matheison, took out patents relating to the electrode material and the use of added gases in the discharge. Since the cathode fall region is not effective in producing hydrazine the energy dissipated in this region should be reduced to a minimum by coating the electrodes with alkali earth metals and oxides (a very similar patent was taken out by T. Rummel in 1940).[119] Unfortunately, it is not possible to draw any definite conclusions about their effectiveness because the working lifetime of the electrodes is not given. The use of small amounts of acyclic alkyl compounds added to the discharge gases increased the yield and conversion by upto 3 times, but the addition of N_2, O_2, N_2O, NO, I_2, Hg and C_3H_8 had only slight or disadvantageous effects. However, the low conversions to hydrazine and low operating pressures made the process commercially unattractive.[3] To some extent Andersen solved both these problems. By using a high frequency generator he extended the pressures to which a discharge could be maintained upto 400 mmHg and achieved conversions to hydrazine upto 0.34 mole%. The high frequency discharge has the advantage that the negative glow does

not exist as such, hence the problem of lost energy in the cathode fall is not present. It was found that the yield was independent of both the discharge frequency and temperature but it increased to a maximum with increasing flowrate, decreasing pressure, current, and gap width. The yields, however, do increase with gap width if they are corrected to a constant residence time. Relating the rate of ammonia decomposition to a theoretical model of the discharge[86] gave the electron energy in the discharge as 4.2ev. This is not sufficient to ionize the gas (10.2ev.) which supports the views of Ouchi, Devins and Burton, that the reaction proceeded through free radicals. The mechanism proposed by Mc.Donald et al[90] (see later) was found to fit the data reasonably well. At about this time Schueler[127] also achieved conversions of 0.33% with yields upto 10.3gm/kwh by lining the reactor tube with fused glass powder. This was yet another indication of the part played by the walls of the tube. Other effects were investigated with less success. The use of nozzles and venturies to increase the gas flowrate or to jet one gas into another[53, 43, 117] and hence increase the yield, again gave low

conversions and were not developed commercially. In Britain, Imperial Chemical Industries looked into the possibilities of commercial development and produced several patents about 1960.[70] One of these one is rather surprising in that it states that the addition of small amount of oxygen nearly doubled the yield of hydrazine, whereas Manion and Westhaver found it had little or disadvantageous effects.[70] The other patents described two different effects:- (a) The use of a liquid adsorbent in the discharge and (b) an extension of Ouchi's work on the pulsing of the discharge. These could be used separately or in conjunction with each other. The advantage of the liquid spray system is that the hydrazine is removed very soom after it is formed in the reactor and this means that an equilibrium position will not be reached. Also the liquid absorbent can be recycled around the system (providing it is not itself decomposed) until a sufficient concentration of hydrazine has built up. The patents indicate that the spray can be introduced through a nozzle, rotating disc, or ultrasonically, giving a drop size in the range 0.2 - 2.0 mm diameter.

The pulsing system described used much shorter pulse on times than Ouchi in the range 20μsec to 500μsec and off times in the range 20,- 44m. sec. The yields were, however, much lower than those of Ouchi, reaching only 20 gm/kwh but insufficient information is given in the patents to help explain why this is so. No details of the conversions are given but since further commercial development was not undertaken it can be assumed that they were prohibitively low.

Even higher conversions were obtained by Rubstova[118] using platinum as a catalyst in an ozonizer discharge and after freezing out the hydrazine recirculating the ammonia. In this way conversions up to 5% were obtained with energy yields of 0.36 gm/kwh. The precise value of the energy yield cannot be ascertained since the power factor was not measured.

Skorokhodov et al[130] obtained comparatively high conversions to hydrazine of 0.5% but since they were mainly concerned with studying possible free radical mechanisms the energy yield was not measured. By using the Vasilev[147] parameter, which is a function of the main variables of power, flowrate and pressure, it was found that the correlation indicated the NH_2 radical was primarily responsible for

the formation of hydrazine (see free radical section). Since the reactor wall temperature had no effect on the yield it was also concluded that hydrazine was not formed on the walls.

A sign of the increasing engineering interest in the production of hydrazine is to be found in Marchellos'[23,24,25,88] work in the Chemical Engineering Department of Maryland University and the work carried out by the Chemical Engineering Department of Newcastle University.[140,141,142,132]

Carbaugh[24] measured emmission spectra from the glow discharge and from this was able to find the effect of residence time on NH_2 and H atom concentrations. The NH_2 concentration remained unchanged with residence time but the hydrogen atom concentration increased steadily at least up to 0.4 seconds residence time.

Following the success of the sensitizer work in radiochemistry Carbaugh added krypton to the ammonia in the discharge but it was found to have no effect. This is probably because the electrons do not have sufficient energy to ionize the gas appreciably. Unfortunately, no attempt was made to measure the power dissipated in the discharge so no energy yields could be determined.

142

Charlton, at Newcastle University, investigated the effect the type of reactor had on the yield of hydrazine, and related this to the Chemical Engineering aspects of synthesis. Concentric tube reactors of different sizes were built with a rotating central electrode through which a spray of the absorbent ethanediol could be admitted. This was said to prevent the degradation of hydrazine and could increase yields by up to a factor of 10, with yields up to 10 gm/kwh being reached. By using a pulsing system similar to the one used by I.C.I. yields of up to 20 gm/kwh were reached. Under these conditions as absorbent spray had no effect which indicates that under pulsing conditions hydrazine degradation was negligible.

Outlined in these papers are the essential features needed to make the large scale production of hydrazine from ammonia in a glow discharge a commercial proposition, and methods of achieving these features are discussed.

2.2 Formation of hydrazine from liquid ammonia.

The formation of hydrazine in or just above a liquid ammonia surface affords interesting possibilities since the hydrazine can be readily

absorbed. This upsets any possible equilibrium and should give high yields and conversions.

However the work of Ingraham[71] on the preparation of hydrazine by the arc electrolysis of liquid ammonia was rather unpromising. Operating his D.C. discharge at up to 60 mA, 4kV between platinum electrodes he obtained a conversion of 0.2% but the energy yield was only about 10^{-3} gm/kwh. From these results it was concluded the essential processes forming hydrazine occurred in the vapour above the liquid surface.

This was later confirmed by Hickling[64] et al, who have carried out most of the work on the glow discharge formation of hydrazine in liquid ammonia. The results improved such that in 1962 patents were taken out with N.R.D.C.[65] describing methods of preparing solutions of liquid ammonia containing over 3% hydrazine, with energy yields at about 6gm/kwh. A diagram of the apparatus is shown in fig. 4a. The anode was a platinum wire above the surface of the liquid and the discharge could be operated at 100 mmHg. The formation of hydrazine differs from that in a gaseous system in that the cathode fall region is used to

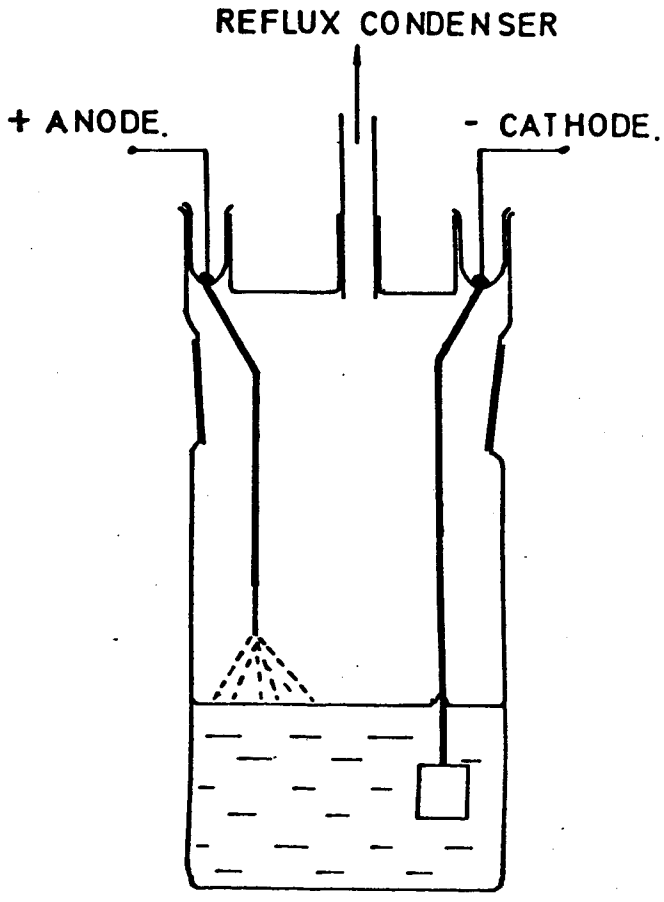

fig4 a. HICKLINGS REACTOR.

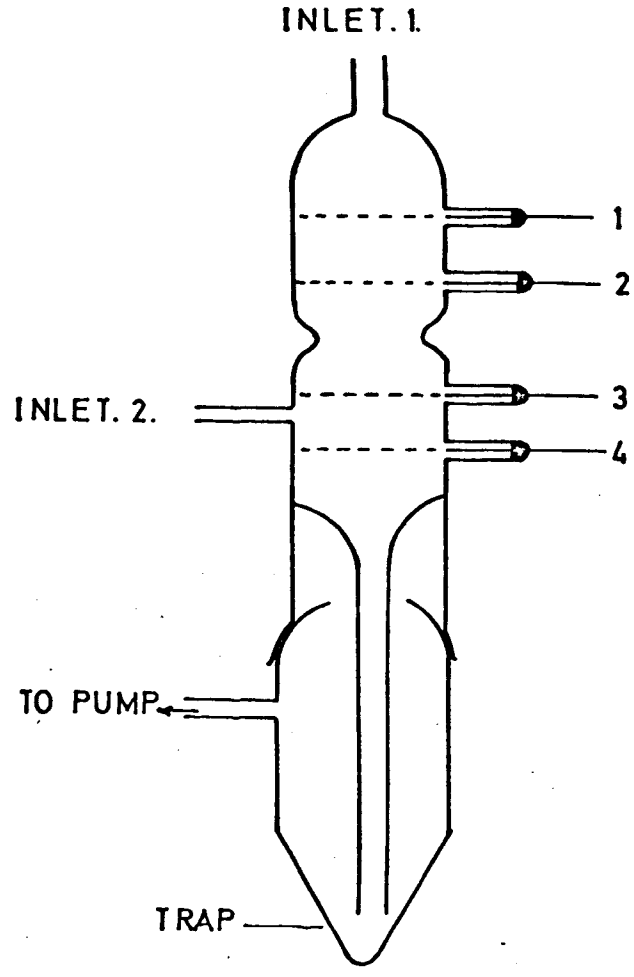

fig 4b. VARNEYS REACTOR.

accelerate gaseous ions into the liquid where they react to form hydrazine. If the electrodes are reversed, so that the positive column is next to the liquid surface the yield is reduced by almost 50%. The yield is substantially independent of changes in pressure, current, electrode distance and the surfaces of the electrodes and walls. Hickling concludes that positive ions (NH_3^+) enter the liquid phase and form NH_2 radicals by charge transfer.

$$NH_3^+ + NH_3 \longrightarrow NH_4^+ + NH_2$$

The hydrazine being formed by

$$NH_2 + NH_2 \longrightarrow N_2H_4$$

with the possibility of degradation by hydrogen atoms.

A convenient method of operating the discharge at atmospheric pressure is to immerse the anode in the liquid and then increase the applied voltage until a glow discharge is formed. Yields are slightly lower by this method but this may be offset by the economic advantages of operating at higher pressures.

2.3 Formation of hydrazine from nitrogen and hydrogen.

Results on the formation of hydrazine from nitrogen and hydrogen are rather contradictory.

In 1930 Steiner studied the reaction between hydrogen and nitrogen atoms and molecules. Each gas was fed through a separate discharge at about 1½mm.Hg and 200 mA. The exit gases from the discharge were then mixed and the products analysed. Reactions were carried out between:-

i) hydrogen atoms and nitrogen molecules

ii) hydrogen atoms and nitrogen atoms.

iii) nitrogen atoms and hydrogen molecules.

It was found that (i) hydrogen atoms did not react with nitrogen molecules, (ii) nitrogen atoms and hydrogen atoms formed ammonia, (iii) nitrogen atoms and hydrogen molecules formed ammonia and hydrazine.

The ammonia being formed by the reactions

$$N + H + X \longrightarrow NH + X$$

$$NH + H_2 \longrightarrow NH_3$$

and hydrazine by the reactions

$$N + H_2 + X \longrightarrow NH_2$$

$$2NH_2 \longrightarrow N_2H_4$$

If these mechanisms are correct, one would also expect hydrazine to formed in case (ii) by the reaction

$$N + H_2 \longrightarrow NH_2$$

$$2NH_2 \longrightarrow N_2H_4$$

but because of the high H atom concentration it would probably be rapidly degraded. The mechanism given for the formation of hydrazine in case (iii) does not explain how the large

quantities of ammonia found were formed. The mechanism is probably much more complex than that given above.

When both the nitrogen and hydrogen were mixed together in high and low frequency arc discharges, Briner and Hoeffer[19] could detect no hydrazine even though ammonia was formed. These findings were confirmed later.[155,42,28]

Steiners experiments (i) and (iii) were repeated in 1955 by Varney[146] using the reactor shown in fig. 4 b. The reactor has two inlets, and four electrodes, 1 to 4. Electrode 2 was a perforated cathode to allow positive ions to pass through it. A variable potential could be applied between electrode 2 and 3 so that ions could be drawn through or held back from the next field region. With nitrogen admitted at inlet 1 to give active nitrogen, and hydrogen admitted at inlet 2, ammonia was formed but no hydrazine was detected. The potentials of electrodes 2 and 3 were then set to aid or prevent the motion of ions but the products were the same indicating the reaction was not ionic in character. With hydrogen admitted at inlet 1 and nitrogen at 2 no hydrazine was formed.

This last result is in agreement with Steiners work but Varney disagrees with Steiner

in saying that hydrazine is formed by the reaction between active nitrogen and molecular hydrogen.

Experiment (ii), performed by Steiner, was investigated by Gvenbaut[55] in 1961. Active nitrogen and hydrogen were formed in an electric discharge and allowed to react in a spherical vessel. The emission spectra of the NH radical was observed and when the products were cooled to 77°K, ammonia with a small amount of hydrazine was found. This is roughly in agreement with Steiners results of 1930 but the mechanism given is

$$NH_3 + NH \longrightarrow N_2H_4$$

rather than that of Steiner.

A system of jetting active nitrogen into ammonia was patented by I.C.I.[70] in 1958 and 1959. The nitrogen was activated in an electrodeless discharge at 40 mm. Hg, the walls being kept cool by a sheath of unactivated gas. Yields and conversions were both low at 1.84 gm/kwh and 0.01% respectively. If ammonia itself was passed through the discharge, yields increased up to 3.3gm/kwh.

The results of this work indicates that the economic advantages of using nitrogen and hydrogen as starting materials are more than offset by the low conversions and energy yields.

2.4 Free Radical and Ionic Studies in Ammonia and Hydrazine.

A knowledge of the free radical reactions leading to the formation and destruction of hydrazine is essential in the full understanding of the chemistry of the glow discharge.

For clarity H atoms, nitrogen containing radicles and ions are treated separately here but one must consider their combined effect in the mechanism and kinetics of the discharge.

(i) Hydrogen atom reactions.

Boehm and Bonhoeffer[16] in 1926 investigated the possibility of reaction between hydrogen atoms and ammonia but observed none. However, the photochemical work of Wigg and Kistiakowsy[154] and the electric discharge work of Koenig and Wagner[79] prompted a further investigation by Dixon.[37] Atomic hydrogen was produced in an electric discharge and its concentration measured calorimetrically by recombination on a sheet of platinum. The atomic hydrogen was allowed to react with both ammonia and hydrazine. With ammonia only a very slight reaction occurred (cf 100). Even though the hydrogen atoms were ten times in excess, only about 2% of the ammonia was decomposed, the reaction suggested being $H + NH_3 \rightarrow NH_2 + H_2$ 1. with an activation energy of 8.5 k.cal/mole.

With hydrazine from 42 - 100% decomposition occurred, low percentage decomposition being favoured by low hydrogen atom concentration and high flowrates. Each mole of hydrazine decomposed produced approximately 1 mole of ammonia and 1 mole of permenent gas in agreement with Wigg and Kistiowsgy's mechanism of

$$H + N_2H_4 \longrightarrow H_2 + N_2H_3 \qquad 2.$$

$$2N_2H_3 \longrightarrow 2NH_3 + N_2 \qquad 3.$$

the reaction $H + N_2H_4 \rightarrow NH_3 + NH_2$ was discounted. 4.

By considering the collision efficiency and diffusion effects Brise and Melville[20] showed that this would not signficantly reduce the hydrogen atom concentration in the decomposition of ammonia. Using deuterium atoms instead of hydrogen atoms Schiavalo and Volpi[124] found that 95% of the ammonia formed was undeuterated. They substantiated reaction (2) and (3) and calculated the rates as

$$k_2 = 3.5 \times 10^{+11} \; e^{-2000/RT} \text{ mole}^{-1} \text{ cc sec}^{-1}$$

$$(1.25 \times 10^7 \text{ lit/m.sec}) \; {}^{300^\circ K}$$

$$k_3 = 3 \times 10^{+12} \text{ mole}^{-1} \text{ cc sec}^{-1} \quad (\text{at } 150^\circ C)$$

The rate for the ammonia reaction is given as approximately 10^7 mole $^{-1}$ cc sec $^{-1}$ at 150°C. The luminescence reaction $H + N_2H_4 \rightarrow NH_3 + NH_2$ $(^2A_1)^*$ was investigated by Gosh and Bair[50] using a 10 M/C discharge with pulse on times of 1 - 2 millisecs and off times of about 50 m.secs who

found with a rate $k_4 = 1.2 \times 10^5 e^{-2600/RT}$, ($1.5 \times 10^3$ at 300^oK) the reaction was relatively insignificant. However they did find an unusually high NH_2 concentration thought to be due to the reaction.

$$N_2H_3 + H \longrightarrow 2NH_2 \qquad 5.$$

occurring at high hydrogen atom concentrations.

(ii) NH and NH_2 radicoles reactions.

NH and NH_2 radicoles have been stated to be responsible for the formation of hydrazine from ammonia in a glow discharge. E.J. Bair[7] and co-workers have been investigating the formation and disappearance of these radicoles for a number of years. In 1956 a method of studying these radicles was developed by absorption spectroscopy following a pulsed discharge. A block diagram of the apparatus is shown in fig. 5a. By adjusting the discharge pulse and measuring pulse time intervals the rise and decay of the NH_2 radical could be measured. A typical plot is shown in fig. 5b for ammonia at 1 mm.Hg.
It was found that the optimum radical concentration depended on discharge repetition frequency, flow rate, pulse width, pressure, power supply capabilities and discharge characteristics.

Nelson and Ramsey[102] studied the radicals formed in the discharge by this method using a 10μF condenser to give 20μsec pulses in ammonia and hydrazine at a few mm.Hg pressure. NH and NH_2 radicals were observed in each case. In 1962 Haines and Bair[57] also found NH and NH_2 radicals but the NH was only observed in the emission spectra and only after 50 - 100 discharges. Using 500μsec pulses at a frequency of 15 pulses/sec the rate of recombination of the NH_2 radicals in ammonia was found to be second order with a rate constant $k_6 = 2.3 \times 10^9$ lit/mole sec. This led to the conclusion that the NH_2 recombination was of the form

$$NH_2 + NH_2 \longrightarrow N_2H_4 \qquad -6$$

rather than $NH_2 + H \longrightarrow NH_3$ -7

Diesen[36] who was working on shock tube experiments at higher pressures suggested that the NH_2 disappearance observed by Haines and Bair may be the reaction.

$$NH_2 + NH_2 \longrightarrow NH_3 + NH \qquad -8$$

rather than (6). To investigate this possibility Salzman and Bair[121] used a flash photolysis method at 5 and 10 torr. They found reaction (8) did occur at a rate approx. $k_8 = 0.5 \times 10^9$ lit/mole sec, this is also supported by work on the NH radical.

A mass spectrometric study of the NH radical produced in a pulse discharge was made by Foner and Hudson.[45] They found its ionization potential 13.1ev and its appearance potential 10.1ev. It should be pointed out that in previous work[45] on the decomposition of hydrazine and ammonia in a continuous electric discharge they were unable to detect the NH radical.

The most recent study of the NH radical is by Mantei and Bair[95] using kinetic spectroscopy following flash photolysis in ammonia at 1 mm.Hg. It was shown that since there was a delay in the appearance of the NH radical it was formed by secondary reactions either

$$NH_2 + H \longrightarrow NH + H_2 \qquad (9)$$

or

$$2NH_2 \longrightarrow NH + NH_3 \qquad (8)$$

and that it decays by the insertion reaction

$$NH + NH_3 \longrightarrow N_2H_4 \qquad (10)$$

with a high pressure limit rate constant of

$$k_{10} = 1.1 \times 10^{10} \text{ l/mole sec at } 300^{\circ}K.$$

This shows that hydrazine, can be formed from both NH radicals and NH_2 radicals (reactions (10 and (6)) but the formation of NH_2 radicals is the primary reaction in each case.

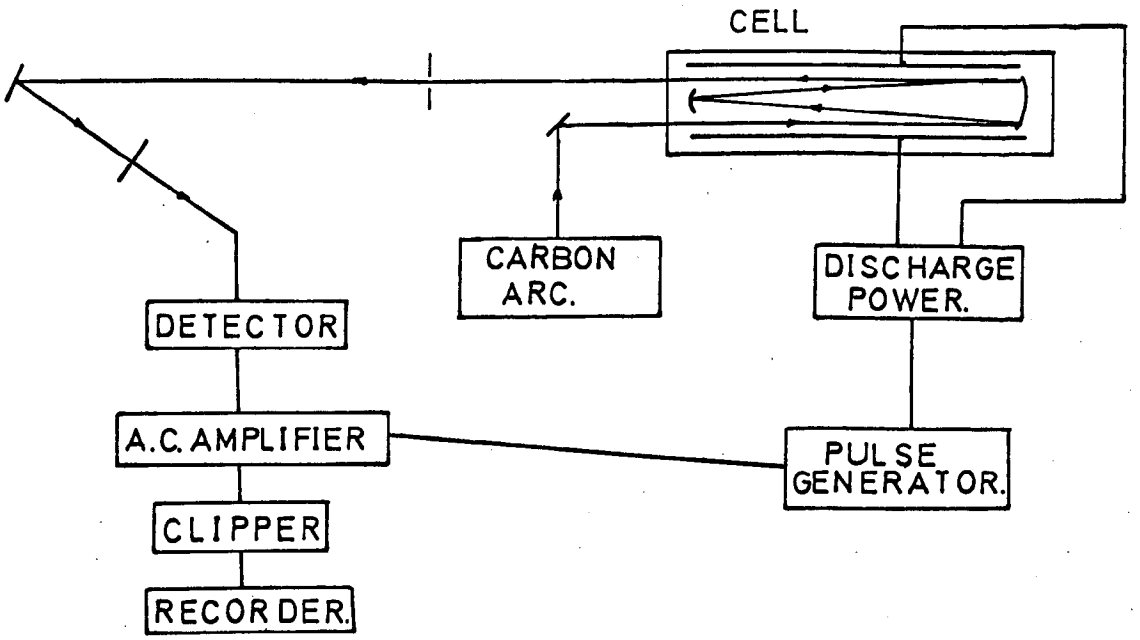

fig 5a. BLOCK DIAGRAM OF BAIRS APPARATUS

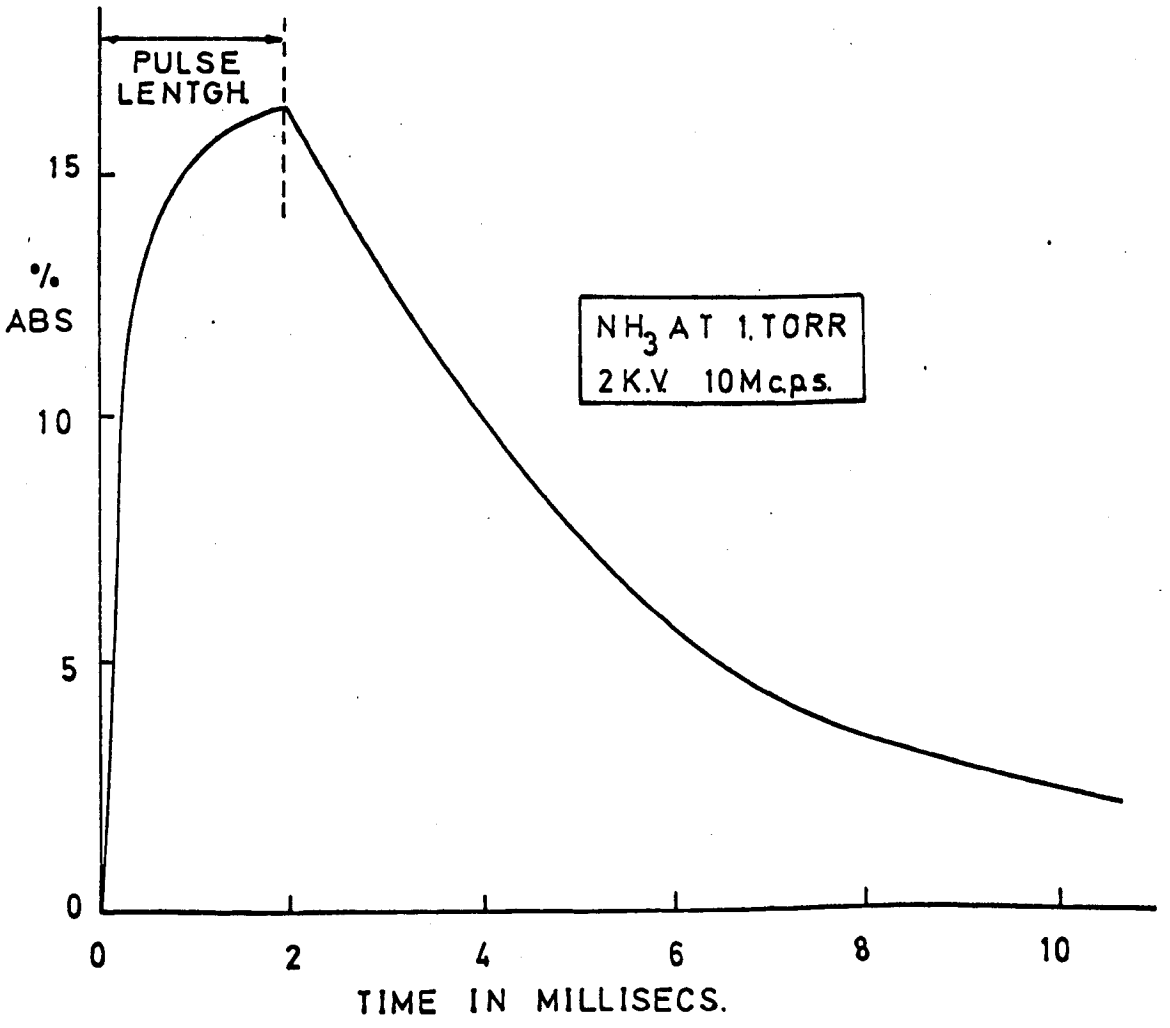

fig 5b. FORMATION & DECAY OF NH_2

Hydrogen atoms have been shown to have little effect on ammonia but to seriously degrade hydrazine (reactions (2) and (3)). This degradation can be minimised by keeping the hydrogen atom concentration small and by using high flowrates.

2.5 Thermodynamic data, collision cross sections and bond energies.

Heats of formation, bond dissociation energies[35] and other useful thermodynamic data[2,122] are found in references[137, 145, 149].

A great deal of work has been carried out in measuring appearance potentials[94,98,96], collision cross sections[10,11,67], ion and electron mobilities etc.[120,61,103,109] but much of it is theoretical or with electron energies at or above the ionization potential[47,32].

References selected here cover in some part the conditions encountered in a glow discharge. It appears from these references that (i) the appearance potentials of the principle ions of ammonia and hydrazine are all above 10ev and that (ii) only a small proportion of the hydrazine formed from the electron impact of ammonia is formed from ion molecule reactions[143,27,59,56] (iii) 99% of all ion molecule reactions form NH_2 or NH and that these reactions occur very quickly.

2.6 Photochemical production of hydrazine.

The extensive work carried out on the photochemistry of ammonia[39,91,8,139] has added considerably to the understanding of the processes which might occur and the effect of parameters on these processes, in the glow discharge.

Different wavelengths of light have associated with them corresponding energies (3000Å = 4ev, 2000Å = 6 ev, etc.) hence by conducting reactions at various wavelengths the threshold energies for dissociation reactions and ionization can be found.[148,150] Using this technique it has been shown that the NH radical only appears with light of wavelength below 1600Å (i.e. above 7.8ev)[107,54,10,125] but NH_2 radicals appear above and below 1600Å. The work of McNesby et al[91] using C_2D_4 as a scavenger for hydrogen atoms also showed that at 1894Å (= 7ev) ammonia decomposed almost entirely into NH_2 and H whereas at 1236Å (= 10ev) 1/6 of the hydrogen is formed from molecular processes of the form $NH_3 \rightarrow NH + H_2$. These radicals can then react by secondary processes to form products including hydrazine.

The formation of hydrazine from the photochemical decomposition of ammonia has been studied extensively by McDonald et al[90] using both static and flow systems. They found that

i) The Quantum yield of ammonia decomposition varied with cell size, light intensity, but surface to volume ratio had little effect over the range 0 - 100 and constant over the range 100 - 560.

ii) The percentage ammonia converted, converted to hydrazine increased with increasing flowrate up to 84% (at 1750 cc/sec) and then started to decrease.

iii) The quantum yield of ammonia decomposition was independent of linear flow.

The most important reactions were thought to be

$$NH_3 \xrightarrow{h\nu} NH_2 + H$$

$$H + NH_2 \longrightarrow NH_3^*$$

$$NH_3^* \longrightarrow NH_2 + H$$

$$NH_3^* + M \longrightarrow NH_3 + M$$

$$2NH_2 \longrightarrow N_2H_4$$

$$H + N_2H_4 \longrightarrow N_2H_3 + H_2$$

$$2N_2H_3 \longrightarrow 2NH_3 + N_2$$

$$H + \text{wall} \longrightarrow \tfrac{1}{2} H_2 + \text{wall}$$

This reaction mechanism is often used to help

describe the glow discharge system and the effect of variable parameters (e.g. flowrate, added gases) are found to be similar in both systems.

The photochemical decomposition of ammonia to form hydrazine has not been exploited commercially. This is probably because the conversion of the electrical energy in the lamp, to light energy of a suitable frequency is very inefficient. In a glow discharge the electrical energy is used directly to initiate the reaction.

2.7 Radiochemical production of hydrazine.

The radiochemical production of hydrazine from ammonia has been studied from both pure and commercial view points. It has been found that many of the relationships applying to gas discharges also hold for the radiochemical reactions even though higher electron energies are used and ion molecule reactions assume greater importance. Viz. The hydrazine yield increases with increasing flowrate,[76] decreasing irradiation intensity,[22A,66] decreasing pressure and that at lower pressure, wall effects became important.[22A,B] Again degradation of the hydrazine by hydrogen atoms was thought to account for the low yields. The use of scavengers has been used extensively[48,131,74,76,128] to reduce the hydrogen atom concentration and to show

the effect of radical, ionic and electron processes. It was shown that the use of ethylene effectively scavanged atomic hydrogen with a corresponding increase in the hydrazine yield and that only a very small amount of molecular hydrogen was formed by direct processes.

Another method of decreasing the hydrogen atom concentration is to carry out the reaction in the presence of a noble gas sensitizer.[82, 62] This gas absorbs nearly all the radiation energy and transfers it to the ammonia at a precise energy level. If this energy level is just high enough to ionize the ammonia but not dissociate it, reaction proceeds as

$$NH_3 \rightarrow NH_3^+ + e$$

$$NH_3 + NH_3^+ \longrightarrow NH_4^+ + NH_2$$

$$NH_4^+ + e \longrightarrow NH_2 + H_2$$

without the formation of hydrogen atoms rather than the reaction,

$$NH_3 \longrightarrow NH_2^+ + H$$

which would occur without the sensitizer. Unfortunately, for sensitizers to be really effective they must constitute up to 90% of the gas mixture and this limits their use commercially because of the separation costs.

Most commercial applications consist, essentially, of suspending small UO_2 particles in liquid ammonia, preferably just above its freezing point[84,128,80,131,30,83,77] and then separating the hydrazine by extraction and distillation. This is also necessary to reduce the radiation level in the hydrazine product but adds to the cost of the process. Preliminary cost estimates carried out by the U.S.A.F.[46] indicate that hydrazine produced by this method would cost between 1/- to 3/- lb. of anhydrous hydrazine (1961). This compares very favourably with present production costs.

TABLE OF SOME IMPORTANT RESULTS.

AUTHOR	DISCHARGE TYPE	CONDITIONS CURRENT	CONDITIONS VOLTAGE	CONDITIONS PRESSURE	CONDITIONS FLOW	ENERGY YIELD	CONVERSION TO HYDRAZINE
Anderson et al	High Frequency	100 mA	565v	90 TORR	600 cc/sec	6gm/kwh	0.34%
Bredig et al	Seimens	1 mA	6,670v	-	150mg/ min	3.9gm/kwh	0.016%
Charlton et al	Liquid spray concentric cylinder	0.047 watt/cc		10 TORR	0,018 sec/res time	8gm/kwh	0.5%
Devins et al	Glow Pt Wall Reactor	4 mA	385v	7 TORR	4.6cc/sec	43 gm/kwh	0,094%
Hickling	Discharge into Liqu NH_3	25mA	900v	100 TORR	-	5.9gm/kwh	3.2%
I.C.I. Patents	Active N_2 jetted into ammonia	1200mA	100v	400 TORR	1000lit/ hr	1.8 gm/kwh	0.014%
Manion	Glow coated electrodes	6.3mA	585v	5 TORR	3.4g/ hr	23gm/kwh	-

AUTHOR	DISCHARGE TYPE	CONDITIONS CURRENT	VOLTAGE	PRESSURES	FLOW	ENERGY YIELD	CONVERSION TO HYDRAZINE
Ouchi	Pulsed Glow	50mA max	1020v mean	40 TORR	780cc/ sec	46.1gm/kwh	0.014%
Rubstova	Ozonizer NH_3 recycled	12.5mA	10kV	600 TORR	-	0.36 gm/ kwh	4.8%
Schuler	500 H_Z Discharge	2.4mA	6400v	6 TORR	3.25 gm/ min	13.6 gm/kwh	0.11%

3.0 Scope of investigation.

The synthesis of hydrazine from ammonia in a glow discharge was studied using a parallel flow cylindrical reactor operating at 10 torr. Power was supplied to the reactor continuously and in short discrete pulses of 5μsec to 220μsec duration.

The successful production of hydrazine in a glow discharge depends on a high energy yield, a high conversion to hydrazine and a low conversion to unwanted by products (nitrogen and hydrogen). Energy yields of upto 47 gms N_2H_4/kwh and conversions to hydrazine of upto 4.8% have been reported. In some experiments over 80% of the ammonia converted formed hydrazine. Unfortunately, all these desirable features do not occur under any one set of operating conditions. If the energy yield is increased the conversion drops and vice versa. The need for optimisation is apparent.

Previous work indicated that high energy yields are formed at low residence times created by fast gas flow or a pulsed discharge system. The fast flow system has the disadvantage that the costs of pumping gas at a low pressure and fast flowrate are very high whereas the costs of electrical switching needed to operate the pulsed

discharge system are comparatively low. A pulsed discharge system gives a low "active residence time", θ', where θ' is defined as the total time a molecule experiences a discharge whilst it is in the reactor i.e.

$$\theta' = \frac{\text{Pulse on time x Gas residence time}}{\text{Pulse on time + pulse off time}}$$

It was thought the active residence time could be used to correlate both the fast flow system and the pulsed discharge system and if both systems had the same active residence times similar energy yields and conversions would be achieved. This hypothesis was tested by carrying out experiments in both systems over a range of active residence times from 4×10^{-2} seconds to 1.12 seconds. When it was found that the pulsed d.c. system gave higher energy yields and higher conversions to hydrazine a fuller study of this system was made. The effect of pulse on time and repetition rate on the energy yield and conversion to hydrazine were determined over a power input range of 10 to 200 watts.

The effect of wall reactions on the pulsed and continuous d.c. systems was investigated by packing the reactor with glass wool to increase the wall area.

Investigations were made into the effect of the cathode fall and positive column zones of the discharge by flowing most of the gas through each zone separately.

In order to increase the mean electron energy in the discharge of the continuous d.c. system, helium was added in varying proportions and its effects on yield and conversion of ammonia to hydrazine measured.

The current voltage characteristics of the d.c. discharge were measured and the prebreakdown current of the non-selfsustaining discharge measured for an applied voltage of a few hundred volts.

From the data obtained the response surfaces were plotted and from these the optimum operating conditions could be ascertained. Possible chemical reactions occurring were considered and a simple kinetic model of the systems set up.

This particular programme of work was carried out to find the optimum operating conditions for the discharge reactor and to give a greater understanding of the processes occurring in the glow discharge synthesis of hydrazine.

4.0 EXPERIMENTAL.

4.1 Choice of Operating Parameters.

Certain parameters were always kept constant partly through constraints imposed by the equipment and partly by the length of time available to carry out the measurements. The effect and reason for the choice of these parameters is explained below.

A gap width of 6.3 cm. was chosen, to fully cover the porous glass wall area and have striking voltages within the range of electrical supply equipment. This gap width is also in the range studied by Rathsack, Westhaver, Ouchi and Devins and Burton. As shown in section 2.1 increasing the gap width at constant residence time should increase the yield accordingly. Hence it should be possible to increase the yield this way.

With a tube radius of 1.8 c.m. it is not too difficult to maintain a uniform discharge but with larger tube diameters the discharge tends to be more intense in some parts of the tube. Work by Devins and Burton indicated that the maximum yield of hydrazine occurs at a reduced tube radius (Rp) of about eight whereas in this work the reduced tube radius was nine.

This difference in value should not change the value of the field strength very much but because the yield is shown to be so critically dependent upon field strength the subsequent difference in yield may be significant.

'Aged' or worked in stainless steel electrodes were used in order to obtain consistent and reproducible results. The reaction between ammonia and steel in glow discharge results in the 'nitriding' of the steel surface, similarly, with aluminium the nitride is formed but it is not known whether the changes in yield with ageing are associated with the discharge voltage characteristics or to some catalytic effect. The use of aged electrodes also corresponds more closely to industrial practice where long down times to change the electrodes would be unacceptable.

Platinum has been shown to be the best electrode material for the synthesis of hydrazine but the use of such a material in amount necessary for large scale production is not feasable because of the prohibitive cost. Similarly the use of very low pressures would mean that large reactors and high flow rates would have to be used to give commercial quantities of product. Previous results indicate

that the maximum yields of hydrazine occurs in the pressure range of 5-10 mm. Hg. A pressure of 10 mm. Hg. was chosen in this case but further experiments below this pressure may be worthwhile. The yield is critically dependent upon X/p and small changes in pressure may effect large changes in the yield.

In the synthesis of hydrazine certain electrical characteristics are apparent in the glow discharge. These characteristics will determine the action of the electrons in the discharge which will in turn effect the rate of primary reactions and hence the rate of production and degradation of hydrazine.

4.2 Experimental Equipment.

4.2.1 Discharge reactor.

A readily available discharge reactor had been designed to be as versatile as possible so that a range of experiments could be carried out with the same reactor. Figures 6 & 7 show a photograph and diagram of the reactor. The reactor body consists of a 1.8 cm. diameter fused silica tube 10" long with the centre section replaced by a porous borosilicate glass tube 5.3 cm. long. Porous glass was used to increase the wall area for recombination and also allow gas to be taken out through the

fig. 6. REACTOR

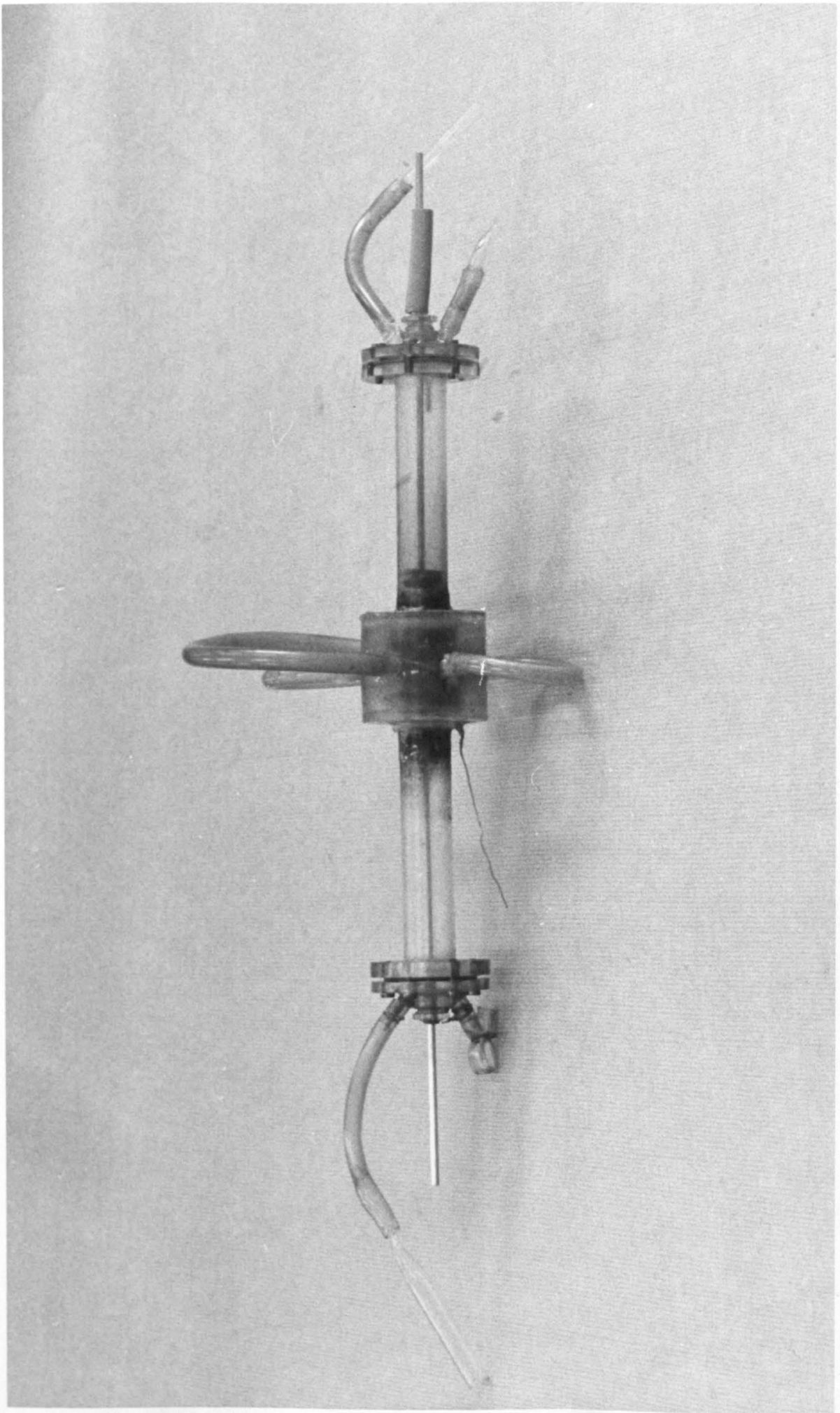

fig. 6. REACTOR

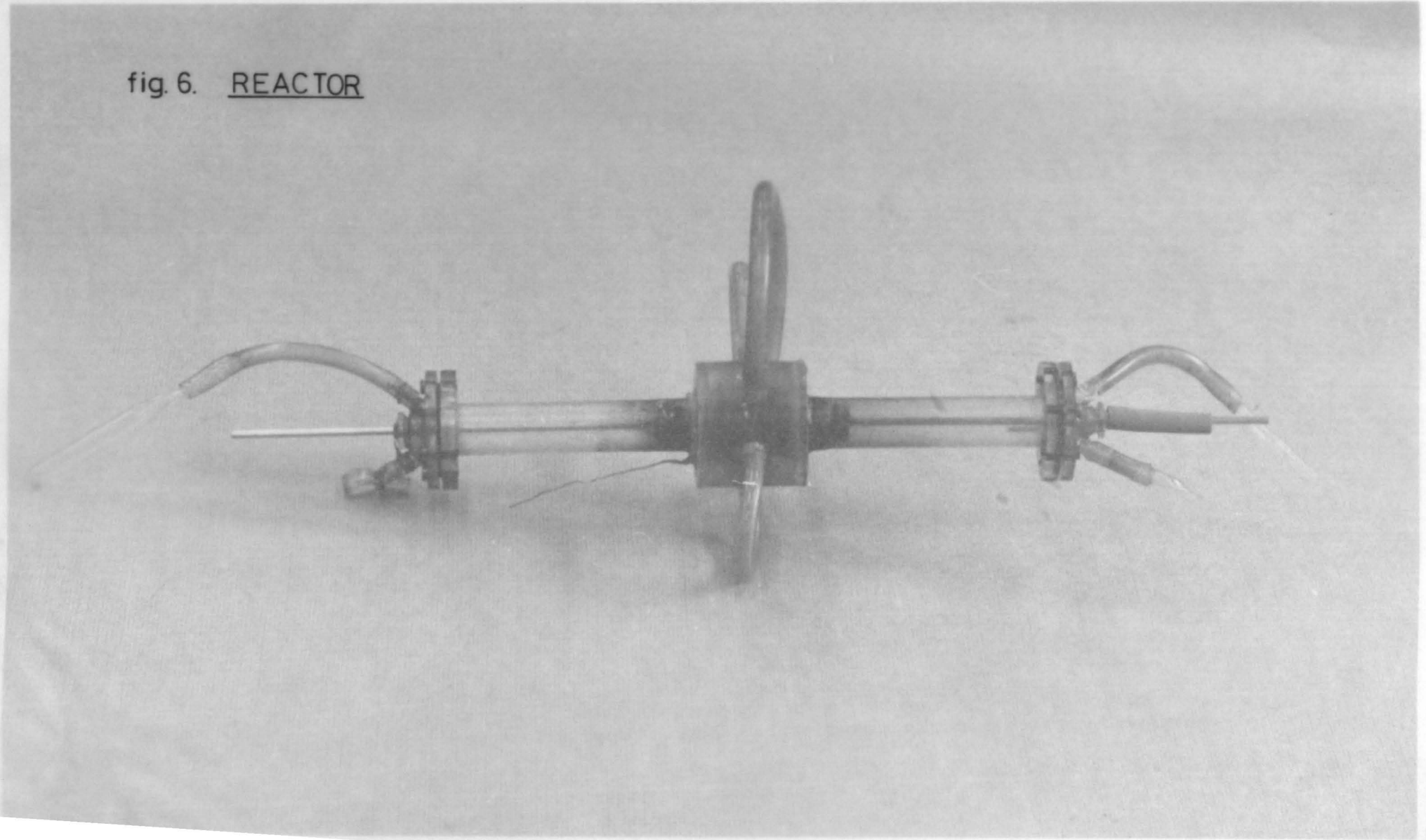

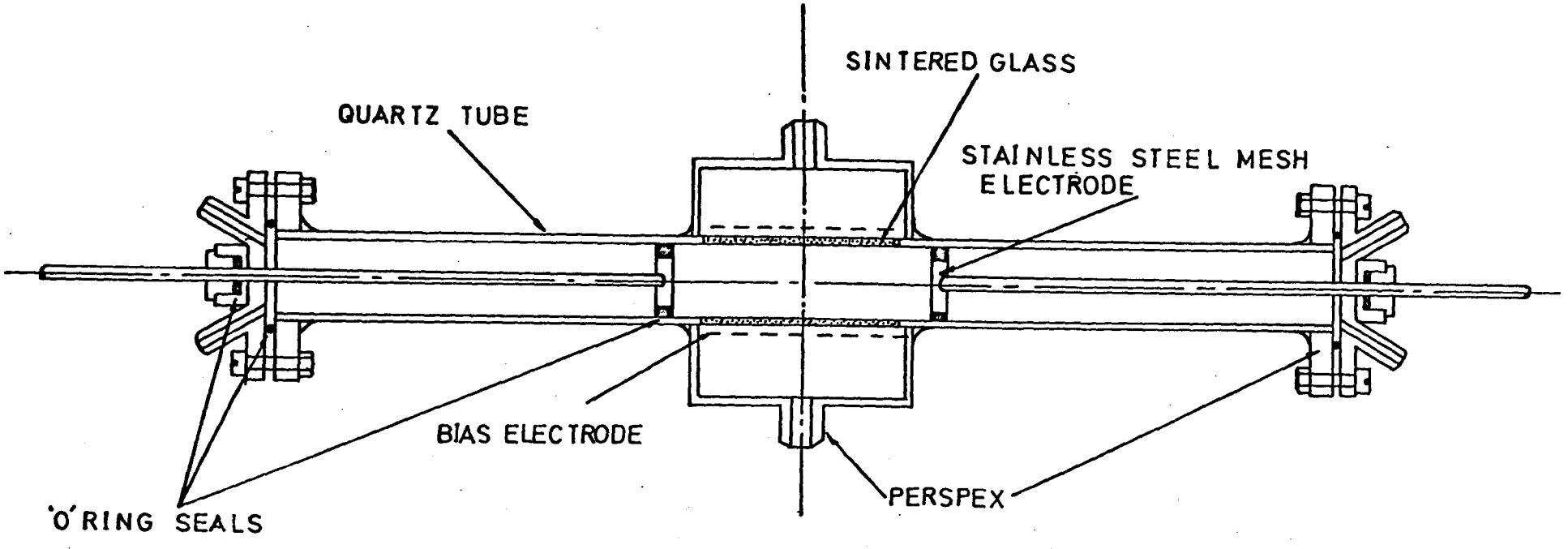

SCALE : 2/3 FULL SIZE

fig 7. DISCHARGE REACTOR

reactor walls. Gas could be taken out through the outlets in the perspex enclosing tube.

An "outer ring electrode" made of copper gauze was wrapped around the outside of the glass section and a lead taken out through the perspex. The electrode could then be used for possible investigations into the effects of positive and negative ions on the reaction, however, it has not been used in any experiments to date. 1 cm. diameter stainless steel mesh discs mounted on $\frac{1}{8}$" stainless steel rods were used as electrodes. Gas could be passed through the discs which were sealed to the sides of the reactor by rubber sealing rings. The steel rods passed through Gaco 'o' rings in the ends of the reactor in such a way that a vacuum tight seal was made but the rods could still be moved in and out to give various inter-electrode distances. Electrical circuitry was connected to the electrode ends by crockodile clips. Inlets and outlets for gas were provided at the ends of the tube and access would be gained to the reactor body by unscrewing the end plates, removing the 'o' rings and electrodes.

In experiments where a high rate of power input was applied the electrodes had to be cooled by a blast of compressed air directed

onto the ouside of the reactor by a suitably shaped piece of glass tubing.

4.2.2 Flow arrangement.

A line diagram of the apparatus is given in fig. 8. In building the apparatus particular attention was paid to the maintenance of high vacuum and prevention of air leaks. Half inch diameter glass tubing was used wherever possible and connections were made with ground glass ball and socket or cone and socket joints High vacuum stopcocks were used throughout as was Apeizon high vacuum grease (Types M and N) To prevent corrosion by ammonia, metallic parts of the apparatus were made from stainless steel. The apparatus was supported on a rigid Lablox frame, see photograph fig. 9.

Reactant gases were supplied from cylinders. Distilled anhydrous ammonia containing less than 200ppm impurities of mainly oil and water, and 99.99% pure helium with less than 1ppm. oxygen were used. Only one cylinder of each gas was used for most experiments so the gas composition can be considered as constant. High pressure gas from the cylinders was reduced to just above atmospheric pressure by needle valves V1 and V2 and then to the operating pressure by valves V4 and V5. The inlet flowrate and temperature to the reactor were measured using a flowrater F and thermometer Th 1, the exit temperature being measured by thermometer Th2,

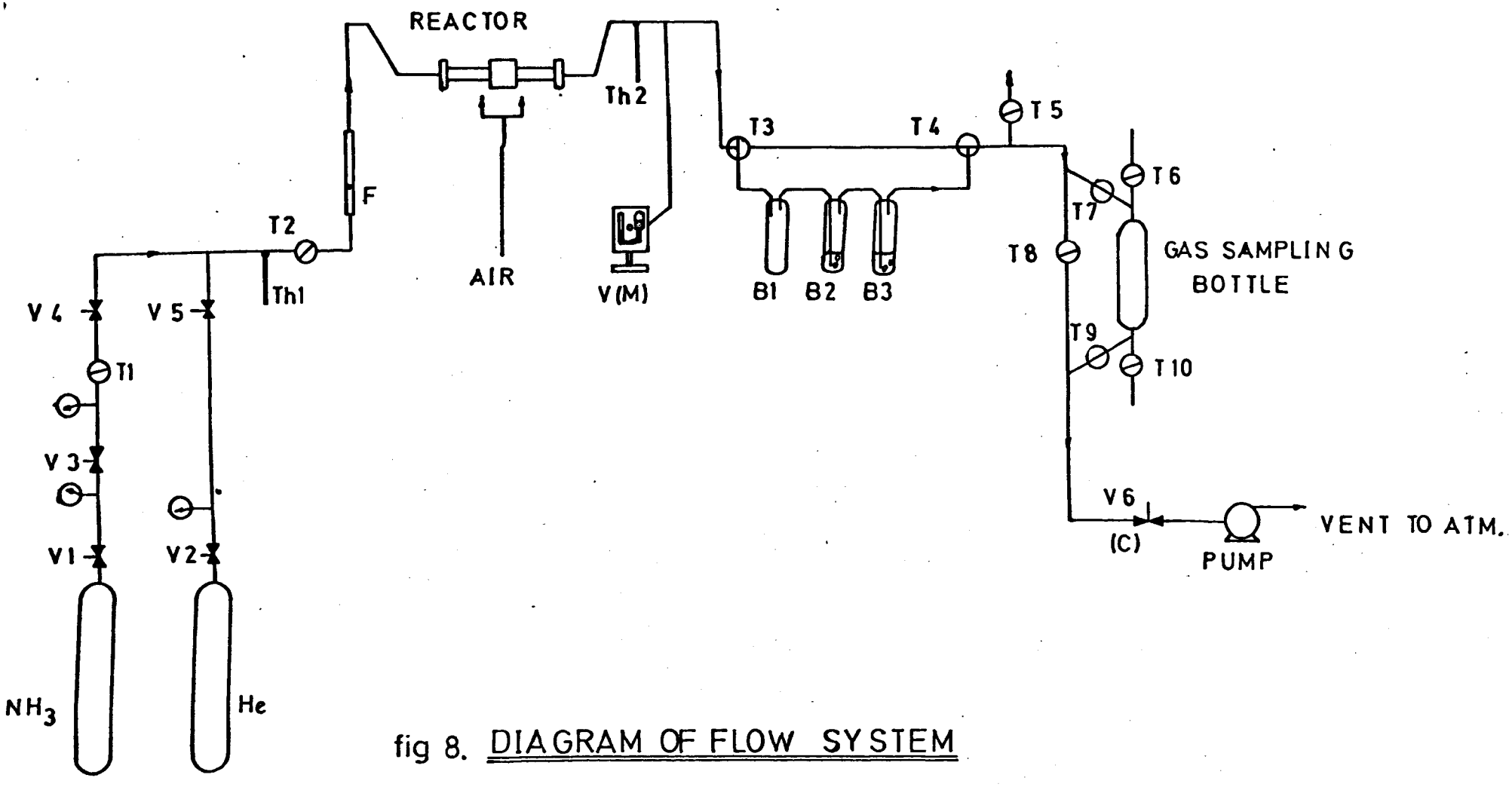

fig 8. DIAGRAM OF FLOW SYSTEM

fig.9. APPARATUS

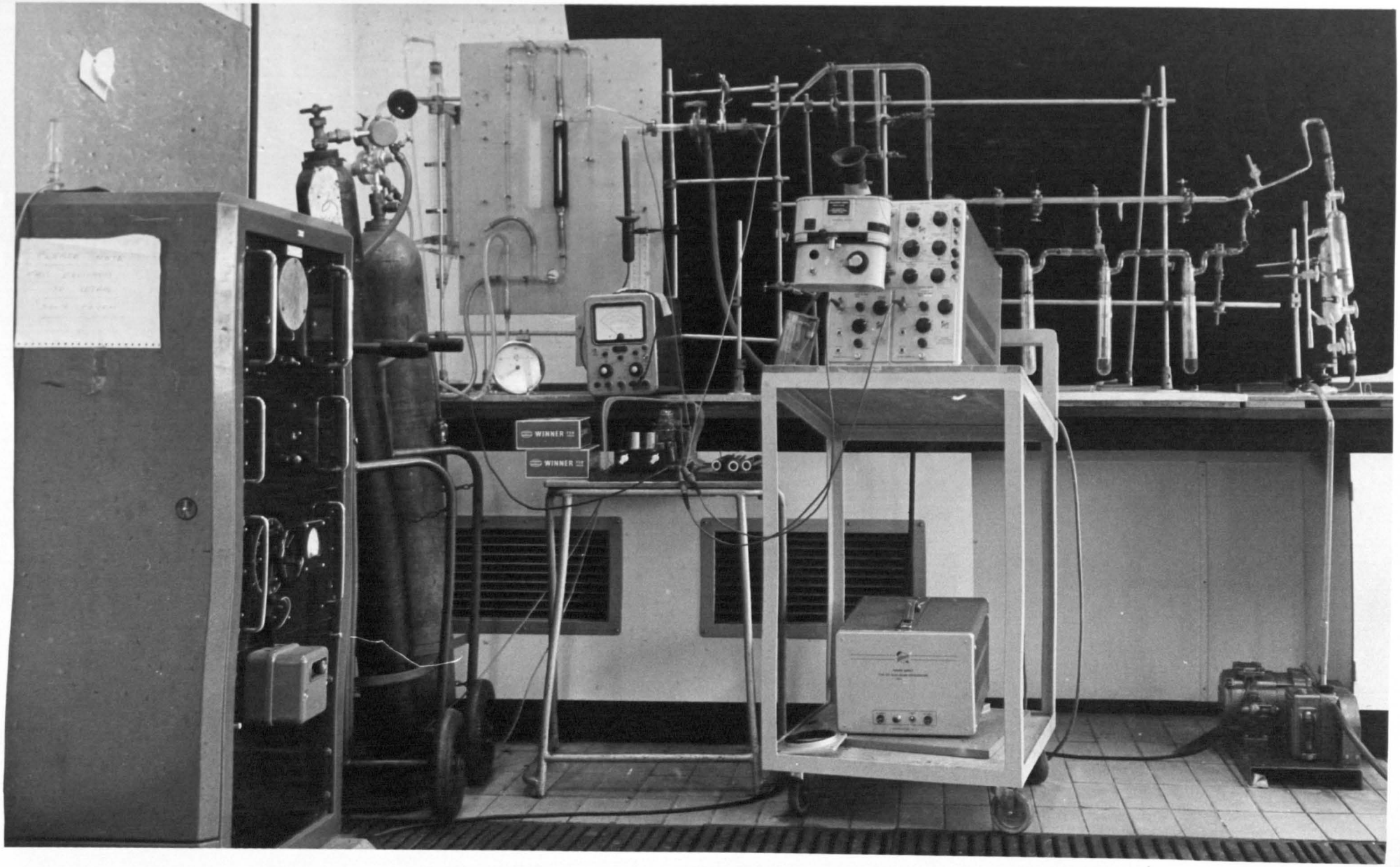
WINNER
WINNER

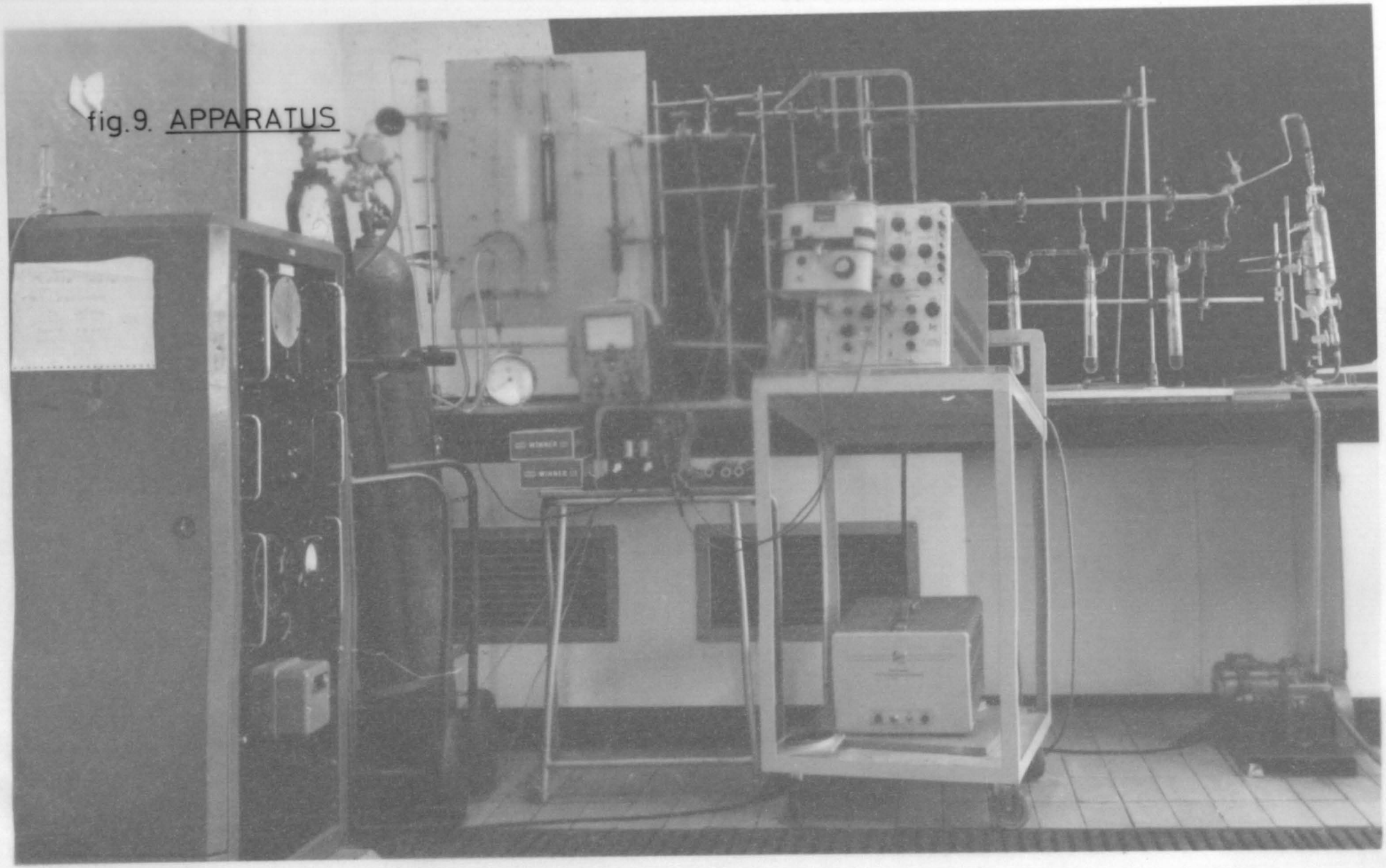

fig.9. APPARATUS

A vacustat gauge model 1B2 or a mercury manometer and barometer V(M) were used to measure the operating pressure. The vacustat gauge operates on the same principle as a McLeod gauge over the range 10 - 10^{-2} torr. Gas leaving the reactor could be directed along the bypass line or through the absorption bottles by stopcocks T3 and T4. The first absorption bottle was empty and acted as a "suck back" trap. B.D.H. 99.9% pure ethane diol was used as the hydrazine absorbent in the second and third absorption bottles. Unused ethane diol was tested for traces of hydrazine but none could be detected. This absorbent was used because of its low vapour pressure at room temperature and its efficiency at absorbing hydrazine.
Gas samples were taken using the gas sampling bottle shown in fig. 10. By adjusting the stopcocks on the bottle gas could be made to flow into the bottle or down the side limb. In this way the bottle could be flushed out by the gas and a sample taken without interrupting the flow.

An Edwards Speedivac ES 35 rotary vacuum pump was used. The pump could reach a vacuum of 0.5 torr and flowrates of 35 litres/min but the ammonia seemed to react with the oil in the pump and reduce its efficiency somewhat.

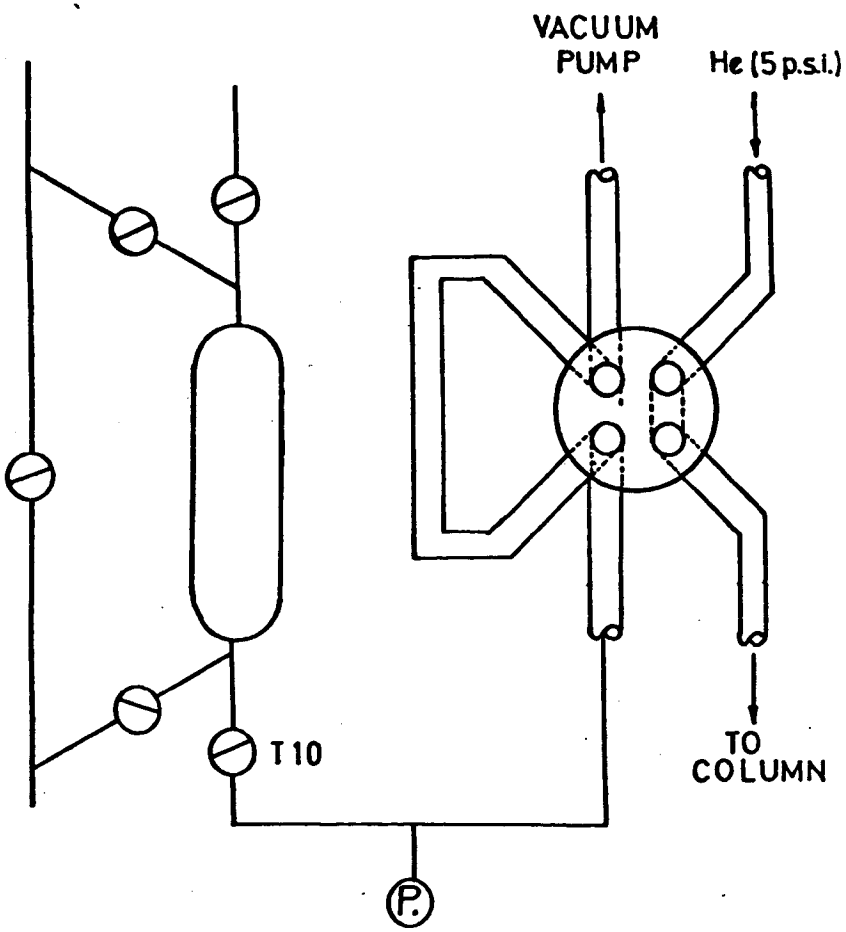

(A) LINE BEING EVACUATED

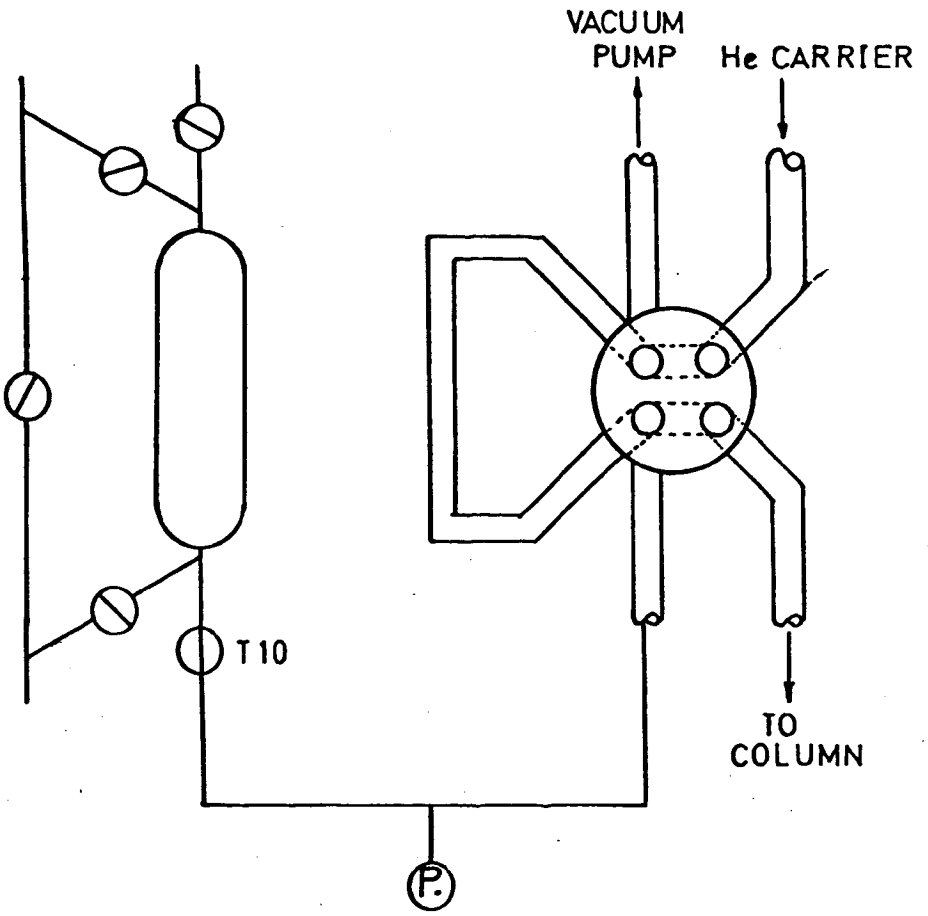

(B) SAMPLE BEING ANALYSED

fig 10. GAS SAMPLING SYSTEM

4.2.3 Electrical Equipment.

(i) Continuous d.c. apparatus.

High voltage d.c. supply.

Fig. 11 shows a circuit diagram of the d.c. supply. The voltage to the primary of the transformer is controlled by the variac at 0 -250v giving an output from the secondary of upto 3.5kV and 300 mA. Smoothing of the output was achieved using a 10 Henry coil and 4 μF high voltage capacitors.

To increase the safety of the equipment microswitches were provided on the supply cabinet doors and on the variac. Both primary and secondary circuits were protected by fuses and a thermal delay was provided on the H.T. to the rectifier valves. In some experiments the smoothing capacitors remained charged to a high potential and had to be discharged with a large insulated perspex switch mounted on top of the cabinet. A 5K ohm resistance was connected in series with the switch to prevent undue arcing.

Ballast Resistance.

A ballast resistance had to be placed in series with the reactor to prevent the glow discharge developing into an arc discharge. The most suitable value of this resistance was found to be 17K ohms. Since the power dissipated in the resistor could be over 100 watts.

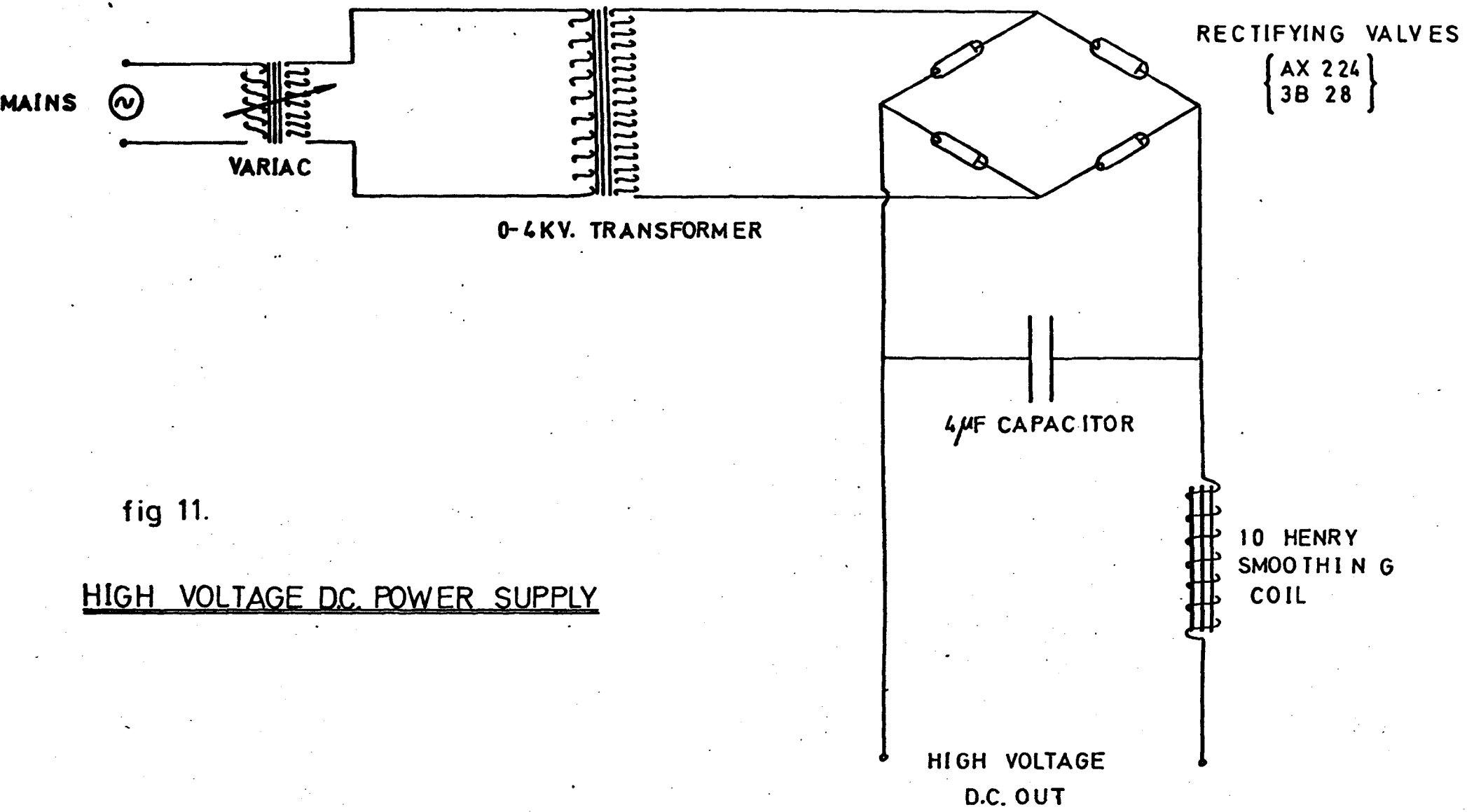

fig 11.

HIGH VOLTAGE D.C. POWER SUPPLY

Welwyn type C47 enamel covered wire wound resistors were used. The same resistor was used in both the continuous d.c. and pulsed d.c. experiments.

Voltmeter.

The discharge operated at high voltages and low currents so a voltmeter with a very high input impedence had to be used. An Airmex valve voltmeter type 314 with a d.c. multiplier probe type 372 gave an input resistance of 2,000M ohms. The instrument could operate from 300mV to 30kV but under normal experimental conditions the voltage measured was only about 1kV. Under these conditions the current drawn by the meter would be approximately 0.5μA, less than 0.01% of the total current. Manufacturers quote an accuracy of $\pm$ 5% full scale deflection and when the instrument was checked against a direct reading galvanometer no difference in readings could be detected visually.

Milliameter.

A standard 0 - 100mA moving coil milliameter was used to measure the direct current. The meter was checked against a calibration instrument and no difference in readings could be detected.

Electrical circuit.

The arrangement of the instruments described above is shown in the circuit diagram fig. 12a. The power dissipated in the discharge was calculated simply by multiplying the current by the voltage.

(ii) Pulsed d.c. apparatus.

The high voltage supply and ballast resistor were the same as those used in the continuous d.c. experiments. Circuit diagrams are shown in fig. 13, and photograph fig. 14.

Pulse generator.

High voltage pulses are created by using a valve to switch the voltage from the d.c. supply to the reactor for a short interval of time. The switch is essentially in three parts

i) a multivibrator and capacitor to generate the pulse

ii) a pulse amplifying stage

iii) a grid switching output stage.

The first valve (v1) an ECC81 acts as a multivibrator switch oscillating at a rate determined by the values of variable resistors R3, and capacitors C1 and 2. Range changes were made by changing C1 and 2 and fine adjustments with R.3. The output from R.3 of the multivibrator is fed to capacitor C.3 so that as the voltage suddenly changes a pulse is generated.

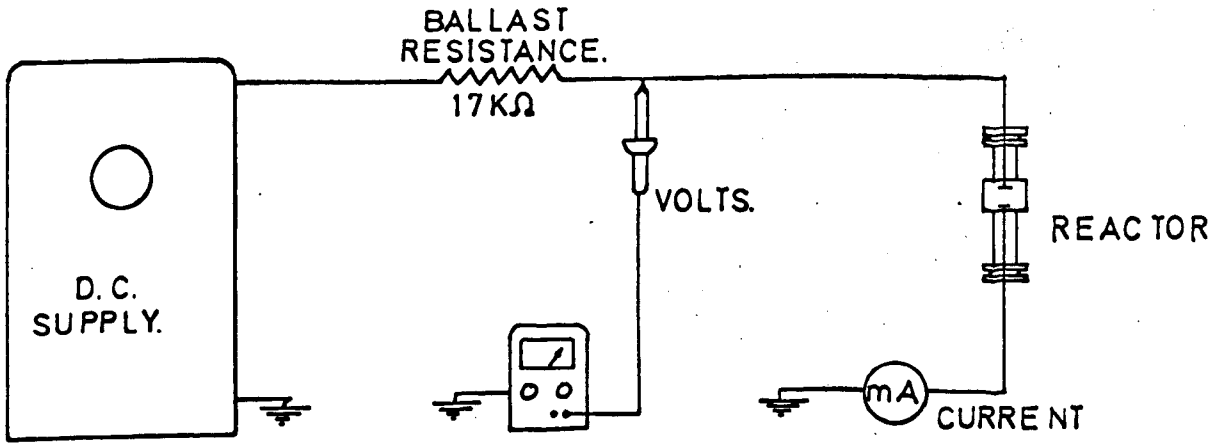

fig 12a.

D.C. MEASURING CIRCUIT.

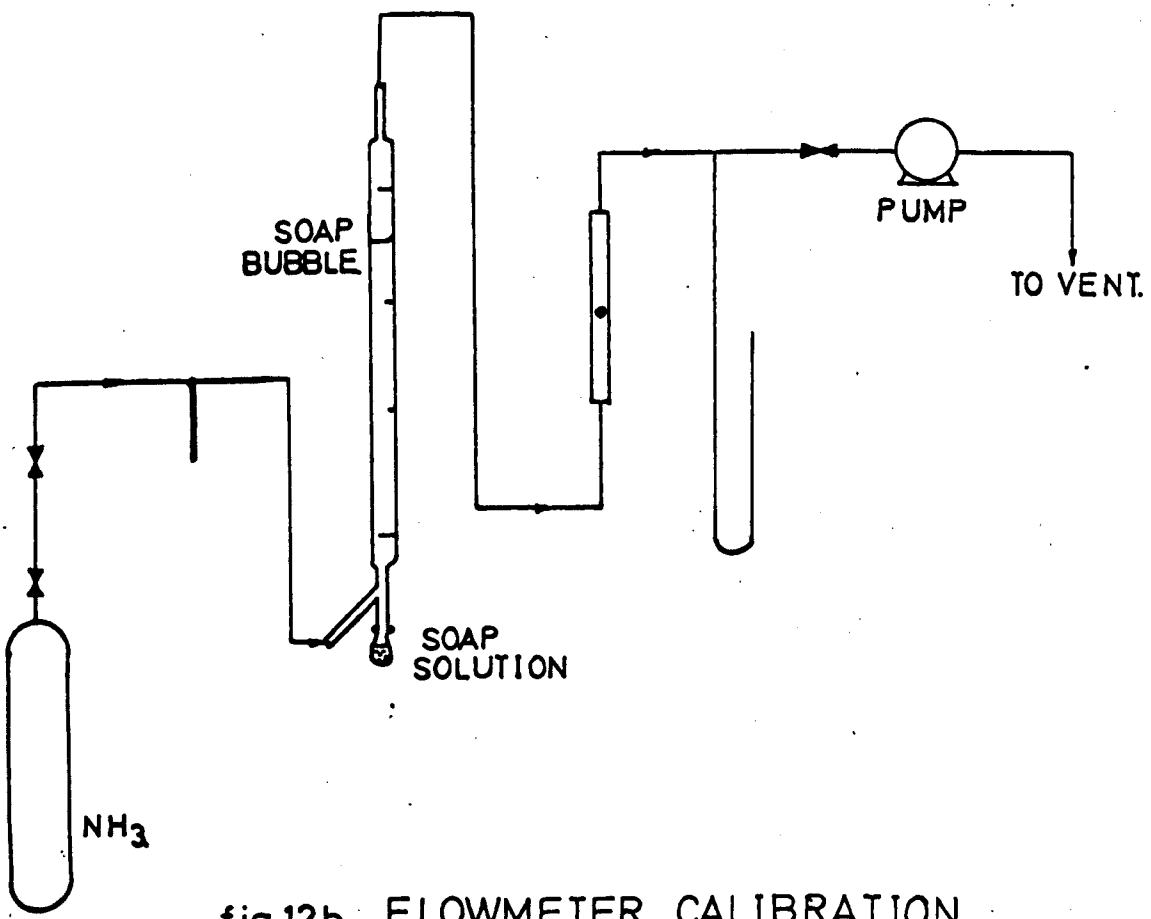

fig 12b. FLOWMETER CALIBRATION.

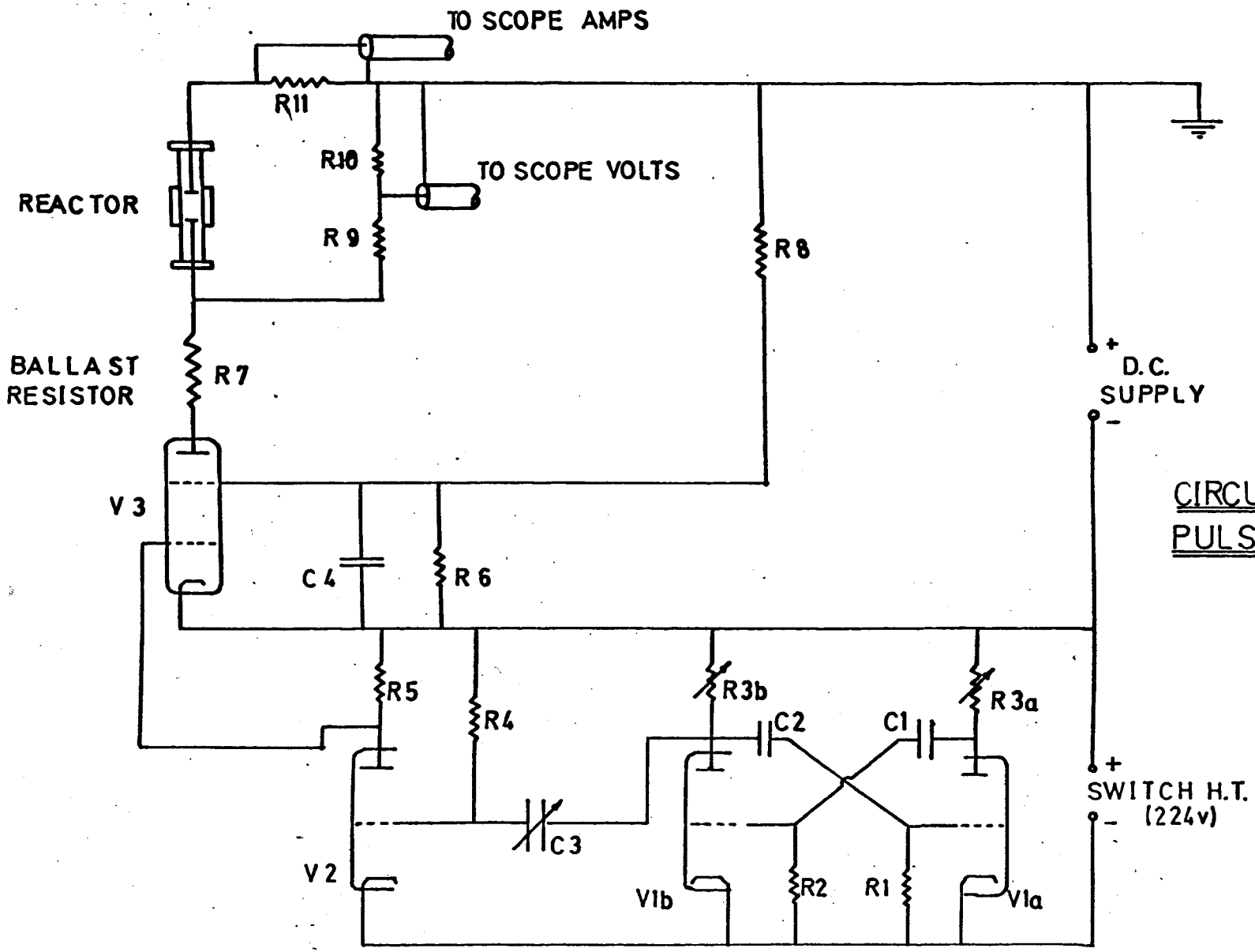

fig 13.

CIRCUIT DIAGRAM UNDER PULSED D.C. CONDITIONS

fig. 14. PULSE.CCT.

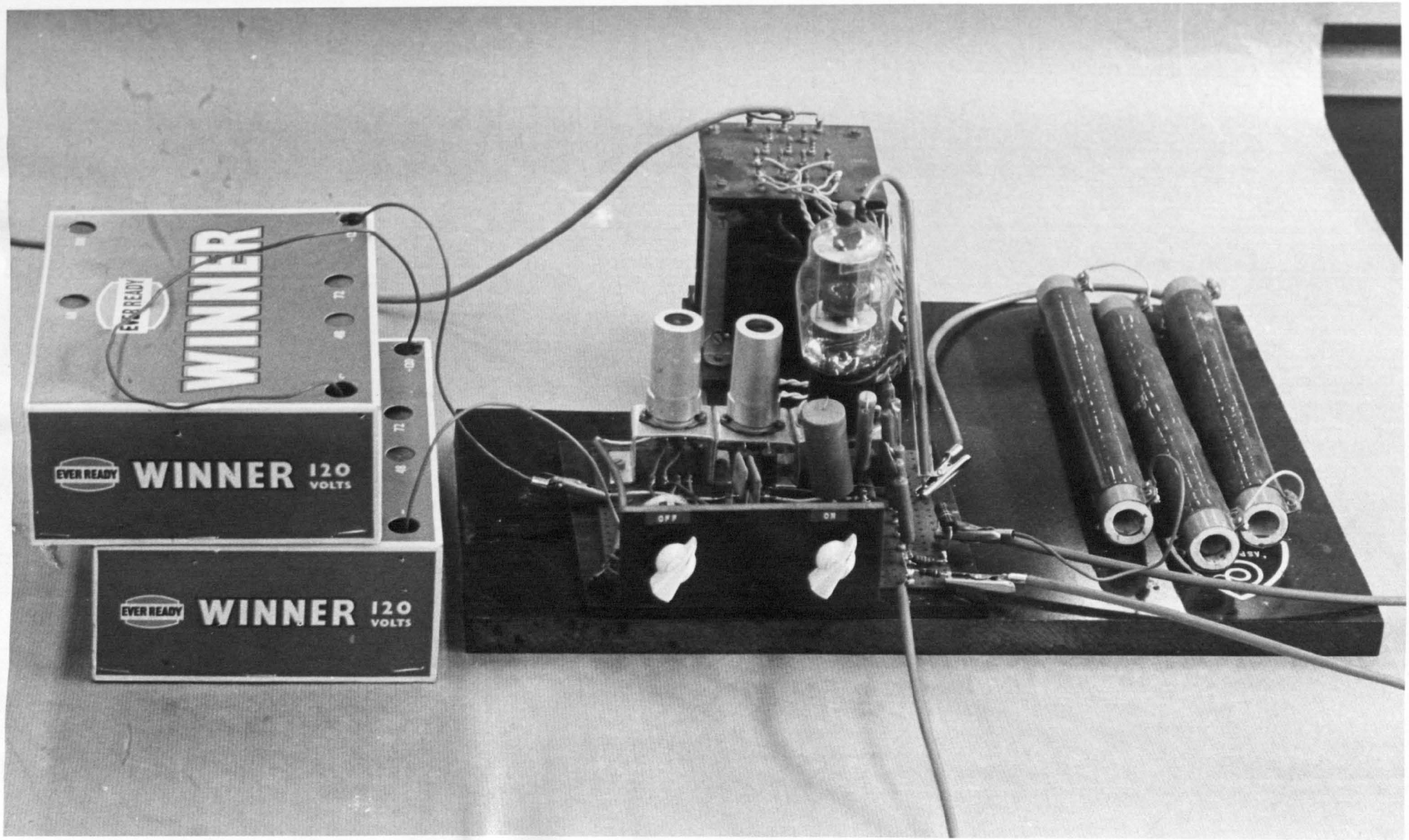
EVER READY
WINNER
EVER READY WINNER 120 VOLTS
EVER READY WINNER 120 VOLTS
OFF
ON

fig. 14. PULSE. CCT.

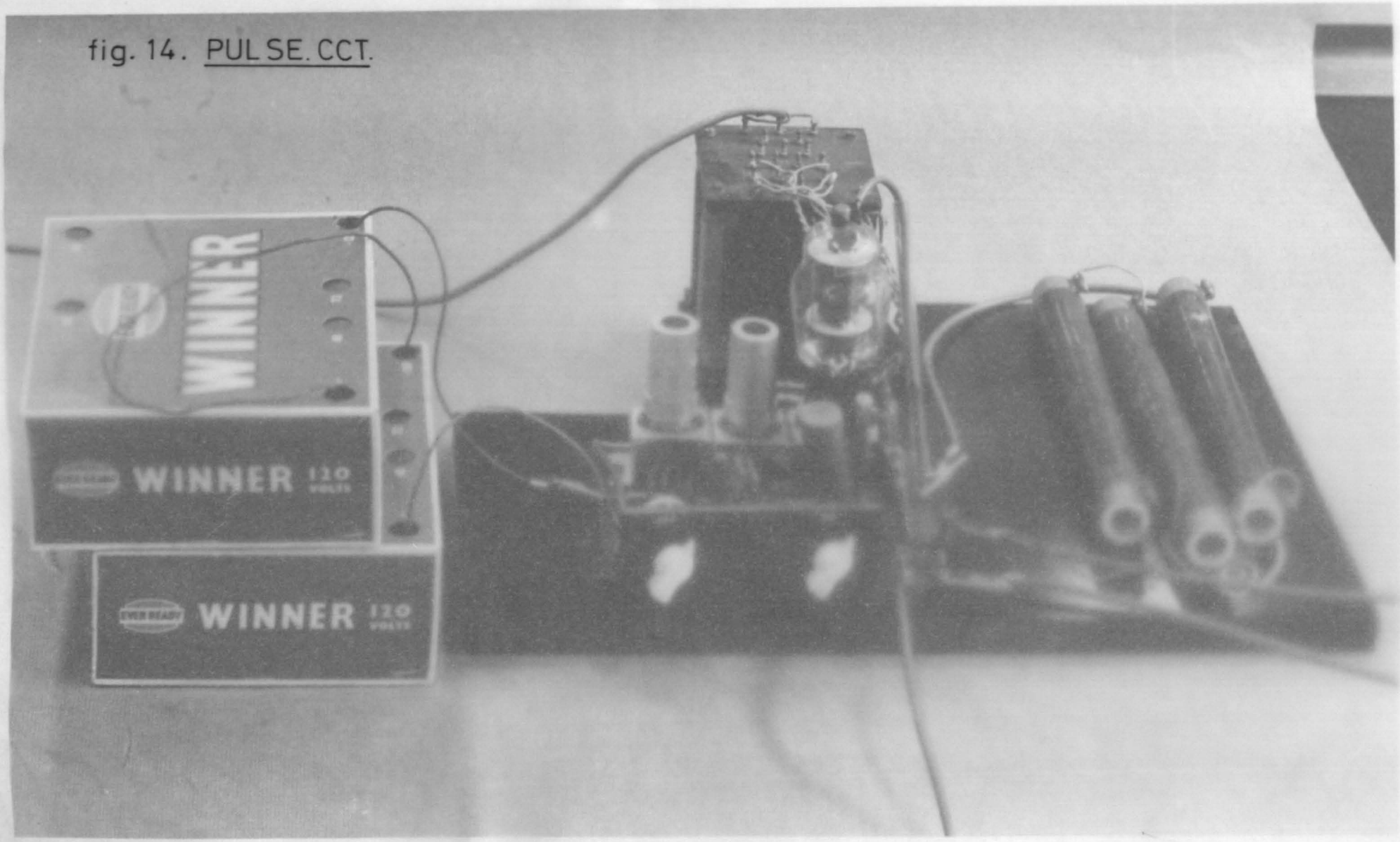

The duration of this pulse will depend upon the value of C.3. The pulse was amplified by half of the second ECC 81(V2) and fed to the grid of the output pentode 807(V3) Grid 3 of this valve is fed with h.t. from the d.c. supply via resistor R. This voltage "holds off" the valve until the input pulse switches it on. The input pulses causes the valve to conduct and hence the high voltage supply is fed to the reactor creating a discharge until such times as the pulse voltage to the grid falls to a level where the valve is "switched off" and the discharge ceases. It was not possible to produce a particularly square voltage pulse but this was largely due to the loading effect caused by the gas resistance suddenly dropping as breakdown occurred. More spphisticated switch designs also suffered from this problem. Although this switch is of simple design it proved an effective method of producing pulses of variable frequency and width. The time between successive pulses could be varied from 10 μ sec. to over two seconds and pulse widths from less than 5 μsec to over a millisecond. A great deal of care had to be exercised in operating the switch because it floated at operating voltages of upto over 3kV.

Oscillascope.

A Tektronic Type 551 dual beam oscillascope and a Shackman camera were used to record the voltage and current waveforms. In order to measure accurately the high speed transients in the discharge pulses type K fast rise preamplifier plug in units were used. These had a rise time of 0.006 μsec and the instrument had an overall response time of 0.014 μsec. Both the horizontal and vertical sweep amplifiers were accurate to within 3% of the control setting.

4.3 Experimental procedure.

4.3.1 Flowmeter calibration.

The gas flowrate was measured using an F & P precision bore flowrator type FP 1/8-20-G-5/84. First the meter had to be calibrated using the soap film technique see fig. 12b. Gas from the rotameter entered the measuring tube as shown and the flowrate found by noting the time taken for the soap film formed to travel up a given volume of the tube. Unfortunately the flowmeter could not be calibrated at the operating pressure of 10 torr because at room temperature the vapour pressure of the water in the soap solution would be significant and a high reading would be obtained. To overcome this problem the

meter was calibrated at 350 torr and from manufacturers data supplied with a rotameter and the physical properties of the gas the flowrate calibration was corrected to 10 torr. See appendix 3. fig 56.

4.3.2 Experimental Routine.

The cleaned, washed and dried absorption bottles were filled with ethane diol from a pipette and connected to the apparatus. Taps T3 and T4 were set such that gas would flow through the absorption bottles. Reducing valve V1 was adjusted to give slightly above atmospheric pressure on valve V3. With tap T2 closed the apparatus was evacuated, taps T8 and T9 closed and the pressure noted. If no leaks were present the pressure did not change over a period of minutes. Where a leak was present its position was found using a Teslar coil type leak detector. Having established no leaks were present taps T2, T8 and T9 were opened and gas allowed to flow through the apparatus. By adjusting valves V4 and V6 it was possible to set both the flow and pressure to the required value. Once set these valves required only a small amount of adjustment for each experiment.

A Cartesian manostat (C) was used to control the pressure in some of the first experiments but it was found to cause a considerable pressure drop, so it was replaced by a needle valve. Some fluctuations in the position of the float in the flowmeter occurred as a result of the gas bubbling through the absorption bottles. At approximately $\pm$ 0.1 the desired value this was not serious but it could not be eliminated completely. In order to flush all the air out of the apparatus, gas was allowed to pass through the apparatus for at least an hour after reaching its operating conditions. Gas was then diverted along the bypass line and the discharge struck and allowed to reach a steady condition. Having done so the gas was passed back through absorption bottles for the duration of the experiment. During the experiment the inlet and outlet temperatures were noted, the pressure and flowrate checked. After an appropriate length of time the discharge was switched off and gas allowed to flow for another four or five minutes tap T4 was then closed, the pump switched off and the apparatus allowed to come upto atmospheric pressure. The ethane diol in the two absorption bottles was mixed together, diluted if necessary and analysed. A check showed a negligable

amount of hydrazine was absorbed in the second bottle.

The procedure for taking gas samples is described on page 71.

When helium was mixed with the ammonia the procedure was exactly the same, the helium cylinder being connected as shown by the dotted line in fig. 8.

At the end of each experiment the absorption train was dismantled, thoroughly washed in water and dried in a hot oven to remove traces of ethane diol.

Operation of discharge.

i) Continuous d.c. experiments.

The discharge was initiated by slowly increasing the voltage until breakdown occurred. The voltage was then rapidly reduced to give the desired current, this current being maintained at a constant value throughout the experiment by adjusting the variac slightly. Voltage changes occurring during an experiment were not more than about 3%, the weighted mean is given in the data.

ii) Pulsed d.c. experiments.

The pulse generator was adjusted to give pulses of the required repetition rate and pulse width using the variable resistors and capacitors. Initiation of the discharge was carried out in the same way as for the continuous d.c. system

except that it was not possible to set the current at a given value. At long off times greater than 0.1 seconds it was sometimes necessary to reduce the pressure of the system before the discharge would strike but once the discharge had been initiated the pressure could be increased without too much difficulty and the experiment continued in the normal way.

The oscilloscope time base, vertical amplifiers and triggering were regulated to give waveforms of a suitable size and at least three photographs were taken at intervals during the experiment. In experiments where the variance between pulses was high more photographs were taken. At the end of the experiment after the discharge had been turned off and the voltage reduced to zero the oscilloscope trace was allowed to free run to provide the baseline photograph for the current and voltage waveforms.

4.3.3 Power measurement.

Continuous d.c. power was measured simply by multiplying the voltage by the current but for a discharge pulse the total power in the pulse W, is given by

$$W = \int_0^T V_t \times i_t \, dt$$

where V_t and i_t are the instantaneous values of voltage and current at time t and T is the time duration of the pulse.

The current waveform signal was taken across a gold standard high stability resistor R11 and the voltage from the voltage divider circuit R9 and R10 with a X10 tuned attenuator probe of 10M ohm resistance and 8$\mu\mu$F input capacitance.

A small phase shift between these two traces could cause quite high errors in the power measurement. To make sure no phase shift occurred because of the measuring circuit used, square wave pulses from a Marconi type TF 675F dual pulse generator were fed to points R9 and R11.. The resulting oscillascope traces showed no phase shift relative to each other indicating no significant errors were caused in this way.

Photographs of the oscillascope traces were enlarged by a known amount onto a sheet of graph paper. Great care was taken in this and succeeding stages not to distort the waveform in any way. The graph paper was mounted on the table of a "Digitised decoder output serializer", a machine which could trace the waveforms and display the X - Y coordinates on a screen. By pressing a switch the coordinates V_t and i_t could be punched onto computer tape ready for subsequent processing. The multiplication and integration were carried out using the computer programme given in the appendix. 1.

4.4 Chemical Analysis.

4.4.1 Analysis of hydrazine.

At room temperature the only stable products formed by the action of a glow discharge on ammonia are nitrogen, hydrazine and ~~ammonia~~ hydrogen.

Hydrazine in the exit gas from the reactor was absorped in ethane diol and then analysed. The concentration of hydrazine in the ethane diol was only of the order of a few parts per million so a colourimetric method of analysis using p-dimethylaminobenzaldehyde was used. The analysis was carried out in the manner described by Watt and Chrisp[151]. A standard hydrazine solution was prepared using hydrazine sulphate, quantatively analysed by titration against standard potassium iodate with chloroform as indicator. The hydrazine solution was then carefully diluted to the concentration range required, 0.01 to 0.2 ppm, for the colourimetric analysis. A calibration curve of % absorption at 458 μ against p.p.m. hydrazine was plotted using these standard solutions in a Unicam SP500 spectrophotometer see fig.57 appendix. 3. The experimental solutions could then be determined against this curve.

The experimental ethanediol/hydrazine solutions from the absorption bottles were diluted with distilled water to a suitable

concentration and compared together with a blank and a standard solution against the calibration curve. The experimental solutions were made up as soon as possible after the experiment and the colour allowed to develop for 15 minutes before analysis. In experiments with low conversions to hydrazine the ethane diol was not diluted and it was found ammonia absorbed in the ethane diol caused the normal yellowish green colour formed to turn dark green. This upset the analysis and had to be eliminated. Bubbling nitrogen through the ethane diol solution removed the ammonia and analysis could then proceed normally.

Although analytical grade p-dimethylamino-benzaldehyde was used its appearance and colour developing properties varied slightly from batch to batch so new colour solutions were always recalibrated. Colour solutions and standard hydrazine solutions could be kept for a month without deterioration.

4.4.2 Analysis of ammonia.

Literature indicated the ammonia conversion could be estimated by bubbling the ammonia from the exit gas through acid and backtitrating any unneutralised acid. Attempts were made using this method with acidified ethylene glycol but results were not reproducible. Errors were probably caused by the difficulty in absorbing all the ammonia.

4.4.3 Analysis of Nitrogen and Hydrogen.

A Perkin Elmer gas chromatograph with a thermal conductivity detector was used to try to estimate the percentages of nitrogen and hydrogen in the product gas. A five foot type 4A molecular seive column operating at room temperature with Helium carrier gas was found to separate the nitrogen and hydrogen in prepared calibration gas samples containing ammonia, nitrogen and hydrogen. Exit gases from the reactor were collected in the gas sampling bottle, the bottle was then isolated, disconnected from the apparatus and attached by a short length of tube to the gas sampling valve of the chromatograph (fig. 10). With the valve in position A and all the stopcocks closed the line to the vacuum pump was evacuated to less than 1 torr, the valve was then turned to the "in" position B and a sample of residual gas injected into the column. The valve was then returned to its "out" position so the helium which filled the gas sampling loop now filled the other line as well. This process was repeated until no air could be detected in the residual gas and the line contained only helium at less than 1 torr. Stopcock T.10 was opened and the

gas from the bottle allowed to fill the gas sampling loop at a pressure given by gauge P. The gas was injected and the results recorded on a Kent recorder. Even though the detector was set at its maximum sensitivity only very small nitrogen peaks and no hydrogen peaks could be detected in product gases.

5.0 EXPERIMENTAL RESULTS.

5.1 Electrical characteristics of discharge.

5.1.1 Continuous d.c. operation.

A typical set of voltage current characteristics for the continuous d.c. discharge in ammonia at 10 torr pressure, with an interelectrode distance of 6.3 cm. and "aged" electrodes is shown in fig. 15. These characteristics changed slightly if very high gas velocities were used. The discharge was more difficult to strike at high gas flowrates and it could even be "blown out" by suddenly increasing the flow of gas. A high voltage of approximately 3kV was needed to initiate the discharge but once the discharge had been initiated the voltage fell because of the loading on the supply. A further reduction in voltage to less than one k.V. could be made and the discharge still maintained. If, however, the current was reduced to below about 15mA fluctuations in voltage and current occurred as the discharge became unstable. At lower currents insufficient electrons were released into the discharge for it to maintain itself and it was eventually extinguished. Currents much higher than 50mA were not used because the reactor became quite hot near the electrodes and there was a danger of the tube cracking.

5.1.2 Pulsed d.c. operation.

Similar effects to those described above for continuous d.c. operation were found in the pulsed d.c. system. At low power inputs the discharge became unstable, indicated by rapid fluctuations of the current waveform. With pulsing conditions of very short off times the discharge could be operated in the same way as the continuous d.c. discharge but as the off time was increased the discharge became progressively more difficult to strike and maintain. With pulse off times greater than 0.1 seconds the breakdown voltage could be applied for several minutes before breakdown actually occurred and once the discharge had been initiated the voltage could only be reduced very slightly, if at all, before the discharge became unstable and was extinguished.

Some typical oscilloscope photographs of the voltage and current waveforms are shown on page 96a to 96g. figs. 23-29.

It can be seen from these photographs that the voltage rises rapidly until breakdown occurrs. At breakdown the resistance of the gas suddenly decreases and the load on the

GRAPH OF DISCHARGE CHARACTERISTICS

fig 15.

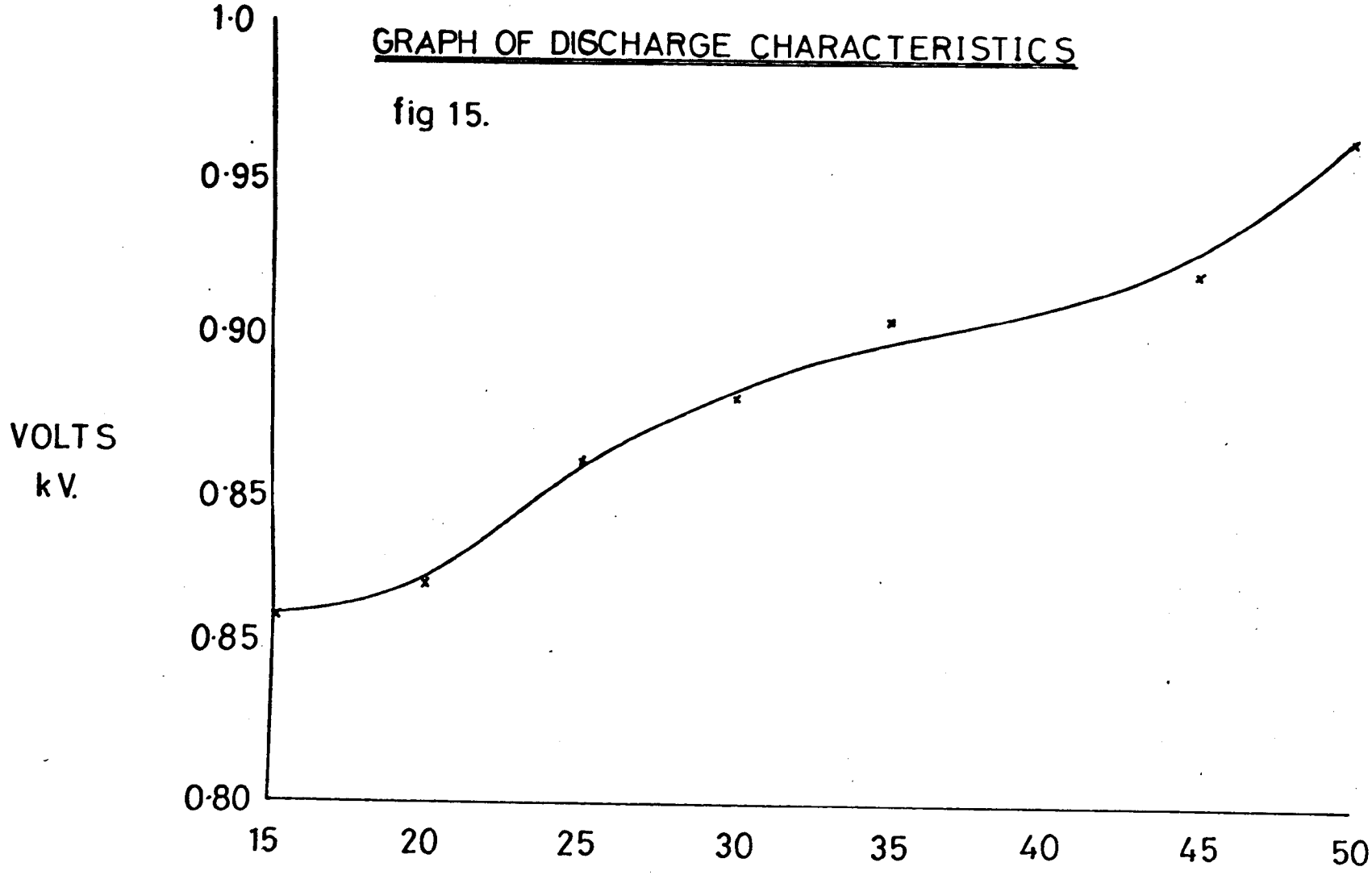

output valve is increased causing the voltage to drop slightly. After breakdown the current starts to build up tending to some equilibrium value dependent upon the applied voltage. When the valve is switched off by the triggering pulse the voltage falls again to a value at which the discharge cannot be sustained of its own accord and so is extinguished.

The residual voltage then decays slowly through resistors R6 and R8.

Errors in power measurement at long off times could be introduced if the prebreakdown current of the nonself sustaining discharge was high. This current was measured using a Rank general radiological D.C. amplifier and found to be extremely small at approximately 0.5×10^{-10} amps.

5.2 Synthesis of hydrazine in a continuous d.c. glow discharge.

5.2.1 Effect of flowrate on energy yield and conversion to hydrazine.

All results on hydrazine synthesis are for an operating pressure of 10 torr with "aged"

electrodes at an interelectrode distance of 6.3 cm. Conversions of ammonia to hydrazine are expressed as a weight percent

$$\text{Conversion} = \frac{\text{gms hydrazine formed X100}}{\text{gms of ammonia passed}} \%$$

The percentage molar decomposition of ammonia cannot be given since the full analysis of all products is not available.

The conversion of ammonia to hydrazine in terms of moles of hydrazine formed per mole of ammonia passed is

$$0.53 \text{ X wt } \% \text{ conversion}$$

Energy yields are expressed as

$$\text{Energy yield} = \frac{\text{gms of hydrazine formed}}{\text{killowatt hrs power input into reactor.}}$$

Energy yields do not include the power dissipated in the ballast resistor.

The continuous d.c. and pulsed d.c. systems are treated separately below but their relation to each other is reported in the discussion of results section.

Experiments were carried out at flowrates from 14 cc/sec to nearly 400 cc/sec, measured at operating conditions giving residence times in the reactor from over one second to about four hundreths of a second. The pumping capacity of the system prevented much higher flowrates being used.

The effects of flowrate or gas residence time on the energy yield of hydrazine is shown on fig. 16 and the effect on the conversion to hydrazine is shown on fig. 17. Data for these graphs is taken from series 1, 2, 8, 9, 16, 20 and 21 experiments. The range of gas residence times in these experiments covers the conditions where the maximum in conversion occurs.

5.2.2 Effect of power input on yield and conversion to hydrazine.

Experiments were carried out over a range of power densities (Π) from 0.63 to 4.3 watts/cc of reactor volume. Since the interelectrode distance was not changed the total power input was always 16Π. For each

flowrate when the log energy yield was plotted against the power density a linear correlation of the form.

$\log_e$ (Energy yield of hydrazine) = a - bπ

was obtained. The lines were fitted by the least squares method and the coefficient a and b together with the statistical variation are given in the data in appendix 2.

The conversion to hydrazine was found to increase with increasing power input reaching a maximum, which was dependent upon the operating conditions. Further increase in power decreased the conversion.

The variation of yield and conversion over a range of power densities is given in appendix .2 . and fig 44. and 45.

5.2.3 Effect of removing products through reactor wall.

Two sets of experiments were conducted with the product gases from the discharge being withdrawn through the porous glass wall in the body of the reactor. A flowrate of 389 cc/sec was used but it is difficult to give a meaningful residence time for the system. In the first set of experiments series 10, the gas entered the reactor through the cathode and into the negative glow region and in the second set series 11, the electrodes were reversed so the gas entered

through the anode into the positive column and out through the porous wall. The second arrangement with gas entering through the anode gave higher yields and conversions to hydrazine than with the gas entering through the cathode but the results were lower than those found with gas passing straight through both electrodes in the normal way. The results are given in the appendix under runs 10 and 11.

5.2.4 Influence of packing reactor on yield and conversion.

In order to investigate the effect of wall reactions on the formation and degradation of hydrazine the positive column area of the reactor was packed with glass wool. By weighing the wool and measuring the fibre diameter using a travelling microscope the surface area was found to be 1800 cm^2 but the volume of the reactor was reduced by less than 2% by the addition of the glass. Experiments were carried out at a constant flowrate of 45.7 cc/sec giving a gas residence time of 0.35 seconds. Series 18 and series 19 runs were with and without the packing respectively. The results are shown in fig. 55. and appendix. 2. Yields and conversions were found to increase by approximately 100% on adding the glass wool packing to the reactor.

fig 16. COMPARISON OF EFFECT OF PULSED AND D.C. CONDITIONS ON YIELD.

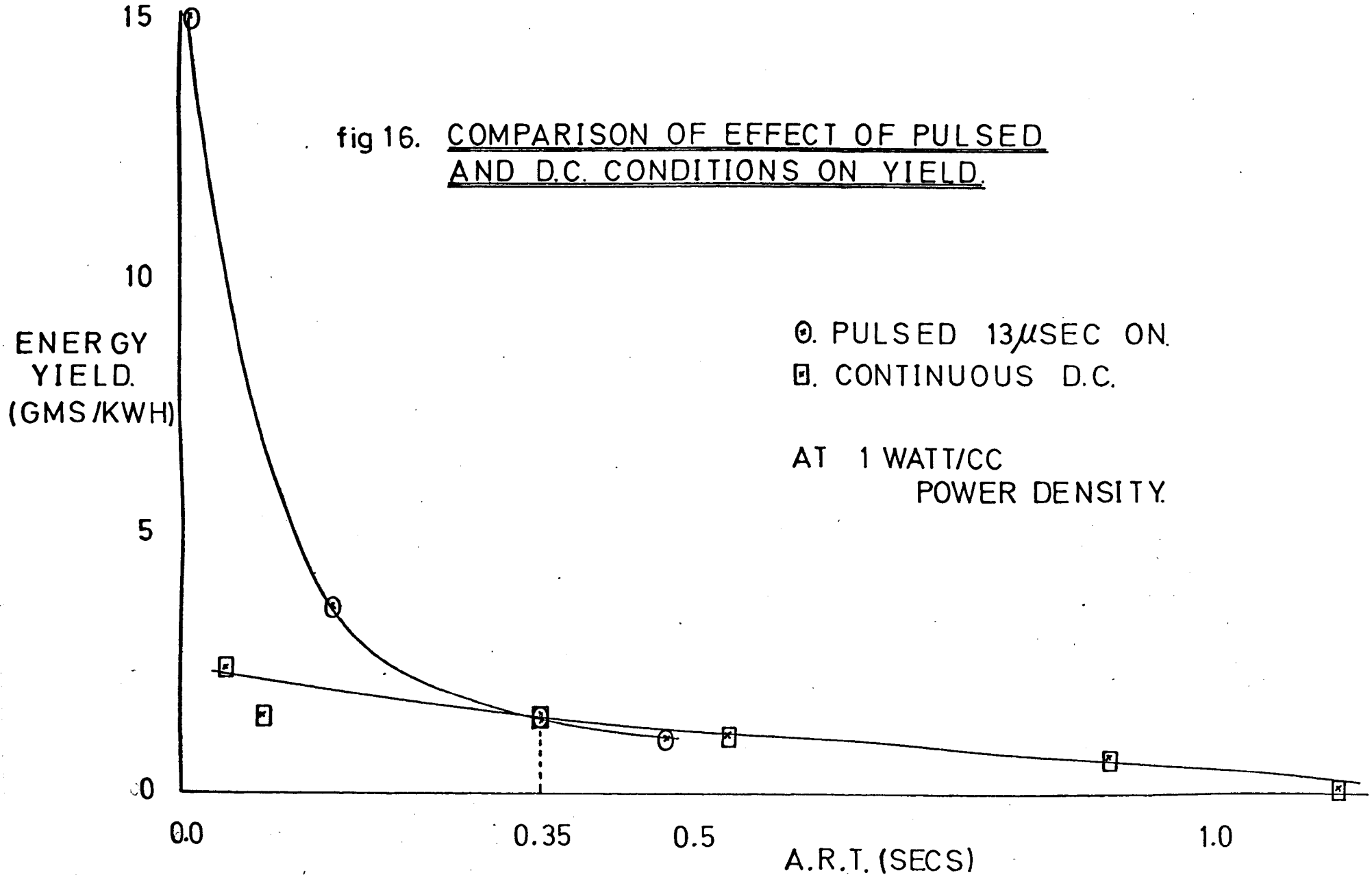

fig 17. COMPARISON OF EFFECT OF PULSED AND D.C. CONDITIONS ON CONVERSION.

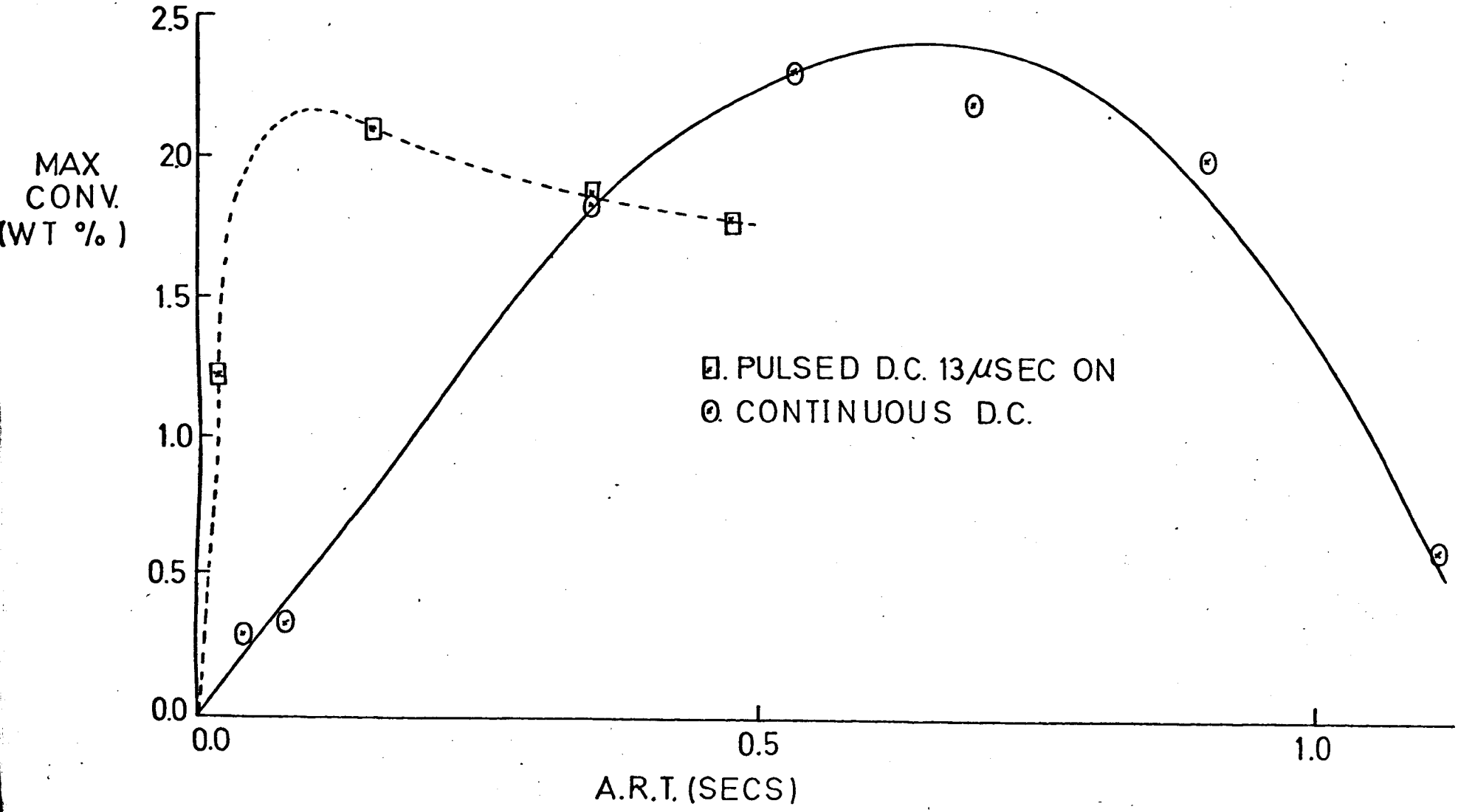

5.2.5 Change in yield and conversion on adding helium to the discharge.

Helium was added to the ammonia in the discharge to try and increase the mean electron energies and hence increase the yield. Experiments were performed with no helium, approximately 15% and 50% helium in the reactant gas. The energy yield and conversion were found to decrease with the addition of helium to the discharge. Results are tabulated in appendix.2.

5.2.6 Conversion of ammonia to nitrogen and hydrogen.

Analyses of nitrogen and hydrogen were made at the position of maximum conversion but no hydrogen peaks could be detected. The nitrogen peaks found were very small corresponding to less than 1% of the product gas. The chromatograph was not sensitive to such low concentrations and the figures given above can only be considered to give a general guide.

No changes in gas pressure or temperature could be detected in the course of the experiments even through the reactor walls became hot near the electrodes at high power input levels.

5.3 Synthesis of hydrazine in a pulsed d.c. discharge.

5.3.1 Effect of flowrate on yield and conversion to hydrazine.

Preliminary experiments were conducted at

flowrates of 1.8, 14.3 and 30.4 cc/sec with a pulse on time of 13μsec and a pulse off time of 100μsec. The energy yield was found to increase with increasing flowrate but the conversion to hydrazine reached a maximum at approximately 14.3 cc/sec so this flowrate was chosen for the other work on the pulsed d.c. system. The effects of flowrate on yield and conversion are shown in fig. 18. Data for the graphs is taken from series 2, 4 and 5 experiments.

5.3.2 Influence of pulsing conditions on yield and conversion to hydrazine.

Most of the work presented in this thesis is concerned with the effects of pulse on time and pulse off time on the yield and conversion to hydrazine. Pulse on times were varied from 5μsec to 220μsec and pulse off times from 18μsec to 1.12 seconds. Apart from the experiments described in (5.3.1) above the flowrate was always 14.3 cc/sec giving a gas residence time of 1.12 seconds. The active residence time ranged from 13μsec to 0.47 seconds.

To give a clearer picture of the complex relationship between yield, conversion, power input, pulse on time and pulse off time some three dimensional models were built. A photograph of the model showing the effect of power density and pulse OFF time on the conversion for a constant on time is given in fig. 19.

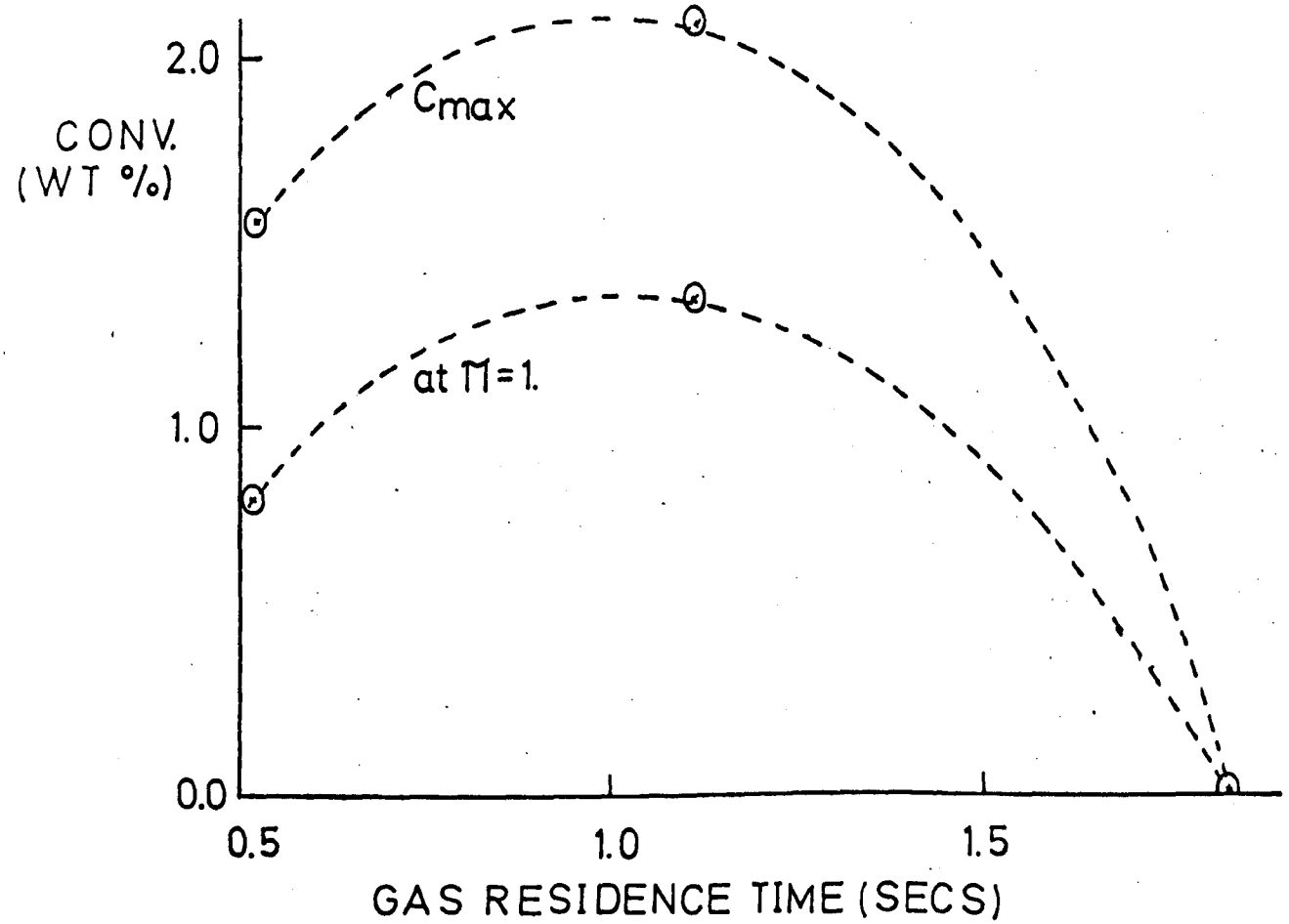

fig 18. EFFECT OF FLOW ON YIELD AND CONVERSION UNDER PULSING CONDITIONS. [13μON::100μOFF]

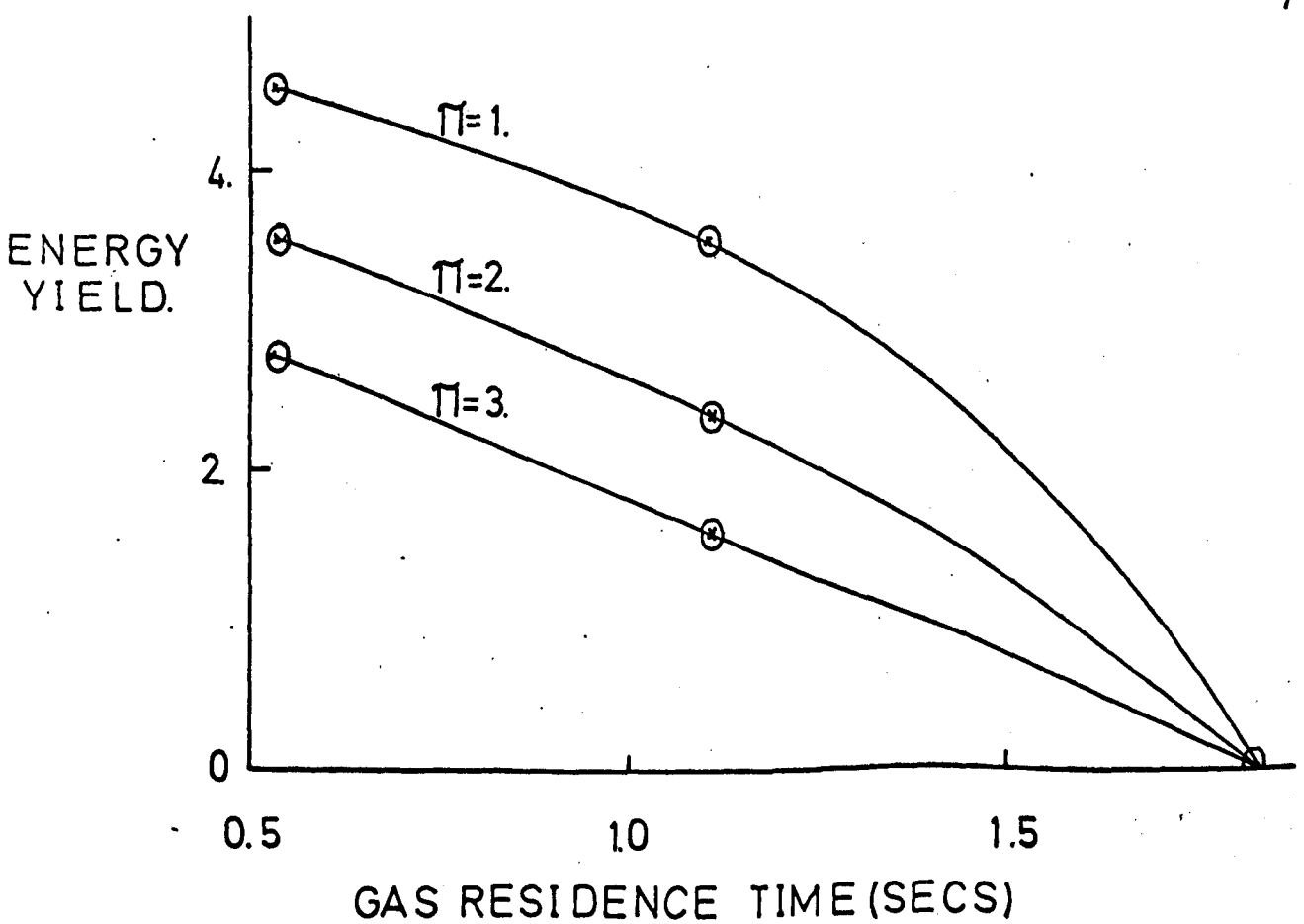

fig. 19.

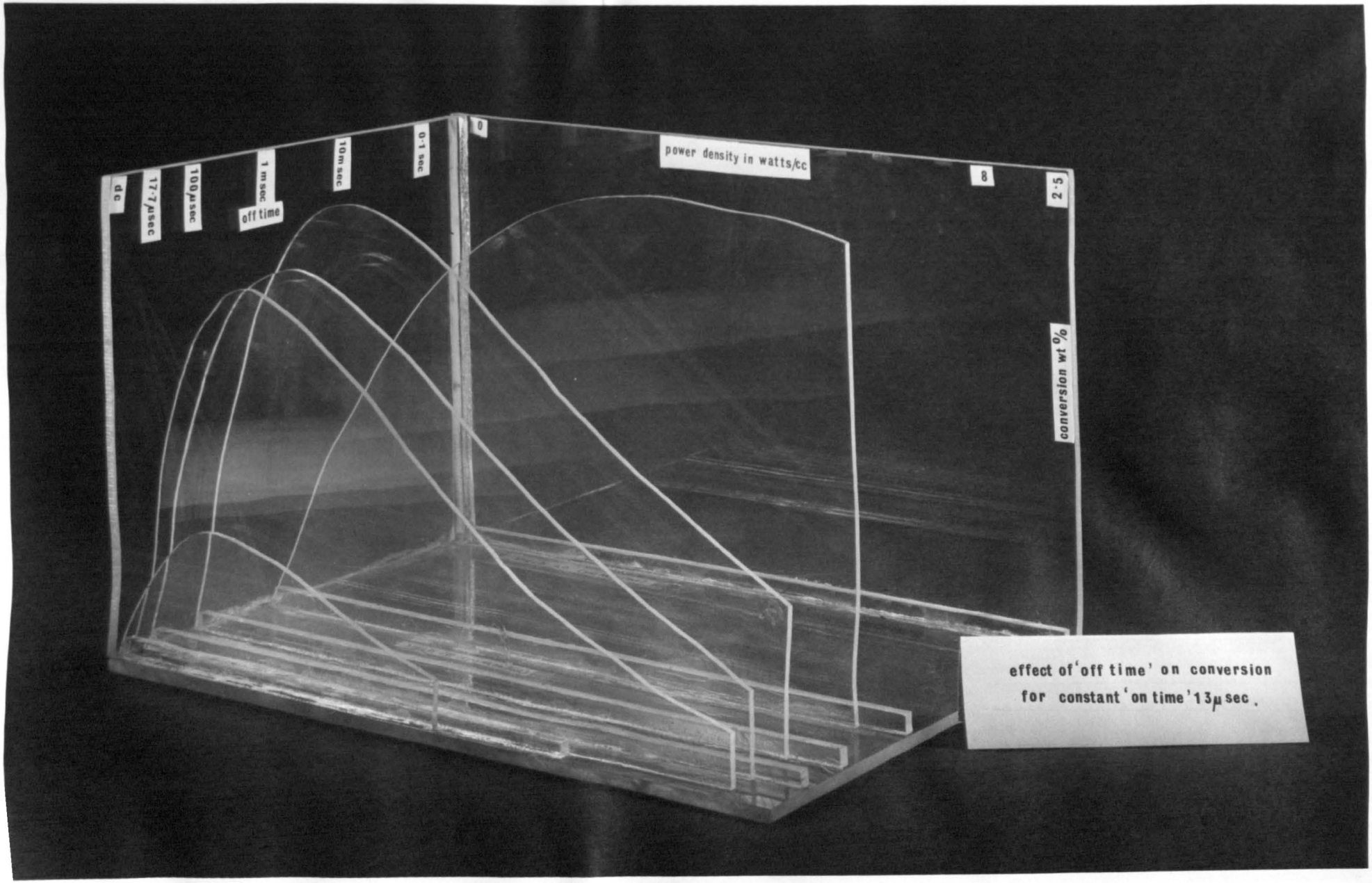

effect of 'off time' on conversion for constant 'on time' 13 μsec.

fig. 19.

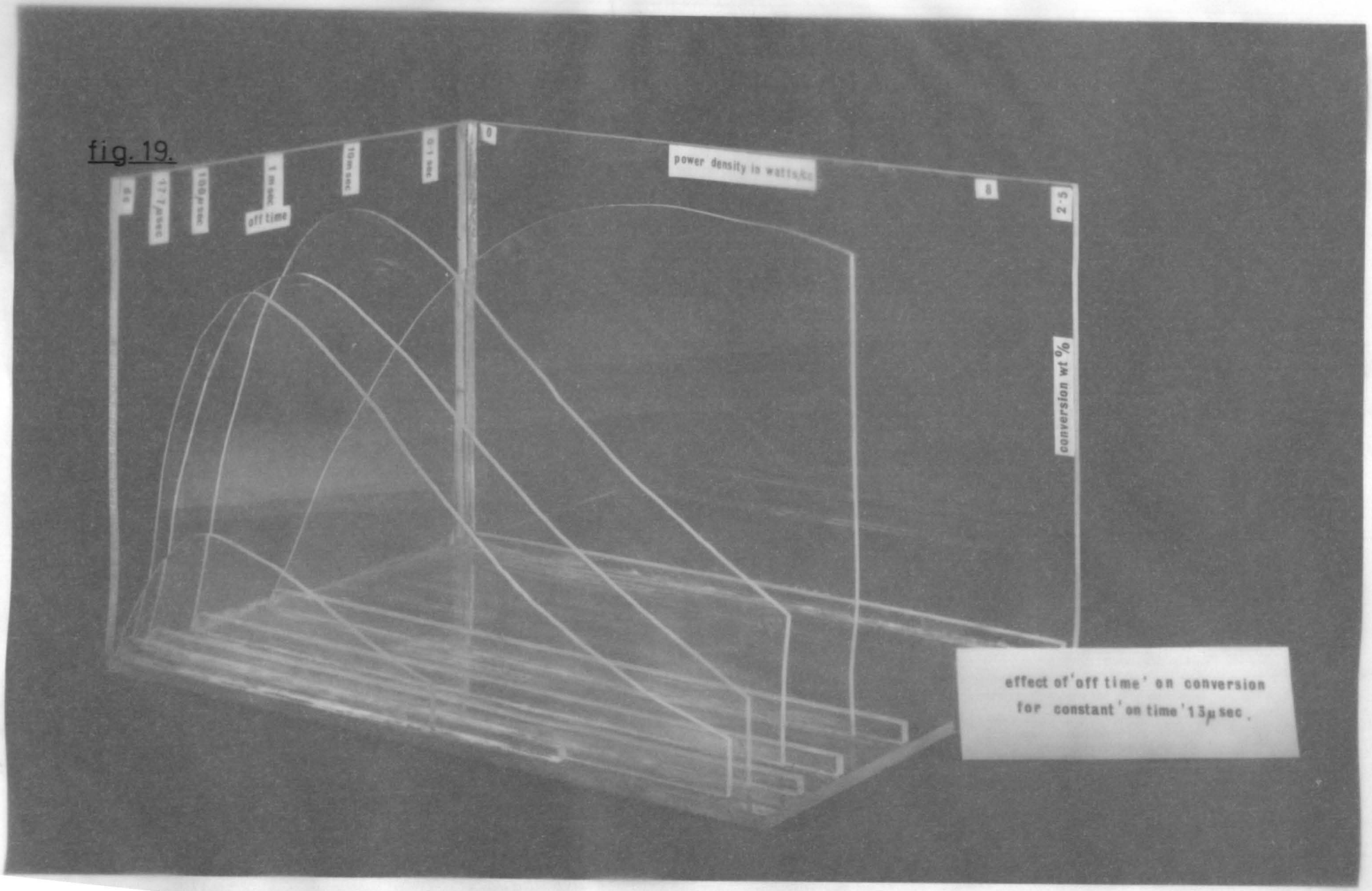
power density in watts/cc
0
8
2·5
conversion wt %
off time
1 msec
10m sec
0·1 sec
effect of 'off time' on conversion
for constant 'on time' 13μ sec.

fig. 20.

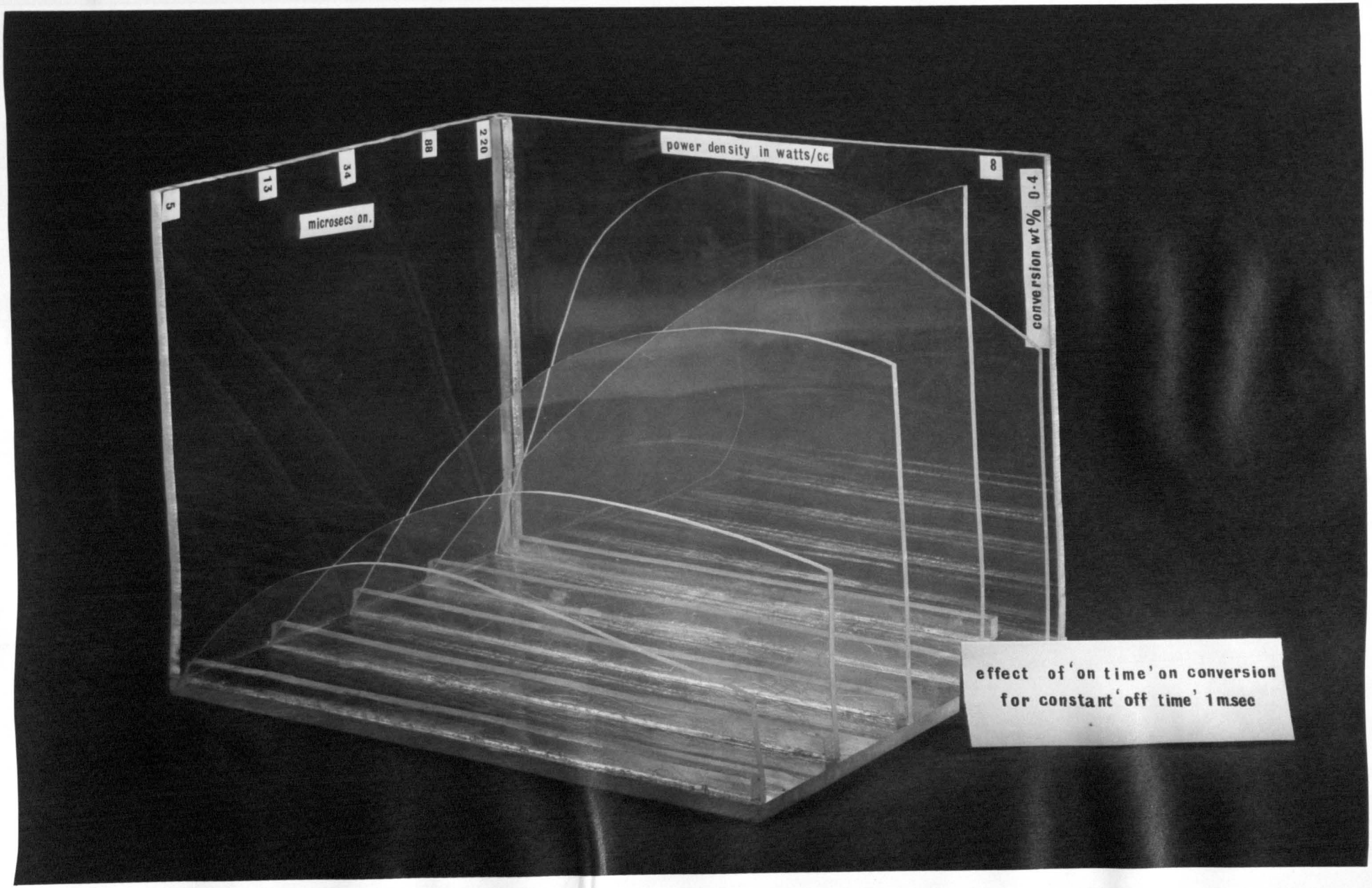
5
13
34
88
220
microsecs on.
power density in watts/cc
8
conversion wt% 0·4
effect of 'on time' on conversion
for constant 'off time' 1msec

fig. 20.

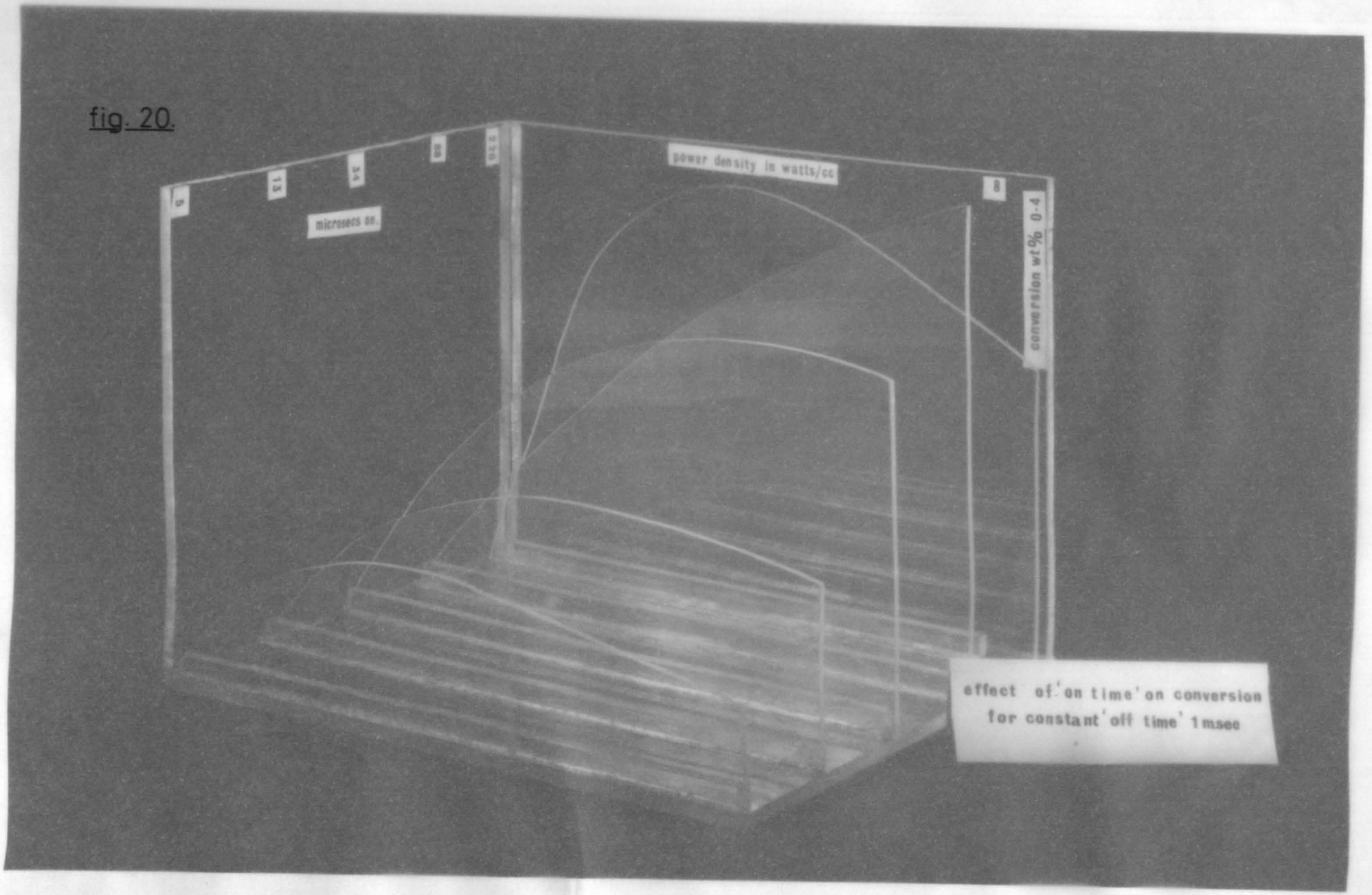
5
13
25
80
320
microsecs on.
power density in watts/cc
8
conversion wt% 0-4
effect of 'on time' on conversion
for constant 'off time' 1msec

fig 21. GRAPH SHOWING EFFECT OF ON & OFF TIMES ON YIELD.

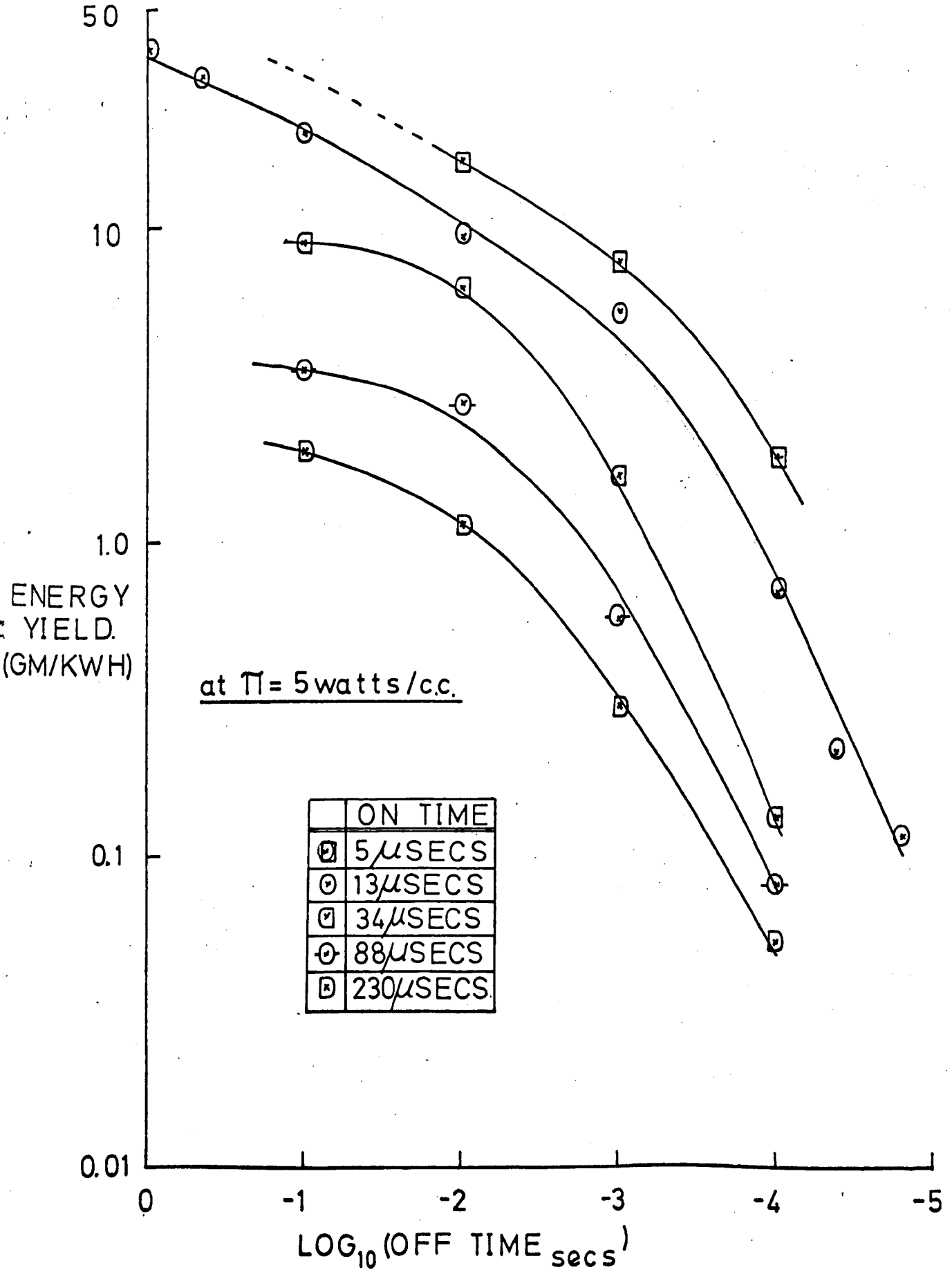

fig 22. EFFECT OF ON AND OFF TIMES ON MAXIMUM CONVERSION

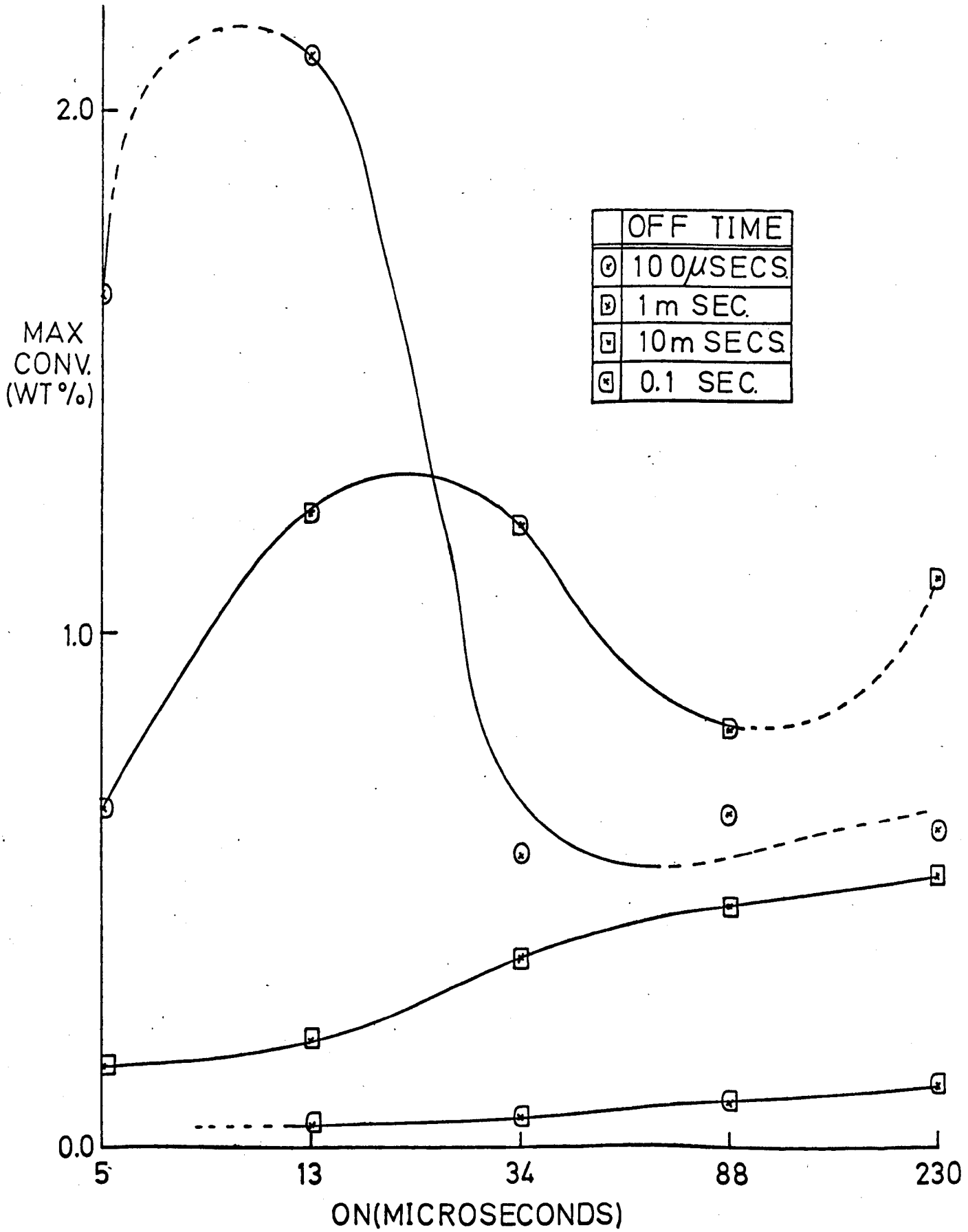

A similar photograph of the model showing the effect of pulse ON time at constant off time is given in fig. 20. The effect of pulse on time and pulse off time on the energy yield for a constant power density is given in fig. 21 and the effect on maximum conversion to hydrazine is given in fig. 22. It can be seen high yields are favoured by short pulse on time and long pulse off times but the conversion to hydrazine passes through a maximum with increasing on time but the position and value of this maximum depends upon the off time.

A full set of graphical results is given in the appendix, data is taken from series 4, 7, 12 - 17, 22 - 38.

5.3.3 Influence of packing reactor on yield and conversion to hydrazine.

The reactor was packed in the same way as described in 5.2.4. Pulse conditions were set at a pulse on time of 13μ sec and a pulse off time of 28.6μ sec giving an active residence time of 0.35 seconds, the same as with the continuous d.c. system. Experiments were carried out with and without packing, series 19 and 15 respectively. The yield and conversion were found not to change on packing the reactor.

This contrasts with the continuous d.c. system where a 100% increase was found on packing the reactor with glass wool. Results are shown in fig. 55.

5.3.4 Effect of power input on yield and conversion to hydrazine.

As with the continuous d.c. system the yield was found to increase with decreasing power, results being correlated by the relation

$$\log_e \text{Energy yield} = a - b\tau$$

Conversion to hydrazine passed through a maximum with respect to power.

Again in common with the continuous d.c. system no changes in temperature or pressure occurred in the course of the experiments and no nitrogen or hydrogen peaks could be detected by chromatography at the position of maximum conversion.

6.0 DISCUSSION OF RESULTS.

6.1 Electrical characteristics of discharge.

6.1.1 Continuous direct current discharge.

The range of currents used in this work was limited to 15-50 mA for reasons given in section 5. This is a much higher range than that of 0.6 to 2 mA used by Devins and Burton and Rathsack but it must be remembered that their experiments were conducted at a pressure of only 3 mm. Hg. where it is possible to maintain these currents. At a pressure of 8 mm. Hg. and a gap distance of 8.3 cm. Westhaver found he could operate in the range of 10-50mA and Skorokhodov et al operated in the range 50-250 mA for pressures between 5 and 10 mm mercury. This indicates that the currents used in this work are what we would expect for the pressure range considered.

In order to strike a discharge a high voltage is necessary and once the gas is ionised this high voltage will cause very high currents to flow. If this current is allowed to build up and continue a glow to arc transition will occur and it will be impossible to maintain the glow discharge. To prevent this occurring a ballast resistance is added to the circuit (fig. 12a), this prevents the current build up and stabilises the

discharge in the glow region. The value of 17 kil ohm used in this work was found by trial and error to give a reasonable range of operating currents, however the addition of a high resistance ballast resistor has certain disadvantageous effects in that the power it dissipates is lost as heat and represents an overall loss in efficiency of the process. At 15 mA, 3.8 watts are dissipated in the resistor representing over 20% of the total power and at 50 mA, 42.5 watts are dissipated or nearly 45% of the total power. This clearly shows that using low currents will increase the overall efficiency of the discharge circuit. One possible method of over coming the loss in efficiency due to the ballast resistors is to use other gas discharges in the circuit to provide the necessary resistance. The resistance of the discharge is nearly 60 kohm at 15 mA and about 22 kohm at 50 mA so by putting three discharges operating at 15 mA in parallel with each other and in series with a discharge taking 45 mA current, as shown below we could theoretically get a stable situation.

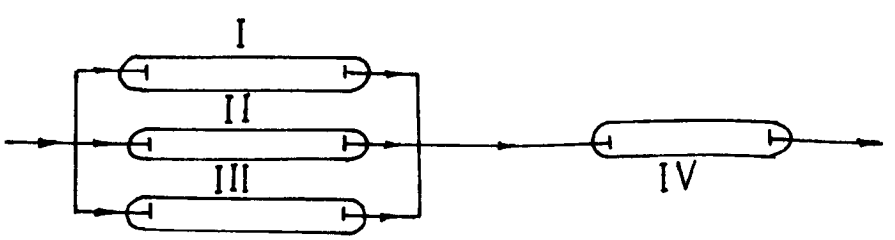

Here each reactor experiences a 20 kohm ballast effect but reactor IV is operating at a current fo 45 mA which it has been shown leads to low energy yields. One method of over coming this is to use two lots of three reactors in parallel as shown below.

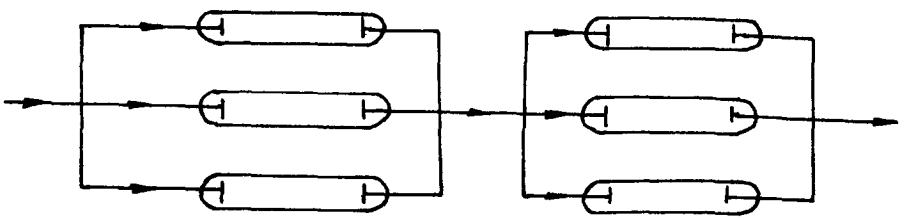

This would in theory eliminate the loss in overall efficiency caused by the ballast resistor but the practical difficulties of switching in each reactor in turn and maintaining an absolutely balanced system would make the method extremely difficult in practice. A more direct control can be made using a feedback system to control the input voltage as shown below.

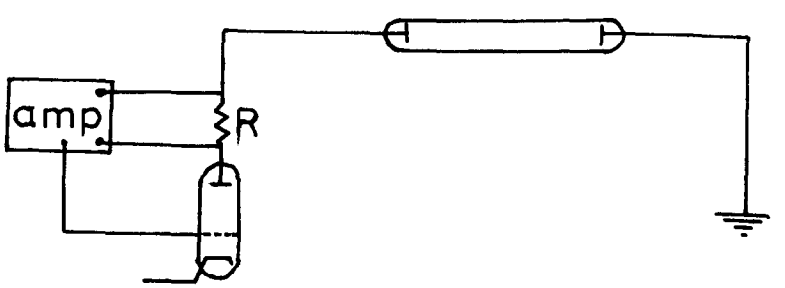

The small voltage generated across the low resistance is amplified and fed to the grid of the output pentode, so controlling the d.c. supply voltage. The power loss in such a

system should be less than 1%. Since the power losses suffered in the ballast resistor can be substantially reduced it seems unreasonable to include them in overall estimates of the efficiency and energy yields. For this reason all efficiencies and energy yields given in the results are based on thepower dissipated only in the reactor.

Voltage Current Characteristics.

The voltage current characteristics curve shows (fig.15) that an increase in current must be accompanied by a small increase in voltage. Voltage current characteristics measured by other workers seem to vary, Rathsack found the voltage descreased with current whereas Devins and Burton operating under the same conditions of gap width, pressure current and tube diameter found that the voltage increased with current.. The reason for the increase or decrease in voltage with current is that at low currents and low current densities only a small part of the gas in the tube is conducting, ions diffuse out of this region and are neutralized. As the current builds up the voltage falls and then levels off, at this level stage any increase in current is met by an increase in the area of ionized gas for the current to flow

through, so that the current density remains constant. The current can be increased until the whole of the discharge space is fully conducting and then any further increase in current must be accompanied by an increase in the current density, the current density can only be increased by an increase in the voltage so the voltage starts to increase with current. The reactor used in this work exhibits this relationship, therefore one can imply that in this work the whole of the reactor volume was filled with conducting gas. Any gas entering the reactor therefore would have to pass through the discharge so no by-passing could take place and this must help to increase the conversion per pass. It has been suggested that the work or voltage increase required to maintain the increased current density may be responsible for the fall in energy yield of hydrazine found with increasing power density. Although this may be true to some extent an analysis of the results shows it is of minor importance. If we increase the current from about 15 mA to 50 mA the voltage increases from about 0.86 k volts to 1.01 k volts, an increase of some 17%. The power density has increased from about 0.8 watts/cc to 3.2 watts/cc

and taking the results from series 3 experiments we find the energy yield drops about 75% over this range. The fall in energy yield under other continuous direct current conditions is even greater. Hence, we see that an increase in voltage of about 17% corresponds to a decrease in energy yield of about 75% therefore the increase in voltage required to maintain the higher current density cannot be totally responsible for the drop in energy yield. Other factors of course come into play, the current increases with increasing power density and this will in turn alter the amount of primary reaction occurring. The effects of this and other reactions are discussed in more detail when considering the kinetics of the reactions.

In the course of an experiment it was found that the reactor near the electrodes became quite hot and so the thermionic emission from the electrodes must have increased during the experiment. However the voltage needed to maintain a given current changed only slightly suggesting that thermionically emitted electrons play only a small part in maintaining the discharge. These results are confirmed by Rathsack who also showed that the electrode temperature has no effect on the energy yield of hydrazine.

The voltage required to strike the discharge was about 3kv which is roughly what one would expect from Paschens Law with a De value of 63 mm Hg cm. Once the gas had been broken down the voltage could be reduced to less than 1kv and the discharge still maintained. Paschens Law states the voltage needed to break down the gas $V_B = f(De)\rho$ where ρ is the pressure and De the interelectrode distance. This function is of the form shown below.

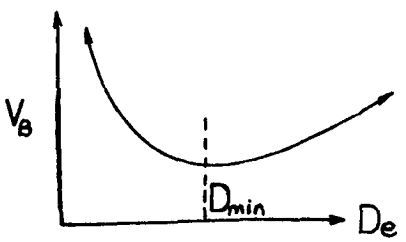

Once the gas is broken down a positive space charge is built up by the positive ions in the gas and this acts as an 'effective anode' nearer the cathode at a distance, say D'e hence the required voltage falls to $V'_B = f(D'e)\rho$
As the current grows, the effective distance falls to D_{min}, any further reduction in D'e would now require an increase in V'_B so once this minimum is reached the discharge becomes stable and can be operated at the lower voltage.

Using the method of calculating breakdown potential given by von Engel (p.195) we get

$$V_B = \frac{Bx\ (\ De)}{C + In\ \ (\ De)}$$

where $C = In \left(\frac{A}{in\ \ (1+1/\gamma} \right)$

Where A and B are constants ν is the number of ions.

Since A, B and are not known exactly they are estimated from fig.45p97 and table 71 as A=15 B=350 and $\nu = 1.5 \times 10^{-2}$ De = 63.0

Substituting in the equations above we get

V_B = 3.14 kv.

6.1.2 Pulsed d.c. discharge.

Pulsed discharges with discharge durations of from 5 micro seconds to 220 micro seconds were investigated. These are very short times and the current build up and decay form a significant part of the total discharge time. Since the discharge is largely in a non-equilibrium state any voltage current characteristics will depend on the time from initiation of discharge as well as the power input, pulse duration, pulse repetition rate, pressure, interelectrode distance and gas flow rate. The breakdown of the gas was also found to depend on some of the above conditions. In general it was easier to strike the discharge under conditions of low pressure, low gas velocity, long pulse duration and a fast repetition rate also once the discharge had been struck it could often be maintained at a lower voltage than the striking voltage. One exception to this was

with long pulse off times from about 10 millisec upwards, here if the voltage was reduced the discharge became unstable or stopped. Similarly it was found that it was easier to break down the gas if the pulse off times were short. Possible reasons for these effects can be found by considering the break down of the gas and the formation of the discharge in more detail. As described previously the breakdown time is a function of the statistical and formative time lags. The statistical time lag for a gas volume of 16 cc should be less than 5 millisecs[40] therefore for a pulse duration of 13 μ sec with an off time of 0.1 seconds and a voltage greater than the breakdown voltage applied for

$\frac{(5 \times 10^{-3}) \times (0.1)}{13 \times 10^{-6}}$ = 40 seconds, the gas should breakdown because the sum total of the 13 μ second pulses is greater than 5 milliseconds. It was found in practice that often under these conditions the voltage had to be applied for up to 3 minutes before breakdown would occur. What may have been happening is that although electron avalanches were occurring they didn't have sufficient time to build up to a level where a self maintained discharge could exist. With shorter off times ions formed

in the previous pulse would not have had time to decay away completely so they would help in the breakdown under the action of the next discharge pulse. The calculations of the rate of diffusion of positive ions given below cannot be considered to be very accurate but they do give an estimate of the orders of magnitude which are adequate for the discussion.

At a reduced field strength of about 10 volts /cm/mm Hg in the positive column the drift velocity of the electrons in ammonia is approximately 5×10^6 cm/sec[61] with a current of about 20 mA the number of electrons per centimeter of discharge tube length would be

$$\frac{20 \times 10^{16}}{1.6 \times 5 \times 10^6} \text{ electrons /cm of tube.}$$

and for the 1.8 cm diameter tube this is equivalent to 10^{10} electrons/cc. For lower currents of about 1 mA in a decaying pulse this value falls to approximately 3×10^9 electrons/cc. At electron densities greater than about 10^9 electrons/cc ambipolar diffusion occurs[12] and for a long tube of radius r the average lifetime (τ) of the diffusing species is given by[59]

$\tau = \frac{1}{Da} \frac{(r)^2}{(2.4)^2}$ where Da is the ambipolar diffusion coefficient. Data for the diffusion coefficient for ammonia is not avilable but the coefficient is mainly dependent upon pressure and molecular weight so that for Neon (MW20) has been taken[40] at 10 mm Hg as 700 cm^2/sec. Therefore for the reactor used in this work

$$\tau = \frac{1}{700} \left(\frac{0.9}{2.4} \right)^2 = 200 \mu \text{ sec}$$

The ion concentration decays exponentially so 1 millisecond after the pulse has 'stopped' 10^8 ions/cc will be present, at the longer off times of 10 m sec - 0.1sec the ions will have decayed away. Discharge breakdown depends upon the acceleration of electrons and positive ions to produce more ions and electrons and so form a self maintaining discharge. This is far easier if there is aconcentration of electrons and ions already in the reactor. The above calculation shows ions remain in the reactor for off times less than 10 m sec and this may account for the ease with which the discharge could be maintained at low off times. Since the completion of this work Brown and Howarth[21] have shown the peak pulse voltage increases with increasing pulse off time reaching a maximum at approx. 10 m sec. The

position of the maximum occurs at longer off times with higher currents in agreement with the above theory.

The formative time lag was thought to be the time for a positive ion to travel from one electrode to the other. This can be calculated assuming 3 kv prebreakdown voltage with an interelectrode distance of 6.3 cm. Using Newtons laws of motion we get the acceleration F

$$F = \frac{Ee}{M}$$

where E is the field strength e the charge on the positive ion and M the mass of the ion

$$\therefore \quad F = \frac{3000}{6.3} \times \frac{1.6 \times 10^{-19}}{17} \times 6 \times 10^{23}$$

$$\text{volt } \frac{\text{coulomb}}{\text{cm gm}}$$

$$= 2.7 \times 10^{13} \text{ cm/sec}^2$$

$\therefore$ assuming an initial velocity of zero the transit time t_f

$$t_f = \left(\frac{2 \times 6.3}{2.7 \times 10^{13}}\right)^{\frac{1}{2}} \text{ secs.}$$

$$= \underline{0.68 \mu\text{sec}}$$

From the discharge pulse photographs it can be seen that the formative time lag must be much less than this. If however the applied voltage

is only one or two percent higher than that required for breakdown the formative time lag is reduced by about 75% or in this case to 0.17 μ sec.

It was found with discharges of short pulse duration times that the discharge did not appear to fill the whole discharge volume but only the area around the axis of the tube. One reason for this is that the electrons spread in a lateral direction at a finite speed which is well below their random velocities. Very little data is available on lateral spreading of electrons in the positive column but an extrapolation of available data[40] indicates the time taken for electrons to spread to the side of the tube would be about 1 μ sec.

The photographs shown in the thesis show the effect of power density, the effect of on time at constant off time and the effect of off time at constant on time. The power density does not alter the shape of the voltage and current wave forms but does alter the steady state values of current and voltage. This must mean that the rate of ionization and the equilibrium electron concentration are both proportional to the power supply. Figs. 23 and 24.

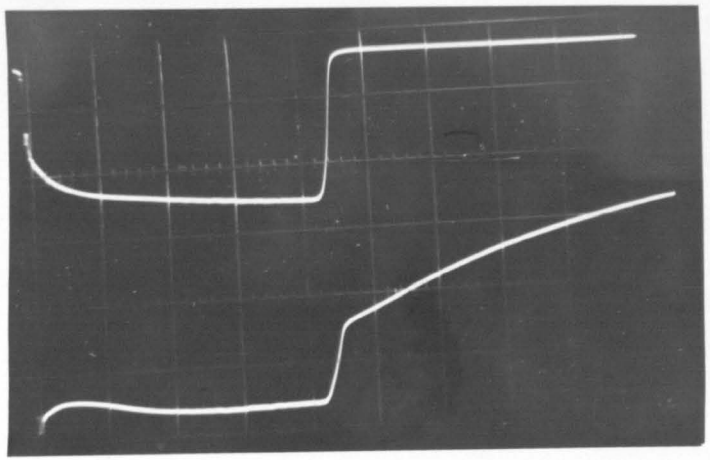

RUN 21.

ON TIME =	88 μ	SEC
OFF TIME =	1·0m	SEC
CURRENT =	5·0	VOLTS/CM
VOLTAGE =	1·0	VOLTS/CM
π =	9·47	WATTS/CC

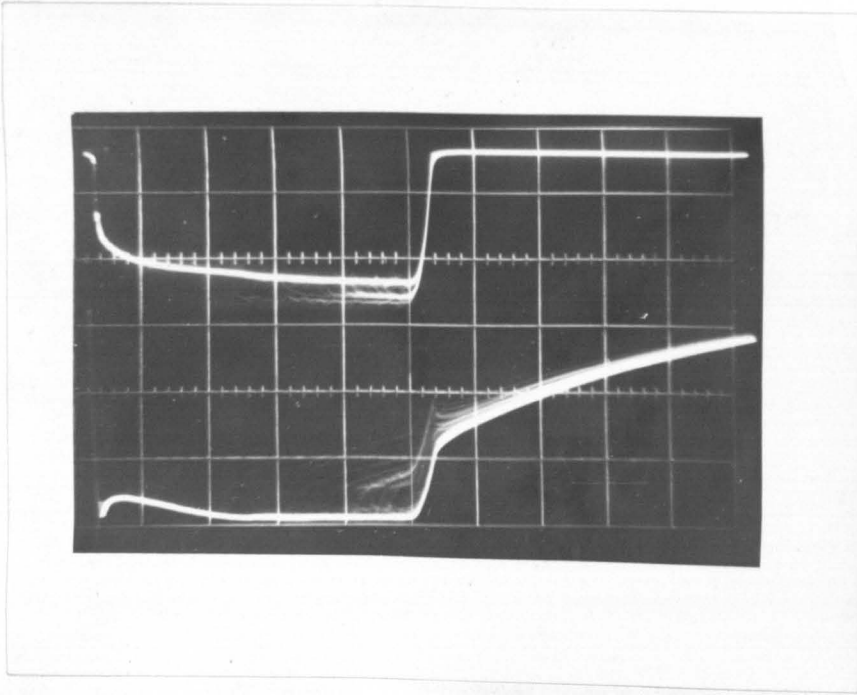

RUN 18.

ON TIME =	88 μ	SEC
OFF TIME =	1·0m	SEC
CURRENT =	5·0	VOLTS/CM
VOLTAGE =	1·0	VOLTS/CM
π =	4·65	WATTS/CC.

fig 23.

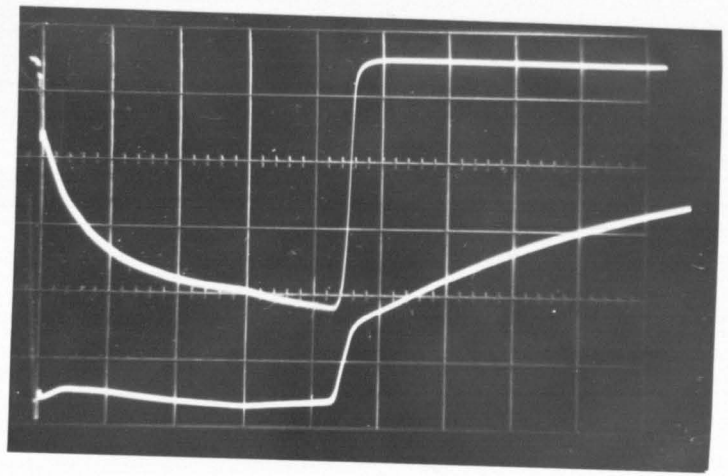

RUN 22.

ON TIME =	88 μ	SEC
OFF TIME =	1·0m	SEC
CURRENT =	2·0	VOLTS/CM
VOLTAGE =	1·0	VOLTS/CM
π =	5·88	WATTS/CC

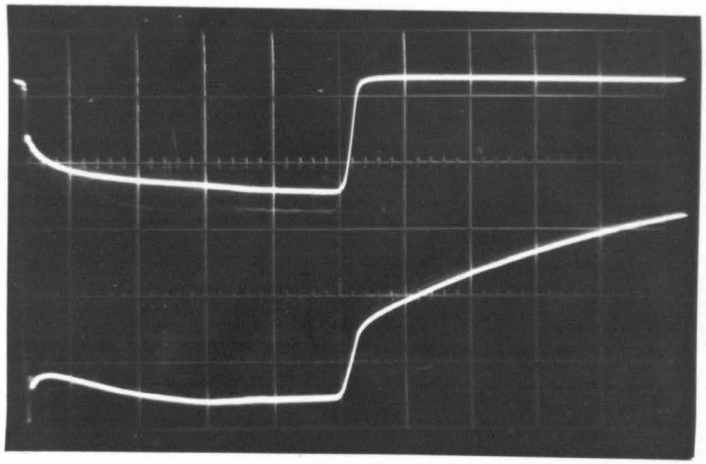

RUN 19.

ON TIME =	88 μ	SEC
OFF TIME =	1·0m	SEC
CURRENT =	5·0	VOLTS/CM
VOLTAGE =	1·0	VOLTS/CM
π =	6·66	WATTS/CC.

fig 24.

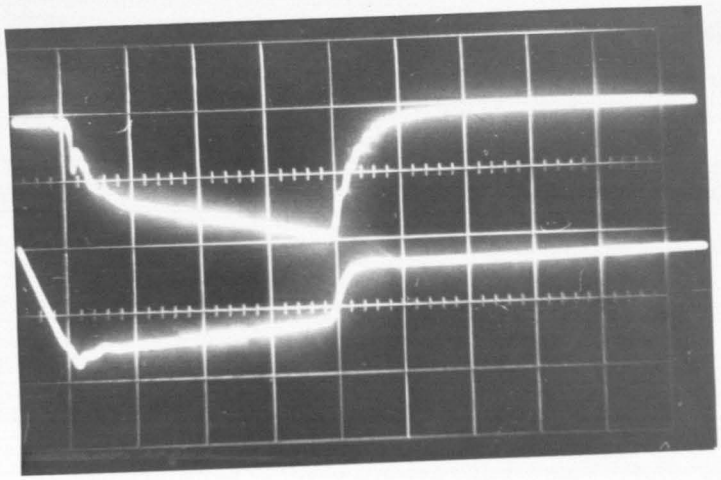

RUN 70.

ON TIME = 5·0 μ SEC.

OFF TIME = 10·0m SEC.

CURRENT = 5·0 VOLTS/CM

VOLTAGE = 2·0 VOLTS/CM.

π = 5·27 WATTS/CC.

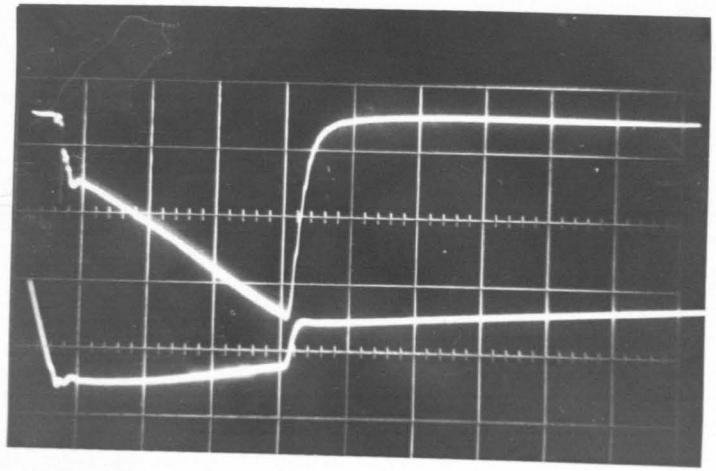

RUN 72.

ON TIME = 13·0 μ SEC.

OFF TIME = 10·0 m SEC.

CURRENT = 2·0 VOLTS/CM.

VOLTAGE = 2·0 VOLTS/CM.

π = 3·21 WATTS/CC.

fig 25.

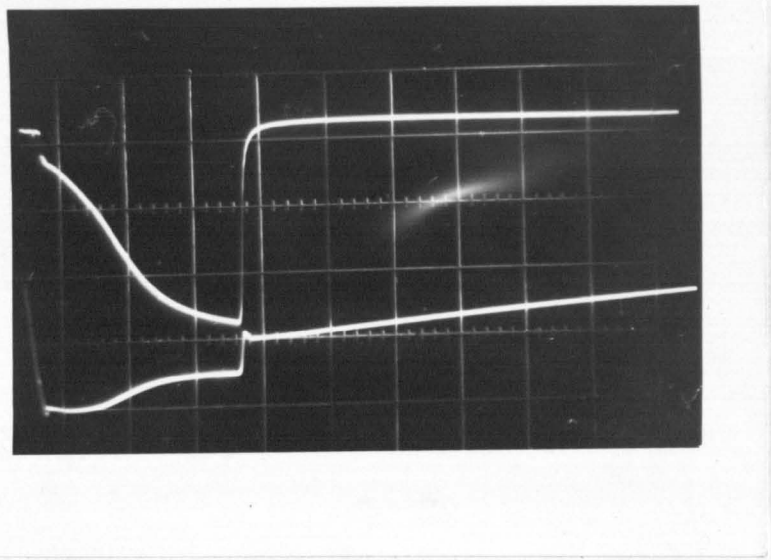

RUN 79.

ON TIME =	33 μ	SEC.
OFF TIME =	10·0m	SEC.
CURRENT =	2·0	VOLTS/CM.
VOLTAGE =	2·0	VOLTS/CM.
π =	3·98	WATTS/CC.

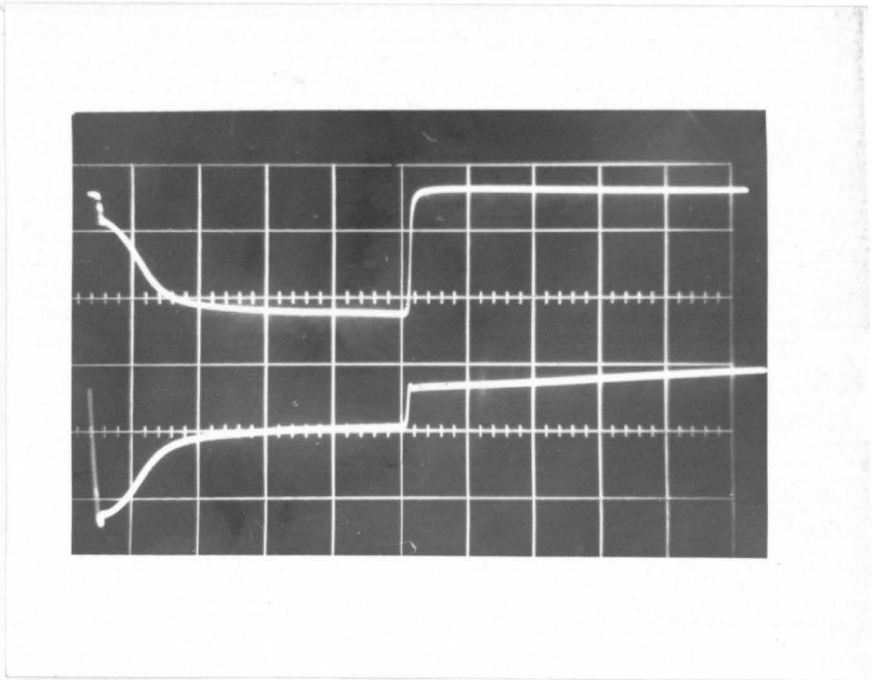

RUN 86

ON TIME =	88 μ	SEC.
OFF TIME =	10·0m	SEC.
CURRENT =	5·0	VOLTS/CM.
VOLTAGE =	1·0	VOLTS/CM.
π =	4·87	WATTS/CC.

fig 26.

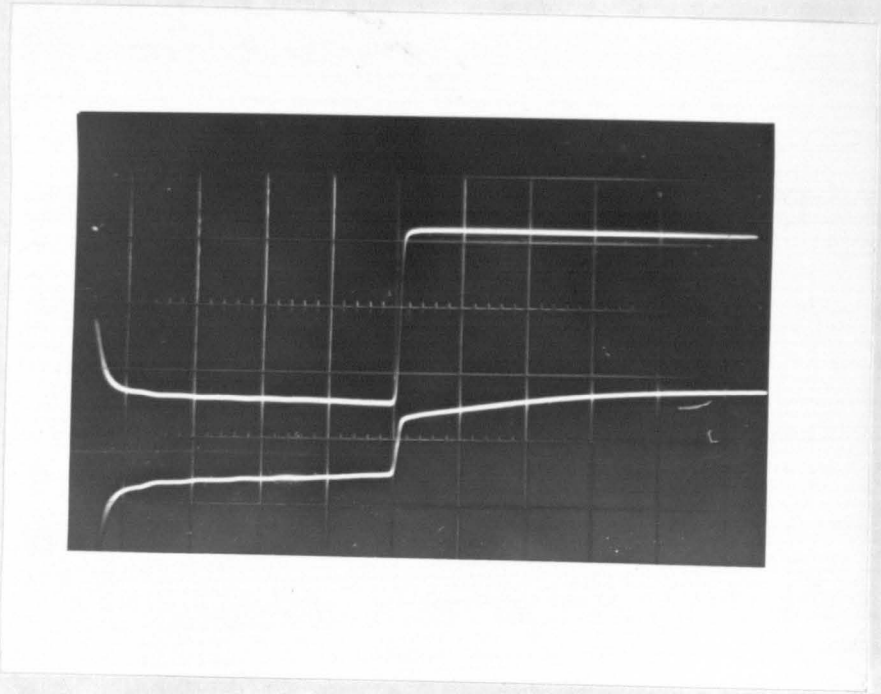

RUN 95.

ON TIME	= 227μ	SEC
OFF TIME	= 10·0m	SEC
CURRENT	= 5·0	VOLTS/CM
VOLTAGE	= 2·0	VOLTS/CM
π	= 11·0	WATTS/CC

fig 27.

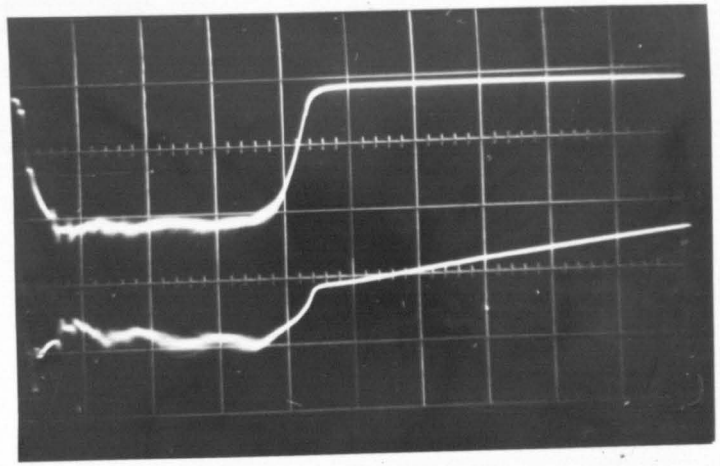

RUN 56

ON TIME	= 34	μ SEC
OFF TIME	= 100	μ SEC
CURRENT	= 5·0	VOLTS/CM
VOLTAGE	= 1·0	VOLTS/CM
π	= 6·43	WATTS/CC

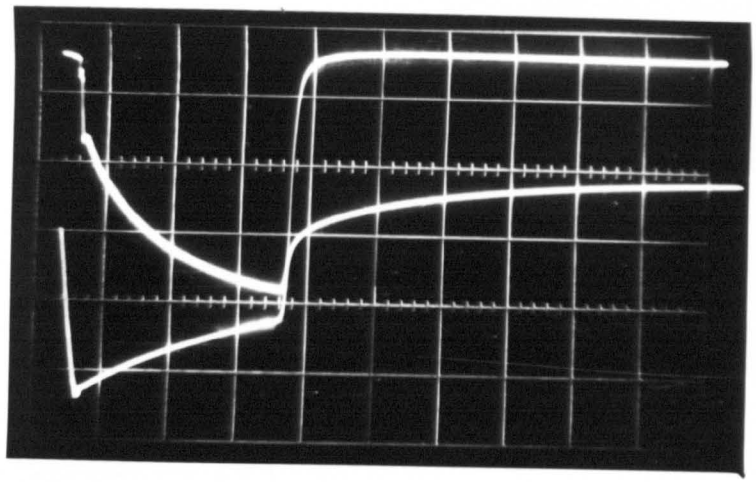

RUN 17

ON TIME =	34	μ SEC
OFF TIME =	1·0m	SEC
CURRENT =	2·0	VOLTS/CM
VOLTAGE =	2·0	VOLTS/CM
π =	5·4	WATTS/CC.

fig 28.

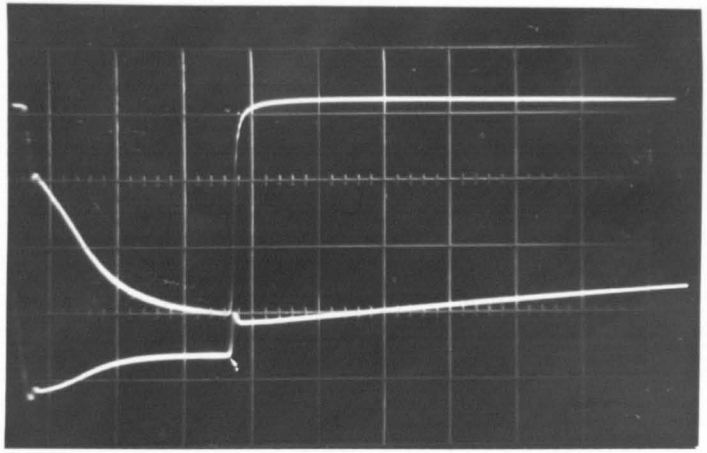

RUN 80.

ON TIME	=	33 μ	SEC
OFF TIME	=	10·0m	SEC
CURRENT	=	2·0	VOLTS/CM
VOLTAGE	=	2·0	VOLTS/CM
π	=	4·42	WATTS/CC

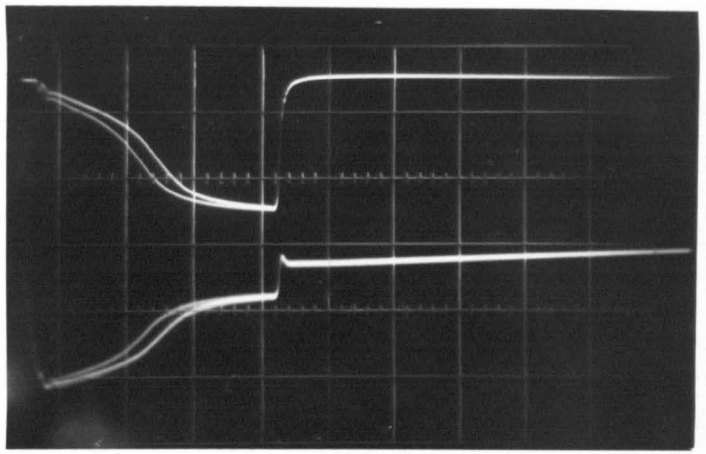

RUN 113.

ON TIME	=	35 μ	SEC
OFF TIME	=	0·10	SEC
CURRENT	=	5·0	VOLTS/CM
VOLTAGE	=	5·0	VOLTS/CM
π	=	9·5	WATTS/CC

fig 29.

Figs. 25 and 27 show the effect of increasing the pulse on time at a constant off time of 10 m sec. The current graduàlly builds up then levels off after about 70μseconds. The 227μ second pulse builds up in the same way as the 88, 33, 13 and 5μseconds pulse but the shorter pulses do not build up to the same extent because the power is removed earlier. The effect of the pulse off time on a constant on time pulse is shown to be significant in figs. 28 to 29. The rate of rise of the current is slower with long off times than with short ones. This is again probably because with long off times few if any positive ions remain in the discharge tube so the rate of ionization and current build up would be expected to be much slower in these circumstances.

6.2 Synthesis of hydrazine in a continuous d.c. system

6.2.1 Effect of flowrate on yield and conversion to hydrazine.

The most simple case to consider first is the continuous d.c. system. Fig.16 shows the effect of flowrate on yield and Fig.17 the effect of flowrate on conversion of ammonia to hydrazine. The reasons for the increase in energy yield flowrate must be due to

(i) the primary species (NH_2) are being produce more effectively by a greater number of ionizing or dissociating inelastic collisions at high flowrates.

(ii) a greater proportion of primary species formed react to form hydrazine.

(iii) less degradation of the hydrazine formed.

Of these (i) is unlikely because the rate of formation of primary species is dependent upon the inelastic collision cross section and the electron energies present not the gas flowrate. The gas flowrate does change the electrical characteristics of the discharge slightly. At high gas velocities ions are removed from the discharge and because of the lower ionic concentration in the discharge a lower maintenance voltage of approximately 0.6 kV is required. The lower maintenance voltage will give a lower field strength and lower mean electron energies which would slightly reduce the rate of primary reaction rather than increase it.

The proportion of primary species reacting to give hydrazine (ii) is also unlikely to change with flowrate. An analysis of possible reaction mechanisms of NH_2 shows the radicle reacts ultimately to give hydrazine or degrade it. Reaction mechanisms and rate constants, as such, will not be affected by flowrate.

Less degradation of the hydrazine formed (iii) at high flowrate is the most likely reason for the increase in yield found. At high flowrates the concentration of hydrazine and presumably hydrogen atoms is low so the degradation of hydrazine will be low with the result that more of the power input will produce undecomposed hydrazine and give a higher energy yield. Also at low flowrate there is a possibility of local heating occurring on the reactor wall surfaces due to the recombination of hydrogen atoms. The recombination reaction is strongly exothermic at 104.2k cal/mole and the rate of recombination would decrease at high temperature leaving a higher hydrogen atom concentration in the reacting gas with consequently higher degree of degradation of hydrazine and low energy yields. The energy yields for the continuous d.c. system are low and not at a commercially viable level. Conversions, however, are high reaching over 2wt % of hydrazine. At high flowrates there is insufficient time for the hydrazine concentration to build up to its maximum but at low flowrates and correspondingly high residence times conversions are also very low. The reason for the low conversions at long gas residence times can again be attributed to the degree of degradation of hydrazine by the hydrogen atoms. This is

described in explaining the low yields at long gas residence times. The low conversions cannot be due to a large decrease in the concentration of ammonia present since this was not detectable by titration and chromatography showed the nitrogen and hydrogen concentrations were very low. Rathsack[114] also explains the increase yields found at lower temperature operation as the greater rate of recombination of hydrogen atoms at low temperatures.

6.2.2 Results on adding helium to the discharge.

Early work by Baily & Duncanson has shown that even if the reduced field strength E/P of a discharge in ammonia can be increased any increase over approx. 20 volts/cm/mmHg will not increase the mean electron energy in the positive column above approximately 2.5 e.v. This is below that required to break the N-H bond in ammonia so most of the electrons present cannot directly dissociate the ammonia. In order to obtain a higher rate of dissociation for a given current and field strength higher energy electrons must be produced.

Examination of graphs of mean electron energies versus reduced field strength for other gases[61] showed that for the reduced field strength values used in this work helium gave higher electron energies viz: at only five volt/cm mm Hg $He \equiv 6.6$ ev and $NH_3 \equiv 0.06$ ev

also the mean electron energy rises still further with increasing reduced field strength and does not level off as is the case with ammonia. It was thought therefore the addition of helium to the ammonia in the discharge may increase the mean electron energy and produce a greater degree of dissociation of the ammonia. Levels of 10% $^{v}/_{v}$ and 50% $^{v}/_{v}$ of helium were tested against a control having no helium added. The electrical characteristics did not change measurably. Contrary to what was expected yields and conversions of ammonia to hydrazine fell when helium was added to the discharge. These results have since been confirmed by Reilly[116] using a concentric tube reactor. This evidence shows addition of helium will not increase yields and conversions but it is not possible to say if the electron energies were increased or not. One possible reason for the decrease in yield and conversion is that the electrons excite the helium molecules by collision but that the excitation energy is not given up to the ammonia molecules. It would be lost to the walls of the tube and/or other helium molecules, hence that energy would not be used for dissociation of ammonia but only in the production of heat.

It is of interest to note the yield and conversion for the control fall on the same line as other results at the same flowrate carried out over 12 months previously (Runs 17-24) indicating no significant changes occurred in either the electrodes or wall surfaces during the course of the experiments reported here. Erratic results did occur when the reactor was first operated due to "ageing" of the electrodes and possibly changes in the reactor wall surfaces. The "ageing" is possibly the nitriding of the stainless steel surface which occurs on exposing steel to an ammonia glow discharge.[65]

6.2.3 <u>The effect of withdrawing product gases through the porous reactor wall.</u>

By withdrawing gas through the reactor walls gas will only pass through one electrode and may pass through only one region of the gas discharge When gas was passed through the anode into the positive column and out through the porous wall the yield and conversion to hydrazine were greater than when gas was passed through the cathode into the cathode fall region and out through the reactor wall. These results are in agreement with the theory that either hydrazine is not formed in the cathode fall region or that it is formed and rapidly

34,108,37
destroyed again. It is very likely that ammonia is decomposed by electron impact in the cathode fall region since high electron energies are present in this region, however, hydrazine could be rapidly destroyed by electron impact and hydrogen atom degradation. It was thought passing gas through the porous glass reactor wall would improve the overall yield and conversion by increasing the recombination of hydrogen atoms on the wall. An increase would also be expected by passing the gas into the reactor through the anode and out through the cathode to avoid the negative glow region. Even with this arrangement the yields and conversions were lower than found by passing the gas in through the cathode and out through the anode at the same flowrate. A possible explanation for this is found by considering the flow through the reactor. When a gas flows straight through the electrodes and the reactor an approximation to plug flow can be said to exist but when the gas is withdrawn through the reactor wall a plug flow nor a fully backmix situation will occurr. A whole range of residence times will be present. The flow can then be considered in simplified form as

shown below

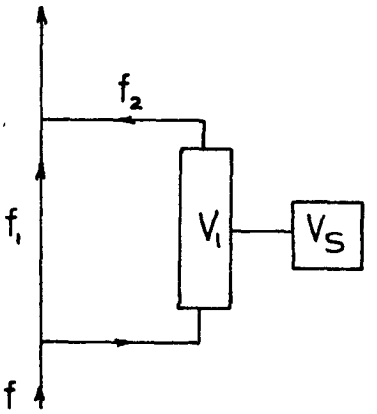

Where Vs is a stagnant portion in the reactor whose total volume is $V_1 + V_s$. The flow is considered in two parts, f_1, passing through the reactor in zero time and hence not being subject to reaction and f_2 remaining in the reactor for a fixed finite time and then leaving the reactor. In this case with low pressure, high velocity gas passing through the reactor walls V_s would be expected to be very small and not to significantly alter the total reactor volume. Since the distance between entering the reactor to leaving it would be less than one centimeter the flow of gas f_1 passing quickly out of the reactor would be large. This would result in a higher residence time in the reactor $(\frac{V_1}{f_2})$ seconds than that calculated from the total flowrate assuming plug flow of $(\frac{V_1}{f_1 + f_2})$ seconds. The higher residence time would result in less hydrazine being formed than in the plug flow case for the same power input, resulting in a lower energy yield.

Since a flow f_1 is "bypassing" the reactor a fall in overall conversion would result.

6.2.4 The influence of power input on energy yield and conversion to hydrazine.

The change in power input to the reactor is largely a measure of the increased current passed because the discharge does not obey Ohms the voltage remaining very nearly constant with increasing current.

As the power input to the reactor is increased the energy yield falls exponentially in all cases and tends to a finite value at zero power. If the energy yield were independent of power input an inverse relationship would result not an exponential one.

Conversions to hydrazine pass through a maximum with increasing power input with the position of the maximum with respect to power input increasing with increasing flowrate. The reason for the shape of the conversion .v. power input graph can be explained as follows. For any given gas residence time at zero power input no reaction occurs therefore the conversion is zero. As the power is increased the H and NH_2 concentrations increased so hydrazine is both formed and destroyed. The extents to which these formation and degradation reactions occur

will depend upon the relative concentrations of NH_2 and H, and hence on the power input. At low power inputs the hydrogen atom concentration will be very low so the hydrazine concentration increases but as the power input increases the hydrogen atom concentration increases faster than the NH_2 concentration so the extent of degradative reaction exceeds the formation reaction and the hydrazine concentration will decrease. At high flowrates free radicle concentrations build up more slowly so a higher power input is needed to increase the radicle concentrations to the point when the extent of degradative reaction exceeds the formation reaction. Therefore the position of the maximum conversion with respect to power input increases with increasing flowrate.

6.3 Synthesis of hydrazine in a pulsed d.c. system.

6.3.1 Variation in energy yield and conversion to hydrazine with flowrate.

Initial experiments were carried out to find the optimum flowrate to carry out the pulsed d.c. experiments. At a pulse on time of 13μ secs and a pulse off time of 100μ secs results indicated the flowrate should be approximately 14.3cc/sec at operating conditions for maximum conversion. This flowrate gives a much lower active residence time of 0.15 seconds than that found

to give maximum conversion in the continuous d.c. system. The difference in graphs of conversion to hydrazine .v. active residence time is shown in fig. 17 . The active residence time has been changed in the pulsed d.c. case by changing the pulse on and off times not be changing the gas flowrate, as in the continuous d.c. case. There is no reason to expect the same flowrate will be the "optimum" for all pulse waveform characteristics and it is possible increases in energy yield and conversion to hydrazine could be made by operating the pulsed d.c. system at different gas flowrates for pulse conditions other than those described above. Ouchi varied the active residence time of his impulse wave system by varying the flow-rate, but it is not possible to determine what the effect of flowrate was because the experiments were carried out at different levels of power input and pressure.

6.3.2 Effect of pulse on times and pulse off times on energy yield and conversion to hydrazine.

Figs. 16. and 17. show pulsed d.c. and continuous d.c. systems behave differently with respect to both energy yield and conversion to hydrazine. Figs. 21. and 22. show the effect of pulse on and off times on yield and

and conversion. The energy yield increases with increasing pulse off time but the rate of increase is slow at long pulse off times. As the pulse off time is increased the conversion to hydrazine falls so the increase in energy yield is offset by the fall in conversion. Similarly with changes in pulse on time, the conversions passed through a maximum with increasing on time with the position of the maximum depending upon the pulse off time. Decreasing the on time also increases the yield but the on time changes has much more effect at long off times than at short off times. At short off times a high level of ionisation is maintained (c.f. page 93 calculation of ionic diffusion rate), the hydrazine can build up to a high concentration and free radicle concentrations will be much nearer their equilibrium value than when long off times are used. Hence the change in these concentrations with pulse on time will be much smaller at short off times than at long off times where the concentrations are much lower.
The lower free radicle and hydrazine concentrations which will be present at short on times and long off times means degradation of hydrazine

would be slight and this explains the high energy yields found under these conditions. Fig. 17. shows the initial slope of the curve conversion to hydrazine .v. active residence time is greater for the pulse d.c. system than the continuous d.c. system. When considered together with the kinetic model data it can be seen this difference in slope is due to the higher rate of primary reaction in a pulse system. When long pulse off times are used at the beginning of a pulse a low level of ionization exists therefore a high breakdown voltage is required for that pulse so initially the average electron energy is high, this will give a higher initial rate of primary reaction and hence increase the slope of the curve. If this higher initial rate of primary reaction exists in the pulsed d.c. system it also explains why the maximum conversion in the pulse system occurs at a low active residence time with respect to pulse on and off time changes and changes in flowrate. The conversion passes through a maximum because of the relative extents of the formation and degradation reactions as described previously. If the rate of primary reaction in a pulse system is high then not only will the hydrazine concentration

rise at a faster rate, but also the H atom concentration, hence the residence time at which the extent of the hydrazine degradation exceeds that of the formation reaction will occur at a lower active residence time. Similar reasoning explains why the maximum conversion with respect to pulse on time varies with off time. With long pulse off times hydrazine and hydrogen atom concentrations are low therefore long pulse on times can be accepted without much degradation taking place. With too long pulse on times, however, the hydrogen atom concentration will build up and more degradation will occur resulting in a drop in the overall conversion to hydrazine. At short pulse off times the hydrazine and H atom concentrations build up more rapidly consequently degradation reactions will predominate at shorter pulse on times.

Conversions to hydrazine of upto 2 % w/w are found in both the pulsed d.c. and continuous d.c. systems but the pulsed d.c. system has the advantage that the maximum conversion occurs at a lower active residence time and hence corresponds to a higher energy yield of hydrazine.

6.3.3 The influence of power input on energy yield and conversion to hydrazine.

The effect of power input is the same as in the continuous d.c. system. The reason for the maximum in conversion to hydrazine .v. power input is also similar except that the pulse on times and off times will also effect the position of the maximum. At faster flowrates, short pulse on times and long pulse off times concentrations of hydrazine and H atoms will be low consequently higher power inputs would be required before the degradation reactions became predominent. In practice this was found to be the case.

6.3.4 Results with the reactor packed with glass wool

It was established that a reactor with no packing operating in a continuous d.c. system at a gas flowrate of 45.7 cc/sec with a gas residence time of 0.35 seconds gave the same yield and conversion to hydrazine as a pulsed d.c. system operating at a flowrate of 14.3 cc/sec with a pulse on time of 13 μ sec and a pulse off time of 28.6 μ sec also giving an active residence time of 0.35 seconds.

When the positive column of the reactor was packed with glass wool of high surface area but

small volume and the experiments repeated yields and conversions doubled in the continuous d.c. system but no significant change occurred in the pulsed d.c. system. A similar effect was noted by Charlton[134] using a concentric tube reactor. In his continuous system an ethane diol spray in the reactor increased the yield but no increase was observed with the spray in the pulse system. This was attributed to the spray absorbing hydrazine from the product gas which may be true to some extent, however, the spray also provides extra surface area for recombination of H atoms and this would explain Charltons results in the same way as with glass packing in this work.

With a continuous d.c. system extra surface area will increase the extent of H atom recombination and hence lower its concentration. In turn the amount of degradation of hydrazine by Hydrogen atoms will be reduced and hence the yield and conversion to hydrazine rises. In the pulsed d.c. system the pulse is 'on' for only 13μsecs therefore the NH_2 and H concentrations will be low. The rate of formation of these radicles is a function of electron energy, which, since the discharge characteristics

did not change on packing, is not a function of surface area. Their rate of dissappearance is a function of surface area, but at low radicle concentrations this has a minor effect, therefore increasing the surface area will not affect the rate of growth of these radicles. When the pulse is switched off the radicle concentrations will decay so their concentration will be lower than in the continuous d.c. system. With extra surface area the free radicles in the packed reactor will decay faster but since they are at a much lower concentration anyway the small difference due to the faster decay will not significantly alter the amount of degradation occurring, therefore the yield and conversion to hydrazine will not be affected.

Further work under different conditions and with different amounts of packing could lead to a much clearer explanation of the changes occurring on packing a reactor.

6.4 Interpretation of results.

6.4.1 Power density and gas residence time.

If log energy yield Y, in gms hydrazine/Kwh energy input into the reactor, is plotted against power density $\bar{\Pi}$, in watts power input into the reactor/cc of reactor volume a linear correlation of the form

$$\log Y = A - B\,\bar{\Pi} \qquad - (i)$$

applies. This correlation is valid for all flowrates in the range investigated and also for

the continuous and pulsed d.c. systems, with constants A and B dependent upon operating conditions. Charlton[142] found the same relationship valid in his work on concentric tube reactors and a replot of Ouchis[108] data for a low pressure a.c. crossflow reactor also shows energy yield correlates with power in an equation of the same form.

The overall rate of production and conversion to hydrazine are related to the above equation viz

$$\text{gms hydrazine produced/sec} = 2.8\times10^{-5}\ W\ e^{\frac{A-BW}{16}} \quad - (ii)$$

$$\text{conversion to hydrazine wt\%} = \frac{2.8\times10^{-5}}{M_f} W\ e^{\frac{A-BW}{16}} \quad - (iii)$$

where M_f is the mass flowrate of ammonia in gms/sec and W is the total power input. Since the reactor volume is always 16cc, $\tau = W/16$.

From these equations it can be seen the conversion passes through a maximum with respect to power Differentiating w.r.t. W we get

$$\frac{d\ Conv}{dw} = \frac{2.8\times10^{-5}}{M_f}\ e^{A-\frac{BW}{16}}\ (1 - BW/16) \quad - (iv)$$

reaching a maximum at a power of $16/B$

hence the maximum conversion to hydrazine

$$= \frac{2.8\times10^{-5}}{M_f}\ \frac{16}{B}\ e^{A-1} \quad - (v)$$

For the continuous d.c. system the constants A and B are both functions of flowrate or gas

residence time (Θ_G) over the range investigated viz:- fig 30.

$A = 1.5 - 1.33\ (\Theta_G)$ - (vi)

$B = 1 - 1.66\ (\Theta_G) + 1.66\ (\Theta_G)^2$ - (vii)

Substituting these constants in (i) and (iii) we get

log energy yield = $1.5-1.33\ (\Theta_G) - \pi$

$(1-1.66\ (\Theta_G) + 1.66\ (\Theta_G)^2)$ - (viii)

and conversion to hydrazine

$= 0.186\ W(\Theta_G)^{\bullet}\ e^{1.5-1.33\ (\Theta_G) - \pi}$

$(1-1.66(\Theta_G) + 1.66\ (\Theta_G)^2)$ - (ix)

therefore we see the yield desreases for all increasing gas residence times and power densities but the conversion reaches a maximum depending upon both the power density and gas residence time.

Differentiating (ix) w.r.t. Θ_G we get

$$\frac{d\ Conv}{d\ \Theta_G} = 0.186\ e^{1.5-1.33\ \Theta_G - \pi\ (1-1.66(\Theta_G) + 1.66(\Theta_G)^2)}\ (1+\Theta_G(-1.33 + \pi(1.66 - 3.33\ (\Theta_G)))$$ - (x)

At a position of maximum conversion $\frac{d\ Conv}{d\ \Theta_G} = 0$

and from (iv) we find the power = $16/_B$

Setting eqn (x) to zero and substituting equations (iv) and (vii) solving the resulting cubic equation in Θ_G shows the maximum conversion in the continuous d.c. system occurs at a gas residence time of 0.56 seconds

fig 30.

CORRELATION OF CONSTANTS IN FUNCTION

Log(yield)= a - bπ WITH GAS RESIDENCE TIME.

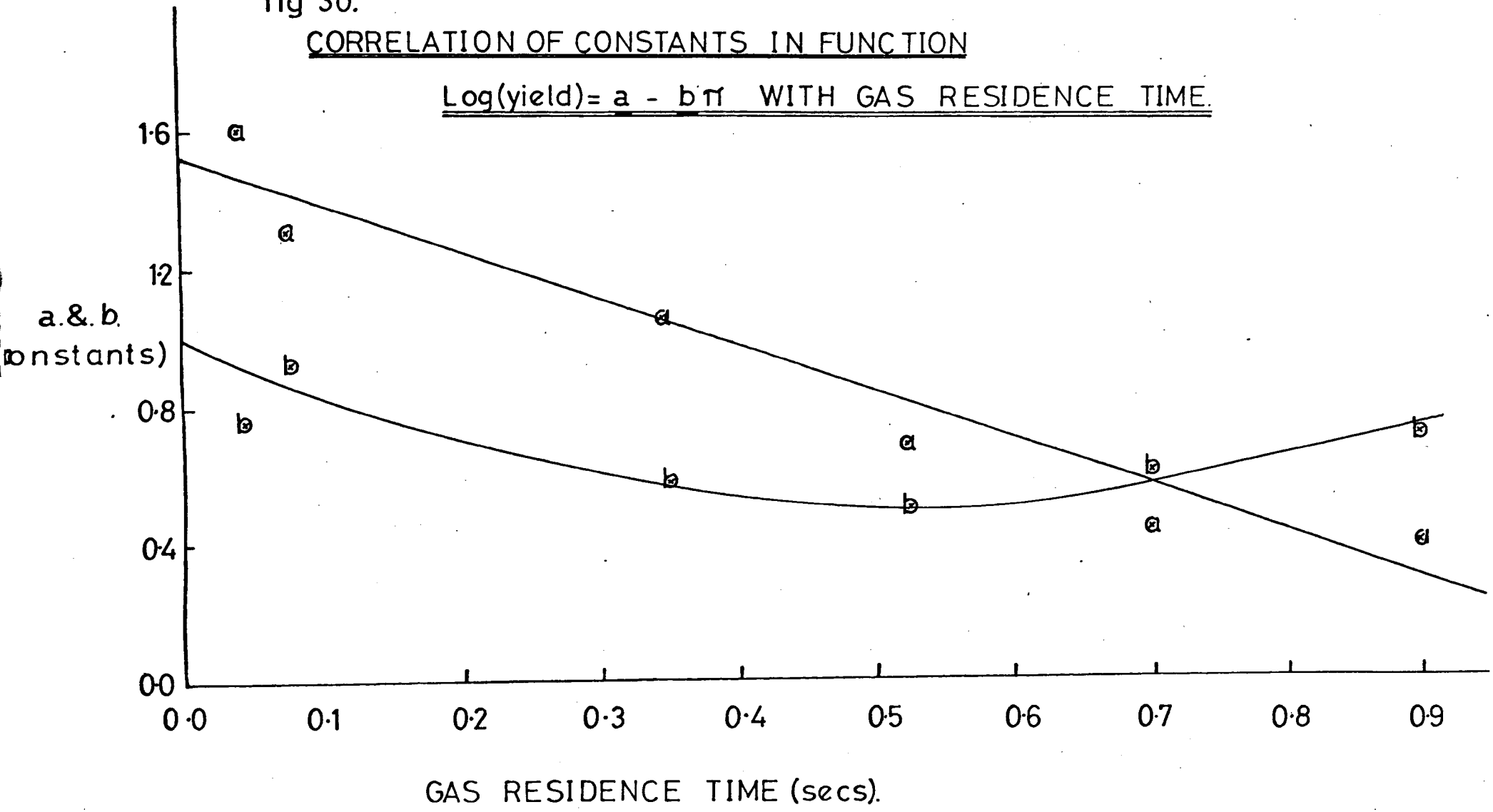

or a flowrate of 28.6 cc/sec and at a power density of 1.69 watts/cc. Under these conditions the maximum conversion is calculated from equations (v) (vi) and (vii) as 2.2 wt %.

The nearest operating conditions to the above were at a gas residence time of 0.53 seconds and a power density of 2 watts/cc. The conversion under these conditions was the maximum recorded at 2.3 wt%.

Although only applying for the particular reactor and pressure used in this work equations (viii) and (ix) can be used to predict the yield and conversion to hydrazine for any power density and flowrate in the continuous d.c. system. Equation (x) will predict the best operating power for maximum conversion at any given flowrate and vice versa. These equations are rather complex being derived from three other equations (i) (vi) and (vii) and therefore it is difficult to,ascertain details of the reaction mechanism behind these results. However let us assume hydrazine is formed by the overall reaction

$$NH_3 + \text{power (W)} \xrightarrow{k} \tfrac{1}{2} N_2H_4 + H$$

Assuming very low N_2H_4 concentrations initially

occuring we get

$$-\frac{d\,NH_3}{dt} = \frac{2\,d\,N_2H_4}{dt} = k\,W\,NH_3 \qquad - (xi)$$

integrating $$\frac{N_2H_4}{NH_3} = \tfrac{1}{2}\,k\,W\,t \qquad - (xii)$$

where t = gas residence time in reactor.

Comparing equation (xii) with equation (ix) we see that these equations are identical apart from the exponential term in equation (ix) representating degradation and back reactions. Converting equation (ix) to a molar basis and comparing with equation (xii) we find

$$k = 0.00\ 88 \quad \text{sec}^{-1}\ \text{watts}^{-1}$$

This low rate of reactions, suggests the fast free radicle and ion molecule reactions do not represent the rate controlling step for formation of hydrazine. The rate of inelastic collision of electrons with ammonia therefore must be the slowest rate step in the formation of hydrazine.

6.4.2 Correlation of pulse on times and pulse off times.

It was not possible to relate the constants A and B of equation 6.4.1 (i) with the active residence time of a pulsed d.c. system. This is not very suprising when one considers a given active residence time can be achieved by several combinations of pulse on times and pulse off times and all these combinations cannot

be expected to give the same energy yields and conversions to hydrazine.

The results of the statistical analysis of the response surfaces of (i) on time, off time, power density and yield

(ii) on time, off time, power density and conversion are given below:-

In the range of pulse on times 5 - 34 μ sec

Energy yield of hydrazine

$$= 17.8 - 5.6X_1 - 10.5X_2 + 10.3X_3 - 1.85X_1^2 + 3.5X_2^2 - 3.0X_3^2 + 1.39X_1X_2 - 5.5X_1X_3 - 0.14X_2X_3$$

Conversion to hydrazine wt%

$$= 0.31 + 0.12X_1 + 0.04X_2 - 0.31X_3 - 0.19X_1^2 + 0.03X_2^2 - 0.12X_3^2 - 0.11X_1X_2 - 0.026X_1X_3 + 0.27X_2X_3$$

where $X_1 = \frac{1}{2}(\pi - 3)$, $X_2 = 0.4 \quad (\log_{10}(\text{on time}) - 1.1)$, $X_3 = \log_{10}$ off time + 2

In the range of pulse on times 34 - 220 μ sec

Energy yield of hydrazine

$$= 4.88 - 1.4X_1 - 3.1X_2 + 2.6X_3 + 1.4X_1^2 + 0.78X_2^2 - 0.65X_3^2 + 0.38X_1X_2 - 2.1X_1X_3 - 2.5X_2X_3$$

Conversion to hydrazine wt %

$$= 0.36 + 0.15X_1 + 0.013X_2 - 0.28X_3 + 0.009X_1^2 + 0.005X_2^2 - 0.15X_3^2 - 0.04X_1X_2 - 0.01X_1X_3 - 0.01X_2X_3$$

Where $X_1 = \frac{1}{2}(\pi - 3)$, $X_2 = 0.41 (\log_{10} \text{on} - 1.95)$
$X_3 = \log \text{off} + 2$.

Further details of the statistical analysis can be found in appendix I . It must be emphasised these results cannot be used outside the range of conditions given.

The stastical analysis above is useful in predicting yields and conversion under any given pulsing conditions but the equations are valid only over a limited range of conditions also they can only contain first and second order linear terms. In view of these limitations it is not possible to draw any general conclusions about maximum yields and conversions attainable or any theoretical basis behind the results. To overcome some of these limitations a simpler functional relationship was worked out to correlate the energy yield with pulse on and pulse off times at a constant power density. Consideration of bond energies indicates the maximum energy yield theoretically possible assuming no degradation of product is approximately 165 gms hydrazine/kwh. The function, therefore, should tend to a value not greater than this at zero pulse on time, where no back reaction can occur, and at zero pulse off time the energy yield should tend to the continuous d.c. system. The

function which best fits the experimental data and the above conditions is given below.

$$\text{Energy yield} = 146 \left(1 - e^{\frac{-4.6 \times 10^{3}}{\log (tn+1)\ (\Theta')^{1/2}}} \right) \quad - (i)$$

The plot of yield .v. the function is shown in fig. 31 . This indicatesahigh energy yield is favoured by low active residence times and short pulse on times. If the rates of reaction were not affected by pulse on times, as such, one would expect, at constant power, the energy yield to only be a function of the active residence time Θ'. A pulsed d.c. system, therefore, is not only a means of producing low active residence times but short pulse on times will increase the energy yield more than that expected from the decrease in active residence time they produce. The maximum energy yield predicted by the function is 146 gm/kwh only 11½% below that predicted from bond energy considerations. For the case at zero pulse off time agreement with the continuous d.c. system is not as good with a yield of 0.067 gm/kwh predicted compared with a yield of approximately 0.01 gm/kwh projected from experimental data. This discrepancy may be due to the heating effects occurring in the continuous d.c. system at low flowrates as explained in 6.2.1.

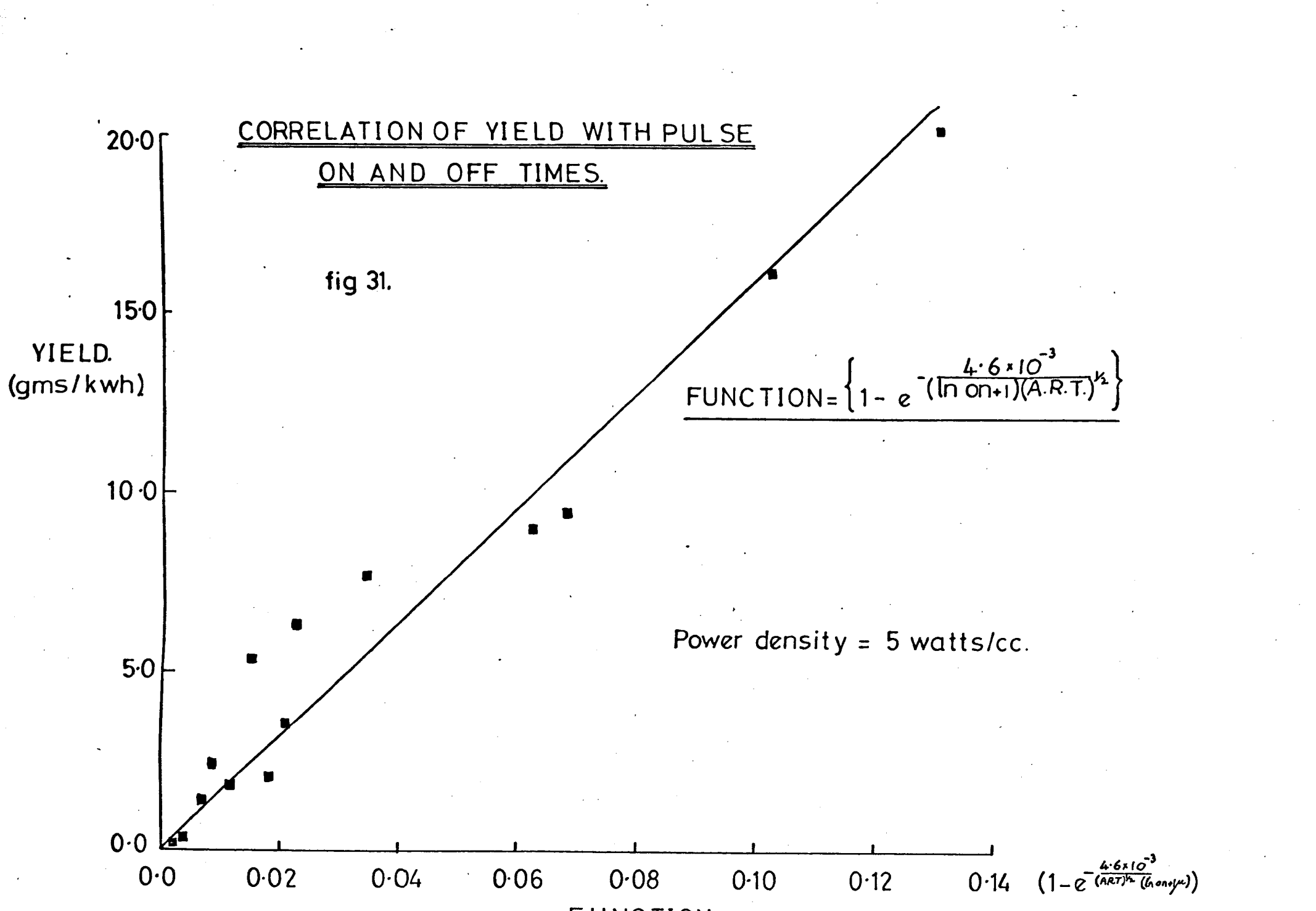
CORRELATION OF YIELD WITH PULSE ON AND OFF TIMES.
fig 31.
YIELD. (gms/kwh)
20·0
15·0
10·0
5·0
0·0
0·0
0·02
0·04
0·06
0·08
0·10
0·12
0·14
FUNCTION = $\left\{1 - e^{-\frac{4\cdot6\times10^{-3}}{(\ln on+1)(A.R.T.)^{1/2}}}\right\}$
Power density = 5 watts/cc.
$(1-e^{-\frac{4\cdot6\times10^{-3}}{(ART)^{1/2}(\ln on+\mu)}})$
FUNCTION

Differentiating eqn (i) w.r.t. pulse off time we get

$$\frac{d\,Y}{d\,(tf)} = \frac{3.36\times10^{5}}{\log\,(tn+1)}\,\frac{(tn+t_f)^{-\frac{1}{2}}}{(\Theta_G \times tn)^{\frac{1}{2}}}\; e^{\frac{-4.6\times10^{-3}}{\log\,(tn+1)}\,(\Theta')^{\frac{1}{2}}} \qquad - (ii)$$

Hence it can be seen the energy yield will always increase with increasing pulse off time, tending to a limit of 146 gm/kwh at infinite off time. The rate of increase will decrease with increasing pulse off time but the yield will increase faster with increasing pulse off time at short pulse on times than at long pulse on times. viz.

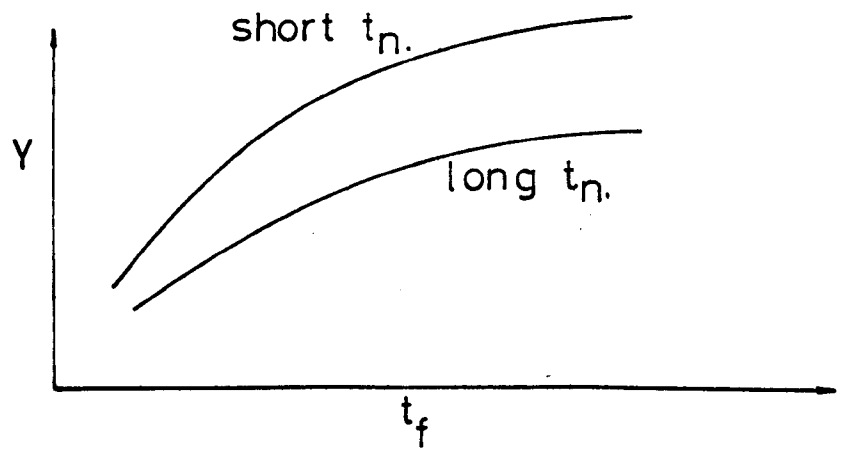

Similarly differentiating w.r.t. pulse on time t_n we get

$$\frac{d\,Y}{d(t_n)} = -\frac{3.36\times10^{5}((t_f)\,(\log\,(t_n+1))+2(tn+t_f))\,e^{\frac{-4.6\times10^{-3}}{\log(t_f+1)}(\Theta')^{\frac{1}{2}}}}{(\Theta_G)^{\frac{1}{2}}\,(t_n+t_f)^{\frac{1}{2}}\,(t_n)^{3/2}\,(\log\,(t_n+1))^{2}} \qquad - (iii)$$

This must always be negative, showing short pulse on times give the highest yield. At long pulse off times the on time + off time = off time.

therefore (iii) reduces to

$$\frac{d\,Y}{d\,(t_n)} = -\frac{3.36\times10^{5}}{(\Theta_G)^{\frac{1}{2}}} \left\{ \frac{(t_f)^{\frac{1}{2}} \left(\log (t_n+1) + 2\right)}{(t_n)^{3/2} \left(\log (t_n+1)\right)^2} \right)$$

$$e^{\frac{-4.6\times10^{-3}(t_f)^{\frac{1}{2}}}{\log(t_n+1)\ (\Theta_G \times t_n)^{\frac{1}{2}}}} \quad -(iv)$$

indicating the energy yield will change faster with changes in pulse on time at long off times. The rate of change of energy yield with pulse on time is also seen to be faster at short on times than long on times. Unfortunately a reduction in on time results in a reduction in conversion to hydrazine. The overall conversion to hydrazine in weight percent is expressed as

$$\text{Conversion wt\%} = 0.186\ WX\ \Theta' \left\{ 146 \left(1 - e^{\frac{-4.6\times10^{-3}}{\log(t_n+1)\ (\Theta')^{\frac{1}{2}}}} \right) \right\} \quad -(v)$$

Hence we see the conversion is zero at active residence times of zero and infinity and passes through a maximum which is dependent upon pulse on time viz.

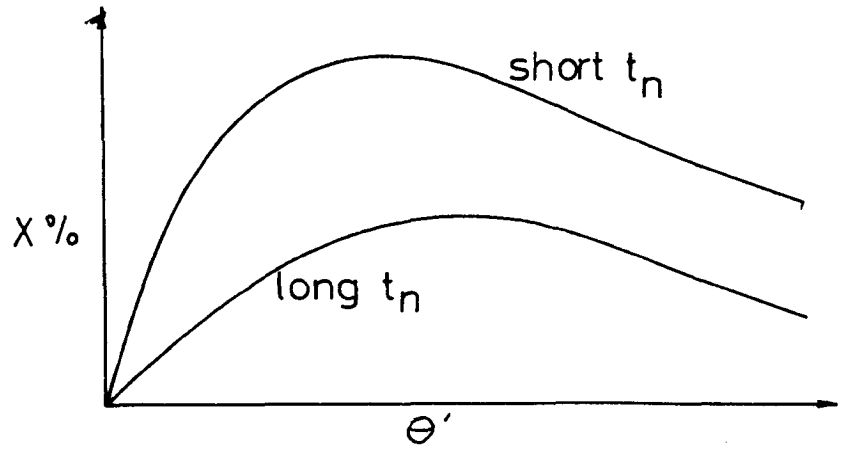

Equ (v) also indicates high conversions will be found for the shortest pulse on and off times for a given active residence time. This is seen in experimental data viz.

θ'	OFF TIME (t_f)	ON TIME(t_n)		CONV. wt%
5.3_{10}-2	100 μsec	5 μsec	4.7	1.58
3.7_{10}-2	1 m sec	33 μsec	4.9	1.04
36.8_{10}-4	10 m sec	33 μsec	5.4	0.36
25.2_{10}-4	0.1 sec	225 μ sec	5.4	0.074

The differentials of conversion with respect to pulse on and off times are complex and not readily solved purely analytically.

6.4.3 Justification and use of W/F parameter.

One of the most commonly used correlating parameters for both yield and conversion is the power input per unit flowrate W/F. The theoretical justification for using W/F and the parameter used in 6.4.1 is given below.

Some simplifying assumptions have been made

1) Diffusion and convection not important
2) Source of electrons, eg. ioniaation, secondary emmission, cosmic radiation, have been ignored.
3) Loss of electrons energy to walls and by radiation are ignored.
4) Number of reactant molecules constant.
5) Single energy electrons. This assumption does not alter the analysis but the collision cross section is a function of the electron energy distribution therefore the cross section Q should read

$$\int_{o}^{\infty} f(E)\, Q \; dE$$

The primary step in reactions occurring in a glow discharge is the collision between an electron and the reactant molecule (m) with energy E_{em} being transferred from the electron to the molecule as

$$e + M \xrightarrow{k_{em}} \text{Product} \qquad \Delta E = E_{em}$$

The rate of inelastic collision is given by

$$\frac{d\,Nm}{dt} = - N_m N_e \overline{v_e}\; Q = - k_{em}\; N_e N_m \qquad - (i)$$

Where

Q = inelastic collision cross section

$\overline{v}_e$ = average electron velocity.

N_e = number of electrons

N_m = number of reactant molecules.

The rate of loss of energy from the system/unit vol

$$\frac{1}{V}\frac{dE_{em}}{dt} = -\frac{dN_m}{dt} E_{em} = E_{em} N_m N_e \overline{v_e} Q \qquad - (ii)$$

The average electron energy $\overline{v_e}$ will be such that the gain in energy from the electric field, X_f will equal the rate of loss of energy given in (ii). If the electron gains energy E_{em} its average velocity $\overline{v_e}$ from Newtons Laws is given by

$$\overline{v_e} = \left\{\frac{2E_{em}}{m}\right\}^{\frac{1}{2}} \qquad - (iii)$$

The mean free path λ is related to the collision crosssection by

$$\lambda = \frac{1}{N} Q \qquad - (iv)$$

and if the time between collisions is t_c assuming zero initial velocity after a collision we get

$$\lambda = \frac{X_f}{2m} t_c^2 \qquad - (v)$$

Where m = mass of an electron

From (iii) (iv) and (v) we find

$$\overline{v_e} = \frac{X_f}{(8e E_{em})^{\frac{1}{2}} N Q} \qquad - (vi)$$

The current density J is also related to the average electron velocity by

$$J = N_e \overline{v_e} \qquad - (vii)$$

So substituting (vi) and (vii) in (i) we get

$$- \frac{d\,N_m}{dt} = k_{e\,m}^{1}\ \frac{N_m}{N}\ JX_f \qquad \text{- (viii)}$$

where $k_{em}^{i} = k_{em}/(8m\,E_{em})^{\frac{1}{2}}\,Q$ - (ix)

JX_f is the power input/unit volume or Π .

Hence the rate of primary reaction is proportional to Π as

$$- \frac{d\,N_m}{dt} = k_{em}^{1}\ \frac{N_m}{N}\ \Pi = k_{em}^{1}\ \frac{N_m}{N}\ \left(\frac{W}{V}\right) \qquad \text{- (x)}$$

And the fractional conversion

$$\frac{d\,N_m}{N_m} = - k_{em}^{1}\ \left(\frac{W}{V}\right)\ \frac{dt}{N} \qquad \text{- (xi)}$$

But in a flow reactor $dt = \frac{dV}{F}$

where V = volume of reaction

F = volumetric flowrate.

and at constant volume

$$\frac{d\,N_m}{N_m} = \frac{k_{em}^{1}}{N}\ d\left(\frac{W}{F}\right) \qquad \text{- (xii)}$$

Therefore we find the fractional conversion is proportional to W/F.

i) <u>Correlation of energy yield with W/F.</u>

Fig.32. shows the continuous d.c. results for energy yield plotted against W/F. The parameter does not give a very good correlation over the range of powers and flowrates used here but in general high energy yields are found to occurr at low values of W/F. The most noticeable aspects of this graph are the low energy yields at a flowrate of 14.3 cc/sec and the relatively low

fig 32. GRAPH OF YIELD.v. Wx GRT.

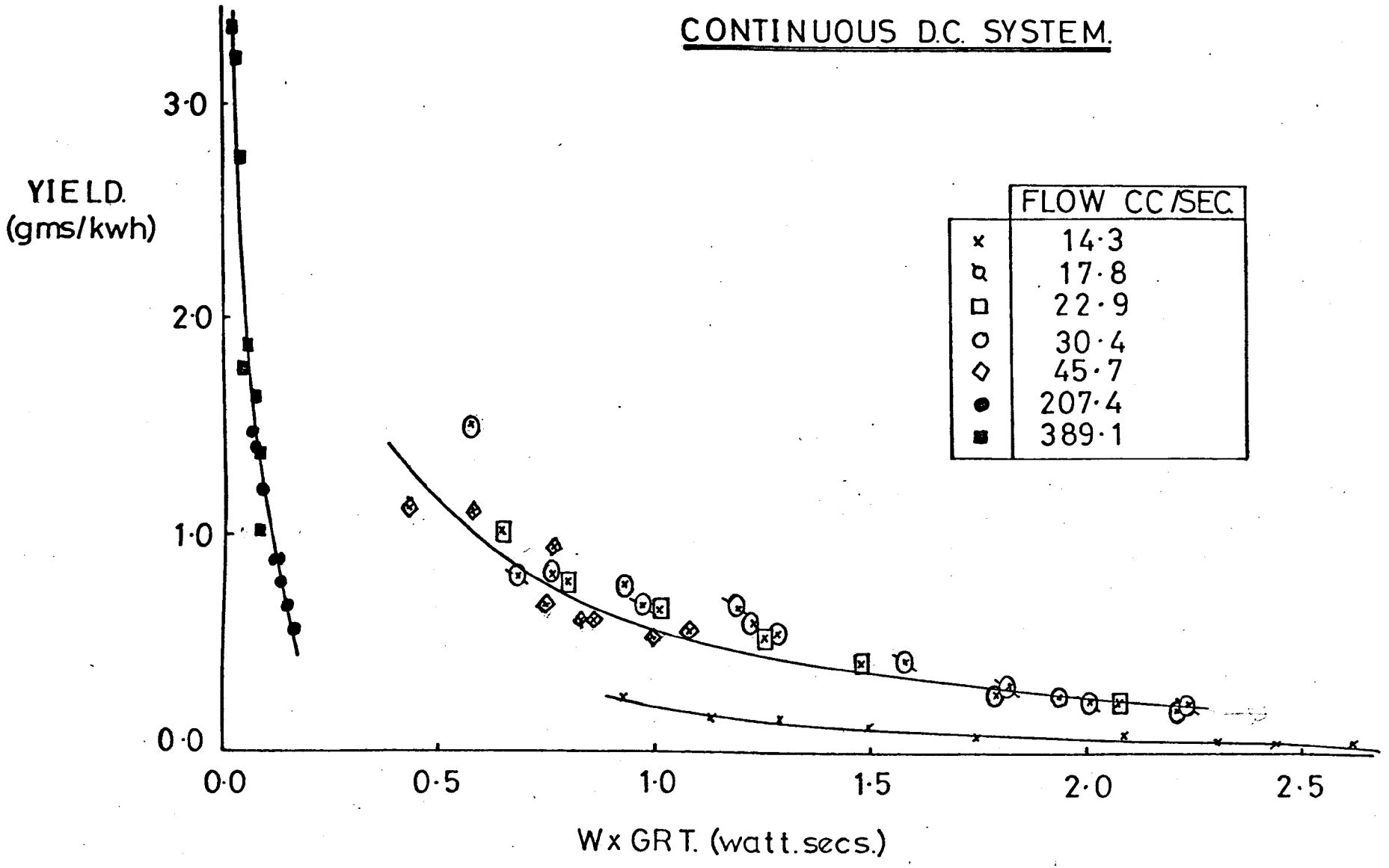

yields at W/F values less than 0.5. The reason for the low yields at low flowrates may be the local heating as discussed earlier. The relatively low energy yields at high gas velocities are probably the result of a change in the electrical characteristics of the discharge. At high gas velocities ions are removed from the discharge and because of the lower ionic concentration a lower maintenance voltage of approximately 0.6Kv is required. This in turn will give a lower mean electron energy, a lower rate of primary reaction and hence a lower energy yield.

With a pulsed d.c. system the gas residence time is not a real measure of the operating conditions of the discharge so the active residence time (Θ') is used and the energy yield correlated against $W \times \Theta'$. Ouchi also used this correlation in his pulsed d.c. work. Figs. 33. and 34. show the correlation in the ranges $0 - 10^{-2}$ and $0 - 10^{-3}$ respectively. It can bee seen $\Theta' \times W$ correlates results for a given off time but does not bring all the results together for different pulse on times. The graphs show high enery yields are favoured by low values of $W \times \Theta'$ and for a given value of $W \times \Theta'$ high energy yields are

fig 33. GRAPH OF YIELD v. W x A.R.T.

PULSED D.C. SYSTEM.

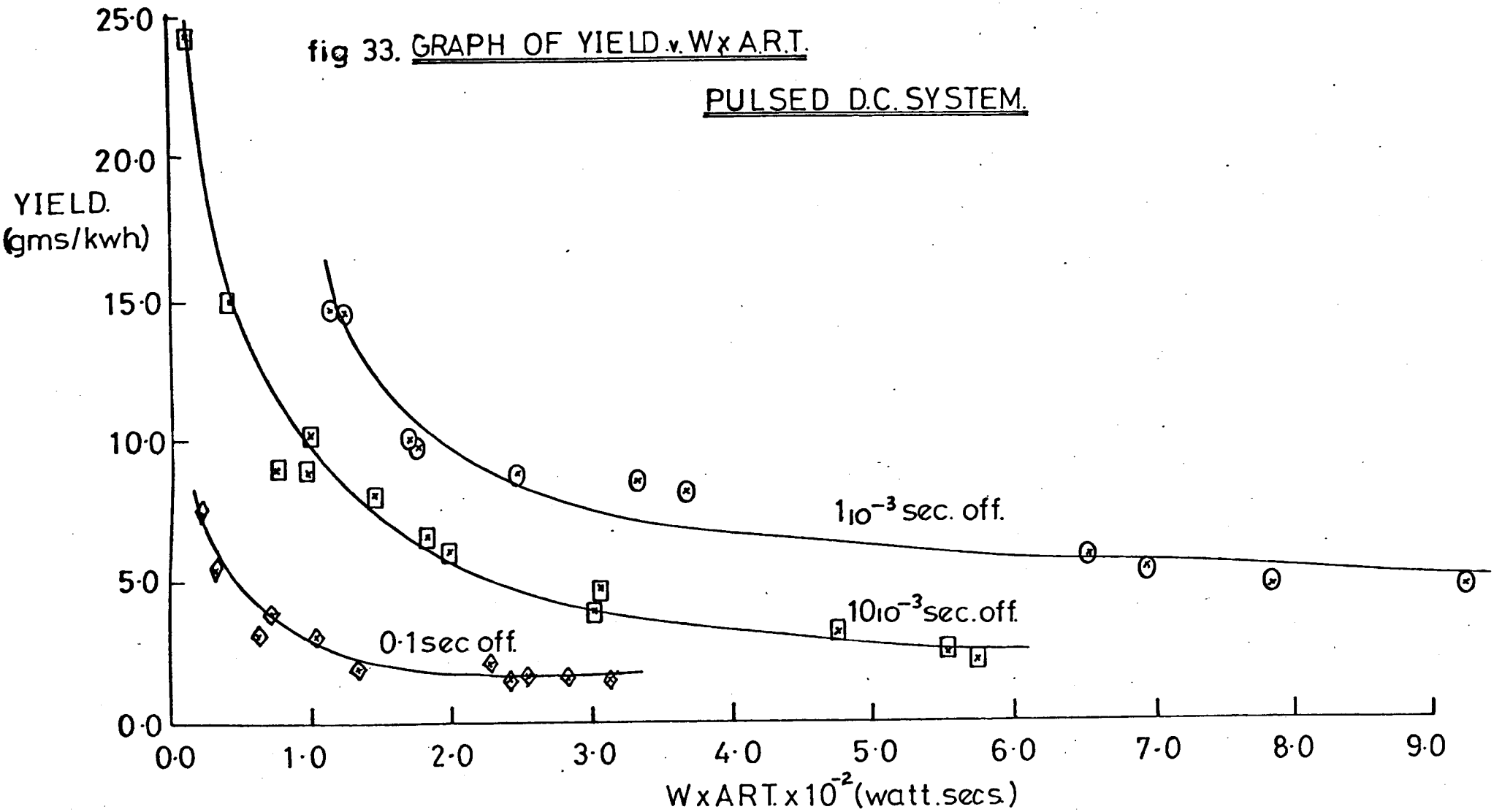

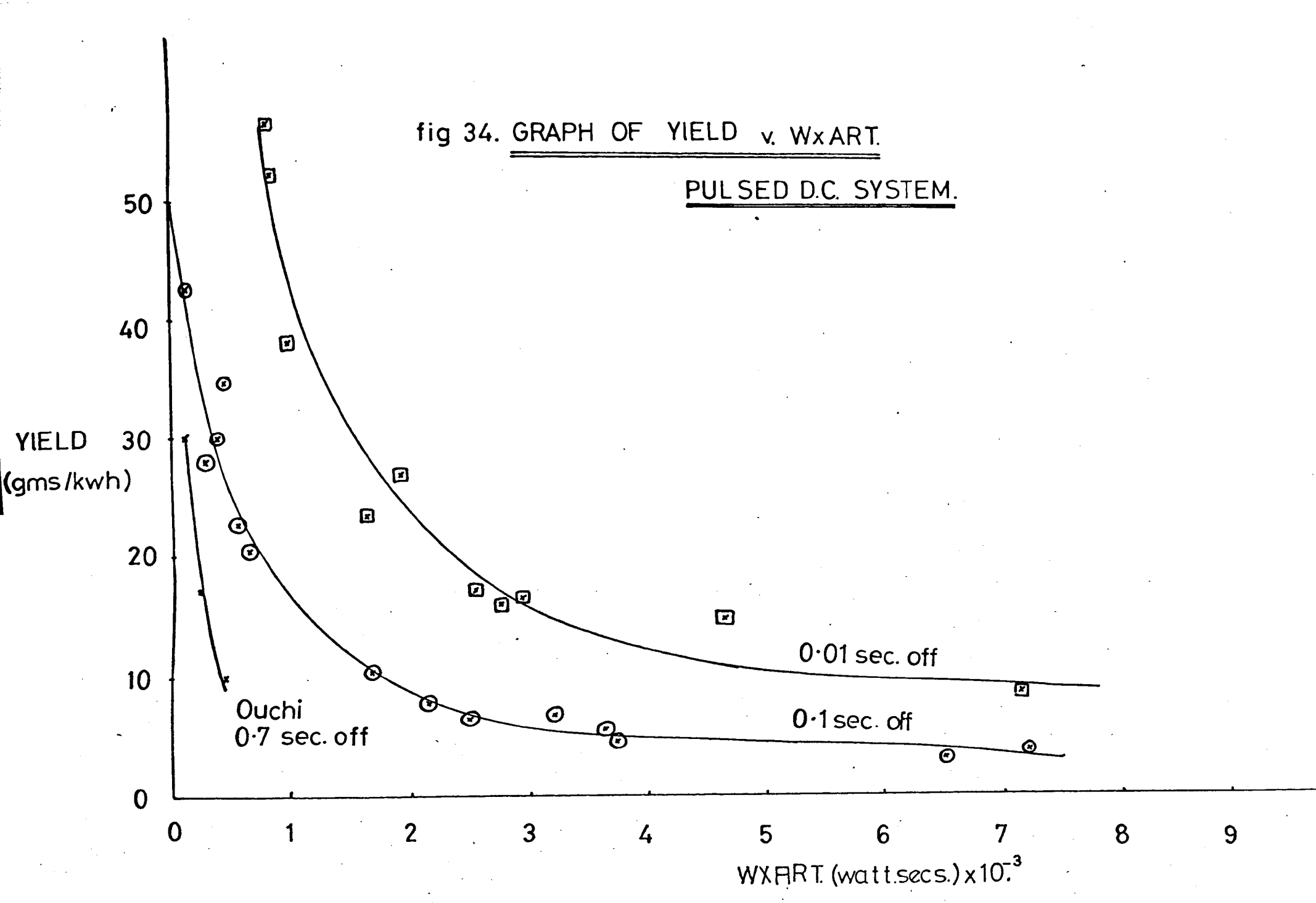
fig 34. GRAPH OF YIELD v. WxART.
PULSED D.C. SYSTEM.
YIELD (gms/kwh)
50
40
30
20
10
0
0·01 sec. off
0·1 sec. off
Ouchi
0·7 sec. off
0
1
2
3
4
5
6
7
8
9
WXART. (watt.secs.) x10.-3

fig 35.

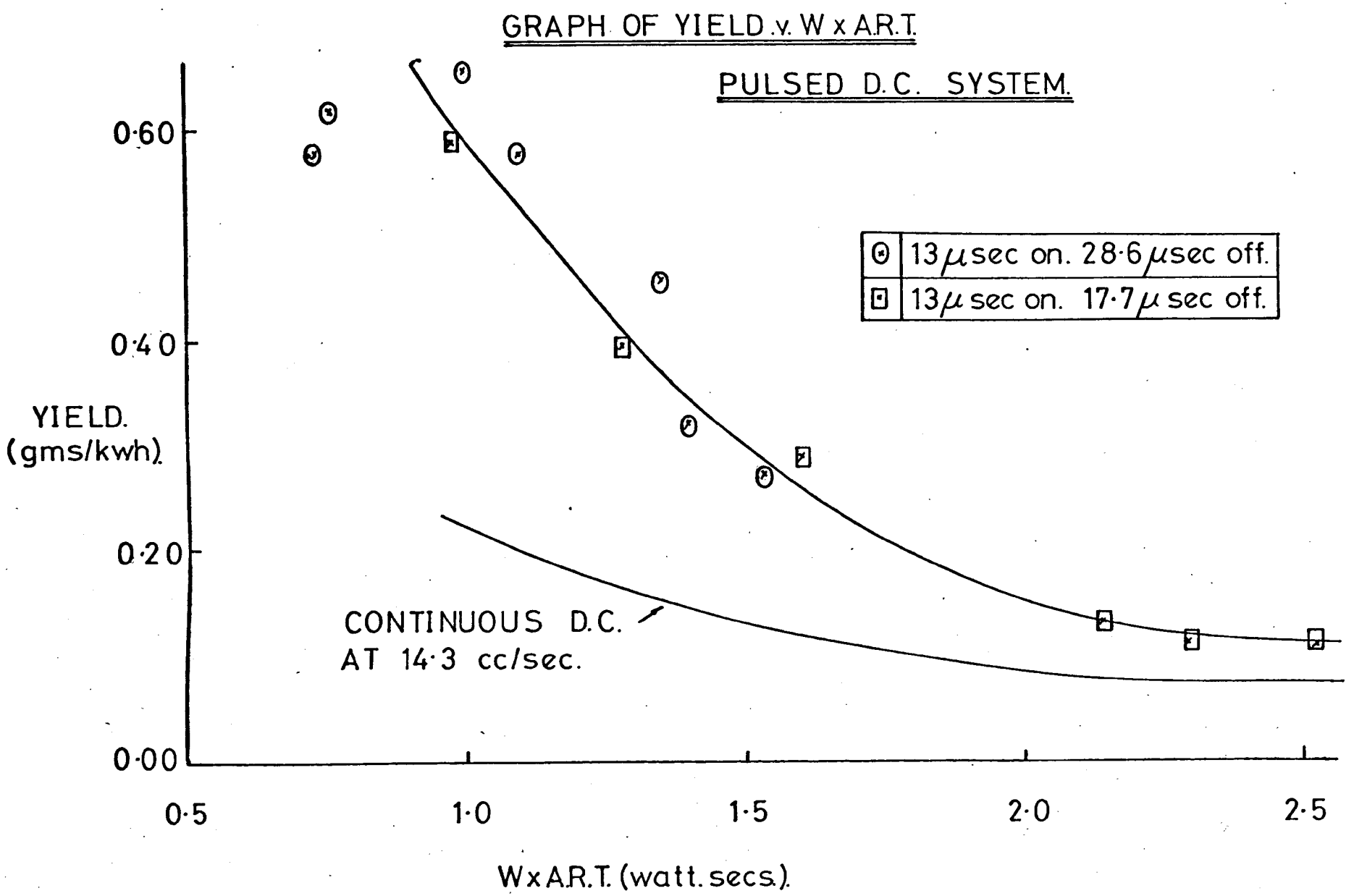
GRAPH OF YIELD v. W x A.R.T.
PULSED D.C. SYSTEM.
0·60
0·40
0·20
0·00
YIELD.
(gms/kwh)
13 μsec on. 28·6 μsec off.
13 μsec on. 17·7 μsec off.
CONTINUOUS D.C.
AT 14·3 cc/sec.
0·5
1·0
1·5
2·0
2·5
W x A.R.T. (watt. secs.)

favoured by short pulse off times. The apparent contradiction of short pulse off times giving high yields for a given value of Wx Θ' is resolved when we consider the corresponding pulse on times. A tenfold increase in pulse off time for a given Wx Θ' means a tenfold decrease in pulse on time, so the fact that short pulse off times give high energy yields for a given Wx Θ' means a decrease in pulse on time gives a greater increase in energy yield than the equivalent increase in pulse off time. Ouchi's experiments were carried out at pulse on and off times of 2.5msec and 0.71 seconds respectively and the results lie in the region one would expect for a pulse off time of 0.71 seconds as shown in fig. 34.

(ii) Correlation of conversion to hydrazine with W/F.

The graph of conversion to hydrazine .v. W/F for the continuous d.c. system falls into two distinct regions, one for low gas velocities and one for high gas velocities. This is again in agreement with previous results and shows more degradation than one would expect occurs at a gas flowrate of 14.3 cc/secs. The other curve is typical of a product being formed then degraded, reaching a maximum conversion to hydrazine of 2.2 wt % at a W/F value of 1.2 watt secs. Unfortunately this W/F value corresponds to an energy yield of less than 1 gm N_2H_3/kwh.

fig 36 GRAPH OF CONVERSION .v. W × GRT.

CONTINUOUS D.C. SYSTEM

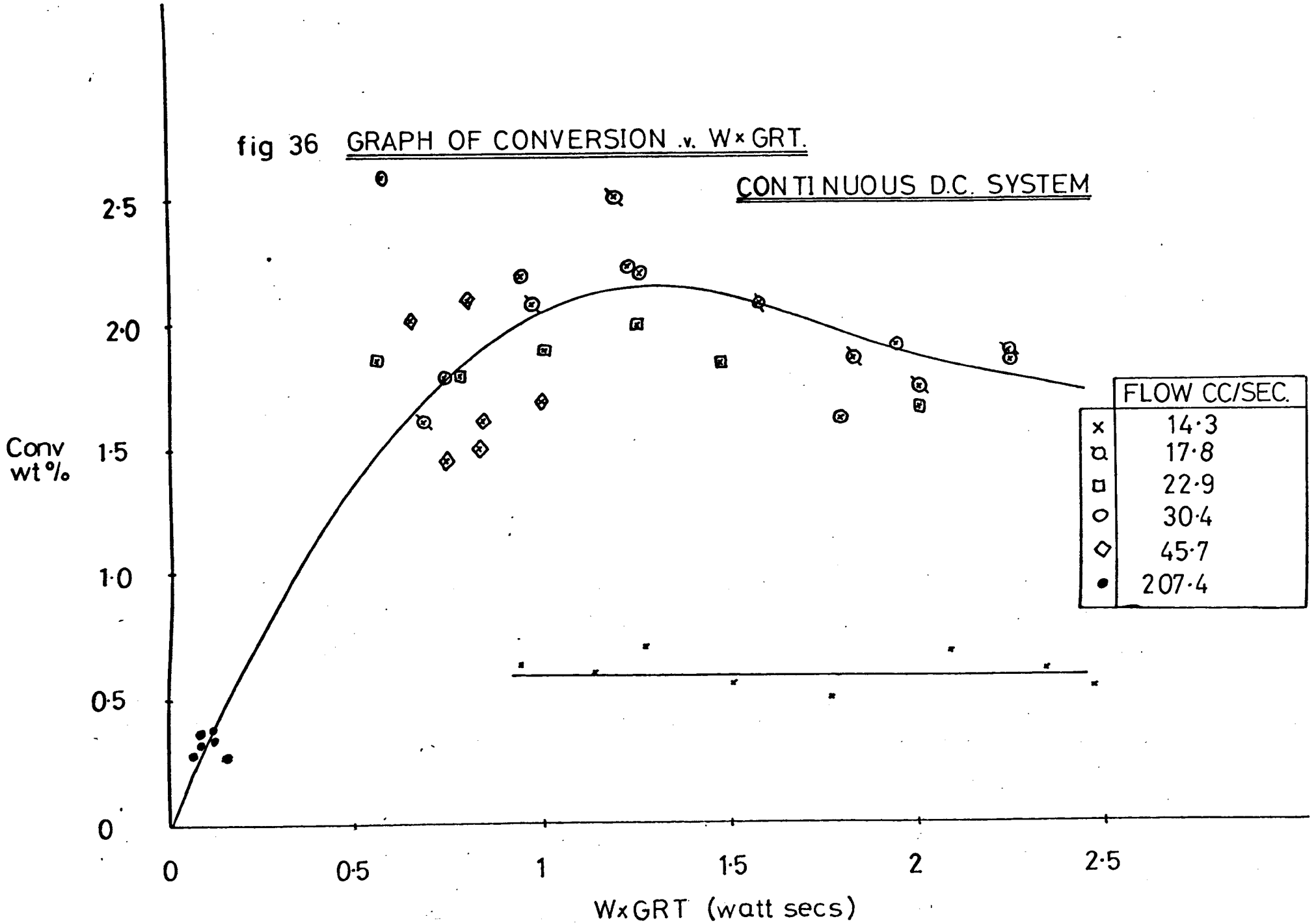

For the pulsed d.c. system the results lie on different curves for different off times as is the case with energy yield. Graphs plotted in the ranges of $WX\Theta'$ from $0 - 10^{-2}$ and $0 - 10^{-3}$ show high conversions are favoured by high values of $WX\Theta'$ and short pulse off times. The curves do not pass through a maximum in these ranges because the values of $WX\Theta'$ are not high enough. Some pulsed d.c. experiments were carried out at very short pulse off times giving active residence times in the range of the continuous d.c. results. When these are plotted fig.39 we get a similar graph to the continuous d.c. graph fig.36. The conversion to hydrazine passes through a maximum at just under 2 wt % conversion and a $WX\Theta'$ value of approximately 1.1 watt seconds. The conversion falls faster than in the continuous d.c. case but tends to the value found in the d.c. case at the same gas flowrate. This is what one would expect because at high active residence times, pulse off times are short and hence the pulse system tends to a continuous d.c. case.

6.5 Simplified kinetic model of discharge processes.

The correlations given above are useful in predicting results of different operating conditions and to give a general guide to the effects occurring in the discharge. An attempt has been made to study the rapid changes occurring in a glow

fig 37. GRAPH OF CONVERSION v. W x ART.

PULSED D.C. SYSTEM.

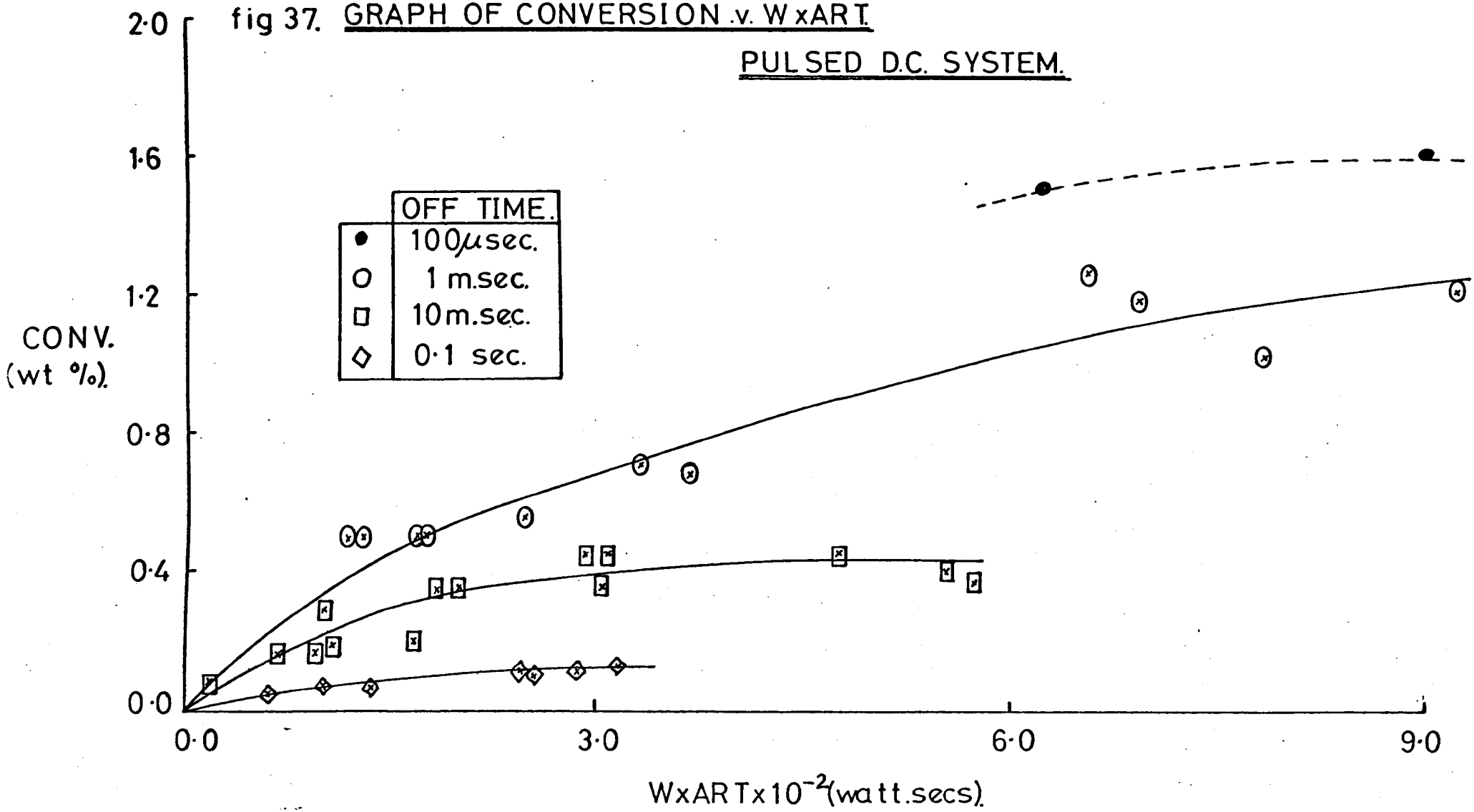

fig 38. GRAPH OF CONVERSION v. WxART.

PULSED D.C. SYSTEM.

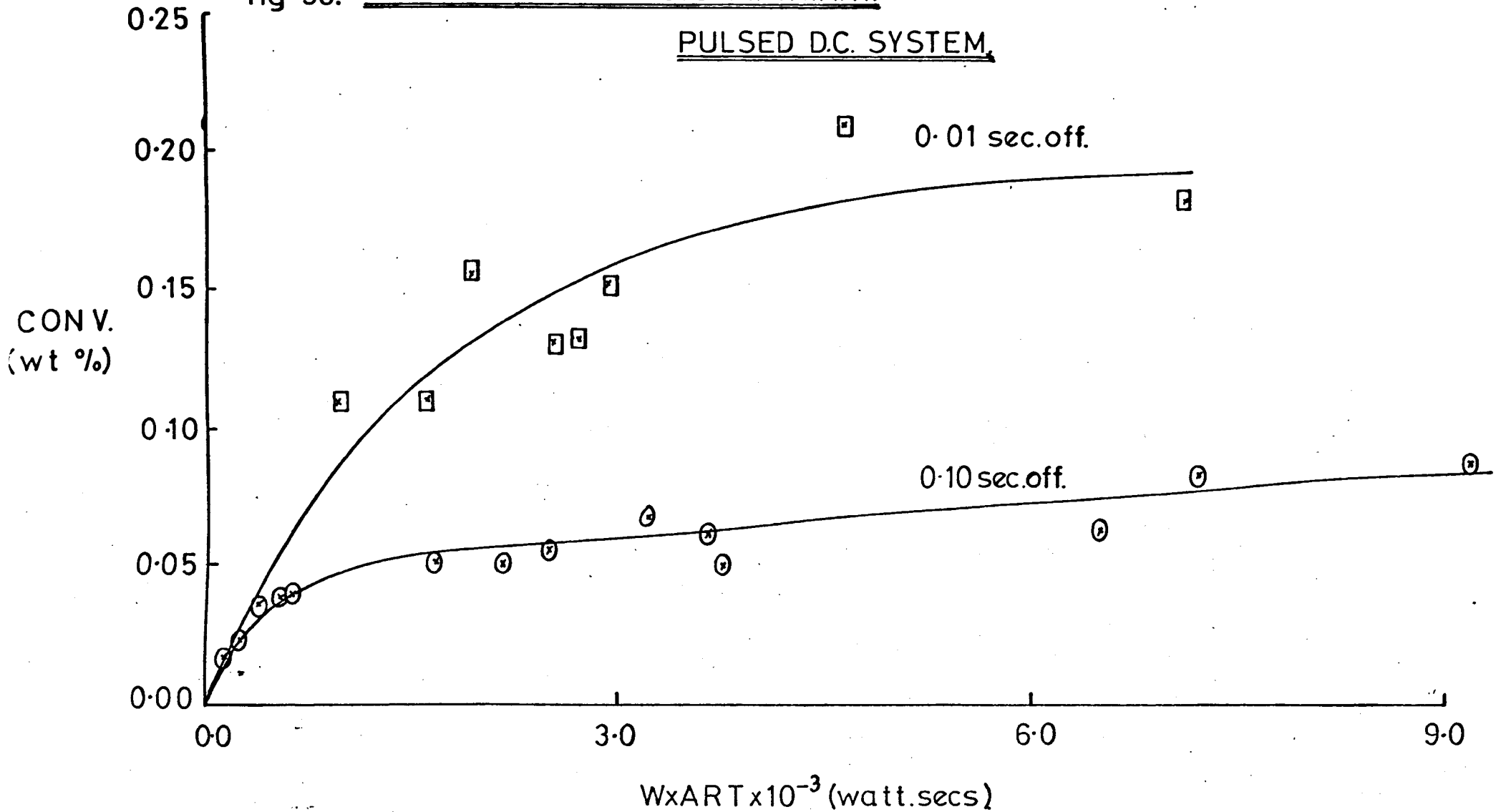

fig 39. GRAPH OF CONVERSION v W x A.R.T.

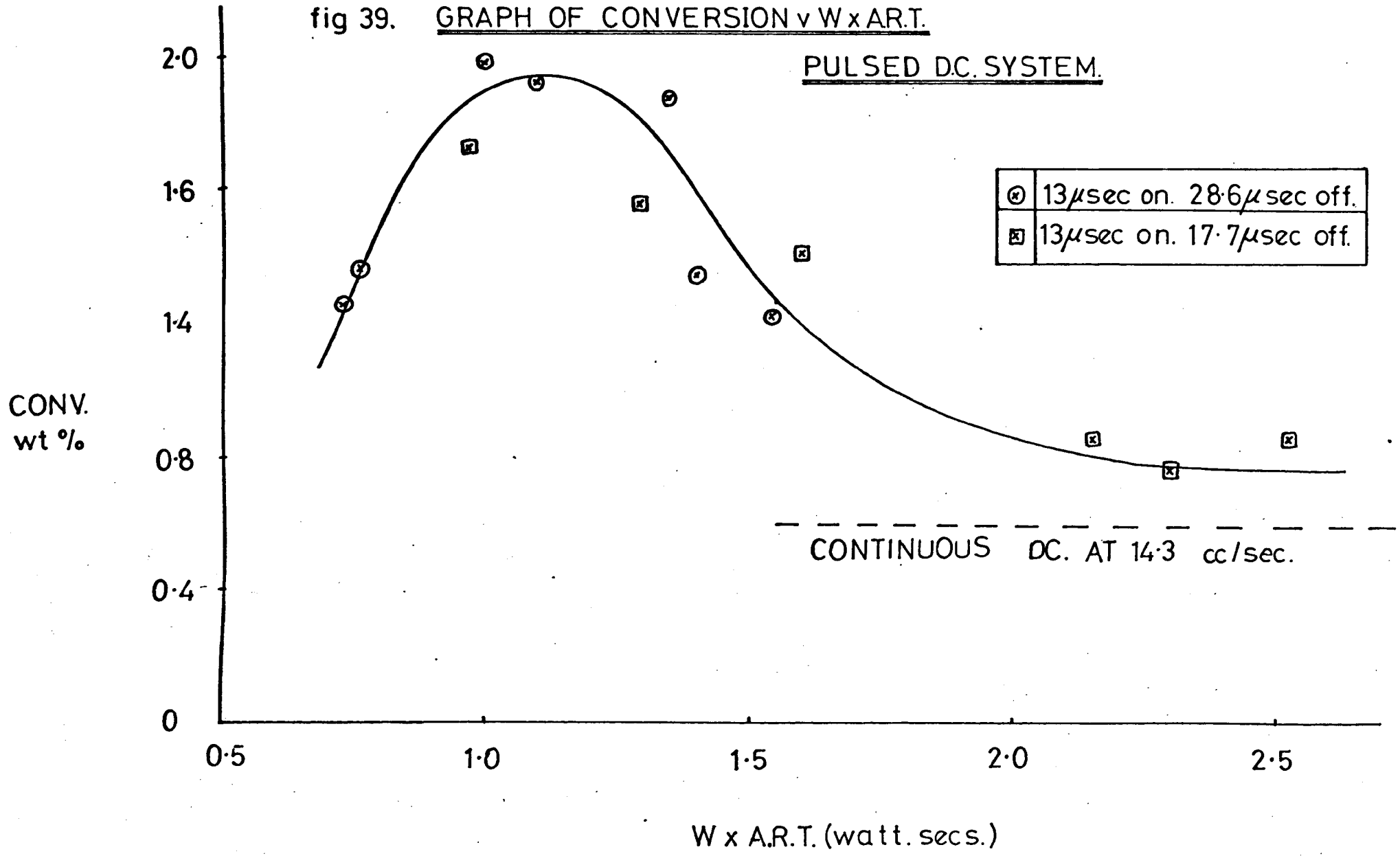

discharge by setting up a mathematical model of the reactions occurring.

Over fifty different free radicle and ionmolecule reactions are possible in the glow discharge decomposition of ammonia. Obviously it is not feasible to cover all these reactions. Using Andersons[3] review of reactions six major reactions were considered.

$NH_3 + e \longrightarrow NH_2 + H$ (i)

$H + \text{wall} \longrightarrow \frac{1}{2} H_2$ (ii)

$NH_2 + NH_2 \longrightarrow N_2H_4$ (iii)

$NH_2 + \text{wall} \longrightarrow \frac{1}{2} N_2H_4$ (iv)

$H + N_2H_4 \longrightarrow {}^{5}/_{4} H_2 + N_2$ (v)

$NH_2 + N_2H_4 \longrightarrow 3H_2 + {}^{3}/_{2} N_2$ (vi)

Ionmolecule reactions are not included since ions have been shown to account for only a small proportion of the reaction products[98]. Recent work by Mantei and Bair[95] has shown the reaction.

$NH_3 + e \longrightarrow NH + H_2$ (vii)

not to be the primary decomposition reaction, rather that NH is produce via

$NH_3 + e \longrightarrow NH_2 + H$ (i)

$2NH_2 \longrightarrow NH_3 + NH$ (viii)

$2NH_2 \longrightarrow N_2H_4$ (iii)

$NH_3 + NH \longrightarrow N_2H_4$ (ix)

Since reaction (viii) occurs at a much slower rate than reaction (iii), only reaction (iii) is considered. The rates of reactions (iii) and (v) are known from the literture so we only need to know the rates for (ii) (i) (vi) and (iv). However, there is also the possibility of hydrazine being broken down by electron impact in the discharge. Some estimate must be made of the rate at which this will occur. The relative rates of electron decomposition of ammonia and hydrazine must be some function of the proportion of electrons with sufficient energy to break the chemical bonds in those molecules and the collision cross sections. The ineleastic collision cross sections for hydrazine and ammonia are not known at the electron energies occuring in the discharge so it is assumed the ratio of the collision cross sections is proportional to the cross sectional areas of the molecules.
With the above assumptions the rate of hydrazine decomposition by electron impact can only be an order of magnitude guide but this may be sufficient to ascertain what the effect the precise control of electron energies in the discharge would have on discharge processes. It has been shown in appendix 1 the average electron energy in the positive column is approximately 1.25 ev.

Knowing the electron energy distribution and the bond strengths of N-H and N-N as 104 ev/mole and 58 ev/mole respectively, we find 6.5% of the electrons present have sufficient energy to break the N-H bond and 25% sufficient energy to break the N-N bond. Taking the cross sectional areas of N_2H_4 to NH_3 as 2:1 we obtain as a first approximation the ratio of the rate of electron decomposition of hydrazine to that of ammonia as 7.7:1. Another indication of the relative rates of reaction between electrons, hydrazine and ammonia can be found from the work of the Takahashi[138] using a 100 MC discharge. From her initial slope data and assuming no difference between the electron energies in the 8.4 mmHg and 11.0 cm discharges, we find the rate of reaction of hydrazine with electrons is 10.0 times faster than that of the reaction of electrons with ammonia. This is very close to the previous estimate despite the inherent assumptions of both methods. Subsequent analysis has shown the kinetic fit is not very sensitive to the rate constant for electron degradation of hydrazine over the range above.

With this and other known data the mathematical model was solved to give the best fit to the experimental results for the continuous d.c. system.

Fig.40. shows the model fits the experimental results well for residence times of less than one second but over one second there is a large discrepancy. Further trials were made to try and find a kinetic model and reaction rates which fitted data over the whole range, for example, reducing the hydrogen recombination rate constant makes the hydrazine conversion pass through a maximum but the shape of the curve would not then fit all the initial results. Among the reasons for the discrepancy at high active residence times could be

(i) Other unknown important reactions are occurring

(ii) Published reaction rates and mechanisms are not totally correct.

(iii) Primary reactions rates change with time.

(iv) Temperature effects are occurring in the discharge.

Of these (iv) is the most likely, with the previous correlations also showing this difference for the low flowrates results.

Fig.41. shows the NH_2 radicle concentration build up and reaches an equilibrium value very rapidly because of the extremely fast rate of reaction (iii). The H atom concentration also builds up very rapidly but falls again as the hydrazine concentration increases indicating the H atom concentration is decreased by reaction with the hydrazine. On this basis conversions

fig 40.

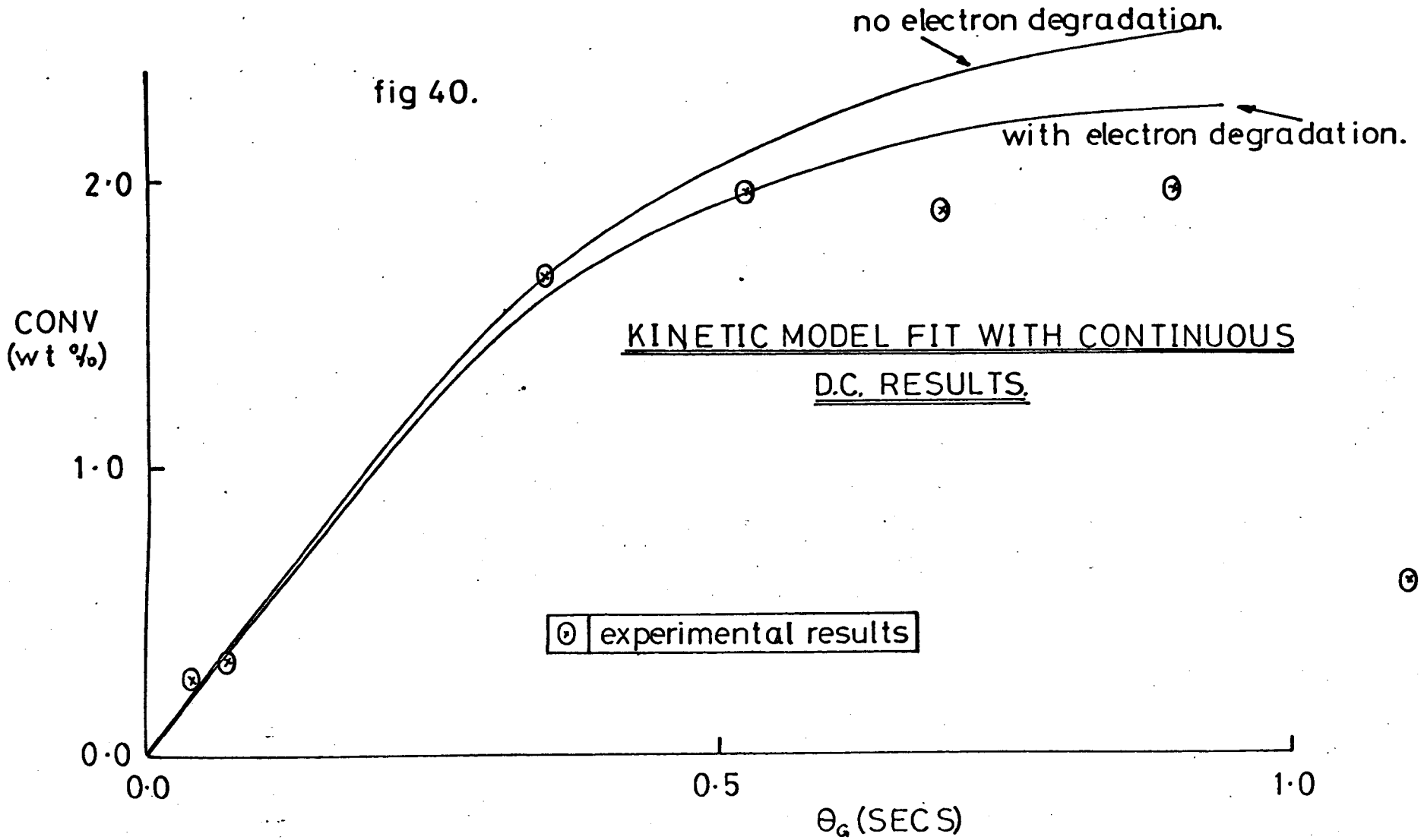
no electron degradation.
with electron degradation.
KINETIC MODEL FIT WITH CONTINUOUS
D.C. RESULTS.
experimental results
CONV
(wt %)
2·0
1·0
0·0
0·0
0·5
1·0
θ_G (SECS)

in the continuous d.c. system could be increased by reducing the H atom concentration by providing extra wall area. When the rate constant for the H atom recombination was increased pro rata with the increase in wall area with the glass wool packing the model predicted a conversion of 2.71 wt% to hydrazine at a residence time of 0.35 seconds. This is not far from the conversion of 3.30 wt% found experimentally.

The model indicates electron degradation of the hydrazine does make a slight difference to the conversion to hydrazine. If the mean electron energy could be reduced it should decrease the amount of degradation of hydrazine, but it would also decrease the rate of primary reaction and this in turn could decrease the energy yield. An optimum electron energy must exist for the continuous d.c. system and it should be possible by adjusting the reduced field strength to arrive at a mean electron energy at this optimum value. However, it must be remembered a range of electron energies will be present in the glow discharge.

The rate data calculated from the continuous d.c. system was used to predict the conversion of a single 13μsec pulse (series 13). The model predicted a conversion of 0.57×10^{-4} wt% to hydrazine whereas experimentally the conversion was found to be higher at 0.004 wt%. In a pulsed

d.c. discharge with long pulse off times, at the start of the pulse the gas is at a very low level of ionization so a high voltage of approximately 3kV is needed before breakdown occurs. This results in a very high initial field strength and consequently high rate of primary reaction. Free radicles are formed very rapidly but the discharge pulse is so short very little hydrazine is actually formed whilst the discharge power is on. The radicles react in the pulse off time period to give hydrazine free of electron degradation therefore high electron energies can be tolerated provided they do not fragment the ammonia into only nitrogen and hydrogen atoms.

Examination of the rate constants shows the kinetic model predicts a primary rate of 2.2×10^{-3} sec $^{-1}$ mA^{-1} whilst converting the value given from correlation data in section 6.4.1 to sec^{-1} mA^{-1} gives a primary rate of 7.3×10^{-3} sec $^{-1}$ mA^{-1}. Ouchi also calculated the rate of primary reactions for an interelectrode distance of 6.3cm at 20 mA but at 6mmHg ammonia pressure, as 0.86×10^{-3} sec $^{-1}$ mA^{-1}. These rates of reaction agree to within an order of magnitude only. Further work at different pressures and currents with complete analysis of all products should enable a more accurate estimate of the primary rate of reaction to be made.

fig 41. FORMATION OF HYDRAZINE AND FREE RADICLES WITH PULSE ON TIME.

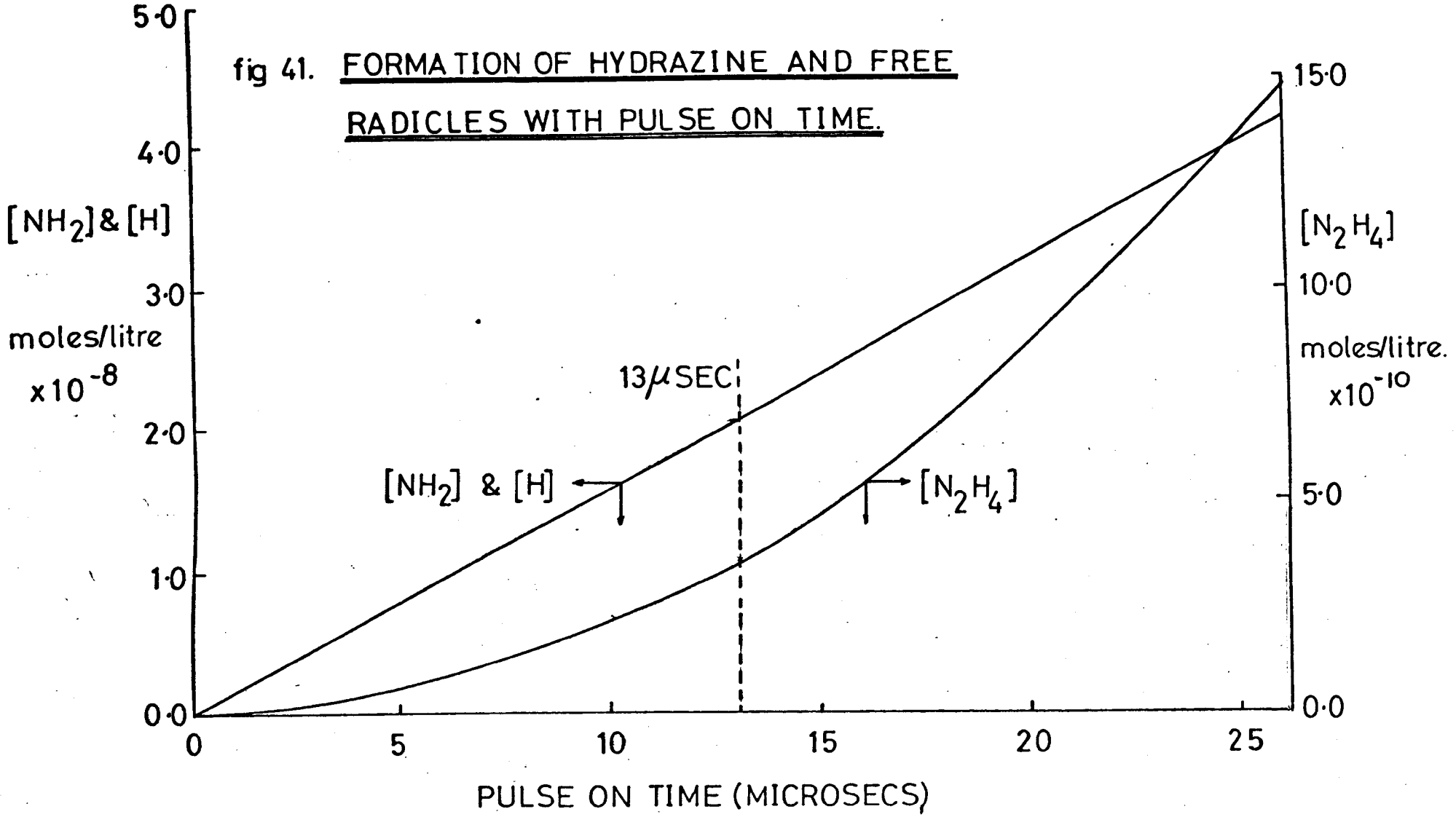

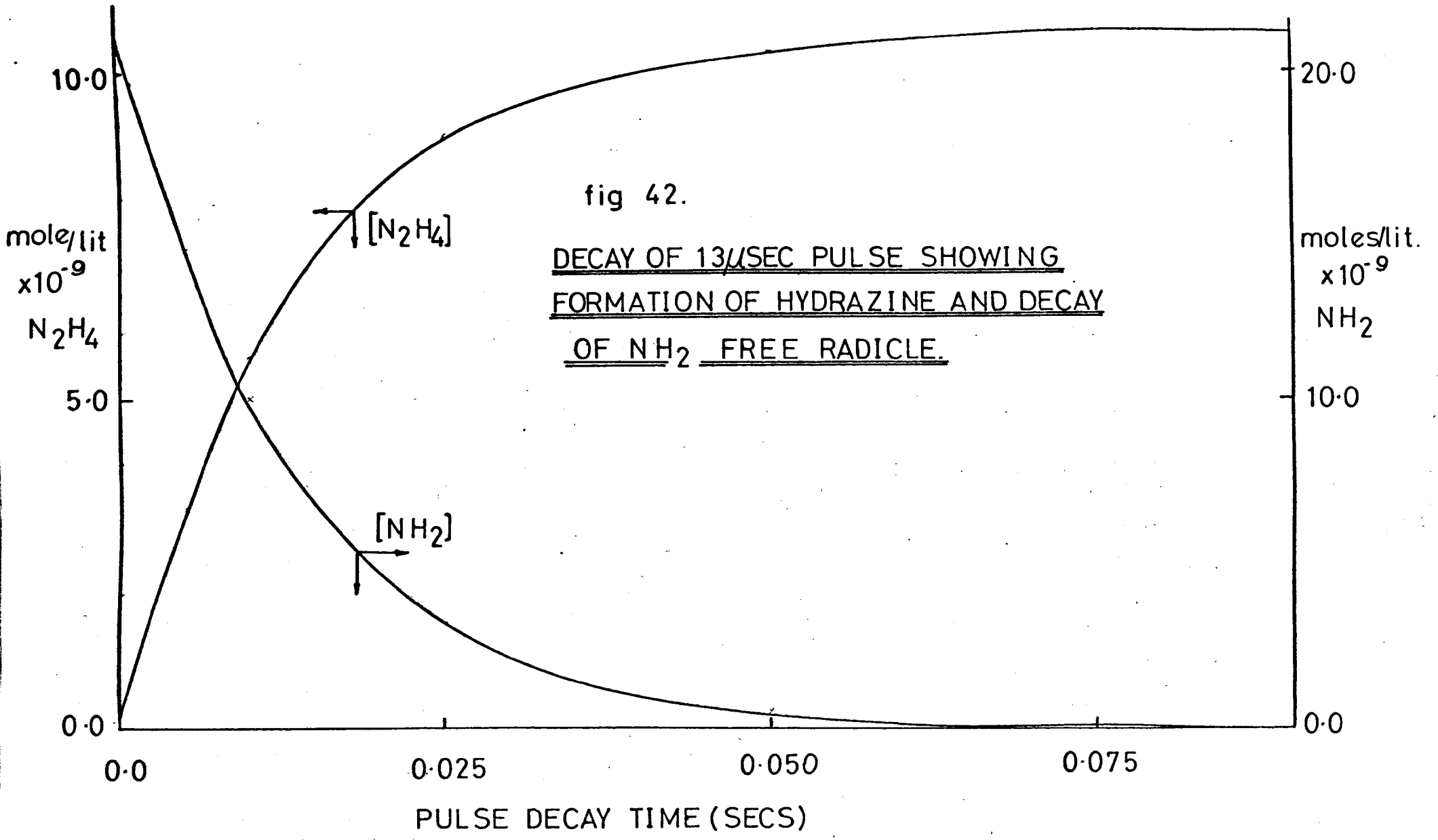

fig 42.

DECAY OF 13μSEC PULSE SHOWING FORMATION OF HYDRAZINE AND DECAY OF NH_2 FREE RADICLE.

The rate of wall recombination of 2.1 $sec^{-1}cm^{-2}$ determined by the kinetic model seems slightly high but this is probably due to the action of the discharge itself. High rates of recombination have been reported in discharges[113] and discharges have been used to increase absorption rates in absorption columns.[144]

6.6 Accuracy of Data.

An indication of the experimental errors occuring is shown in the scatter of results about the fitted regression lines. The standard deviation and varience of the slope of the lines is given together with the results in appendix.2.

The pressure within the apparatus remained constant during a run and could be maintained and measured to within 0.5 torr. Flowrate, as measured on the flowmeters oscillated very slightly because of bubbles forming in the absorption bottle tubes. This resulted in adjustment and reading of flow to $\pm$ 0.1 of the desired value, representing an error of the less than 4% in the flowrate.

One of the major sources of error was the colourimetric analysis of the hydrazine absorbed in the ethane diol. Although great care was taken the percentage absorption readings obtained on the spectrophotometer could only be reproduced to 1%, representing an error of some 6% in the quantity of hydrazine present.

Potentiometric titration of hydrazine may improve this accuracy for higher concentrations of hydrazine but the colourimetric method was still the most accurate at the time of completion of this work.

Errors in the measurement of power input for the continuous d.c. system result from inaccuracies in measuring and reading voltages and current. The milliameter could be read to within $\pm$ 0.5 mA or within $\pm$ 3.3% error at 15mA. The valve voltmeter could be read to within 2% of the voltage reading, however, non random errors occur and manufacturers quote an overall accuracy of only 5% full scale deflection.

The measurement of power dissipated in a pulsed discharge constitutes a major source of error. Errors occur in the measurement, recording, enlarging and integrating of waveforms.

To find the error in the enlarging and integrating of waveforms, tests were carried out using triangular and semi-circular waveforms whose integrated area could be calculated mathematically The difference between the calculated result and the computer result was less than 1%. With actual pulsed discharge waveform greater irregularities occur and repeat integrations showed computed

areas varied by ± 2% from the mean. With long pulse off times variation between pulses within an experimental run was a major problem. Individual pulses could vary from the mean by upto 20% but by taking a series of photographs and averaging the integrated area the percentage error at a 95% confidence limit was reduced to 11.9% in the worst case of a 13 μ sec pulse on time and a pulse off time of 1.12 seconds. With very short pulse off times the variance between pulses was very much less and one waveform photograph represented the average waveform of several oscillascope trace sweeps. Non random errors could have been introduced by the oscillascope since both horizontal sweep and vertical deflection amplifiers were only accurate to 3%. The limited frequency response of the amplifiers may also cause very high frequency components of the waveform not to be detected but errors introduced in this way are probably very small. Despite errors in the equipment the oscillascope used is one of the best available for this type of work.

7.0 Recommendations for future work.

The work presented in this thesis was all carried out with one reactor system. The number of different reactor systems and parameters which could be studied is enormous but any system should aim to minimise unwanted degradation reactions and maximise the efficient utilization of power input.

In any direct current system the negative glow region is inefficient in producing hydrazine and the fraction of energy dissipated in this region should be minimised. This can easily be done, providing suitable d.c. power supplies are available, by increasing the interelectrode distance. The power dissipated in the negative glow region will remain the same but power in the positive column will increase hence increasing the fraction of useful power dissipated in the positive column. As the interelectrode distance is increased, higher gas velocities must be used to maintain low residence in a parallel flow arrangement. With a cross flow arrangement much lower gas residence times can be achieved for a given gas velocity and as such is the preferable arrangemtnt to use in future work. The use of a cross flow arrangement with long interelectrode distances should lead to high energy yields.

One of the best ways of increasing the conversion of ammonia to hydrazine is by reducing the degradation of hydrazine by hydrogen atoms. Addition of scavenger gases will effectively reduce the hydrogen atom concentration but the subsequent separation of hydrazine from the product gases will be more complex and costly. The use of platinum on the reactor walls and electrodes to reduce the hydrogen atom concentrations is also prohibitively expensive commercially. Apart from the glass wool packing used in this work a spray of liquid ammonia could be added to the reactor to provide extra area of recombination and also absorb some of the product. No additional purification step would be required and the low temperature of the liquid could prevent heating up of the reactor. Charlton[142] reported increased energy yields of hydrazine by spraying ethane diol into the glow discharge, The droplets in the spray provide extra area for recombination of hydrogen atoms and results correspond closely to results with glass wool packing in this work, in that with the spray or packing, energy yields increased in the continuous d.c. system but did not change in the pulsed d.c. system.

With a pulsed d.c. system high yields result from high rates of primary reaction and short pulse on times. Pulse on times were limited to 5 μ sec in this work because of lack of equipment giving short high power discharge pulses, however, equipment is now available giving pulse on times as low as 1 μ sec. Use of such equipment should give high energy yields and also provide data to give a more accurate prediction of the effect of pulse on times and off times upon energy yield of hydrazine.

The problems of measuring the power in short pulses are considerable. Errors are introduced in each stage of measuring the signals, photographing, enlarging, and integrating the traces. The process is very time consuming and does not provide an immediate indication of the power input so the power cannot be set to a predetermined value. An analogue network to continuously monitor, multiply and integrate the voltage and current, would overcome most of these problems. A suitable circuit is shown in fig.43. which will give the power in any given number of pulses. Unfortunately multiplying units are not available with a high enough frequency response to deal with the very rapid voltage changes occuring in the discharge pulse without

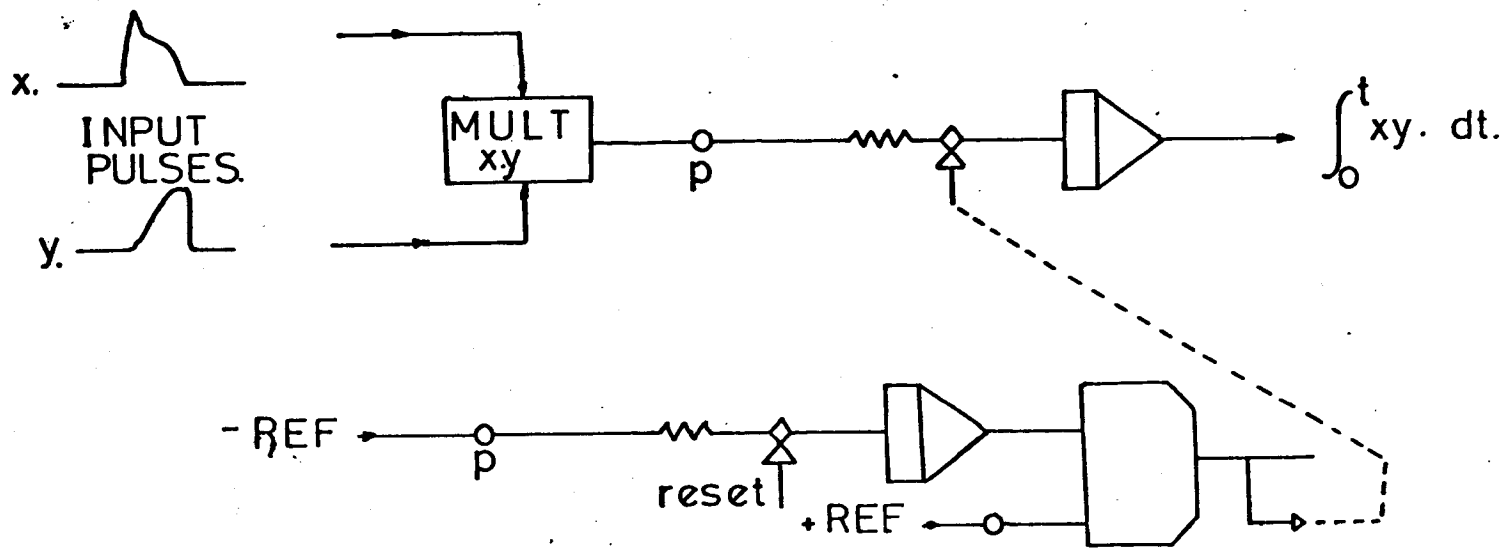

fig. 43. ANALOGUE NETWORK TO CONTINUOUSLY MEASURE AND DISPLAY POWER INPUT INTO PULSED D.C. DISCHARGE.

causing oscillations or severe damping of waveforms.

To be commercially viable a process for the glow discharge synthesis of hydrazine must be capable of producing large quantities of product. This suggests the use of large reactors operating at higher pressures, however, very little is known of the scale up of glow discharge reactors. Similarity criteria are known and it would be interesting to test these criteria in simple reactors of different sizes. One of the parameters used is the reduced tube radius, R_p cm mmHg. R_p has been shown to effect the reduced field strength value in the discharge and the yield of product. Work by Devins and Burton[34] indicates the optimum reduced tube radius is approx 8 cm mmHg c.f. a value of 9 cm mmHg used in this work. The low optimum value of the reduced tube radius severely limits the range of reactor tube diameters and operating pressures which can be used. Several small reactors connected together may well be a better solution to the problem of high throughputs

rather than one large reactor with the wrong physical characteristics. Further work is needed on the control of power input into several discharges connected in series or parallel

The glow discharge can easily produce free radicles and it should be possible to react these radicles with other molecules. A considerable amount of work has been carried out with ammonia and other molecules to form amino compounds in a glow discharge.[29,97,99,101,112] This is a promising field which may well give useful results.

A full understanding of glow discharges and the reactions occuring in them will only be possible when more basic data is known. The inelastic collision cross section for low energy electrons say 0 - 50 e.v. in ammonia are needed in order to accurately determine the primary rate of reaction at different electron energies and operating conditions. A greater understanding of the pulsed d.c. system would result from mass spectrometer sampling from the discharge, especially the pulse decay. The work on the kinetic model could be extended with this data to cover further pulsing conditions, pressures, flowrates, added gases and reactor systems.

With this sort of information perhaps we could look forward to more rapid progress in the utilization of glow discharges for chemical synthesis.

8.0 CONCLUSIONS.

8.1 Chemical Effects.

8.1.1 Continuous direct current discharge.

(i) The power input to the reactor effects both the yield and conversion of ammonia to hydrazine. The energy yield decreases exponentially with increasing power giving an equation of the form

$$\log(\text{energy yield}) = 1.5 - 1.33(\theta_G) - \pi\,(1 - 1.66(\theta_G) + 1.66(\theta_G)^2)$$

The conversion of ammonia to hydrazine passes through a maximum with increasing power. The position of the maximum occurs at increasing power density with increasing gas flowrate. Analysis showed the maximum conversion should occur at a gas flowrate of 28.6 cc/sec and at a power density of 1.69 watts/cc of reactor volume. The maximum conversion recorded was 2.3 wt %.

(ii) High gas flowrates give higher energy yields than low gas flowrates but the conversion passes through a maximum with flowrate.

(iii) The above findings are probably due to the fact that rate of formation of hydrazine increases with power input and its concentration tends to increase with time. However, as the

hydrazine concentration increases, the extent of the degradation of hydrazine with free radicles also increases so giving the observed maxima.

Consideration of bond energies, electron energies and a tentative kinetic model indicate only a small amount of hydrazine is degraded by electron impact.

The abnormally low conversions found at long residence times of approx 1 sec can be explained by heating effects. Hydrogen atoms combining on the wall would heat up the reactor walls. This would reduce their subsequent rate of recombination and hence increase the concentration of hydrogen atoms in the gas. In turn the increased concentration of hydrogen atoms would increase the extent of the degradation of hydrazine and hence reduce the conversion.

(iv) An experiment to check the effect of area available for recombination of hydrogen atoms was carried out using glass wool packing in the reactor to increase the wall area. Under these conditions the energy yield and conversion to hydrazine increased by approx 100%. This indicates that solid surfaces are beneficial in increasing the recombination rate

of hydrogen atoms and hence in reducing the degradation rate of hydrazine.

(v) A kinetic model showed that the rate of electron inpact was low at 2.2×10^{-3} sec^{-1} mA^{-1}.

(vi) Addition of helium to the discharge gas caused a fall in yield and conversion to hydrazine probably because energy gained by the helium from electron impact was not transferred to the ammonia.

(vii) The parameter W/F correlated the results with respect to conversion but the correlation falls into three regions with respect to energy yield. These regions can be accounted for in terms of electrical and wall effects.

8.1.2 Pulsed direct current discharge.

(i) The effect of power input and flowrate on the energy yield and conversion to hydrazine are the same as in the continuous d.c. case. The conversion passes through a maximum with respect to both flowrate and power input. Energy yield decreases with decreasing flowrate and decreases exponentially with increasing power.

(ii) A plot of energy yield and conversion to hydrazine for the continuous d.c. and pulsed d.c. systems over the same range of active residence times showed that the pulsed d.c. system gave higher energy yields and conversions.

A pulsed d.c. discharge is not merely a method of acheiving low active residence times but must have physical and chemical attributes which give rise to faster reaction rates and less degradation of product.

(iii) High energy yields of hydrazine are formed by long pulse off times and short pulse on times but for high conversions to hydrazine we need short pulse off times. The conversion passes through a maximum with increasing pulse on time, with the position of the maximum dependent upon the pulse off time. Energy yields of hydrazine of over 40 gms/kwh were found using a pulsed system.

(iv) The addition of glass wool packing to the reactor had no effect on energy yield or conversion to hydrazine indicating little if any significant reduction in degradation occurred.

(v) The expression which best correlates the energy yield with pulse on time and pulse off times within the theoretical constraints of the system is

$$\text{Energy yield} = 146\left\{1 - e^{\frac{-4.6\times10^{-3}}{\log(\text{on time} + 1)\,(\Theta')^{\frac{1}{2}}}}\right\}$$

(vi) A kinetic model showed the reason for the higher yields and conversions to hydrazine

were due to a higher rate of electron impact. A high field strength exists in a pulse giving higher energy electrons and hence a higher rate of electron impact. The free radical concentrations build up rapidly whilst the discharge power is on but react very quickly afterwards so the overall radical concentration is low hence degradation of the hydrazine is reduced.

8.2 Electrical effects.

(i) The continuous d.c. discharge operated in the abnormal glow region where an increase in current is accompanied by a slight increase in voltage.

(ii) The mean electron energy in the positive column of the continuous d.c. discharge was calculated to be approx 1.25 ev.

(iii) The shape of the pulsed d.c. discharge waveform was dependent upon the pulse on time, pulse off time and power input.

(iv) If the pulse off time was increased to 10 milliseconds or longer the discharge became difficult to strike and maintain. This was probably due to charged species diffusing to the walls between pulses.

9.0 NOMENCLATURE.

A = Constant in calculation of V_B

A = Parameter in equ $Y = A - B\pi$

B = Constant in calculation of V_B

B = Parameter in equ $Y = A - B\pi$

C = $\mathrm{Ln}\left(\frac{A}{\mathrm{ln}\,(1+1/\gamma)}\right)$

D_a = Ambipolar diffusion coefficient

D_e = Interelectrode distance

D_e^1 = Effective interelectrode distance

E = Field strength

E_{em} = Energy transfer

e = Charge of electron

F = Acceleration

f = Gas flow rate

h = Planks constant

i_t = Instanteous current at time t.

J = Current density.

k = Rate constants

k_+ = Positive ion mobility

M = Mass of molecule or ion

M_f = Mass flowrate of ammonia

m = Mass of electron

N_e = Number of electrons

N_m = Number of molecules

P = Pressure of gas

Q = Collision cross section

R = Tube radius

R_p = Reduced tube radius

T = Pulse on time

T_e = Electron temperature

T_f = Formative time lag

T_g = Molecular gas temperature

T_s = Statistical time lag

t = Instantaneous time

t_f = pulse off time (secs)

t_{on} = pulse on time (microsecs)

U = Energy change

V = Reactor volume

V_B = Breakdown voltage

V_B^1 = Maintenance voltage

V_i = Ionization potential

V_{min} = Minimum maintenance voltage

v = Velocity of electron

$\bar{v}$ = Mean electron velocity

V_t^e = Instantaneous voltage

W = Power input

X = Conversion to hydrazine

X_f = Electric field strength

Y = Energy yield of hydrazine (gm/kwh)

γ = Number of ions

λ = Mean free path of electron

Π = Power density (watts/cc)

Θ_G = Gas residence time (secs)

Θ' = Active residence time (secs)

ρ = Gas pressure.

10.0 References

1 Akerlof G.C. U.S.pat. 2,728,723 (1955).

2 Altshuller A.P. J. Chem. Phys. 22 1947 (1952)

3 Anderson W.H. Zwolinski B.J. Parlin. R.B. Ind Eng. Chem. 51 527 (1959)

4 Andrews J.G. & Varey R.H. Nature 225 270 (1970).

5 Audrieth L.F. & Mohr Chem. Eng. News 26 3746 (1948)

6 Audrieth L.F. & Ogg B.A. "The Chemistry of Hydrazine" Wiley (1951).

7 Bair E.J. Lund J.T. & Cross P.C. J. Chem. Phys. 24 (5) 961 (1956)

8 Bamford C.H. Trans Farad Soc 35 568 (1939).

9 Baxter Aircraft Eng. 19 249 (1947).

10 Bayes K.D. Becker K.H. & Welge K.H. Z.Nat. 18a 900 (1963)

11 Bayes K.D. Kivelson D & Wong S.C. J. Chem. Phys 37 1217 (1962)

12 Beck A.H.W. Handbook of vacuum physics vol a partl Fundermentals of electric discharges in gases Macmillan (1967)

13 Berghaus B. Ger 736, 568 (1943)
& Steache M. Ger 1, 193, 921 (1965)

14 Besson A. Compt. Rend 152 1850 (1911)

15 Blanc M.L. Z Electrochem 14 361-6 (1908)

16 Boehm E & Bonhoeffer K.F. Z. Phys Chem. 119 385 (1926)

17 Bredig G. Koenig H & Wagner O.M. Z. Phys Chem. 139A 211 (1928)

18 Brewer A.K. & Westhaver J.W.
J Phys Chem 33 883 (1929)
ibid 34 153 (1930)

19 Briner E & Hoefer H Helv Chim Acta 25 96 (1942)

20 Brise E.A. & Melville H.W. Proc. Roy Soc A175 164 (1940)

21 Brown B.A. Howarth C. Newcastle University. Private Communication.

22 Bruche E. Ann Physik 1 93 (1929)
ibid 83 1065 (1927)

23 Carbaugh D.C. ph.D thesis Maryland University (1967)

24 Carbaugh D.C. & Marchello J.M. J.Opt. Soc Am 56 (6) 836 (1966).

25 Carbaugh D.C. Marchello J.M. & Munno F.J. J. Chem Phys 47 (12) 5211 (1967)

26 Cotton W.J. Tran. Electrochem. Soc. 91 407,409 (1947)
U.S. patsp 2,468,173-7
2,485,476-7

27 Court G.R. & Sayers J. Brit.J.Appl.Phys 15 923 (1964)

28 Cress A. Fr. pats. 1,002,329-30 (1952)

29 Cznchajowski L. Halina F & Wanda G.
Recz Chem. (in English) 42 (4) 697-702 (1968)
ibid 869-74

30 Dainton F.S. Trans. Farad. Soc. 60 1068 (1964)

31 Davies J.H. Z.Phys Chem. 64 657 (1908)

32 Dawson P.H. & Tickner A.W. J.Chem. Phys. 40 3745 (1964)

33 Derwish G.A.W. Galli A. Guidoni A.G. & Volpi GG. J. Chem. Phys 39 (6) 1599 (1963)

34 Devins J.C. & Burton M. J.Am Chem. Soc. 76 2618 (1954)
Brit. pat. 735, 655
Ger. pat. 1,036, 229
U.S. pat. 2,849, 357 (1955)

35 Dibeler V.H. Frankling J.L. & Reese R.M. J.Am Chem. Soc. 81 68-73 (1959)

36 Diesen R.W. J. Chem. Phys 39 2121 (1963)

37 Dixon J.K. J. Am.Chem. Soc. 54 4262 (1932).

38 Dundas P.H. Thorpe M.L. Chem. Eng. (6) 123 (1969)

39 Elgin J.C. & Taylor H.S. J. Am.Chem. Soc. 51 2059 (1929)

40 Von Engel A. "Ionized Gases" 2nd Ed. OUP (1965)

41 Faraday M "Researches in electricity" London 1844.

42 Fillippov Yu V. Zh Fiz Khim 24 1009 (1950)
ibid 24 845 (1950)

43 Finch G.I. Ger. pat. 1,132, 897 (1962)

44 Fite W.L.

45 Foner S.N. & Hudson R.L. 28 719 (1958)
J.Chem. Phys 29 442 (1958)
Advances in Chem.Ser 36 34 (1962)
J.Chem Phys 45 40 (1966)

46 Fritsch C.P. Chem. Eng. Prog. 57(3) 37-41 (1961)

47 Frost D.C. McDowell G.A.
Can. J. Chem 45 1343 (1967)
ibid 36 39 (1958)

48 Gaussens G. Compt. Rend. C262 1613 (1966)
Fr. pat. 1,464, 158 (1966)

49 Gredye G.R. Rideal E.K. J.Chem.Soc. 1932 1169

50 Ghosh K.P. & Bair E J.Chem.Phys 45 4738 (1966)

51 Gray P. Trans. Farad Soc. 60 1047 (1964)

52 Gregory S.A. Chem.Eng. (London) CE 329 (1966)

53 Griesheim K. Ger.pat. 1,114,238 (1962)

54 Groth W, Welge K.H. Bull Soc.Chim. Belge 71 705 (1962)

55 Guenebaut H Pannetier G & Gondmand P.
J.Chem. Phys 58 513 (1961)

56 Gunther P. Holzapfel L. Zph. Chem. B38 211 (1957)

57 Haines M.H. & Bair E.J. J.Chem Phys 38 672 (1962)

58 Harrie & Von Engel J.Chem.Phys 19 514 (1951)

59 Harrison A.G. & Thyme J.C.J. T. Farad Soc. 62 2804 (1966)

60 Helland E.J. U.S.pat. 3,444,061 (1966)

61 Henley R.H. Reed J.W. "The behavior of slow electrons in gases" Amalgamated Wireless Ltd. p81 (1941)

62 Hertel G.R. & Koski W.S. J.Am.Chem. Soc. 86 1683 (1964)

63 Hickling A. N.R.D.C. Brit. pat. 896,113 (1962)

64 Hickling A & Newns G.R. Proc.Chem.Soc. 272 (1959)
ibid 368 (1959)
J.Chem.Soc. 5177 (1961)
ibid 5186 (1961)

65 Hornberg H. Haertere:- Tech Mitt 17 82 (1962)

66 Horscraft R.C. Trans Farad Soc. 60 323 (1964)

67 Howard R.R. & Smith W.V. Phys.Rev. 79 128 (1950)

68 Howard & Browne J.Am. Chem.Soc. 55 1968 (1963)
ibid 3211 (1963)

69 Howatson A.M. "An Introduction to gas dicharges" Pergammon (1965).

70 Imperial Chemical Industries.
Brit. pat. 958, 776 - 8 (1964)
966, 406 (1964)
948, 772

71 Ingraham T.R. Can. J. Chem. 30 168 (1952)

72 Jackson K. & Bloom M.S. Brit.pat 915,771

73 Jogaro A & Sastri B.S.R. J. Sci.Ind.Res (India) 18B 197 (1968)

74 Johnson G.R.A. & Simic M. Adv.chem.series 82 197 (1968)
Nature 216 479 (1967)

75 Jolly W.L. Tech. Imorg. Chem. 1 179 (1963)

76 Jones F.T. & Sworski T.J. Trans Farad Soc. 63 2411 (1963)

77 Kahn S & Standefer F.R. A.E.C. AccNo 40947 Rept No AGN 8137 (Vol 1)

78 Klarfeld B.N. "Investigations into Electrical Discharge in gases" McMillan (1964)

79 Koeing A & Wagner O,M. Z.Phys Chem. 144A 213 (1929)

80 Kolditz L. Zh Phys. Chem. 218 108 (1961)

81 Kouzmine E. Fr. pat. 966, 320 (1950)

82 Lampe F.W. Koski S.W. & Williams Trans Farad Socp 63 2426

83 Landsman D.A. Noble C.H., Atomic Energy Res.Memo M921 (1961)

84 Levy B. Epstein L.M. Handler G. Int. J. Nucleonics 18 128 (1960)

85 Llewelyn-Jones F.
"The glow discharge and an introduction to plasma physics" Methuen (1966)
"Ionization, breakdown in gases" Methuen (1966)

86 Loeb L.B. "Basic processes in gaseous electronics" Univ. California press (1955)

87 Loeb L.B. Fundamental processes of Electrical discharges in gases Ch.XI Wiley 1939.

88 Logan F.E. Marchello J.M. Diss.Abs.29B 2858 (1969)

89 McDaniel E.W. "Collision phenonema in ionized gases" Wiley (1964)

90 McDonald C.C. Gunning H.E. J.Chem.Phys 23 532 (1955)

91 McNesby J.R. & Okabe H & Tanaka I J.Chem.Phys 36 605 (1962)

92 Manion J.P. US pat. 2,849,356 (1958)
3,020,223 (1958)

93 Manion J.P. & Losin E.T. Brit. pat. 1,140,460
US. pats. 3,401,108
3,396,098

94 Mann M.M. Hustralid A & Tate J.T. Phys Rev. 58 340 (1940)

95 Mantei K.A. & Bair E.J. J.Chem. Phys 49 3248 (1968)

96 Marx R & Manchaite G. Adv. Chem. Ser 82 212 (1968)

97 Matsuda T. Odo K. & Sugino K Nippon Kagaku Zasshi 79 324 (1958)

98 Melton C.E. J.Chem.Phys 45 4414 (1966)

99 Miyazaki S Takahashi S
Nippon Kagaku Zasshi 78 552 (1958)
ibid 79 17 (1958)
c.f. Takahashi S.

100 Moore G.E. Schular K.E. Silverman S & Herman R. J.Phys.Chem. 60 813 (1956)

101 Mueller U & Greiner A Chem.Tech 18(6) 327 (1966)

102 Nelson L.S & Ramsey D.A. J.Chem.Phys 25 372 (1956)

103 Neilson R.A. & Bradbury N.E. Phys Rev. 51 69 (1937)

104 Mishikawa M N Shinohara & Maysura N Bull.Chem.Soc.Jap. 40 (8) 1993 (1967)

105 Noyes J. Am.Chem Soc. 47 1003 (1925)

106 Noyes Hammond & Pitts Advances in photochemistry, 3.

107 Okab H & Lenzi M. J.Chem.Phys 47 5241 (1967)

108 Ouchi K. Sci.Repts.Res inst Tohoku Univ.A4 203 (1952)
c.f. also J. Electrochem Soc. Jap 17 285 (1949)
20 164,168,233, 381,378
21 75, 132 (1953)

109 Pack J.L. Voshall R.E. Phelps A.V.
Phys Rev. 127 2084 (1962)

110 Papoular R "Electrical phenonema in gases" Elsevier (1965)

111 Peeters J.L. Rundle H.W. Deckers J.M. Can.J.Chem. 44 2981 (1966)

112 Prilezheava N & Nother H Acta Physiochem URSS (In Eng) 7 811 (1937)

113 Rassou J Optick 23 (4) 362 (1965)

114 Rathsack H.A. Z Phys Chem. 206 285 (1957)
214 101 (1960)
216 246 (1961)

115 Reikrundel E.M. Kustova A.V. & Zimelev A.G.
Z. Tekh Fiz. 24 1179 (1954)

116 Reilly R. Newcastle University Private communication.

117 Rouy A.L.M.A. Peterson CH. Glassock G.B. U.S. 3,003,939 (1955)

118 Rubstova E.A. & Eremin E.N.Zfiz. Khim 40 3110 (1966)
Russ J. Phys Chem. 40 1671 (1966)
Z Fiz Khim 42 1022 (1968)

119 Rummel T. Brit.Pat, 527,899 (1940)

120 Russel A.N. & Bradbury N.E. Phys Rev. 51 69 (1937)

121 Salzman J.D. Bair E.J. J Chem.Phys 41 3654

122 Sasaki N & Ohta Y J.Chem. Soc. Jap 63 1491 (1942)

123 Schenk P.W. Agnew Chem. 50 535 (1937)

124 Schiavello M & Volpi G.G. J.Chem.Phys. 37 1510 (1962)

125 Schnepp O. & Dressler K J.Chem.Phys 32 1682 (1960)

126 Schueler H & Degenhart V. Z Naturforsch 7a 753 (1952)
ibid 8a 251 (1953)

127 Schueler H Ger.pat. 1,116,638 (1959)

128 Schwarz E. Atomstrahlung Med Tech. 284 (1964)

129 Semiokhin LA Andreev Yu P Salimova K.M. &
Garrat F Yu Russ. J.Phys Chem. 42 473 (1968)

130 Skorokhodov II Nekrasov L.I., Kobozev, N.I. & Filonova A.D.
Russ. J.Phys.Chem. 35 503 (1961)

131 Sorokin Yu A. Zh.Fiz.Chim. 39 1955 (1965)

132 Spedding P.L. Nature 214 124 (1967)
Industrial Fellows Rept. Inst Chem.Eng (1968)

133 Srikantan B.S. J. Indian Chem. Soc. 13 79 (1936)

134 Steiner W. Z. Electrochem. 36 807 (1930)

135 Sutton J. Am. Rocket Soc. 72 2 (1947)

136 Suzuki M. Shinku Kagaku 9 61 (1961)
Nippon Kagaku Zasshi 77 873 (1956)

137 Szwarc M. Proc. Roy.Soc. A198 267 (1949)

138 Takahashi S Bull Chem. Soc. 33 1350 (1960)

140 Thornton J.D. Chem.Processing XII (2) 56 (1966)
153rd Nat. Meeting Am.C. Soc.
Div.of Fuel Chem. 2 (2) 291 (1967)
Rev. pure & applied Chem. (Aust) (18) 197 (1968)

141 Thornton J.D. & Spedding P.L. Nature 213 1118 (1967)

142 Thornton J.D. Charlton W.D. & Spedding P.L. "Hydrazine
synthesis in a Silent Electric discharge" 153rd
Nat. Meeting Am.C.Soc. April (1967) 2 pt 1, 128.

143 Turner J.E. Phys. Rev 141 21 (1966)

144 Uchigasaki K et al Kagaku Kagaku 31 (9) 878 (1967)

145 Uhara I Kitagawe J Electrochem. Soc. Japan 16 112 (1948)

146 Varney R.N. J.Chem.Phys 23 866 (1955)

147 Vasilev & Eremin Z. Fiz Khim 7 619 (1936)

148 Vilesov F.I. Kurbatov B.L. Terenin A.N. English translation of Dok Akad Nauk. 122 623 (1958)

149 Van Vorst W.D. & Ahlert R.C. J.Chem. Eng. Data 9 345 (1964)

150 Watanbe K. J.Chem.Phys 22 1564 (1954)

151 Watt G.W. Chrisp J.D. Anal.Chem 24 2006 (1952)

152 Westhaver J.W. J.Phys Chem. 37 897 (1933)

153 Wiener & Burton J.Am.Chem. Soc. 75 5815 (1953)

154 Wigg & Kistickowsky J.Am.Chem Soc. 54 1806 (1932)

155 Wijnen M.H. Austin H. J.Chem.Phys 21 233 (1953)

156 Willey E.J.B. Trans Farad Soc. 39 234 (1943)
Proc. Roy Soc. A152 158 (1935).

A P P E N D I C E S

APPENDIX 1 PAGE

SPECIMEN CALCULATIONS

CALCULATION FROM EXPERIMENTAL RESULTS.

Reactor volume.

Average internal diameter of discharge tube as measured by a telescopic micrometer = 0.7062"

∴ For electrodes 6.3 cm apart reactor volume

= 16.0 ml.

Series 33 Run 89

Energy yield of hydrazine

(i) Grams of hydrazine.

The dreschel bottles contained 100 mls of ethane diol. A sample of the diol was diluted by a factor of 10 and 20 ml of the diluted solution added to the acidified colour solution to make a total volume of 50 ml. This solution contained 0.125 p.p.m. of hydrazine. Therefor number of grams of hydrazine in dreschel bottles

$$= \frac{0.125}{10^6} \times \frac{50}{20} \times 10 \times 100 \quad \text{gms}$$

$$= \underline{3.13 \times 10^{-4} \text{ gms.}}$$

(ii) Energy input.

Power/pulse = Power pulse area x v/cm(volts) x v/cm(amps) x μ sec/cm x enlargement factor x pulse circuit factor x conversion to Kwh

$$= 90.8 \times 2.0 \times 5.0 \times 20.0 \times 0.061 \times 4.34 \times 0.287 \times 10^{-12}$$

$$= \underline{13.4 \times 10^{-10} \text{ Kwh/pulse}}$$

No of pulses = $\frac{\text{Run time}}{\text{Pulse on + off time}} = \frac{8.0 \times 60}{1.009 \times 10^{-2}}$

$= \underline{4.81 \times 10^{4}}$

(iii) Energy yield.

Energy yield = $\frac{\text{Gms hydrazine}}{\text{kwh/pulse x no pulses}}$

$= \frac{3.13 \times 10^{-4}}{13.4 \times 10^{-10} \times 4.81 \times 10^{4}}$

$= \underline{4.92 \text{ gms/kwh.}}$

Power density.

Power density = $\frac{\text{Power/pulse}}{(\text{Pulse time}) \times (\text{Reactor volume})}$

$= \frac{13.4 \times 10^{-10} \times 10^{3} \times 2.54 \times 3600}{12.2 \times 20 \times 10^{-6} \times 16}$

$= \underline{3.13 \text{ Watts/cc reactor volume.}}$

Conversion to hydrazine

Conversion = $\frac{\text{Grams hydrazine formed} \times 100}{\text{Grams ammonia passed}}$ wt %

Ammonia passed in 8 mins = 14.3 x 8 x 60 cc at operating conditions

$$= \frac{14.3 \times 8 \times 60}{10^3} \times \frac{10}{760} \times \frac{273}{293} \times \frac{17}{22.4} \text{ gms}$$

$$= 0.0637 \text{ gms } NH_3$$

$$\therefore \text{ Conversion} = \frac{3.13 \times 10^{-4} \times 100}{0.0637} \text{ wt \%}$$

$$= \underline{0.494 \text{ wt \%}}$$

CALCULATIONS OF MEAN ELECTRON ENERGY. -

Method 1.

Bailey & Duncanson measured the ratio of mean electron temperature to molecular gas temperature for different reduced field strengths in ammonia. Hence if the reduced field strength can be found the mean electron energy can be determined.

We are interested in this mean electron energy in the positive column since this is the area where most of the hydrazine is formed. From Ouchis data it is seen for an interelectrode distance of 6.3 cm the positive column would be 5 cm long. Westhaver measured the cathode fall voltage for aged electrodes as 350 volts hence for the reactor used in this work operating at 10 mm Hg with a total applied voltage of approx. 950 v we get the reduced field strength in the positive column as:-

$$\frac{950 - 350}{5 \times 10} = 12 \quad \text{volts/cm/mmHg.}$$

From Bailey & Duncansons data we find Te/Tg = 32
Hence if the molecular gas is at 293°K the mean electron energy in the positive column = 1.23 ev

Method 2.

Method 2 uses the reduced tube radius data given in von Engel. VonEngel measured the ratio of electron temperature to ionization potential for different values of C.P.R. i.e.

$$Te/Vi = f(CPR)$$

Where $C = \dfrac{(a\, V_i^{\frac{1}{2}})^{\frac{1}{2}}}{k^+ \quad P}$

Ionization potential V_i = 11.2 e.v.

Pressure P = 10 mm Hg

Tube radius R = 0.9 cm

In the absence of more accurate data:-

the mobility k_+ is taken as 0.7×10^3 cm/sec/volt/

the constant a is taken as 25×10^{-2}

Hence $C = \left(\left(\dfrac{25 \times 10^{-2} \times (11.2)^{\frac{1}{2}}}{0.7 \times 10^3 \times 10}\right)\right)^{\frac{1}{2}} = 1.1 \times 10^{-2}$

$\therefore$ $CPR = 1.1 \times 10^{-2} \times 10 \times 0.9 = 9.9 \times 10^{-2}$

At a CPR value of 9.9×10^{-2}, $Te/Vi = 8.6 \times 10^2$

$\therefore$ Mean electron energy $= \dfrac{8.6 \times 10^2 \times 11.2}{7740}$ e.v.

$= \underline{1.25 \text{ ev}}$

Although the value calculated from both methods agree very closely this agreement must not be taken as a measure of the accuracy of the determination. Method 1 is sensitive to small changes in the E/P value and Method 2 uses extrapolated and inadequate data. The values given are probably only accurate to within 50%. Despite this the results are accurate enough to give an indication of the extent of electron degradation of hydrazine.

Computer programme for calculation of power in discharge pulse.

The programme multiplies the instantaneous voltage with the instantaneous voltage and integrates the result w.r.t. time. A trapezium rule intregration method is used.

Data fed in is of the form:-

q = number of sets of data

X = initial time coordinate

Y = initial instantaneous current coordinate

Z = initial instantaneous voltage coordinate.

x, y = current x,y coordinate.

ex, z = voltage x,y coordinates.

- 1 = terminating number for that set of data.

```
QE08 D SAVAGE VOLT AMP CURVE INTEGRATION→

begin
real l,x,ex,avx,y,z,t,avt,h,a,sum,X,Y,Z;
integer q,m,i,f,n;
open(20); open(30);
f:=format([ss-d.ddddₓ+nd]);
q:=read(20); m:=0;
SET: m:=m+1; if m>q then goto END;
begin
sum:=0;  l:=0;
X:=read(20); Y:=read(20); Z:=read(20);
L:x:=read(20); if x>0 then
begin
y:=read(20);ex:=read(20);z:=read(20);
avx:=(x+ex)/2;
t:=(z-Z)×(y-Y);
avt:=(t+l)/2;
h:=avx-X;
a:=avt×h;
sum:=sum+a;
X:=avx;   l:=t;
goto L;
end
else  begin
write(30,f,sum);
newline(30,1);
goto SET;
end;
END: end;close(20); close(30);
end→
```

Computer programme for calculation and analysis of results.

The programme determines if the results are for a continuous or pulsed d.c. systems, calculates the energy yield, conversion to hydrazine and power density from the experimental measurements. The coefficients of the linear regression log yield = a - bπ are then calculated together with the variance of b and the standard deviation.

Data fed in is of the form:-

flow = gas flowrate in cc/sec at operating conditions

pulsed = +1 if pulsed d.c. run, - 1 if continuous d.c.

n = no of sets of results.

dil = factor by which ethane diol was diluted.

runt = duration of run.

IF pulsed d.c.

out = pulse on time microseconds

oft = pulse off time seconds.

ppm = p.p.m. hydrazine analysed

kwhpulse = kwh/pulse as previously calculated

tlen = base length of pulse in cm.

IF continuous d.c.

ppm = p.p.m. hydrazine analysed.

watts = mean power input.

Results were also checked manually.

```
CED3   D SAVAGE  PULSED...D.C. RESULTS→


begin
real flow,ont,oft,dil,runt,ppm,kwhpulse,
    tlen,watts,a,b,xbar,ybar,resid,sigma,varb,
pie,logey,YN2H4,GMN2H4,GMNH3,conv;
integer pulsed,f,f1,f2,i,n;

procedure
       wkpls(n,dil,runt,ont,oft,ppm,
         kwhpulse,tlen,gm,kwh,yield,pi);
real
    ont,oft,dil,runt,ppm,kwhpulse,tlen;
array gm,kwh,yield,pi;
integer n;
        begin
          writetext(30,[***ppm[6s]kwhpulse[7s]gm[10s]
          kwh[9s]yield[9s]pi[c]]);
    write(30,f1,ppm);
     write(30,f1,kwhpulse×10-10);
    gm[i]:=ppm×10×dil×10-6/0.04;
    write(30,f1,gm[i]);
    kwh[i]:=runt×kwhpulse×10-10/oft;
   write(30,f1,kwh[i]);
    yield[i]:=gm[i]/kwh[i];
    write(30,f1,yield[i]);
   pi[i]:=kwhpulse×1.429×4/tlen;
    write(30,f1,pi[i]);
    newline(30,2);
    end ;
```

```
procedure
        wkdc(n,dil,runt,ppm,watts,
        kwh,gm,yield,pi);
    real dil,runt,ppm,watts;
array gm,yield,pi,kwh;
    integer n;

begin
      writetext(30,[***ppm[10s]gm[10s]watts[8s]
          kwh[9s]yield[9s]pi[c]]);
     write(30,f1,ppm);
  gm[i]:=ppm×10×dil×10-6/0.04;
    write(30,f1,gm[i]);
    write(30,f1,watts);
    kwh[i]:=watts×runt×1×10-3/3600;
    write(30,f1,kwh[i]);
  yield[i]:=gm[i]/kwh[i];
    write(30,f1,yield[i]);
    pi[i]:=watts/16;
  write(30,f1,pi[i]);
  newline(30,2);
end of wkdc poc;


procedure
        STATS(m,x,y,a,b,xbar,ybar,resid,sigma,varb);
real resid,sigma,varb,xbar,ybar,a,b;
array x,y;  integer m;
```

```
begin
        real ssx,ssy,spxy,
             sumx,sumy,
               sumx2,sumy2,sumxy;
      integer df,i;

writetext(30,[****Xbar[7s]Ybar[11s]a=[10s]b=[8s]RESID[7s]
              SIGMA[8s]VARb[c]]);
sumx:=0:sumy:=0:sumx2:=0;sumy2:=0;sumxy:=0;

for i:=1step 1until m do
  begin

sumx:=sumx+x[i];
sumy:=sumy+ n(y[i]);
sumx2:=sumx2+x[i]↑2;
sumy2:=sumy2+ n(y[i])↑2;
sumxy:=sumxy+x[i]× n(y[i]);

end;

ssy:=sumy2-sumy↑2/m;
ssx:=sumx2-sumx↑2/m;
spxy:=sumxy-sumx×sumy/m;

  b:=spxy/ssx;

xbar:=sumx/m;ybar:=sumy/m;

   a:=ybar-b×xbar;

resid:=ssy-spxy↑2/ssx;

  df:=m-2;

sigma:=sqrt(resid/df);

varb:=sigma↑2/ssx;



write(30,f1,xbar);      write(30,f1,ybar);
write(30,f1,a);    write(30,f1,b);
write(30,f1,resid);    write(30,f1,sigma);
write(30,f1,varb);
end of stats proc;


open(20); open(30);
f:=format([s-ddd.dd]);
f1:=format[[ss-d.ddd10+nd]];
f2:=format[[-d.ddd10+nd]];


writetext(30,[***experimental*results]);
newline(30,2);
flow:=read(20); pulsed:=read(20); n:=read(20);
  dil:=read(20); runt:=read(20);
```

```
writetext(30,[flow=]);    write(30,f,flow);
begin
    array gm[1:n],kwh[1:n],yield[1:n],pi[1:n];


if pulsed=+1 then
begin
      writetext(30,[******pulsed*dc]);
       newline(30,1);

 ont:=read(20); oft:=read(20);
writetext(30,[***on*time=]);  write(30,f2,ont);
writetext(30,[sec**off*time=]);  write(30,f2,oft);
writetext(30,[sec]);  newline(30,4);



    for i:=1 step 1until ndo
    begin
       ppm:=read(20);
        kwhpulse:=read(20);
      tlen:=read(20);
    wkpls(n,dil,runt,ont,oft,ppm,
          kwhpulse,tlen,gm,kwh,yield,pi);
    end;
end

else
     begin writetext(30,[*****straight*dc]);
       newline(30,4);


   for i:=1 step 1 until n do
    begin
      ppm:=read(20);
       watts:=read(20);
   wkdc(n,dil,runt,ppm,watts,
                kwh,gm,yield,pi);
   end;end;

newline(30,4);
writetext(30,[statistical*linear*regression*on*results]);
newline(30,2);

STATS(n,pi,yield,a,b,xbar,ybar,resid,sigma,varb);

newline(30,1);


writetext(30,[[p]**watts/cc**conversion]);
newline(30,2);

for pie:=1  step 0.2until 8do
begin
         logey:=a+b×pie;
         YN2H4:=exp(logey);
         GMN2H4:=16×pie×YN2H4;

if flow<14.35 then GMNH3:=4.75₁₀+2
```

```
e_se GMNH3:=10.14**+2;

conv:=GMN2H4x1000/GMNH3;
write(30,f1,pie);write(30,f1,conv);
newline(30,1);
end;
close(20);close(30);
end;
end→
```

Computer programme for determining regression coefficients of a centre cube factorial design.

The form of data required is a centre cube composite design.

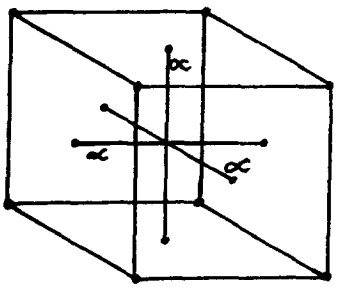

The cube represents a 2^3 factorial design and in this case $\alpha = 1$. In all there are fifteen points.

The value of yield or conversion (y) is given by

$$y = \beta_0 x_0 + \beta_1 x_1 + \beta_2 x_2 + \beta_3 x_3 + \beta_{11} x_1^2 + \beta_{22} x_2^2 + \beta_{33} x_3^2 + \beta_{12} x_1 x_2 + \beta_{13} x_1 x_3 + \beta_{23} x_2 x_3$$

A matrix of these equations is set up and the regression coefficients determined.

Data fed in is of the form

k = number of independent variables (TT, ontime, offtime)

n = number of data points to be fed in (15)

t = number of regression coefficients (9)

steps = an accuracy term (25)

Experimental data

(1,1,1) ; (1,2,2) ; (1:3); y(1);

(3,1,1) ; (3 ;2) ; (3,3) ; y(3);

10^7 = terminating number.

I would like to thank Mr. K.A. Jones for the loan and explanation of this programme.

```
CE03 D SAVAGE RES SURFACE→

begin library A0,A6,A12; integer t,fa; real pmax,pmin,tc;

begin integer i,j,k,m,n,steps,f; real ym,y,ye;

procedure SP(k,n,D,S,RHS,XMV,YM);
value k,n; integer k,n; real YM;
array D,S,RHS,XMV;

comment on entry:

k=number of indipendent variables
n=number of sets of values
D[1:n,1:k+1] contains the sets of values with
the dependent variable y in the last column
if m=k+k×(k+1)/2 then on exit:
S[1:m,1:m] contains the normal equations,the
variables being taken in the order;
x[1],...x[k],x[1]×x[1],x[1]×x[2],...,x[1]×x[k],
x[2]×x[2],....,x[k]×x[k]
RHS[1:m] contains the righthand sides for the
normal equations
XMV[1:m] contains the means of the indipendent
variables in the equations
YM is the mean value of the dependent variable;

begin integer i,j,m,p,q;

m:=k×(k+1); m:=k+m/2;

comment clear space for sums;
YM:=0;
fori:=1 step 1 until m do
begin XMV[i]:= RHS[I]:=0;
for J:=1 step 1 until m do S[i,j]:=0end;

comment form crude sums;
begin array z[1:m];
for I:=1 step 1 until n do
begin for J:=1 step 1 until k do z[j]:=D[i,j];
j:=k+1;
for p:=1 step 1 until k do
for q:=p step 1 until k do
begin z[j]:=z[p]×z[q]; j:=j+1 end;

for p:=1 step 1 until m do
begin for q:=p step 1 until m do
S[p,q]:=S[p,q]+z[p]×z[q];
RHS[p]:=RHS[p]+z[p]×D[i,k+1];

XMV[p]:=XMV[p]+z[p]
end;
YM:=YM+D[i,k+1]
end

end;
```

```
comment form means and corrected sums of products;
for I:=1 step 1 until m do
begin S[1,I]:=S[I,I]-XMV[I]/n×XMV[1];
XMV[I]:=XMV[1]/n;  RHS[1]:=RHS[1]-XMV[1]×YM;
for J:=1+1 step 1 until m do
S[I,J]:=S[J,I]:=S[I,J]-XMV[I]×XMV[J]
end;
YM:=YM/n
end of SP;


procedure GAUSSRI(a,b,n,m,FAIL,pmax,pmin);
value m,n; integer m,n; array a,b; real pmax,pmin; label FAIL;

begin integer i,j,k; real t;
for I:=1 step 1 until n-1 do
begin
t:=0;
for J:=i step 1 until n do
if abs(a[J,I])>abs(t) then
begin
t:=a[J,i];k:=J;
end;

if t=0 then goto FAIL ;
if k≠1 then
begin
for J:=1 step 1 until n do
begin
t:=a[i,J];a[i,J]:=a[k,J];a[k,J]:=t;
end;
for J:=1 step 1 until m do
begin
t:=b[i,J];b[i,J]:=b[k,J];b[k,J]:=t;
end;
end;
for J:=1+1 step 1 until n do
begin
t:=a[J,i]/a[i,i];
for k:=1+1 step 1 until n do
a[J,k]:=a[J,k]-t×a[i,k];
for k:=1 step 1 until m do
b[J,k]:=b[J,k]-t×b[i,k];
end;
end of pivotel condensation;

if a[n,n]=0 then goto FAIL;
for J:=1 step 1 until m do
begin
for I:=n step -1 until 1 do
begin
t:=0;
for k:=1+1 step 1 until n do
t:=t+a[i,k]×b[k,J];
b[i,J]:=(b[i,J]-t)/a[i,i];
end;
end of back substitution;
pmax:=pmin:=a[1,1];
for i:=2 step 1 until n do
if abs(a[I,I])<abs(pmin) then pmin:=a[i,i]
else if abs(a[i,i])>abs(pmax) then pmax :=a[i,i];
end of procedure GAUSSRI;
```

```
procedure DIAG(A,N,W,Z,steps);
value N; integer N,steps; array A,W,Z;
comment A is lower triangle of symetric N×N matrix (N>1),
(i.e. all elements A[i,j] for which i>j must be given),
W is array of roots in (100,-100) in decreasing order,
Z is array of eigenvectors such that Z[i,j] is the jth component of
iht vector;

begin integer m1; real norm; array C,B[1:N]; boolean array d[0:N];
procedure Htd(n,c,b,a);
value n; integer n;array a,b,c;

begin
integer j,i,k;
real ai,sigma,h,bj,bigk,bi;
array q[1:n-1];
for I:=n step -1 until 3 do
begin sigma:=0;
for k:=1 step 1 until i-1 do
sigma:=sigma+a[i,k]×a[i,k];
ai:=a[i,i-1];
if ai>0 then bi:=-sqrt(sigma) else bi:=sqrt(sigma);
b[i-1]:=bi;

if bi≠0 then
begin
h:=sigma-ai×bi;
a[i,i-1]:=ai-bi;

for j:=i-1 step -1 until 1 do
begin bj:=0;
for k:=i-1 step -1 until j do
bj:=bj:=bj+a[k,j]×a[i,k];
for k:=j-1 step -1 until 1 do
bj:=bj+a[j,k]×a[i,k];

q[j]:=bj/h
end;
bigk:=0;
for j:=i-1 step -1 until 1 do
bigk:=bigk+a[i,j]×q[j];
bigk:=bigk/(2×h);

for j:=i-1 step -1 until 1 do
q[j]:=q[j]-bigk×a[i,j];
for j:=i-1 step -1 until 1 do
begin
for k:=j step -1 until 1 do
a[j,k]:=a[j,k]-a[i,j]×q[k]-a[i,k]×q[j];
end
end
end;

for i:=n step -1 until 1 do
c[i]:=a[i,i];
b[1]:=a[2,1];
b[n]:=0
end;

procedure tdbs 1 (c,b,n,gu,go,t,w,norm,m1);
value n,gu,go,t;
integer n,t,m1;
```

```
real gu,go,norm;
array c,b,w;

begin
integer i,j,k,a1,a2,d;
real t,g,h,lambda,p1,q1,y;
array p[1:n];
procedure sturm;
begin
p1:=0;q1:=1;a1:=0;
for i:=1step 1 until n do
begin
y:=(c[i]-lambda)×q1-p[i]×p1;
p1:=q1;q1:=y;
if p1>0 eqv q1>0
then a1:=a1+1
end;
If q1=0 and p1>0 then a1:=a1-1
end;

if gu>go then
begin g:=gu;gu:=go;go:=g
end;

norm:=abs(c[1])+abs(b[1]);
for i:=2 step 1 until n do
begin t:=abs(b[i-1])+abs(c[i])+abs(b[i]);
if t>norm then norm:=t
end;
  norm:=norm×1.000000001;
for i:=1 step 1 until n-1 do
begin p[i+1]:=b[i]×b[i];
if p[i+1]=0 then p[i+1]:=2↑(-78)×norm×norm
end;p[1]:=0;
if gu>norm or go<-norm then
begin m1 :=0; goto noeig
end;

if go>norm then go:=norm;
if gu<-norm then gu:=-norm;
lambda:=gu;
sturm;
a2:=a1;
if q1=0 then  a2:=a1+1;
lambda:=go;
sturm;
m1:=a2-a1;
d:=a1;
for k:=1 step 1 until m1 do
begin d:=d+1;
g:=go;h:=gu;

for j:=1 step 1 until t do
begin lambda:=(g+h)/2;
sturm;
if a1 ≥d then h:=lambda else g:=lambda
end;
w[k]:=(g+h)/2
end;
noeig :end;

procedure trii1(c,b,n,w,norm,m1,z);
value n,m1,norm;
```

```
integer n,m1; real norm;
array c,b,w,z;

begin
integer i,j;
real bi,bi1,lda,u,v,h,eps,eta;
arraym,p,q,r,int[1:n],x[1:n+2];
lda:=norm;eps:=2↑(-39)×norm;
for j:=1 step 1 until m1 do
begin lda:=lda-eps;
if w[j]<lda then lda:=w[j];
u:=c[1]-lda; v:=b[1];
if v=0 then v:=eps;
for i:=1 step 1 until n-1 do
begin bi:=b[i];
if bi=0 then bi:=eps;

bi1 :=b[i+1];
if bi1=0 then bi1:=eps;
if abs(bi)>abs(u) then
begin m[i+1]:=if abs(u)<eps and abs(bi)≤eps then 1 else u/bi;
p[i]:=bi;
q[i]:=c[i+1]-lda;
r[i]:=bi1 ; u:=v-m[i+1]×q[i];
v:=-m[i+1]×r[i];
int[i+1]:=1
end

else
begin m[i+1]:=bi/u;
p[i]:=u; q[i]:=v;
r[i]:=0;
u:=c[i+1]- da-m[i+1]×v;
v:=bi1; int[i+1]:=-1
end
end;

p[n]:=u; q[n]:=r[n]:=0;
x[n+1]:=x[n+2]:=0; h:=0; eta:=1/n;
for i:=n step -1 until 1 do
begin  u:=eta-q[i]×x[i+1]-r[i]×x[i+2];
if p[i]=0 then x[i]:=u/eps else x[i]:=u/p[i];
h:=h+abs(x[i])
end;
h:=1/h;
for i:=1 step 1 until n do
x[i]:=x[i]×h;

for i:=2 step 1 until n do
begin if int[i]>0 then begin u:=x[i-1];
x[i-1]:=x[i];
x[i]:=u-m[i]×x[i-1]
end
else x[i]:=x[i]-m[i]×x[i-1]end;

h:=0; bi:=0;
for i:=n step -1 until 1 do
begin u:=x[i]-q[i]×x[i+1]-r[i]×x[i+2];
if p[i]=0 then x[i]:=u/eps
else x[i]:=u/p[i];
v:=abs(x[i]);  if v>bi then bi:=v;
end;
```

```
for i:=n step -1 until 1 do
begin x[i]:=x[i]/bi;
h:=h+x[i]×x[i]
end;
h:=1/sqrt(h);
for i:=1 step 1 until n do
z[j,i]:=x[i]×h
end
end;

procedure bktr(a,b,z,n,m1);
value n,m1;
integer n,m1;  array a,b,z;

begin
integer i,j,k;  real s;
for j:=1 step 1 until m1 do
for k:=3 step 1 until n do

if b[k-1]≠0 then
begin s:=0;
for i:= 1 step 1 until k-1 do
s:=s+a[k,i]×z[j,i];
s:=s/(b[k-1]×a[k,k-1]);
for i:=1 step 1 until k-1 do
z[j,i]:=z[j,i]+s×a[k,i]
end
end;
procedure seperate(w,n,norm,deg); value norm,n;
array w; real norm; integer n; boolean array deg;
begin
integer t,i,k; real a;
for i:=1 step 1 until n-1 do deg[i]:=w[i]-w[i+1]<10-7×norm;
deg[n]:=deg[0]:=false;
for i:=1,i+1 while i<n do
if deg[i] then
begin a:=w[i];  t:=1;
for k:=i,k+1 while deg[k] do
begin i:=k;  t:=t+1;  a:=a+w[k+1] end;
w[i+1]:=a/t-(t-1)×510-9×norm;
for k:=i,k-1 while deg[k] do w[k]:=w[k+1]+10-8×norm
end
end;

procedure orth(z,deg,n);  value n;
array z;  boolean array deg;  integer n;
begin real a,b;  integer i,j,k,l;  array v[1:n];
for i:=1 ,i+1 while i<n do
if deg[i] then
begin for j:=i,j+1 while deg[j] do
begin for k:=1 step 1 until n do v[k]:=z[j+1,k];
for l:=1 step 1 until j do
begin a:=0; for k:=1 step 1 until n do a:=a+z[l,k]×z[j+1,k];
for k:=1 step 1 until n do v[k]:=v[k]-a×z[l,k]
end;
b:=0; for k:=1 step 1 until n do b:=b+v[k]↑2;
b:=sqrt(1/b); for k:=1 step 1 until n do z[j+1,k]:=b×v[k]
end;  i:=l
end
end;
```

```
for i:=1 step 1 until m do write(30,f,xmv[i]);
writetext(30,[[ss]]);  write(30,f,ym);
newline(30,6);  writetext(30,[matrix*inversion*of*composite*design[cc]])
begin integer c;
for I:=1 step 1 until t do
begin
for J:=1 step 1 until t do
b[I,J]:= If I=J then 1 else 0 ;
b[i,t+1]:=rhs[i];
end;

GAUSSRI(s,b,t,t+1,END,pmax,pmin);
c:=0;
for i:=1 step 1 until t do
for j:=1 step 1 until t do
begin
c:=c+1;
if c=c+txt then write(30,fa+1,b[i,j])
else write(30,fa,b[i,j]);
end;
writetext(30,[[c]]);
end;

begin real s,rss,rms;
tc:=0;
for i:=1 step 1 until n do
tc:=tc+d[I,k+1]xd[I,k+1];
tc:=tc-nxym↑2;
s:=0;
for i:=1 step 1 until t do
s:=s+b[i,t+1]xrhs[i];
rss:=tc-s;
rms:=rss/(n-1-m);
newline(30,3);
writetext(30,[[25s]anova*table[cc]]);
writetext(30,[S.OF.V[13s]S.S[12s]D.F[15s]M.S[cc]mult*regn[4s]]);
write(30,fa,s);  space(30,8);  write(30,format([dd]),m);
space(30,11);  write(30,fa+1,s/m);  newline(30,1);
writetext(30,[residual[5s]]);  write(30,fa,rss);  space(30,8);
write(30,format([dd]),n-1-m);  space(30,11);  write(30,fa+1,rms);
newline(30,1);  writetext(30,[total[8s]]);  write(30,fa,tc);
space(30,8);  write(30,format([dd]),n-1);  newline(30,3);

begin
comment calculation of the expected value of y i.e.b0;
writetext(30,[expected*value*of*y[c]b0**]);
ye:=ym;
for i:=1 step 1 until t do
ye:=ye-xmv[I]xb[I,t+1];
write(30,fa+1,ye);
end;
writetext(30,[[p]]);
writetext(30,[regression*coefficients*[cc]]);
for i:=1 step 1 until t do
write(30,fa,b[i,t+1]);
newline(30,2);
begin real array se[1:t];
comment the standard errors provided by the square
root of the variance are based on the experimental error varince(rms);

for i:=1 step 1 until t do
for j:=1 step 1 until t do
if i=j then

se[i]:=sqrt(b[i,j]xrms);
```

```
if N=1 then begin W[1]:=A [1,1]; Z[1,1]:=1 end
else
begin
HHd(N,C,B,A);
tdbs1 (C,B,N,-100,100,steps,W,norm,m1);
seperate(W,N,norm,d);
trii1(C,B,N,W,norm,m1,Z);
bktr(A,B,Z,N,m1);
orth(Z,d,N);
end;

end of DIAG;


procedure REGEQ(k,ba,y,bb,e);
value k,ba;  real y; integer k,ba;  real array bb,e;
comment this procedure evaluates the regression equation;
begin Integer p,s,c,d,ee,a,i;
a:=0;
for i:=1 step 1 until k do
y:=y+bb[i]xe[i];
for i:=k+1 step k-(a-1) until (2xk)+ba do
begin comment calculation of quadratic effects;
a:=a+1;
y:=y+e[a]↑2xbb[i];
end;
begin real array q[1:ba];
comment calculation of interaction effects;
for d:=1 step 1 until k do
for c:=d+1 step 1 until k do
q[d]:=e[d]xe[c];
p:=s:=k;
d:=0;
for ee:=0 step 1 until k-1 do
begin
s:=s+(k-ee);
for i:=p+2 step 1 until s do
begin
d:=d+1;
y:=y+q[d]xbb[i];
end;
p:=s;
end;
end;
end of procedure REGEQ;

open(20);open(30);
fa:=format([ss-d.ddddb-nd]);
writetext(30,[COMPOSITE*DESIGN*MATRIX[cc]]);
k:=read(20);  n:=read(20);  t:=read(20);  steps:=read(20);
m:=kx(k+1);  m:=k+m/2;
begin array d[1:n,1:k+1],s,g[1:m,1:m],rhs,xmv[1:m],b[1:t,1:t+1];
for i:=1 step 1 until n do
for j:=1 step 1 until k+1 do d[i,j]:=read(20);
SP(k,n,d,s,rhs,xmv,ym);

f:=format([s-ndd.dddd]);
  writetext(30,[[cc]]);
for i:=1 step 1 until m do
begin writetext(30,[[c]]);
for j:=1 step 1 until m do write(30,f,s[i,j]);
writetext(30,[[ss]]);  write(30,f,rhs[i]);
end;

writetext(30,[[cc]]);
```

```
writetext(30,[standard*errors[c]]);
for i:=1 step 1 until t do
write(30,fa,se[i]);
end;

end;
begin array A[1:k,1:k],b1[1:k,1:1];  integer ab,q,g,z;

comment calculation of the coords of centre,for variables x1.....xk;
for I:=1 step 1 until k do  b1[i,1]:=-b[i,t+1];
q:=z:=k;  ab:=0;
for g :=0 step 1 until k-1 do
begin
ab:=ab+1;
z:=z+(k-g);
for i:=q+1 step 1 until z do
begin
if g=q+ab-1 then A[g+1,i+ab-(q+1)]:=b[i,t+1]x2
else begin
A[g+1,i+ab-(q+1)]:=b[i,t+1];
A[i+ab-(q+1),g+1]:=A[g+1,i+ab-(q+1)];
end;
end;
q:=z;
end;

GAUSSRI(A,b1,k,1,END,pmax,pmin);
writetext(30,[[cc]contour*system*center*coords[cc]]);
 for i:=1 step 1 until k do
 write(30,fa,b1[i,1]);
 newline(30,2);
 begin integer ba ;  real array bb[1:t],e[1:k];
 comment calculation of yield at center coords;
 ba:=0;   y:=ye;
 for i:=1 step 1 until k do
 ba:=ba+(k-1);
 for i:=1 step 1 until t do
 bb[i]:=b[I,t+1];
 for i:=1 step 1 until k do
 e[I]:=b1[I,1];
 REGEQ(k,ba,y,bb,e);

 writetext(30,[[cc]y*value*at*centre*coords[cc]]);
 write(30,fa+1,y);
 begin
 comment calc of expected values from the fitted equ;
 writetext(30,[[cc]comparison*of*expected*and*
 experimental*values[cc4s]expected[10s]actual
 [10s]residual[c]]);

 for i:=1 step 1 until n do
 begin
 for J:=1 step 1 until k do
 e[J]:=d[i,J];
 y:=ye;
 REGEQ(k,ba,y,bb,e);
 write(30,fa,y);  space(30,4);
 write(30,fa,d[i,k+1]);  space(30,4);
 write(30,fa+1,y-d[i,k+1]);
```

```
end;
new line(30,2);
end;
end;
end;
begin array Z,E[1:k,1:k],b[1:k]; integer cd,ga,za,qa;
comment calc of eigenvalues and eigenvectors
of the problem;
cd:=0;   qa:=za:=k;
for ga:=0 step 1 until k-1 do
begin
cd:=cd+1;
za:=za+(k-ga);
for i:=qa+1 step 1 until za do
begin
if ga=qa+cd-1 then E[ga+1,i+cd-(qa+1)]:=b[i,t+1]
else begin
E[ga+1,i+cd-(qa+1)]:=b[i,t+1]/2;
E[i+cd-(qa+1),ga+1]:=E[ga+1,i+cd-(qa+1)];
end;
end;
qa:=za;
end;
DIAG(E,k,b,Z,steps);

writetext(30,[[cc]eigenvalues*and*vectors*of*a*real
symmetric*matrix[cc]]);
for i:=1 step 1 until k do
begin
writetext(30,[[c]eigenvalue*=*]);
write(30,fa,b[i]);  writetext(30,[[c]eigenvector**]);
for j:=1 step 1 until  k do
begin
write(30,fa,Z[i,j]);
if j+k×k=j then newline(30,1);
end;
end;
end;
end;
k:=read(20);  if k>6 then goto END else goto L;
end;
END:close(20);  close(30);
end→
```

Computer programme for solving kinetic model.

The programme uses an Algol Kutta Merson integration procedure to solve the simultaneous differential equations, this is a standard programme approximating to a Taylor series.

Data fed in is of the form:-

n = number of differential equations

y(1) = initial concentration of NH_2 radicles.

y(2) = " " " H atoms

y(3) = " " " hydrazine

t = time at which integration starts (normally zero)

range = time interval for integration

acc = the accuracy to which final and previous values of integration step must agree before next step is taken

h = initial integration step length

k1 = rate constant for $NH_3 + e \longrightarrow NH_2 + H$

k2 = " " " $NH_2 + NH_2 \longrightarrow N_2H_4$

k3 = " " " $H + N_2H_4 \longrightarrow 5/4\ H_2 + N_2$

k4 = " " " $NH_2 + wall \longrightarrow \frac{1}{2}\ N_2H_4$

k5 = " " " $NH_2 + N_2H_4 \longrightarrow 3/2N_2 + 3H_2$

k6 = " " " $H + wall \longrightarrow \frac{1}{2}\ H_2$

e = current in mA

c = ratio of ratio of electron degradation of ammonia and hydrazine.

The programme automatically adjusts h, the step length, to reach any given accuracy and the values of

(H), (NH_2), (N_2H_4), and time are printed out after the completion of each step. kl is also adjusted within the programme such that the hydrazine concentration fits the experimental value at 0.35 sec.

The pulse formation and decay is carried out in two separate runs with kl or e set equal to zero for the pulse decay.

```
CE03 HYDRAZINE KINETICS WITH ELECTRON DEGRADATION→

begin library A0,A6,A12;
 real k1,k2,k3,k4,k5,k6,c,e,q,t,range,acc,h;
 integer n,ft;
open(20); open(30);  n:=read(20);
begin array y[1:n];
procedure KM3 (n,t,y,range,fn,acc,h);
value n,range,acc;
integer n; real t,range,acc,h; array y; procedure fn;
begin integer j; real t1,hn,inc,error; boolean finish;
array z,f0,f1,f2[1:n];
t1:=t+range; finish:=false;
L1:if h×(t+h-t1)≥0.0 then
 begin hn:=h; h:=t1-t; finish:=true end;
fn(k1,k2,k3,k4,k5,k6,c,e,t,y,f0);
L2:for j:=1 step 1 until n do
z[j]:=y[j]+f0[j]×h/3;
fn(k1,k2,k3,k4,k5,k6,c,e,t+h/3,z,f1);
for j:=1 step 1 until n do
 z[j]:=y[j]+(f0[j]+f1[j])×h/6;
fn(k1,k2,k3,k4,k5,k6,c,e,t+h/3,z,f1);
for j:=1 step 1 until n do
 z[j]:=y[j]+(0.125×f0[j]+0.375×f1[j])×h;
fn(k1,k2,k3,k4,k5,k6,c,e,t+h/2,z,f2);
for j:=1 step 1 until n do
 z[j]:=y[j]+(0.5×f0[j]-1.5×f1[j]+2.0×f2[j])×h;
fn(k1,k2,k3,k4,k5,k6,c,e,t+h,z,f1);
inc:=h;
```

```
for j:=1 step 1 until n do
        begin f1[j]:=y[j]+(f0[j]+4.0×f2[j]+f1[j])×h/6;
        error:=0.2×abs(1-f1[j]/z[j]);
        if error>acc then begin h:=h/2;
         finish:=false; goto L2 end;
        if error>0.025×acc then inc:=0.0
        end;
t:=t+h;
write(30,ft,t);
h:=h+inc;
for j:=1 step 1 until n do
 begin y[j]:=f1[j]; write(30,ft,y[j]);end;
newline(30,1);
if t>0.34 and t<0.36 then q:=y[3];
if finish then h:=hn else gotoL1
end;

procedure fn(k1,k2,k3,k4,k5,k6,c,e,t,y,f);
 value t;real t,k1,k2,k3,k4,k5,k6,c,e; array y,f;
begin
        if t>0.01 then f[1]:=0 else
                f[1]:=k1×ex5.34₁₀-4-k2×y[1]↑2-k4×y[1];
                f[2]:=k1×ex5.34₁₀-4-k3×y[2]×y[3]-k6×y[2]/2;
        f[3]:=k2×y[1]↑2-k3×y[2]×y[3]+k4×y[1]-k5×y[3]×y[1]-k1×c×exy[3];
end;
y[1]:=read(20);y[2]:=read(20);y[3]:=read(20);
t:=read(20); range:=read(20); acc:=read(20);
h:=read(20);k1:=read(20);k2:=read(20);k3:=read(20);k4:=read(20);
k5:=read(20);k6:=read(20);e:=read(20);c:=read(20);
ft:=format([ssd.ddd₁₀+nd]);
```

```
L3:writetext(30,[[p]hydazine*kinetics*using*km3[c]]);
writetext(30,[*NH3+E**RATE*K1=]);write(30,ft,k1);newline(30,1);
writetext(30,[NH2+NH2**RATE*K2=]);write(30,ft,k2);newline(30,1);
writetext(30,[N2H4+H**RATE*K3=]);write(30,ft,k3);newline(30,1);
writetext(30,[NH2*ON*WALL**RATE*K4=]);write(30,ft,k4);newline(30,1);
writetext(30,[N2H4+NH2**RATE*K5=]);write(30,ft,k5);newline(30,1);
writetext(30,[H*ON*WALL**RATE*K6=]);write(30,ft,k6);newline(30,1);
write(30,ft,e); newline(30,1);
write(30,ft,c); newline(30,1);
writetext(30,[rate*k1=]);write(30,ft,k1);newline(30,2);
writetext(30,[time(secs)**nh2*conc*****h*conc****n2h4*conc**(in*moles/lit)
newline(30,1);

KM3(n,t,y,range,fn,acc,h);

t:=0;
y[1]:=0;y[2]:=0;y[3]:=0;
if q<4₁₀-6 then begin k1:=k1+k1/2; goto L3;end;
ifq>5₁₀-6 then begin k1:=k1-k1/3; goto L3 ;end;
close(20); close(30);
end;
end↠
```

APPENDIX LL

SERIES 1

CONTINUOUS DIRECT CURRENT BALLAST RESISTANCE 17K.OHMS
OPERATING PRESSURE 10MM.HG ROOM TEMPERATURE 100CC OF GLYCOL ABSORBENT USED
INTERELECTRODE DISTANCE 6.3CM REACTOR VOLUME 16CC
AMMONIA FLOWRATE 14.3CC/SEC AT OPERATING CONDITIONS
GAS RESIDENCE TIME 1.12SECS ACTIVE RESIDENCE TIME 1.12SECONDS

RUN NO	CURRENT (MAMPS)	VOLTS (KV)	WATTS	RUN (MINS)	DILUTE *	P.P.M. N2H4	YIELD (GM/KWH)	PWR DNSTY (WATT/CC)	CONV (WT PC)
1	15.0	0.89	13.3	5.0	20	0.064	0.232	0.83	0.64
2	35.0	0.85	29.9	5.0	20	0.068	0.110	1.87	0.69
3	20.0	0.90	18.0	5.0	20	0.071	0.188	1.13	0.71
4	40.0	0.88	35.1	5.0	20	0.053	0.073	2.20	0.54
5	40.0	0.83	33.4	5.0	20	0.061	0.087	2.09	0.61
6	30.0	0.71	21.4	5.0	20	0.056	0.126	1.34	0.56
7	30.0	0.84	25.1	5.0	20	0.050	0.096	1.57	0.50
8	20.0	0.80	16.1	5.0	20	0.059	0.179	1.01	0.60

STATISTICAL ANALYSIS OF RESULTS

LINEAR REGRESSION GIVES LOG(ENERGY YIELD)=-0.960 - 0.730*POWER DENSITY
VARIANCE OF B= 1.10* -2 SIGMA= 1.48* -1
VALUES FROM FITTED REGRESSION LINE

POWER DENSITY	0.0	1.0	2.0	3.0	4.0	5.0	6.0	7.0	8.0
YIELD(GM/KWH)	0.383	0.185	0.089	0.043	0.021	0.010	0.005	0.002	0.001
CONVERSION	0.000	0.616	0.594	0.429	0.276	0.166	0.096	0.054	0.030

SERIES 3

CONTINUOUS DIRECT CURRENT BALLAST RESISTANCE 17K.OHMS
OPERATING PRESSURE 10MM.HG ROOM TEMPERATURE 100CC OF GLYCOL ABSORBENT USED
INTERELECTRODE DISTANCE 6.3CM REACTOR VOLUME 16CC
AMMONIA FLOWRATE 30.4CC/SEC AT OPERATING CONDITIONS
GAS RESIDENCE TIME 0.53SECS ACTIVE RESIDENCE TIME 0.53SECONDS

RUN NO	CURRENT (MAMPS)	VOLTS (KV)	WATTS	RUN (MINS)	DILUTE *	P.P.M. N2H4	YIELD (GM/KWH)	PWR DNSTY (WATT/CC)	CONV (WT PC)
17	50.0	1.10	55.0	2.0	25	0.110	0.300	3.42	1.61
18	55.0	1.08	59.4	2.0	25	0.130	0.328	3.71	1.91
19	50.0	1.38	69.0	2.0	25	0.125	0.272	4.30	1.84
20	35.0	1.11	38.9	2.0	25	0.148	0.574	2.43	2.19
21	40.0	0.09	37.6	2.0	25	0.150	0.600	2.35	2.22
22	35.0	0.88	28.7	2.0	25	0.150	0.776	1.79	2.18
23	30.0	0.75	22.3	2.0	25	0.120	0.810	1.40	1.78
24	25.0	0.70	17.6	2.0	25	0.175	1.500	1.10	2.59

STATISTICAL ANALYSIS OF RESULTS

LINEAR REGRESSION GIVES LOG(ENERGY YIELD)= 0.668 - 0.492*POWER DENSITY
VARIANCE OF B= 3.20* -3 SIGMA= 1.72* -1
VALUES FROM FITTED REGRESSION LINE

POWER DENSITY	0.0	1.0	2.0	3.0	4.0	5.0	6.0	7.0	8.0
YIELD(GM/KWH)	1.95	1.19	0.729	0.446	0.273	0.167	0.102	0.062	0.038
CONVERSION	0.000	1.873	2.291	2.101	1.713	1.309	0.960	0.685	0.479

SERIES 8

CONTINUOUS DIRECT CURRENT BALLAST RESISTANCE 17K.OHMS
OPERATING PRESSURE 10MM.HG ROOM TEMPERATURE 100CC OF GLYCOL ABSORBENT USED
INTERELECTRODE DISTANCE 6.3CM REACTOR VOLUME 16CC
AMMONIA FLOWRATE 207CC/SEC AT OPERATING CONDITIONS
GAS RESIDENCE TIME 7.70* -2SECS ACTIVE RESIDENCE TIME 7.70* -2SECONDS

RUN NO	CURRENT (MAMPS)	VOLTS (KV)	WATTS	RUN (MINS)	DILUTE *	P.P.M. N2H4	YIELD (GM/KWH)	PWR DNSTY (WATT/CC)	CONV (WT PC)
66	29.0	0.65	18.9	3.0	50	0.103	1.370	1.18	0.37
68	40.0	0.65	26.0	3.0	50	0.092	0.890	1.62	0.33
69	45.0	0.59	26.5	3.0	50	0.079	0.740	1.66	0.28
70	30.0	0.64	19.2	3.0	50	0.092	1.200	1.20	0.33
71	50.0	0.60	30.0	3.0	50	0.082	0.630	1.88	0.27
72	55.0	0.61	33.5	3.0	50	0.075	0.560	2.10	0.27
73	20.0	0.64	12.8	3.0	50	0.075	1.480	0.79	0.27

STATISTICAL ANALYSIS OF RESULTS

LINEAR REGRESSION GIVES LOG(ENERGY YIELD)= 1.300 - 0.921*POWER DENSITY
VARIANCE OF B= 1.10* -2 SIGMA= 8.60* -2
VALUES FROM FITTED REGRESSION LINE

POWER DENSITY	0.0	1.0	2.0	3.0	4.0	5.0	6.0	7.0	8.0
YIELD(GM/KWH)	3.67	1.46	0.582	0.232	0.092	0.037	0.015	0.006	0.002
CONVERSION	0.000	0.336	0.268	0.160	0.085	0.042	0.020	0.009	0.004

SERIES 9

CONTINUOUS DIRECT CURRENT BALLAST RESISTANCE 17K.OHMS
OPERATING PRESSURE 10MM.HG ROOM TEMPERATURE 100CC OF GLYCOL ABSORBENT USED
INTERELECTRODE DISTANCE 6.3CM REACTOR VOLUME 16CC
AMMONIA FLOWRATE 389CC/SEC AT OPERATING CONDITIONS
GAS RESIDENCE TIME 4.10* -2SECS ACTIVE RESIDENCE TIME 4.10* -2SECONDS

RUN NO	CURRENT (MAMPS)	VOLTS (KV)	WATTS	RUN (MINS)	DILUTE *	P.P.M. N2H4	YIELD (GM/KWH)	PWR DNSTY (WATT/CC)	CONV (WT PC)
74	40.0	0.60	24.0	3.0	100	0.089	1.850	1.50	0.34
75	20.0	0.64	12.8	3.0	100	0.082	3.200	0.80	0.31
76	15.0	0.67	10.1	3.0	100	0.066	3.280	0.63	0.25
77	25.0	0.62	15.5	3.0	100	0.084	2.710	0.97	0.32
78	30.0	0.65	19.5	3.0	100	0.069	1.770	1.22	0.27
79	35.0	0.62	21.7	3.0	100	0.046	1.060	1.36	0.18
80	50.0	0.60	30.3	3.0	100	0.083	1.380	1.88	0.32
81	45.0	0.63	28.4	3.0	100	0.090	1.600	1.76	0.35

STATISTICAL ANALYSIS OF RESULTS

LINEAR REGRESSION GIVES LOG(ENERGY YIELD)= 1.610 - 0.741*POWER DENSITY
VARIANCE OF B= 4.80* -2 SIGMA= 2.58* -1
VALUES FROM FITTED REGRESSION LINE

POWER DENSITY	0.0	1.0	2.0	3.0	4.0	5.0	6.0	7.0	8.0
YIELD(GM/KWH)	5.00	2.38	1.14	0.542	0.258	0.123	0.059	0.028	0.013
CONVERSION	0.000	0.293	0.279	0.199	0.127	0.076	0.043	0.024	0.013

SERIES 10

CONTINUOUS DIRECT CURRENT BALLAST RESISTANCE 17K.OHMS
OPERATING PRESSURE 10MM.HG ROOM TEMPERATURE 100CC OF GLYCOL ABSORBENT USED
INTERELECTRODE DISTANCE 6.3CM REACTOR VOLUME 16CC
AMMONIA FLOWRATE 389CC/SEC AT OPERATING CONDITIONS
GAS RESIDENCE TIME 1.12SECS ACTIVE RESIDENCE TIME 1.12SECONDS

RUN NO	CURRENT (MAMPS)	VOLTS (KV)	WATTS	RUN (MINS)	DILUTE *	P.P.M. N2H4	YIELD (GM/KWH)	PWR DNSTY (WATT/CC)	CONV (WT PC)
82	30.0	0.62	19.5	3.0	20	0.165	0.890	1.22	0.13
83	40.0	0.59	23.6	3.0	20	0.200	0.850	1.47	0.15
84	20.0	0.61	12.2	3.0	20	0.135	1.110	0.76	0.10
85	20.0	0.64	12.8	3.0	20	0.192	1.000	0.80	9.82» -2

STATISTICAL ANALYSIS OF RESULTS

LINEAR REGRESSION GIVES LOG(ENERGY YIELD)= 0.302 - 0.330*POWER DENSITY
VARIANCE OF E= 6.20» -2 SIGMA= 4.70» -2
VALUES FROM FITTED REGRESSION LINE

POWER DENSITY	0.0	1.0	2.0	3.0	4.0	5.0	6.0	7.0	8.0
YIELD(GM/KWH)	1.35	0.972	0.699	0.503	0.361	0.260	0.187	0.134	0.097
CONVERSION	0.000	0.119	0.172	0.185	0.177	0.159	0.138	0.115	0.095

SERIES 11

CONTINUOUS DIRECT CURRENT BALLAST RESISTANCE 17K.OHMS
OPERATING PRESSURE 10MM.HG ROOM TEMPERATURE 100CC OF GLYCOL ABSORBENT USED
INTERELECTRODE DISTANCE 6.3CM REACTOR VOLUME 16CC
AMMONIA FLOWRATE 389CC/SEC AT OPERATING CONDITIONS
GAS RESIDENCE TIME 1.12SECS ? 0.112 ACTIVE RESIDENCE TIME 1.12SECONDS

RUN NO	CURRENT (MAMPS)	VOLTS (KV)	WATTS	RUN (MINS)	DILUTE *	P.P.M. N2H4	YIELD (GM/KWH)	PWR DNSTY (WATT/CC)	CONV (WT PC)
86	30.0	0.79	23.7	3.0	20	0.240	1.010	1.48	0.18
87	30.0	0.60	18.0	2.5	20	0.170	1.130	1.13	0.16
88	20.0	0.70	14.0	2.5	20	0.190	1.630	0.88	0.18

STATISTICAL ANALYSIS OF RESULTS

LINEAR REGRESSION GIVES LOG(ENERGY YIELD)= 1.080 - 0.750*POWER DENSITY
VARIANCE OF B= 1.04* -1 SIGMA= 1.38* -1
VALUES FROM FITTED REGRESSION LINE

POWER DENSITY	0.0	1.0	2.0	3.0	4.0	5.0	6.0	7.0	8.0
YIELD(GM/KWH)	2.94	1.39	0.657	0.310	0.147	0.069	0.033	0.015	0.007
CONVERSION	0.000	0.171	0.161	0.114	0.072	0.043	0.024	0.013	0.007

SERIES 16

CONTINUOUS DIRECT CURRENT BALLAST RESISTANCE 17K.OHMS
OPERATING PRESSURE 10MM.HG ROOM TEMPERATURE 100CC OF GLYCOL ABSORBENT USED
INTERELECTRODE DISTANCE 6.3CM REACTOR VOLUME 16CC
AMMONIA FLOWRATE 45.7CC/SEC AT OPERATING CONDITIONS
GAS RESIDENCE TIME 0.35SECS ACTIVE RESIDENCE TIME 0.35SECONDS

RUN NO	CURRENT (MAMPS)	VOLTS (KV)	WATTS	RUN (MINS)	DILUTE *	P.P.M. N2H4	YIELD (GM/KWH)	PWR DNSTY (WATT/CC)	CONV (WT PC)
121	29.0	1.30	37.7	0.9	20	0.070	0.608	2.36	1.50
122	35.0	1.06	37.1	1.0	20	0.107	0.865	2.32	2.10
123	34.0	1.13	38.4	1.0	20	0.082	0.641	2.40	1.61
124	40.0	1.14	45.6	1.0	20	0.084	0.563	2.85	1.68
125	28.0	1.20	33.6	1.0	20	0.074	0.661	2.10	1.45
126	24.0	1.24	29.8	1.0	20	0.103	1.037	1.86	2.02
127	50.0	1.03	51.5	1.0	20	0.075	0.434	3.22	1.46
128	27.0	1.10	29.7	1.0	20	0.103	1.040	1.86	2.02

STATISTICAL ANALYSIS OF RESULTS

LINEAR REGRESSION GIVES LOG(ENERGY YIELD)= 1.040 - 0.587*POWER DENSITY
VARIANCE OF B= 1.40* -2 SIGMA= 1.47* -1
VALUES FROM FITTED REGRESSION LINE

POWER DENSITY	0.0	1.0	2.0	3.0	4.0	5.0	6.0	7.0	8.0
YIELD(GM/KWH)	2.83	1.57	0.875	0.486	0.270	0.150	0.084	0.046	0.026
CONVERSION	0.000	1.644	1.828	1.525	1.130	0.785	0.524	0.340	0.216

SERIES 18

CONTINUOUS DIRECT CURRENT BALLAST RESISTANCE 17K.OHMS
OPERATING PRESSURE 10MM.HG ROOM TEMPERATURE 100CC OF GLYCOL ABSORBENT USED
INTERELECTRODE DISTANCE 6.3CM REACTOR VOLUME 16CC
AMMONIA FLOWRATE 45.7CC/SEC AT OPERATING CONDITIONS
GAS RESIDENCE TIME 0.35SECS ACTIVE RESIDENCE TIME 0.35SECONDS

RUN NO	CURRENT (MAMPS)	VOLTS (KV)	WATTS	RUN (MINS)	DILUTE *	P.P.M. N2H4	YIELD (GM/KWH)	PWR DNSTY (WATT/CC)	CONV (WT PC)
136	30.0	0.96	28.8	1.0	40	0.074	1.540	1.83	2.95
137	35.0	1.08	37.8	1.0	40	0.083	1.320	2.40	3.31
138	25.0	1.05	26.3	1.0	40	0.085	1.940	1.67	3.39
139	20.0	1.05	21.0	1.0	40	0.069	1.980	1.34	2.77
140	40.0	0.96	38.4	1.0	40	0.079	1.230	2.45	3.15
141	25.0	1.06	26.5	1.0	40	0.096	2.170	1.69	3.83
142	18.0	1.06	19.1	1.0	40	0.102	3.200	1.21	4.05
143	16.0	1.17	19.3	1.0	40	0.094	2.920	1.23	3.75

STATISTICAL ANALYSIS OF RESULTS

LINEAR REGRESSION GIVES LOG(ENERGY YIELD)= 1.790 - 0.667*POWER DENSITY
VARIANCE OF B= 1.40* -2 SIGMA= 1.47* -1
VALUES FROM FITTED REGRESSION LINE

POWER DENSITY	0.0	1.0	2.0	3.0	4.0	5.0	6.0	7.0	8.0
YIELD(GM/KWH)	5.99	3.07	1.58	0.810	0.416	0.213	0.109	0.056	0.029
CONVERSION	0.000	3.213	3.298	2.539	1.737	1.115	0.686	0.411	0.241

SERIES 20

CONTINUOUS DIRECT CURRENT BALLAST RESISTANCE 17K.OHMS
OPERATING PRESSURE 10MM.HG ROOM TEMPERATURE 100CC OF GLYCOL ABSORBENT USED
INTERELECTRODE DISTANCE 6.3CM REACTOR VOLUME 16CC
AMMONIA FLOWRATE 17.8CC/SEC AT OPERATING CONDITIONS
GAS RESIDENCE TIME 0.90SECS ACTIVE RESIDENCE TIME 0.90SECONDS

RUN NO	CURRENT (MAMPS)	VOLTS (KV)	WATTS	RUN (MINS)	DILUTE *	P.P.M. N2H4	YIELD (GM/KWH)	PWR DNSTY (WATT/CC)	CONV (WT PC)
151	30.0	1.20	36.0	2.5	20	0.086	0.288	2.25	1.74
152	30.0	0.93	27.9	2.5	20	0.103	0.443	1.75	2.08
153	25.0	0.85	21.2	2.5	20	0.124	0.700	1.33	2.50
154	20.0	0.88	17.6	2.0	20	0.082	0.700	1.10	2.07
155	35.0	0.93	32.6	2.0	20	0.074	0.340	2.04	1.86
156	42.0	0.95	39.9	1.7	20	0.066	0.282	2.49	1.88
157	15.0	0.82	12.3	2.0	20	0.064	0.780	0.77	1.61

STATISTICAL ANALYSIS OF RESULTS

LINEAR REGRESSION GIVES LOG(ENERGY YIELD)= 0.379 - 0.693*POWER DENSITY
VARIANCE OF B= 4.40* -3 SIGMA= 1.00* -1
VALUES FROM FITTED REGRESSION LINE

POWER DENSITY	0.0	1.0	2.0	3.0	4.0	5.0	6.0	7.0	8.0
YIELD(GM/KWH)	1.46	0.731	0.365	0.183	0.091	0.046	0.023	0.011	0.006
CONVERSION	0.000	1.960	1.960	1.470	0.980	0.613	0.368	0.215	0.123

SERIES 21

CONTINUOUS DIRECT CURRENT BALLAST RESISTANCE 17K.OHMS
OPERATING PRESSURE 10MM.HG ROOM TEMPERATURE 100CC OF GLYCOL ABSORBENT USED
INTERELECTRODE DISTANCE 6.3CM REACTOR VOLUME 16CC
AMMONIA FLOWRATE 22.9CC/SEC AT OPERATING CONDITIONS
GAS RESIDENCE TIME 0.70SECS ACTIVE RESIDENCE TIME 0.70SECONDS

RUN NO	CURRENT (MAMPS)	VOLTS (KV)	WATTS	RUN (MINS)	DILUTE *	P.P.M. N2H4	YIELD (GM/KWH)	PWR DNSTY (WATT/CC)	CONV (WT PC)
158	30.0	0.96	28.8	2.0	20	0.102	0.530	1.80	1.99
159	25.0	0.92	23.0	2.0	20	0.096	0.625	1.44	1.88
160	15.0	0.88	13.2	2.0	20	0.094	1.070	0.83	1.85
161	20.0	0.89	17.8	2.0	20	0.092	0.775	1.11	1.79
163	35.0	1.36	47.6	2.0	20	0.084	0.265	2.98	1.65
164	30.0	1.13	33.9	2.0	20	0.095	0.415	2.12	1.83

STATISTICAL ANALYSIS OF RESULTS

LINEAR REGRESSION GIVES LOG(ENERGY YIELD)= 0.430 - 0.590*POWER DENSITY
VARIANCE OF B= 1.80* -2 SIGMA= 8.40* -2
VALUES FROM FITTED REGRESSION LINE

POWER DENSITY	0.0	1.0	2.0	3.0	4.0	5.0	6.0	7.0	8.0
YIELD(GM/KWH)	1.54	0.852	0.472	0.262	0.145	0.080	0.045	0.025	0.014
CONVERSION	0.000	1.777	1.970	1.638	1.211	0.839	0.558	0.361	0.229

RESULTS WITH HELIUM ADDED TO DISCHARGE.

AMMONIA FLOWRATE 14.3 cc/sec 10 mm Hg CONTINUOUS DIRECT CURRENT

Run	Current mA	Voltage kv	Helium % vol	Runtime mins	Dil x	N_2H_4 ppm	Yield gm/kwh	π watts/sec	Conversion wt %
125	25	0.88	0	2	20	0.094	0.705	1.38	1.10
126	25	0.865	10	2	20	0.085	0.650	1.35	1.01
127	25	0.95	50	2	10	0.054	0.188	1.48	0.39
128	25	0.80	50	2	10	0.059	0.242	1.25	0.426

SERIES 4

PULSED D.C. PULSE ON TIME 13.0 MICROSECS OFF TIME 1.00. .4SECONDS

OPERATING PRESSURE 10MM.HG ROOM TEMPERATURE

100CC OF GLYCOL ABSORBENT USED

INTERELECTRODE DISTANCE 6.3CM REACTOR VOLUME 16CC

AMMONIA FLOWRATE 14.3CC/SEC AT OPERATING CONDITIONS

GAS RESIDENCE TIME 1.12SECS ACTIVE RESIDENCE TIME 0.15SECONDS

NUMBER OF PULSES PER GAS RESIDENCE TIME 9.90. 3

RUN NO	OSCILLASCOPE SETTINGS V/CM(VOLTS)	V/CM(AMPS)	μSECS/CM	RUN LENTGH (MINS)	DILUTE *	CONC P.P.M.	VARIAC SET AT	COMMENTS (IF ANY)
26	1.0	2.0	20.0	5.0	20.0	0.117	45	
40	1.0	2.0	20.0	5.0	50.0	0.052	47	
42	1.0	2.0	20.0	5.0	50.0	0.057	35	
38	1.0	2.0	20.0	5.0	50.0	0.082	40	
25	1.0	2.0	20.0	10.0	20.0	0.230	45	
47	1.0	5.0	20.0	5.0	50.0	0.036	50	
48	1.0	2.0	20.0	5.0	50.0	0.061	47	
49	1.0	2.0	20.0	5.1	50.0	0.076	35	
51	1.0	5.0	20.0	5.0	50.0	0.039	52	

SERIES 5

PULSED D.C. PULSE ON TIME 13.0 MICROSECS OFF TIME 1.00= =4SECONDS

OPERATING PRESSURE 10MM.HG ROOM TEMPERATURE

100CC OF GLYCOL ABSORBENT USED

INTERELECTRODE DISTANCE 6.3CM REACTOR VOLUME 16CC

AMMONIA FLOWRATE 30.4CC/SEC AT OPERATING CONDITIONS

GAS RESIDENCE TIME 0.56SECS ACTIVE RESIDENCE TIME 6.34= =2SECONDS

NUMBER OF PULSES PER GAS RESIDENCE TIME 4.65= 3

RUN NO	OSCILLASCOPE SETTINGS V/CM(VOLTS)	V/CM(AMPS)	μSECS/CM	RUN LENTGH (MINS)	DILUTE *	CONC P.P.M.	VARIAC SET AT	COMMENTS (IF ANY)
29	1.0	2.0	20.0	5.0	125.0	0.066	40	
35	1.0	2.0	20.0	5.0	125.0	0.050	40	
33	1.0	2.0	20.0	5.0	125.0	0.086	45	
36	1.0	2.0	20.0	5.0	125.0	0.051	45	
31	1.0	2.0	20.0	5.0	125.0	0.050	30	
34	1.0	2.0	20.0	5.0	125.0	0.044	35	
30	1.0	2.0	20.0	5.0	15.0	0.062	35	
52	1.0	5.0	20.0	5.0	62.5	0.077	50	
50	1.0	5.0	20.0	5.0	62.5	0.075	52	

SERIES 7

PULSED D.C. PULSE ON TIME 13.0 MICROSECS OFF TIME 1.77. =5SECONDS

OPERATING PRESSURE 10MM.HG ROOM TEMPERATURE

100CC OF GLYCOL ABSORBENT USED

INTERELECTRODE DISTANCE 6.3CM REACTOR VOLUME 16CC

AMMONIA FLOWRATE 14.3CC/SEC AT OPERATING CONDITIONS

GAS RESIDENCE TIME 1.12SECS ACTIVE RESIDENCE TIME 0.47SECONDS

NUMBER OF PULSES PER GAS RESIDENCE TIME 3.55. 4

RUN NO	OSCILLASCOPE SETTINGS V/CM(VOLTS)	V/CM(AMPS)	μSECS/CM	RUN LENTGH (MINS)	DILUTE *	CONC P.P.M.	VARIAC SET AT	COMMENTS (IF ANY)
60	2.0	5.0	5.0	4.0	10.0	0.067	45	
61	1.0	2.0	5.0	4.0	10.0	0.125	40	
62	1.0	2.0	5.0	4.0	10.0	0.072	45	
63	1.0	5.0	5.0	4.0	10.0	0.068	47	
64	1.0	1.0	5.0	4.0	10.0	0.156	30	
65	1.0	2.0	5.0	4.0	10.0	0.135	35	

SERIES 12

PULSED D.C. PULSE ON TIME 13.0 MICROSECS OFF TIME 0.56SECONDS

OPERATING PRESSURE 10MM.HG ROOM TEMPERATURE

100CC OF GLYCOL ABSORBENT USED

INTERELECTRODE DISTANCE 6.3CM REACTOR VOLUME 16CC

AMMONIA FLOWRATE 14.3CC/SEC AT OPERATING CONDITIONS

GAS RESIDENCE TIME 1.12SECS ACTIVE RESIDENCE TIME 2.60. =5SECONDS

NUMBER OF PULSES PER GAS RESIDENCE TIME 2.0

RUN NO	OSCILLASCOPE SETTINGS V/CM(VOLTS)	V/CM(AMPS)	μSECS/CM	RUN LENTGH (MINS)	DILUTE *	CONC P.P.M.	VARIAC SET AT	COMMENTS (IF ANY)
89	2.0	5.0	5.0	15.0	1.0	0.064	54	
92	1.0	1.0	5.0	15.0	1.0	0.024	40	
94	2.0	2.0	5.0	15.0	1.0	0.052	50	
95	2.0	1.0	5.0	15.0	1.0	0.046	45	
96	1.0	5.0	5.0	15.0	1.0	0.085	60	
97	2.0	5.0	5.0	15.0	1.0	0.084	65	

SERIES 13

PULSED D.C. PULSE ON TIME 13.0 MICROSECS OFF TIME 1.12SECONDS

OPERATING PRESSURE 10MM.HG ROOM TEMPERATURE

100CC OF GLYCOL ABSORBENT USED

INTERELECTRODE DISTANCE 6.3CM REACTOR VOLUME 16CC

AMMONIA FLOWRATE 14.3CC/SEC AT OPERATING CONDITIONS

GAS RESIDENCE TIME 1.12SECS ACTIVE RESIDENCE TIME 1.30= .5SECONDS

NUMBER OF PULSES PER GAS RESIDENCE TIME 1.0

RUN NO	OSCILLASCOPE SETTINGS V/CM(VOLTS)	V/CM(AMPS)	μ SECS/CM	RUN LENTGH (MINS)	DILUTE *	CONC P.P.M.	VARIAC SET AT	COMMENTS (IF ANY)
112	1.0	5.0	5.0	30.0	1.0	0.088	45	
98	1.0	5.0	5.0	40.0	1.0	0.128	64	
99	2.0	5.0	5.0	30.0	1.0	0.082	60	
100	1.0	5.0	5.0	30.0	1.0	0.093	55	
101	2.0	5.0	5.0	30.0	1.0	0.092	50	
102	1.0	5.0	5.0	30.0	1.0	0.063	50	
103	1.0	5.0	5.0	30.0	1.0	0.068	50	

SERIES 14

PULSED D.C. PULSE ON TIME 26.0 MICROSECS OFF TIME 1.12SECONDS

OPERATING PRESSURE 10MM.HG ROOM TEMPERATURE

100CC OF GLYCOL ABSORBENT USED

INTERELECTRODE DISTANCE 6.3CM REACTOR VOLUME 16CC

AMMONIA FLOWRATE 14.3CC/SEC AT OPERATING CONDITIONS

GAS RESIDENCE TIME 1.12SECS ACTIVE RESIDENCE TIME 2.60# =5SECONDS

NUMBER OF PULSES PER GAS RESIDENCE TIME 1.0

RUN NO	OSCILLASCOPE SETTINGS V/CM(VOLTS)	V/CM(AMPS)	μ SECS/CM	RUN LENTGH (MINS)	DILUTE *	CONC P.P.M.	VARIAC SET AT	COMMENTS (IF ANY)
104	1.0	5.0	5.0	25.0	1.0	0.077	60	
105	1.0	5.0	10.0	30.0	1.0	0.083	65	
106	1.0	5.0	10.0	30.0	1.0	0.086	59	
107	1.0	5.0	10.0	30.0	1.0	0.090	55	
108	1.0	5.0	10.0	30.0	1.0	0.091	52	
109	1.0	5.0	10.0	30.8	1.0	0.096	48	
110	1.0	5.0	10.0	30.0	1.0	0.092	45	
111	1.0	2.0	10.0	30.0	1.0	0.065	40	

SERIES 15

PULSED D.C. PULSE ON TIME 13.0 MICROSECS OFF TIME 2.86m =5SECONDS

OPERATING PRESSURE 10MM.HG ROOM TEMPERATURE

100CC OF GLYCOL ABSORBENT USED

INTERELECTRODE DISTANCE 6.3CM REACTOR VOLUME 16CC

AMMONIA FLOWRATE 14.3CC/SEC AT OPERATING CONDITIONS

GAS RESIDENCE TIME 1.12SECS ACTIVE RESIDENCE TIME 0.35SECONDS

NUMBER OF PULSES PER GAS RESIDENCE TIME 2.69m 4

RUN NO	OSCILLASCOPE SETTINGS V/CM(VOLTS)	V/CM(AMPS)	μ SECS/CM	RUN LENTGH (MINS)	DILUTE *	CONC P.P.M.	VARIAC SET AT	COMMENTS (IF ANY)
112	1.0	2.0	5.0	4.0	20.0	0.093	30	
113	1.0	2.0	5.0	4.0	20.0	0.065	35	
114	1.0	1.0	5.0	4.0	20.0	0.099	27	
115	1.0	2.0	5.0	4.0	20.0	0.103	40	
116	1.0	5.0	5.0	4.0	20.0	0.095	45	
117	1.0	5.0	5.0	4.0	20.0	0.059	50	
118	1.0	5.0	5.0	4.0	20.0	0.061	50	
120	1.0	2.0	5.0	4.0	20.0	0.072	35	

SERIES 17

PULSED D.C. PULSE ON TIME 13.0 MICROSECS OFF TIME 1.00= -3SECONDS

OPERATING PRESSURE 10MM.HG ROOM TEMPERATURE

100CC OF GLYCOL ABSORBENT USED

INTERELECTRODE DISTANCE 6.3CM REACTOR VOLUME 16CC

AMMONIA FLOWRATE 14.3CC/SEC AT OPERATING CONDITIONS

GAS RESIDENCE TIME 1.12SECS ACTIVE RESIDENCE TIME 1.50= =2SECONDS

NUMBER OF PULSES PER GAS RESIDENCE TIME 1.10= 3

RUN NO	OSCILLASCOPE SETTINGS V/CM(VOLTS)	V/CM(AMPS)	μSECS/CM	RUN LENTGH (MINS)	DILUTE *	CONC P.P.M.	VARIAC SET AT	COMMENTS (IF ANY)
129	2.0	5.0	5.0	5.0	20.0	0.102	50	
130	2.0	5.0	5.0	5.0	20.0	0.130	45	
131	2.0	5.0	5.0	4.0	20.0	0.092	55	
132	2.0	5.0	5.0	4.0	20.0	0.126	55	
133	1.0	5.0	5.0	4.0	20.0	0.074	58	
134	2.0	5.0	5.0	4.0	20.0	0.077	63	
135	2.0	5.0	5.0	4.0	20.0	0.057	50	

SERIES 19

PULSED D.C. PULSE ON TIME 13.0 MICROSECS OFF TIME 2.86 .5SECONDS

OPERATING PRESSURE 10MM.HG ROOM TEMPERATURE

100CC OF GLYCOL ABSORBENT USED

INTERELECTRODE DISTANCE 6.3CM REACTOR VOLUME 16CC

AMMONIA FLOWRATE 14.3CC/SEC AT OPERATING CONDITIONS

GAS RESIDENCE TIME 1.12SECS ACTIVE RESIDENCE TIME 0.35SECONDS

NUMBER OF PULSES PER GAS RESIDENCE TIME 2.69 4

RUN NO	OSCILLASCOPE SETTINGS V/CM(VOLTS)	V/CM(AMPS)	μSECS/CM	RUN LENTGH (MINS)	DILUTE *	CONC P.P.M.	VARIAC SET AT	COMMENTS (IF ANY)
144	1.0	2.0	2.0	2.0	20.0	0.070	40	
145	1.0	2.0	2.0	2.0	20.0	0.043	35	
146	1.0	2.0	2.0	3.5	20.0	0.076	32	
147	1.0	5.0	2.0	3.0	20.0	0.065	40	
148	1.0	5.0	2.0	3.1	20.0	0.085	45	
149	1.0	5.0	2.0	2.5	20.0	0.050	50	
150	1.0	1.0	2.0	3.5	20.0	0.068	26	

SERIES 22

PULSED D.C. PULSE ON TIME 5.0 MICROSECS OFF TIME 1.00= =3SECONDS

OPERATING PRESSURE 10MM.HG ROOM TEMPERATURE

100CC OF GLYCOL ABSORBENT USED

INTERELECTRODE DISTANCE 6.3CM REACTOR VOLUME 16CC

AMMONIA FLOWRATE 14.3CC/SEC AT OPERATING CONDITIONS

GAS RESIDENCE TIME 1.12SECS ACTIVE RESIDENCE TIME 5.57= =3SECONDS

NUMBER OF PULSES PER GAS RESIDENCE TIME 1.11= 3

RUN NO	OSCILLASCOPE SETTINGS V/CM(VOLTS)	V/CM(AMPS)	μSECS/CM	RUN LENTGH (MINS)	DILUTE *	CONC P.P.M.	VARIAC SET AT	COMMENTS (IF ANY)
1	1.0	2.0	2.0	5.0	20.0	0.078	43	
2	2.0	2.0	2.0	4.0	20.0	0.065	46	
3	2.0	2.0	2.0	4.0	20.0	0.076	48	
4	2.0	2.0	2.0	4.0	20.0	0.048	50	
5	2.0	1.0	2.0	4.0	20.0	0.075	42	
6	2.0	5.0	2.0	4.0	20.0	0.085	52	
7	2.0	5.0	2.0	4.0	20.0	0.078	54	
8	2.0	1.0	2.0	4.0	20.0	0.064	45	

SERIES 23

PULSED D.C. PULSE ON TIME 34.0 MICROSECS OFF TIME 1.00# =3SECONDS

OPERATING PRESSURE 10MM.HG ROOM TEMPERATURE

100CC OF GLYCOL ABSORBENT USED

INTERELECTRODE DISTANCE 6.3CM REACTOR VOLUME 16CC

AMMONIA FLOWRATE 14.3CC/SEC AT OPERATING CONDITIONS

GAS RESIDENCE TIME 1.12SECS ACTIVE RESIDENCE TIME 3.68# =2SECONDS

NUMBER OF PULSES PER GAS RESIDENCE TIME 1.08# 3

RUN NO	OSCILLASCOPE SETTINGS V/CM(VOLTS)	V/CM(AMPS)	μSECS/CM	RUN LENTGH (MINS)	DILUTE *	CONC P.P.M.	VARIAC SET AT	COMMENTS (IF ANY)
9	2.0	5.0	10.0	2.0	10.0	0.057	40	
10	2.0	5.0	10.0	4.0	20.0	0.065	46	
11	2.0	2.0	10.0	4.0	20.0	0.073	38	
12	2.0	5.0	10.0	4.0	20.0	0.055	44	
14	2.0	5.0	10.0	4.0	20.0	0.077	52	
15	2.0	10.0	10.0	4.0	20.0	0.069	54	
17	2.0	2.0	10.0	4.0	20.0	0.070	38	

SERIES 24

PULSED D.C. PULSE ON TIME 88.0 MICROSECS OFF TIME 1.00# =3SECONDS

OPERATING PRESSURE 10MM.HG ROOM TEMPERATURE

100CC OF GLYCOL ABSORBENT USED

INTERELECTRODE DISTANCE 6.3CM REACTOR VOLUME 16CC

AMMONIA FLOWRATE 14.3CC/SEC AT OPERATING CONDITIONS

GAS RESIDENCE TIME 1.12SECS ACTIVE RESIDENCE TIME 9.06# =2SECONDS

NUMBER OF PULSES PER GAS RESIDENCE TIME 1.03# 3

RUN NO	OSCILLASCOPE SETTINGS V/CM(VOLTS)	V/CM(AMPS)	μSECS/CM	RUN LENTGH (MINS)	DILUTE *	CONC P.P.M.	VARIAC SET AT	COMMENTS (IF ANY)
18	1.0	5.0	20.0	4.0	20.0	0.059	45	
19	1.0	5.0	20.0	4.0	20.0	0.050	40	
20	1.0	5.0	20.0	5.0	20.0	0.069	42	
21	1.0	5.0	20.0	5.0	20.0	0.059	50	
22	1.0	2.0	20.0	5.0	20.0	0.067	52	
23	1.0	5.0	20.0	5.0	20.0	0.058	55	

SERIES 25

PULSED D.C. PULSE ON TIME 230 MICROSECS OFF TIME 1.00. =3SECONDS

OPERATING PRESSURE 10MM.HG ROOM TEMPERATURE

100CC OF GLYCOL ABSORBENT USED

INTERELECTRODE DISTANCE 6.3CM REACTOR VOLUME 16CC

AMMONIA FLOWRATE 14.3CC/SEC AT OPERATING CONDITIONS

GAS RESIDENCE TIME 1.12SECS ACTIVE RESIDENCE TIME 0.21SECONDS

NUMBER OF PULSES PER GAS RESIDENCE TIME 9.10. 2

RUN NO	OSCILLASCOPE SETTINGS V/CM(VOLTS)	V/CM(AMPS)	μSECS/CM	RUN LENTGH (MINS)	DILUTE *	CONC P.P.M.	VARIAC SET AT	COMMENTS (IF ANY)
25	1.0	5.0	50.0	5.0	40.0	0.063	38	
26	1.0	5.0	50.0	3.0	20.0	0.052	45	
27	1.0	5.0	50.0	4.0	20.0	0.068	40	
28	1.0	5.0	50.0	4.0	20.0	0.070	50	
29	1.0	2.0	50.0	3.0	20.0	0.050	55	
30	1.0	2.0	50.0	4.0	20.0	0.066	34	
31	1.0	2.0	50.0	4.0	20.0	0.058	31	

SERIES 26

PULSED D.C. PULSE ON TIME 220 MICROSECS OFF TIME 1.00. -4SECONDS

OPERATING PRESSURE 10MM.HG ROOM TEMPERATURE

100CC OF GLYCOL ABSORBENT USED

INTERELECTRODE DISTANCE 6.3CM REACTOR VOLUME 16CC

AMMONIA FLOWRATE 14.3CC/SEC AT OPERATING CONDITIONS

GAS RESIDENCE TIME 1.12SECS ACTIVE RESIDENCE TIME 0.77SECONDS

NUMBER OF PULSES PER GAS RESIDENCE TIME 3.50. 3

RUN NO	OSCILLASCOPE SETTINGS V/CM(VOLTS)	V/CM(AMPS)	μSECS/CM	RUN LENTGH (MINS)	DILUTE *	CONC P.P.M.	VARIAC SET AT	COMMENTS (IF ANY)
33	1.0	2.0	50.0	1.2	1.0	0.130	40	
34	1.0	2.0	50.0	2.0	2.0	0.200	35	
35	1.0	5.0	50.0	1.0	2.0	0.056	50	
36	1.0	2.0	50.0	1.0	2.0	0.126	37	
37	1.0	2.0	50.0	1.0	2.0	0.080	40	
38	1.0	5.0	50.0	1.0	2.0	0.094	45	
39	1.0	2.0	50.0	1.0	2.0	0.085	32	
40	1.0	2.0	50.0	1.0	2.0	0.105	30	
41	1.0	2.0	50.0	1.0	2.0	0.086	27	

SERIES 27

PULSED D.C. PULSE ON TIME 88.0 MICROSECS OFF TIME 1.00= .4SECONDS

OPERATING PRESSURE 10MM.HG ROOM TEMPERATURE

100CC OF GLYCOL ABSORBENT USED

INTERELECTRODE DISTANCE 6.3CM REACTOR VOLUME 16CC

AMMONIA FLOWRATE 14.3CC/SEC AT OPERATING CONDITIONS

GAS RESIDENCE TIME 1.12SECS ACTIVE RESIDENCE TIME 0.52SECONDS

NUMBER OF PULSES PER GAS RESIDENCE TIME 5.96= 3

RUN NO	OSCILLASCOPE SETTINGS V/CM(VOLTS)	V/CM(AMPS)	μSECS/CM	RUN LENTGH (MINS)	DILUTE *	CONC P.P.M.	VARIAC SET AT	COMMENTS (IF ANY)
45	1.0	2.0	20.0	1.0	2.0	0.102	30	
46	1.0	2.0	20.0	1.0	2.0	0.106	27	
47	1.0	5.0	20.0	1.0	2.0	0.080	45	
49	1.0	5.0	20.0	1.0	2.0	0.128	40	
50	1.0	2.0	20.0	1.0	2.0	0.138	35	
51	1.0	5.0	20.0	1.0	4.0	0.071	50	

SERIES 28

PULSED D.C. PULSE ON TIME 34.0 MICROSECS OFF TIME 1.00= .4SECONDS

OPERATING PRESSURE 10MM.HG ROOM TEMPERATURE

100CC OF GLYCOL ABSORBENT USED

INTERELECTRODE DISTANCE 6.3CM REACTOR VOLUME 16CC

AMMONIA FLOWRATE 14.3CC/SEC AT OPERATING CONDITIONS

GAS RESIDENCE TIME 1.12SECS ACTIVE RESIDENCE TIME 0.28SECONDS

NUMBER OF PULSES PER GAS RESIDENCE TIME 8.35= 3

RUN NO	OSCILLASCOPE SETTINGS V/CM(VOLTS)	V/CM(AMPS)	μSECS/CM	RUN LENTGH (MINS)	DILUTE *	CONC P.P.M.	VARIAC SET AT	COMMENTS (IF ANY)
52	1.0	2.0	10.0	1.0	2.0	0.112	30	
53	1.0	2.0	10.0	1.0	2.0	0.107	27	
54	1.0	2.0	10.0	1.0	2.0	0.105	35	
55	1.0	5.0	10.0	1.0	2.0	0.092	40	
56	1.0	5.0	10.0	1.0	2.0	0.096	45	
57	1.0	5.0	10.0	1.0	2.0	0.108	50	

SERIES 29

PULSED D.C. PULSE ON TIME 5.0 MICROSECS OFF TIME 1.00* -4SECONDS

OPERATING PRESSURE 10MM.HG ROOM TEMPERATURE

100CC OF GLYCOL ABSORBENT USED

INTERELECTRODE DISTANCE 6.3CM REACTOR VOLUME 16CC

AMMONIA FLOWRATE 14.3CC/SEC AT OPERATING CONDITIONS

GAS RESIDENCE TIME 1.12SECS ACTIVE RESIDENCE TIME 5.34* -2SECONDS

NUMBER OF PULSES PER GAS RESIDENCE TIME 1.07* 4

RUN NO	OSCILLASCOPE SETTINGS V/CM(VOLTS)	V/CM(AMPS)	μSECS/CM	RUN LENTGH (MINS)	DILUTE *	CONC P.P.M.	VARIAC SET AT	COMMENTS (IF ANY)
58	1.0	1.0	2.0	5.0	40.0	0.085	35	
59	1.0	1.0	2.0	2.0	20.0	0.085	30	
60	1.0	2.0	2.0	2.0	20.0	0.096	35	
61	1.0	2.0	2.0	2.0	20.0	0.090	40	
62	1.0	5.0	2.0	2.5	20.0	0.108	45	
63	1.0	1.0	2.0	2.0	20.0	0.067	32	
64	1.0	5.0	2.0	2.0	20.0	0.095	50	

SERIES 30

PULSED D.C. PULSE ON TIME 5.0 MICROSECS OFF TIME 1.00= =2SECONDS

OPERATING PRESSURE 10MM.HG ROOM TEMPERATURE

100CC OF GLYCOL ABSORBENT USED

INTERELECTRODE DISTANCE 6.3CM REACTOR VOLUME 16CC

AMMONIA FLOWRATE 14.3CC/SEC AT OPERATING CONDITIONS

GAS RESIDENCE TIME 1.12SECS ACTIVE RESIDENCE TIME 5.60= =4SECONDS

NUMBER OF PULSES PER GAS RESIDENCE TIME 1.12= 2

RUN NO	OSCILLASCOPE SETTINGS V/CM(VOLTS)	V/CM(AMPS)	μSECS/CM	RUN LENTGH (MINS)	DILUTE *	CONC P.P.M.	VARIAC SET AT	COMMENTS (IF ANY)
65	2.0	1.0	2.0	4.0	5.0	0.074	40	
66	2.0	1.0	2.0	4.0	5.0	0.085	45	
67	2.0	2.0	2.0	4.0	5.0	0.071	50	
68	1.0	1.0	2.0	4.0	5.0	0.059	37	
69	2.0	0.5	2.0	4.0	5.0	0.070	35	
70	2.0	5.0	2.0	4.0	5.0	0.073	55	
71	2.0	5.0	2.0	4.0	5.0	0.069	52	

SERIES 31

PULSED D.C. PULSE ON TIME 13.0 MICROSECS OFF TIME 1.00= ~2SECONDS

OPERATING PRESSURE 10MM.HG ROOM TEMPERATURE

100CC OF GLYCOL ABSORBENT USED

INTERELECTRODE DISTANCE 6.3CM REACTOR VOLUME 16CC

AMMONIA FLOWRATE 14.3CC/SEC AT OPERATING CONDITIONS

GAS RESIDENCE TIME 1.12SECS ACTIVE RESIDENCE TIME 1.45= ~3SECONDS

NUMBER OF PULSES PER GAS RESIDENCE TIME 1.12= 2

RUN NO	OSCILLASCOPE SETTINGS V/CM(VOLTS)	V/CM(AMPS)	μSECS/CM	RUN LENTGH (MINS)	DILUTE *	CONC P.P.M.	VARIAC SET AT	COMMENTS (IF ANY)
72	2.0	2.0	5.0	6.0	10.0	0.068	40	
73	2.0	0.5	5.0	8.0	10.0	0.048	37	
74	2.0	2.0	5.0	8.0	10.0	0.065	45	
75	2.0	5.0	5.0	8.0	10.0	0.064	50	
76	2.0	5.0	5.0	8.0	10.0	0.054	55	
77	2.0	5.0	5.0	8.5	10.0	0.078	52	

SERIES 32

PULSED D.C. PULSE ON TIME 33.0 MICROSECS OFF TIME 1.00= =2SECONDS

OPERATING PRESSURE 10MM.HG ROOM TEMPERATURE

100CC OF GLYCOL ABSORBENT USED

INTERELECTRODE DISTANCE 6.3CM REACTOR VOLUME 16CC

AMMONIA FLOWRATE 14.3CC/SEC AT OPERATING CONDITIONS

GAS RESIDENCE TIME 1.12SECS ACTIVE RESIDENCE TIME 3.68= =3SECONDS

NUMBER OF PULSES PER GAS RESIDENCE TIME 1.11= 2

RUN NO	OSCILLASCOPE SETTINGS V/CM(VOLTS)	V/CM(AMPS)	μSECS/CM	RUN LENTGH (MINS)	DILUTE *	CONC P.P.M.	VARIAC SET AT	COMMENTS (IF ANY)
78	2.0	2.0	10.0	8.0	10.0	0.069	35	
79	2.0	2.0	10.0	8.0	10.0	0.095	40	
80	2.0	2.0	10.0	8.0	10.0	0.052	45	
81	2.0	5.0	10.0	8.0	10.0	0.094	50	
82	2.0	5.0	10.0	8.0	10.0	0.098	52	
83	2.0	1.0	10.0	8.0	10.0	0.079	35	

SERIES 33

PULSED D.C. PULSE ON TIME 88.0 MICROSECS OFF TIME 1.00* =2SECONDS

OPERATING PRESSURE 10MM.HG ROOM TEMPERATURE

100CC OF GLYCOL ABSORBENT USED

INTERELECTRODE DISTANCE 6.3CM REACTOR VOLUME 16CC

AMMONIA FLOWRATE 14.3CC/SEC AT OPERATING CONDITIONS

GAS RESIDENCE TIME 1.12SECS ACTIVE RESIDENCE TIME 9.80* =3SECONDS

NUMBER OF PULSES PER GAS RESIDENCE TIME 1.11* 2

RUN NO	OSCILLASCOPE SETTINGS V/CM(VOLTS)	V/CM(AMPS)	μSECS/CM	RUN LENTGH (MINS)	DILUTE *	CONC P.P.M.	VARIAC SET AT	COMMENTS (IF ANY)
84	2.0	5.0	20.0	8.0	10.0	0.096	40	
85	2.0	2.0	20.0	8.0	10.0	0.126	35	
86	1.0	5.0	20.0	8.0	10.0	0.124	45	
87	1.0	5.0	20.0	8.0	10.0	0.098	50	
88	1.0	5.0	20.0	8.0	10.0	0.110	47	
89	2.0	5.0	20.0	8.0	10.0	0.125	37	

SERIES 34

PULSED D.C. PULSE ON TIME 227 MICROSECS OFF TIME 1.00# -2SECONDS

OPERATING PRESSURE 10MM.HG ROOM TEMPERATURE

100CC OF GLYCOL ABSORBENT USED

INTERELECTRODE DISTANCE 6.3CM REACTOR VOLUME 16CC

AMMONIA FLOWRATE 14.3CC/SEC AT OPERATING CONDITIONS

GAS RESIDENCE TIME 1.12SECS ACTIVE RESIDENCE TIME 2.49# -2SECONDS

NUMBER OF PULSES PER GAS RESIDENCE TIME 1.09# 2

RUN NO	OSCILLASCOPE SETTINGS V/CM(VOLTS)	V/CM(AMPS)	μSECS/CM	RUN LENTGH (MINS)	DILUTE *	CONC P.P.M.	VARIAC SET AT	COMMENTS (IF ANY)
90	2.0	2.0	50.0	8.0	10.0	0.105	33	
91	2.0	2.0	50.0	5.0	10.0	0.075	35	
92	2.0	5.0	50.0	5.0	10.0	0.081	40	
93	2.0	5.0	50.0	5.0	10.0	0.096	45	
94	2.0	5.0	50.0	5.0	10.0	0.092	50	
95	2.0	5.0	50.0	5.0	10.0	0.096	52	

SERIES 35

PULSED D.C. PULSE ON TIME 225 MICROSECS OFF TIME 1.00, =1SECONDS

OPERATING PRESSURE 10MM.HG ROOM TEMPERATURE

100CC OF GLYCOL ABSORBENT USED

INTERELECTRODE DISTANCE 6.3CM REACTOR VOLUME 16CC

AMMONIA FLOWRATE 14.3CC/SEC AT OPERATING CONDITIONS

GAS RESIDENCE TIME 1.12SECS ACTIVE RESIDENCE TIME 2.52, =3SECONDS

NUMBER OF PULSES PER GAS RESIDENCE TIME 11.2

RUN NO	OSCILLASCOPE SETTINGS V/CM(VOLTS)	V/CM(AMPS)	μSECS/CM	RUN LENTGH (MINS)	DILUTE *	CONC P.P.M.	VARIAC SET AT	COMMENTS (IF ANY)
96	2.0	5.0	50.0	10.0	6.7	0.059	40	
97	2.0	2.0	50.0	15.0	6.7	0.053	35	
98	2.0	5.0	50.0	15.0	10.0	0.072	45	
99	2.0	5.0	50.0	15.0	6.7	0.089	47	
100	2.0	5.0	50.0	15.0	10.0	0.069	50	
101	1.0	5.0	50.0	15.0	10.0	0.069	52	

SERIES 36

PULSED D.C. PULSE ON TIME 87.0 MICROSECS OFF TIME 1.00= =1SECONDS

OPERATING PRESSURE 10MM.HG ROOM TEMPERATURE

100CC OF GLYCOL ABSORBENT USED

INTERELECTRODE DISTANCE 6.3CM REACTOR VOLUME 16CC

AMMONIA FLOWRATE 14.3CC/SEC AT OPERATING CONDITIONS

GAS RESIDENCE TIME 1.12SECS ACTIVE RESIDENCE TIME 9.75= =4SECONDS

NUMBER OF PULSES PER GAS RESIDENCE TIME 11.2

RUN NO	OSCILLASCOPE SETTINGS V/CM(VOLTS)	V/CM(AMPS)	μSECS/CM	RUN LENTGH (MINS)	DILUTE *	CONC P.P.M.	VARIAC SET AT	COMMENTS (IF ANY)
102	2.0	5.0	20.0	15.0	6.7	0.066	40	
103	2.0	5.0	20.0	20.0	10.0	0.060	45	
104	2.0	2.0	20.0	20.0	6.7	0.063	37	
105	2.0	5.0	20.0	20.0	10.0	0.060	47	
106	2.0	5.0	20.0	20.0	10.0	0.061	50	
107	2.0	5.0	20.0	20.0	10.0	0.070	52	

SERIES 37

PULSED D.C. PULSE ON TIME 35.0 MICROSECS OFF TIME 1.00# =1SECONDS

OPERATING PRESSURE 10MM.HG ROOM TEMPERATURE

100CC OF GLYCOL ABSORBENT USED

INTERELECTRODE DISTANCE 6.3CM REACTOR VOLUME 16CC

AMMONIA FLOWRATE 14.3CC/SEC AT OPERATING CONDITIONS

GAS RESIDENCE TIME 1.12SECS ACTIVE RESIDENCE TIME 3.92# =4SECONDS

NUMBER OF PULSES PER GAS RESIDENCE TIME 11.2

RUN NO	OSCILLASCOPE SETTINGS V/CM(VOLTS)	V/CM(AMPS)	μSECS/CM	RUN LENTGH (MINS)	DILUTE #	CONC P.P.M.	VARIAC SET AT	COMMENTS (IF ANY)
108	2.0	5.0	10.0	20.0	6.7	0.071	47	
109	2.0	2.0	10.0	20.0	6.7	0.057	40	
110	5.0	5.0	10.0	20.0	6.7	0.061	45	
111	5.0	5.0	10.0	20.0	6.7	0.068	50	
112	5.0	2.0	10.0	20.0	6.7	0.060	42	
113	5.0	5.0	10.0	20.0	6.7	0.053	52	

SERIES 38

PULSED D.C. PULSE ON TIME 13.0 MICROSECS OFF TIME 1.00# =1SECONDS

OPERATING PRESSURE 10MM.HG ROOM TEMPERATURE

100CC OF GLYCOL ABSORBENT USED

INTERELECTRODE DISTANCE 6.3CM REACTOR VOLUME 16CC

AMMONIA FLOWRATE 14.3CC/SEC AT OPERATING CONDITIONS

GAS RESIDENCE TIME 1.12SECS ACTIVE RESIDENCE TIME 1.45# =4SECONDS

NUMBER OF PULSES PER GAS RESIDENCE TIME 11.2

RUN NO	OSCILLASCOPE SETTINGS V/CM(VOLTS)	V/CM(AMPS)	μSECS/CM	RUN LENTGH (MINS)	DILUTE #	CONC P.P.M.	VARIAC SET AT	COMMENTS (IF ANY)
131	2.0	1.0	5.0	6.0	1.0	0.068	45	
132	2.0	2.0	5.0	6.0	1.0	0.143	47	
133	2.0	2.0	5.0	4.0	1.0	0.074	47	
134	2.0	2.0	5.0	4.0	1.0	0.078	50	
135	2.0	1.0	5.0	5.0	1.0	0.044	42	
136	2.0	2.0	5.0	5.0	1.0	0.096	52	

S

SERIES 4

PULSED D.C. PULSE ON TIME 13.0 MICROSECS OFF TIME 1.00* -4SECONDS

RUN NO	POWER PULSE AREA	KWH/PULSE *.10	PULSE BASE LENGTH	ENERGY YIELD (GMS/KWH)	POWER DENSITY (WATTS/CC)	CONVERSION WT PCENT
26	67.3	1.98	1.8	1.93	3.14	2.329
40	69.7	2.05	1.8	1.06	3.25	1.324
42	53.0	1.56	1.8	1.53	2.48	1.458
38	62.2	1.83	1.9	1.87	2.76	1.983
25	66.0	1.94	1.8	1.98	3.08	2.343
47	46.2	3.40	1.7	0.440	5.90	0.998
48	73.8	2.17	1.8	1.17	3.44	1.547
49	56.1	1.65	1.8	1.17	3.44	1.547
51	55.9	4.11	1.8	0.395	6.54	0.993

STATISTICAL ANALYSIS OF RESULTS

LINEAR REGRESSION GIVES LOG(ENERGY YIELD)= 1.670 - 0.408*POWER DENSITY
VARIANCE OF B= 2.60* -2 SIGMA= 2.11* -1

VALUES FROM FITTED REGRESSION LINE

POWER DENSITY	0.0	1.0	2.0	3.0	4.0	5.0	6.0	7.0	8.0
YIELD(M/KWH)	5.31	3.53	2.35	1.56	1.04	0.691	0.459	0.305	0.203
CONVERGION	0.000	1.357	1.805	1.801	1.597	1.327	1.059	0.822	0.624

SERIES 5

PULSED D.C. PULSE ON TIME 13.0 MICROSECS OFF TIME 1.00* -4SECONDS

RUN NO	POWER PULSE AREA	KWH/PULSE **10	PULSE BASE LENGTH	ENERGY YIELD (GMS/KWH)	POWER DENSITY (WATTS/CC)	CONVERSION WT PCENT
29	80.6	2.37	1.8	2.90	3.68	1.929
35	79.9	2.35	1.8	2.22	3.74	1.501
33	84.7	2.49	1.8	1.80	2.53	0.823
36	88.4	2.60	1.8	2.04	4.14	1.527
31	39.8	1.17	1.7	4.46	1.97	1.588
34	72.4	2.13	1.6	2.15	3.80	1.477
30	58.5	1.72	1.8	3.76	2.73	1.855
52	61.6	4.53	1.6	0.880	7.90	1.257
50	62.0	4.56	1.8	0.856	7.24	1.120

STATISTICAL ANALYSIS OF RESULTS

LINEAR REGRESSION GIVES LOG(ENERGY YIELD)= 1.770 - 0.252*POWER DENSITY
VARIANCE OF B= 2.00* -3 SIGMA= 2.60* -1

VALUES FROM FITTED REGRESSION LINE

POWER DENSITY	0.0	1.0	2.0	3.0	4.0	5.0	6.0	7.0	8.0
YIELD(GM/KWH)	5.87	4.56	3.55	2.76	2.14	1.67	1.29	1.01	0.782
CONVERSION	0.000	0.824	1.281	1.493	1.548	1.504	1.403	1.272	1.130

S

SERIES 7

PULSED D.C. PULSE ON TIME 13.0 MICROSECS OFF TIME 1.77* -5SECONDS

RUN NO	POWER PULSE AREA	KWH/PULSE *.10	PULSE BASE LENGTH	ENERGY YIELD (GMS/KWH)	POWER DENSITY (WATTS/CC)	CONVERSION WT PCENT
60	51.1	1.88	4.5	0.114	4.80	0.774
61	184.9	1.36	4.6	0.294	3.38	1.405
62	236.6	1.74	4.4	0.132	4.52	0.844
63	103.4	1.90	4.1	0.114	5.33	0.859
64	224.1	0.824	4.6	0.595	2.04	1.717
65	148.2	1.09	4.6	0.395	2.70	1.508

STATISTICAL ANALYSIS OF RESULTS

LINEAR REGRESSION GIVES LOG(ENERGY YIELD)= 0.664 - 0.566*POWER DENSITY
VARIANCE OF B= 2.00* -3 SIGMA= 1.28* -1

VALUES FROM FITTED REGRESSION LINE

POWER DENSITY	0.0	1.0	2.0	3.0	4.0	5.0	6.0	7.0	8.0
YIELD(GM/KWH)	1.94	1.10	0.626	0.356	0.202	0.115	0.065	0.037	0.021
CONVERSION	0.000	1.560	1.771	1.509	1.142	0.811	0.552	0.366	0.237

SERIES 12

PULSED D.C. PULSE ON TIME 13.0 MIC OSECS OFF TIME 0.56SECONDS

RUN NO	POWER PULSE AREA	KWH/PULSE *.10	PULSE BASE LENGTH	ENERGY YIELD (GMS/KWH)	POWER DENSITY (WATTS/CC)	CONVERSION WT PCENT
89	829.9	4.16	7.5	23.9	6.36	0.012
92	199.7	1.01	9.7	37.2	1.18	0.003
94	76.3	1.53	8.4	52.3	2.09	0.008
95	156.0	1.57	9.5	45.6	1.89	0.007
96	182.2	4.58	8.3	28.9	6.30	0.014
97	95.5	4.80	9.8	27.3	5.59	0.012

STATISTICAL ANALYSIS OF RESULTS

LINEAR REGRESSION GIVES LOG(ENERGY YIELD)= 3.970 - 0.110*POWER DENSITY
VARIANCE OF B= 1.00* -3 SIGMA= 1.70* -1

VALUES FROM FITTED REGRESSION LINE

POWER DENSITY	0.0	1.0	2.0	3.0	4.0	5.0	6.0	7.0	8.0
YIELD(GM/KWH)	53.0	47.5	42.5	38.1	34.1	30.6	27.4	24.5	22.0
CONVERSION	0.000	0.004	0.007	0.009	0.011	0.012	0.013	0.013	0.014

SERIES 13

PULSED D.C. PULSE ON TIME 13.0 MIC OSECS OFF TIME 1.12SECONDS

RUN NO	POWER PULSE AREA	KWH/PULSE **10	PULSE BASE LENGTH	ENERGY YIELD (GMS/KWH)	POWER DENSITY (WATTS/CC)	CONVERSION WT PCENT
112	158.4	3.92	7.8	34.9	5.70	0.008
98	177.0	4.90	7.7	30.5	7.25	0.009
99	105.4	5.30	6.1	24.1	9.95	0.009
100	161.1	4.06	5.4	35.6	8.60	0.012
101	91.1	4.58	6.0	31.3	8.72	0.011
102	140.9	3.54	4.8	27.7	8.43	0.009
103	141.3	3.55	5.0	29.8	8.12	0.009

STATISTICAL ANALYSIS OF RESULTS

LINEAR REGRESSION GIVES LOG(ENERGY YIELD)= 3.990 - 0.076*POWER DENSITY
VARIANCE OF B= 4.00* -3 SIGMA= 6.70* -2

VALUES FROM FITTED REGRESSION LINE

POWER DENSITY	0.0	1.0	2.0	3.0	4.0	5.0	6.0	7.0	8.0
YIELD(GM/KWH)	54.1	50.1	46.4	43.0	39.9	37.0	34.3	31.8	29.4
CONVERSION	0.000	0.002	0.004	0.005	0.006	0.007	0.008	0.009	0.009

SERIES 14

PULSED D.C. PULSE ON TIME 26.0 MIC OSECS OFF TIME 1.12SECONDS

RUN NO	POWER PULSE AREA	KWH/PULSE **10	PULSE BASE LENGTH	ENERGY YIELD (GMS/KWH)	POWER DENSITY (WATTS/CC)	CONVERSION WT PCENT
104	111.7	5.61	6.9	25.6	4.65	0.009
105	156.0	7.48	7.4	16.5	6.37	0.008
106	165.8	8.33	7.2	16.1	6.58	0.008
107	165.6	8.31	7.3	16.7	6.49	0.008
108	155.8	7.82	6.9	18.1	6.50	0.009
109	147.2	7.40	7.0	20.2	6.04	0.009
110	135.8	6.81	6.8	21.0	5.76	0.009
111	254.0	5.11	6.9	19.8	4.26	0.007

STATISTICAL ANALYSIS OF RESULTS

LINEAR REGRESSION GIVES LOG(ENERGY YIELD)= 3.700 - 0.129*POWER DENSITY
VARIANCE OF B= 2.30* -3 SIGMA= 1.13* -1

VALUES FROM FITTED REGRESSION LINE

POWER DENSITY	0.0	1.0	2.0	3.0	4.0	5.0	6.0	7.0	8.0
YIELD(GM/KWH)	40.4	35.6	31.2	27.5	24.1	21.2	18.7	16.4	14.4
CONVERSION	0.000	0.003	0.005	0.006	0.007	0.008	0.009	0.009	0.009

SERIES 15

PULSED D.C. PULSE ON TIME 13.0 MICROSECS OFF TIME 2.86* =5SECONDS

RUN NO	POWER PULSE AREA	KWH/PULSE *.10	PULSE BASE LENGTH	ENERGY YIELD (GMS/KWH)	POWER DENSITY (WATTS/CC)	CONVERSION WT PCENT
112	54.5	1.37	5.0	0.590	3.13	1.927
113	223.9	0.900	6.2	0.585	2.06	1.258
114	194.0	0.390	7.2	2.20	0.78	1.791
115	336.1	1.35	6.7	0.660	2.86	1.970
116	173.9	1.75	6.5	0.470	3.84	1.884
117	186.5	1.88	6.7	0.320	3.98	1.329
118	196.9	1.98	6.7	0.270	4.35	1.226
120	254.4	1.03	6.8	0.610	2.17	1.382

STATISTICAL ANALYSIS OF RESULTS

LINEAR REGRESSION GIVES LOG(ENERGY YIELD)= 0.856 - 0.490*POWER DENSITY
VARIANCE OF B= 7.00* =3 SIGMA= 2.70* =1

VALUES FROM FITTED REGRESSION LINE

POWER DENSITY	0.0	1.0	2.0	3.0	4.0	5.0	6.0	7.0	8.0
YIELD(GM/KWH)	2.35	1.44	0.883	0.541	0.332	0.203	0.124	0.076	0.047
CONVER ION	0.000	1.505	1.844	1.695	1.384	1.060	0.779	0.557	0.390

SERIES 17

PULSED D.C. PULSE ON TIME 13.0 MICROSECS OFF TIME 1.00* -3SECONDS

RUN NO	POWER PULSE AREA	KWH/PULSE *.10	PULSE BASE LENGTH	ENERGY YIELD (GMS/KWH)	POWER DENSITY (WATTS/CC)	CONVERSION WT PCENT
129	74.7	3.75	8.2	4.56	5.23	1.022
130	6.3	3.17	8.3	6.84	4.37	1.281
131	83.7	4.21	7.8	4.55	6.17	1.203
132	61.9	3.11	7.7	5.97	4.63	1.185
133	205.9	5.16	8.3	2.99	7.11	0.911
134	106.9	5.36	8.2	2.98	7.47	0.954
135	87.6	4.40	7.4	3.82	6.80	1.113

STATISTICAL ANALYSIS OF RESULTS

LINEAR REGRESSION GIVES LOG(ENERGY YIELD)= 2.950 - 0.248*POWER DENSITY
VARIANCE OF B= 9.80* -3 SIGMA= 9.50* -2

VALUES FROM FITTED REGRESSION LINE

POWER DENSITY	0.0	1.0	2.0	3.0	4.0	5.0	6.0	7.0	8.0
YIELD(GM/KWH)	19.1	14.9	11.6	9.08	7.09	5.53	4.31	3.37	2.63
CONVERSION	0.000	0.639	0.997	1.167	1.215	1.185	1.110	1.010	0.901

SERIES 19

PULSED D.C. PULSE ON TIME 13.0 MICROSECS OFF TIME 2.86* =5SECONDS

RUN NO	POWER PULSE AREA	KWH/PULSE *.10	PULSE BASE LENGTH	ENERGY YIELD (GMS/KWH)	POWER DENSITY (WATTS/CC)	CONVERSION WT PCENT
144	315.1	1.26	12.4	0.963	2.90	2.915
145	232.6	0.940	12.0	0.803	2.23	1.869
146	305.9	1.23	12.0	0.611	2.93	1.869
147	135.3	1.30	11.8	0.578	3.15	1.900
148	165.0	1.65	12.0	0.574	3.93	2.355
149	233.1	2.34	12.2	.296	5.48	1.693
150	212.4	4.72	12.6	1.42	1.07	1.586

STATISTICAL ANALYSIS OF RESULTS

LINEAR REGRESSION GIVES LOG(ENERGY YIELD)= 0.657 - 0.337*POWER DENSITY
VARIANCE OF B= 1.79* -1 SIGMA= 3.00* -3

VALUES FROM FITTED REGRESSION LINE

POWER DENSITY	0.0	1.0	2.0	3.0	4.0	5.0	6.0	7.0	8.0
YIELD(GM/KWH)	1.93	1.38	0.983	0.702	0.501	0.358	0.255	0.182	0.130
CONVERSION	0.000	1.437	2.052	2.198	2.092	1.867	1.599	1.332	1.087

SERIES 22

PULSED D.C. PULSE ON TIME 5.0 MICROSECS OFF TIME 1.00* -3SECONDS

RUN NO	POWER PULSE AREA	KWH/PULSE *10	PULSE BASE LENTGH	ENERGY YIELD (GMS/KWH)	POWER DENSITY (WATTS/CC)	CONVERSION WT PCENT
1	461.6	1.36	12.4	9.60	3.14	0.501
2	233.1	1.37	12.9	9.90	3.04	0.500
3	355.8	2.09	13.4	7.60	4.46	0.563
4	473.1	2.78	12.8	3.60	6.21	0.371
5	363.0	1.07	14.5	14.6	2.11	0.512
6	169.6	2.49	11.9	7.10	5.98	0.706
7	178.8	2.63	11.4	6.20	6.59	0.679
8	323.0	0.950	12.2	14.0	2.22	0.516

STATISTICAL ANALYSIS OF RESULTS

LINEAR REGRESSION GIVES LOG(ENERGY YIELD)= 2.930 - 0.174*POWER DENSITY
VARIANCE OF B= 7.50* -4 SIGMA= 1.20* -1

VALUES FROM FITTED REGRESSION LINE

POWER DENSITY	0.0	1.0	2.0	3.0	4.0	5.0	6.0	7.0	8.0
YIELD(GM/KWH)	18.7	15.7	13.2	11.1	9.34	7.85	6.59	5.54	4.66
CONVERSION	0.000	0.261	0.439	0.554	0.621	0.652	0.657	0.644	0.619

SERIES 23

PULSED D.C. PULSE ON TIME 34.0 MICROSECS OFF TIME 1.00* -3SECONDS

RUN NO	POWER PULSE AREA	KWH/PULSE **10	PULSE BASE LENTGH	ENERGY YIELD (GMS/KWH)	POWER DENSITY (WATTS/CC)	CONVERSION WT PCENT
9	110.3	8.11	8.8	1.45	5.27	0.839
10	145.9	10.7	9.0	1.26	6.81	0.942
11	267.9	7.88	9.2	1.93	4.90	1.039
12	131.1	9.64	8.9	1.19	6.19	0.809
14	208.5	15.3	9.1	1.04	9.63	1.100
15	138.5	20.4	8.5	0.710	13.69	1.067
17	287.3	8.45	8.9	1.72	5.43	1.026

STATISTICAL ANALYSIS OF RESULTS

LINEAR REGRESSION GIVES LOG(ENERGY YIELD)= 0.962 - 0.098*POWER DENSITY
VARIANCE OF B= 2.80* -4 SIGMA= 1.32* -1

VALUES FROM FITTED REGRESSION LINE

POWER DENSITY	0.0	1.0	2.0	3.0	4.0	5.0	6.0	7.0	8.0
YIELD(GM/KWH)	2.62	2.37	2.15	1.95	1.77	1.61	1.46	1.32	1.20
CONVERSION	0.000	0.261	0.473	0.644	0.778	0.883	0.961	1.017	1.054

SERIES 24

PULSED D.C. PULSE ON TIME 88.0 MICROSECS OFF TIME 1.00* -3SECONDS

RUN NO	POWER PULSE AREA	KWH/PULSE **10	PULSE BASE LENTGH	ENERGY YIELD (GMS/KWH)	POWER DENSITY (WATTS/CC)	CONVERSION WT PCENT
18	285.9	21.0	12.9	0.063	4.65	0.079
19	392.3	28.9	12.4	0.390	6.66	0.702
20	397.4	29.2	12.7	0.420	6.57	0.745
21	504.5	37.1	11.2	0.290	9.47	0.742
22	838.6	24.7	12.0	0.510	5.88	0.810
23	701.2	51.6	13.2	0.240	11.16	0.724
24	721.6	53.1	13.1	0.196	11.57	0.613

STATISTICAL ANALYSIS OF RESULTS

LINEAR REGRESSION GIVES LOG(ENERGY YIELD)= 0.173 - 0.151*POWER DENSITY
VARIANCE OF B= 1.40* -4 SIGMA= 7.90* -2

VALUES FROM FITTED REGRESSION LINE

POWER DENSITY	0.0	1.0	2.0	3.0	4.0	5.0	6.0	7.0	8.0
YIELD(GM/KWH)	1.19	1.02	0.879	0.756	0.650	0.559	0.480	0.413	0.355
CONVERSION	0.000	0.276	0.475	0.613	0.702	0.755	0.779	0.781	0.768

SERIES 25

PULSED D.C. PULSE ON TIME 230 MICROSECS OFF TIME 1.00* -3SECONDS

RUN NO	POWER PULSE AREA	KWH/PULSE **10	PULSE BASE LENTGH	ENERGY YIELD (GMS/KWH)	POWER DENSITY (WATTS/CC)	CONVERSION WT PCENT
25	390.5	71.8	12.5	0.360	6.56	1.475
26	528.7	97.2	12.5	0.183	8.89	1.016
27	426.6	78.4	12.5	0.220	7.17	0.985
28	686.5	126.2	12.7	0.142	11.40	1.011
29	775.8	138.9	12.7	0.123	12.50	0.960
30	759.9	55.9	12.3	0.303	5.19	0.982
31	548.3	40.3	12.5	0.365	3.69	0.841

STATISTICAL ANALYSIS OF RESULTS

LINEAR REGRESSION GIVES LOG(ENERGY YIELD)=-5.80* -1 - 0.123*POWER DENSITY
VARIANCE OF B= 2.40* -5 SIGMA= 3.76* -2

VALUES FROM FITTED REGRESSION LINE

POWER DENSITY	0.0	1.0	2.0	3.0	4.0	5.0	6.0	7.0	8.0
YIELD(GM/KWH)	0.560	0.495	0.438	0.387	0.342	0.303	0.268	0.237	0.209
CONVERSION	0.000	0.309	0.547	0.725	0.855	0.945	1.003	1.035	1.046

SERIES 26

PULSED D.C. PULSE ON TIME 220 MICROSECS OFF TIME 1.00, -4SECONDS

RUN NO	POWER PULSE AREA	KWH/PULSE *,10	PULSE BASE LENTGH	ENERGY YIELD (GMS/KWH)	POWER DENSITY (WATTS/CC)	CONVERSION WT PCENT
33	575.8	42.3	8.0	0.034	6.05	0.477
34	670.1	49.3	9.3	0.054	6.06	0.753
35	451.1	82.9	9.2	0.018	10.30	0.426
36	810.2	59.6	11.5	0.056	5.92	0.767
37	968.9	71.2	11.7	0.030	6.94	0.478
38	413.1	75.9	11.6	0.033	7.48	0.567
39	626.6	46.1	11.6	0.049	4.54	0.513
40	593.0	39.6	11.1	0.071	4.08	0.662
41	461.7	34.0	11.7	0.068	3.32	0.515

STATISTICAL ANALYSIS OF RESULTS

LINEAR REGRESSION GIVES LOG(ENERGY YIELD)=-1.96, 0 - 0.198*POWER DENSITY
VARIANCE OF B= 1.00, -3 SIGMA= 1.87, -1

VALUES FROM FITTED REGRESSION LINE

POWER DENSITY	0.0	1.0	2.0	3.0	4.0	5.0	6.0	7.0	8.0
YIELD(GM/KWH)	0.141	0.116	0.095	0.078	0.064	0.052	0.043	0.035	0.029
CONVERSION	0.000	0.265	0.435	0.536	0.586	0.601	0.592	0.566	0.531

SERIES 27

PULSED D.C. PULSE ON TIME 88.0 MICROSECS OFF TIME 1.00* -4SECONDS

RUN NO	POWER PULSE AREA	KWH/PULSE **10	PULSE BASE LENTGH	ENERGY YIELD (GMS/KWH)	POWER DENSITY (WATTS/CC)	CONVERSION WT PCENT
45	602.1	17.7	13.0	0.090	3.89	0.547
46	480.1	14.1	13.1	0.118	3.08	0.568
47	368.8	27.1	13.0	0.046	5.96	0.429
49	348.9	25.7	13.1	0.078	5.60	0.683
50	714.2	21.0	13.2	0.103	4.55	0.733
51	443.6	32.6	13.3	0.068	7.01	0.745

STATISTICAL ANALYSIS OF RESULTS

LINEAR REGRESSION GIVES LOG(ENERGY YIELD)=-1.63* 0 - 0.179*POWER DENSITY
VARIANCE OF B= 5.50* -3 SIGMA= 2.39* -1

VALUES FROM FITTED REGRESSION LINE

POWER DENSITY	0.0	1.0	2.0	3.0	4.0	5.0	6.0	7.0	8.0
YIELD(GM/KWH)	0.196	0.164	0.137	0.115	0.096	0.080	0.067	0.056	0.047
CONVERSION	0.000	0.256	0.428	0.537	0.599	0.626	0.628	0.612	0.585

SERIES 28

PULSED D.C. PULSE ON TIME 34.0 MICROSECS OFF TIME 1.00* -4SECONDS

RUN NO	POWER PULSE AREA	KWH/PULSE **10	PULSE BASE LENTGH	ENERGY YIELD (GMS/KWH)	POWER DENSITY (WATTS/CC)	CONVERSION WT PCENT
52	410.9	6.04	10.9	0.207	3.17	0.556
53	333.5	4.90	10.8	0.244	2.59	0.536
54	530.4	7.80	11.5	0.150	3.88	0.493
55	277.3	10.2	11.0	0.101	5.29	0.453
56	346.0	12.7	11.3	0.084	6.43	0.458
57	393.5	14.5	11.2	0.083	7.38	0.519

STATISTICAL ANALYSIS OF RESULTS

LINEAR REGRESSION GIVES LOG(ENERGY YIELD)=-8.83* -1 - 0.238*POWER DENSITY
VARIANCE OF B= 9.70* -4 SIGMA= 1.32* -1

VALUES FROM FITTED REGRESSION LINE

POWER DENSITY	0.0	1.0	2.0	3.0	4.0	5.0	6.0	7.0	8.0
YIELD(GM/KWH)	0.414	0.326	0.257	0.203	0.160	0.126	0.099	0.078	0.062
CONVERSION	0.000	0.276	0.435	0.515	0.541	0.533	0.504	0.464	0.418

SERIES 29

PULSED D.C. PULSE ON TIME 5.0 MICROSECS OFF TIME 1.00* -4SECONDS

RUN NO	POWER PULSE AREA	KWH/PULSE **10	PULSE BASE LENTGH	ENERGY YIELD (GMS/KWH)	POWER DENSITY (WATTS/CC)	CONVERSION WT PCENT
58	494.3	0.730	12.2	4.13	1.70	1.117
59	310.6	0.457	11.2	8.13	1.17	1.513
60	336.4	0.989	11.0	4.25	2.57	1.737
61	469.2	1.38	11.0	2.85	3.59	1.627
62	251.6	1.85	11.3	2.05	4.68	1.526
63	461.6	0.679	11.5	4.32	1.69	1.161
64	268.6	1.98	12.0	2.11	4.70	1.577

STATISTICAL ANALYSIS OF RESULTS

LINEAR REGRESSION GIVES LOG(ENERGY YIELD)= 2.160 - 0.309*POWER DENSITY
VARIANCE OF B= 2.70* -3 SIGMA= 1.86* -1

VALUES FROM FITTED REGRESSION LINE

POWER DENSITY	0.0	1.0	2.0	3.0	4.0	5.0	6.0	7.0	8.0
YIELD(GM/KWH)	8.67	6.37	4.67	3.43	2.52	1.85	1.36	0.997	0.732
CONVERSION	0.000	1.013	1.487	1.637	1.603	1.471	1.296	1.110	0.931

SERIES 30

PULSED D.C. PULSE ON TIME 5.0 MICROSECS OFF TIME 1.00* -2SECONDS

RUN NO	POWER PULSE AREA	KWH/PULSE **10	PULSE BASE LENTGH	ENERGY YIELD (GMS/KWH)	POWER DENSITY (WATTS/CC)	CONVERSION WT PCENT
65	233.7	0.687	13.1	56.5	1.50	0.141
66	558.8	1.64	13.7	27.0	3.43	0.155
67	365.2	2.15	13.5	17.2	4.55	0.131
68	548.1	0.806	13.0	38.1	1.77	0.113
69	478.1	0.703	13.3	52.1	1.58	0.137
70	156.9	2.31	12.5	16.6	5.27	0.146
71	150.8	2.22	13.0	16.1	4.88	0.131

STATISTICAL ANALYSIS OF RESULTS

LINEAR REGRESSION GIVES LOG(ENERGY YIELD)= 4.395 - 0.322*POWER DENSITY
VARIANCE OF B= 9.01* -4 SIGMA= 1.22* -1

VALUES FROM FITTED REGRESSION LINE

POWER DENSITY	0.0	1.0	2.0	3.0	4.0	5.0	6.0	7.0	8.0
YIELD(GM/KWH)	81.0	58.7	42.6	30.8	22.4	16.2	11.7	8.51	6.17
CONVERSION	0.000	0.098	0.142	0.154	0.149	0.135	0.118	0.099	0.082

SERIES 31

PULSED D.C. PULSE ON TIME 13.0 MICROSECS OFF TIME 1.00* -2SECONDS

RUN NO	POWER PULSE AREA	KWH/PULSE *10	PULSE BASE LENTGH	ENERGY YIELD (GMS/KWH)	POWER DENSITY (WATTS/CC)	CONVERSION WT PCENT
72	261.0	3.18	11.3	14.9	3.21	0.207
73	291.0	1.07	11.0	23.4	1.11	0.113
74	276.2	4.06	9.4	8.40	4.94	0.180
75	148.0	5.44	9.2	6.15	6.76	0.180
76	151.2	5.56	8.8	5.07	7.22	0.159
77	132.2	4.86	8.7	7.88	6.39	0.218

STATISTICAL ANALYSIS OF RESULTS

LINEAR REGRESSION GIVES LOG(ENERGY YIELD)= 3.420 - 0.238*POWER DENSITY
VARIANCE OF B= 4.30* -4 SIGMA= 1.10* -1

VALUES FROM FITTED REGRESSION LINE

POWER DENSITY	0.0	1.0	2.0	3.0	4.0	5.0	6.0	7.0	8.0
YIELD(GM/KWH)	30.6	24.1	19.0	15.0	11.8	9.30	7.33	5.78	4.55
CONVERSION	0.000	0.104	0.165	0.195	0.205	0.202	0.191	0.175	0.158

SERIES 32

PULSED D.C. PULSE ON TIME 33.0 MICROSECS OFF TIME 1.00* -2SECONDS

RUN NO	POWER PULSE AREA	KWH/PULSE **10	PULSE BASE LENTGH	ENERGY YIELD (GMS/KWH)	POWER DENSITY (WATTS/CC)	CONVERSION WT PCENT
78	137.5	4.04	8.6	8.86	2.68	0.261
79	210.7	6.20	8.9	8.01	3.98	0.350
80	234.4	6.89	8.9	3.94	4.42	0.191
81	101.4	7.46	8.6	6.58	4.96	0.359
82	116.1	8.54	9.0	6.00	5.42	0.357
83	277.8	4.08	8.6	10.1	2.71	0.301

STATISTICAL ANALYSIS OF RESULTS

LINEAR REGRESSION GIVES LOG(ENERGY YIELD)= 2.700 - 0.165*POWER DENSITY
VARIANCE OF B= 5.90* -4 SIGMA= 6.10* -2

VALUES FROM FITTED REGRESSION LINE

POWER DENSITY	0.0	1.0	2.0	3.0	4.0	5.0	6.0	7.0	8.0
YIELD(GM/KWH)	14.9	12.6	10.7	9.07	7.69	6.52	5.53	4.69	3.97
CONVERSION	0.000	0.139	0.235	0.299	0.338	0.358	0.364	0.361	0.349

SERIES 33

PULSED D.C. PULSE ON TIME 88.0 MICROSECS OFF TIME 1.00* -2SECONDS

RUN NO	POWER PULSE AREA	KWH/PULSE **10	PULSE BASE LENTGH	ENERGY YIELD (GMS/KWH)	POWER DENSITY (WATTS/CC)	CONVERSION WT PCENT
84	88.1	13.0	12.0	3.90	3.08	0.350
85	218.1	12.8	12.0	5.17	3.05	0.459
86	139.1	20.5	12.0	3.19	4.87	0.453
87	333.9	24.6	12.0	2.10	5.85	0.358
88	324.1	23.8	12.1	2.43	5.63	0.399
89	90.8	13.4	12.2	4.92	3.13	0.449

STATISTICAL ANALYSIS OF RESULTS

LINEAR REGRESSION GIVES LOG(ENERGY YIELD)= 2.560 - 0.305*POWER DENSITY
VARIANCE OF B= 2.50* -4 SIGMA= 4.20* -2

VALUES FROM FITTED REGRESSION LINE

POWER DENSITY	0.0	1.0	2.0	3.0	4.0	5.0	6.0	7.0	8.0
YIELD(GM/KWH)	12.9	9.54	7.03	5.18	3.82	2.82	2.08	1.53	1.13
CONVERSION	0.000	0.278	0.410	0.453	0.445	0.410	0.363	0.312	0.263

SERIES 34

PULSED D.C. PULSE ON TIME 227 MICROSECS OFF TIME 1.00* -2SECONDS

RUN NO	POWER PULSE AREA	KWH/PULSE **10	PULSE BASE LENTGH	ENERGY YIELD (GMS/KWH)	POWER DENSITY (WATTS/CC)	CONVERSION WT PCENT
90	330.9	48.7	11.5	1.15	4.85	0.413
91	449.7	66.1	11.8	0.965	6.41	0.459
92	200.8	73.8	11.8	0.937	7.15	0.497
93	263.9	97.0	11.9	0.840	9.32	0.580
94	262.4	96.5	11.7	0.816	9.42	0.570
95	314.8	115.7	12.0	0.680	11.02	0.556

STATISTICAL ANALYSIS OF RESULTS

LINEAR REGRESSION GIVES LOG(ENERGY YIELD)= 0.493 - 0.076*POWER DENSITY
VARIANCE OF B= 5.60* -5 SIGMA= 3.82* -2

VALUES FROM FITTED REGRESSION LINE

POWER DENSITY	0.0	1.0	2.0	3.0	4.0	5.0	6.0	7.0	8.0
YIELD(GM/KWH)	1.64	1.52	1.41	1.30	1.21	1.12	1.04	0.962	0.891
CONVERSION	0.000	0.112	0.209	0.290	0.358	0.415	0.462	0.499	0.529

SERIES 35

PULSED D.C. PULSE ON TIME 225 MICROSECS OFF TIME 1.00* -1SECONDS

RUN NO	POWER PULSE AREA	KWH/PULSE **10	PULSE BASE LENTGH	ENERGY YIELD (GMS/KWH)	POWER DENSITY (WATTS/CC)	CONVERSION WT PCENT
96	266.5	98.0	11.6	1.67	9.65	0.121
97	366.8	53.9	11.4	1.82	5.41	0.074
98	252.4	92.8	11.6	2.15	9.14	0.147
99	276.1	101.5	11.5	1.63	10.09	0.123
100	346.8	127.5	11.6	1.50	12.56	0.141
101	619.4	113.8	11.7	1.67	11.12	0.139

STATISTICAL ANALYSIS OF RESULTS

LINEAR REGRESSION GIVES LOG(ENERGY YIELD)= 0.818 - 0.028*POWER DENSITY
VARIANCE OF B= 4.60* -4 SIGMA= 1.15* -1

VALUES FROM FITTED REGRESSION LINE

POWER DENSITY	0.0	1.0	2.0	3.0	4.0	5.0	6.0	7.0	8.0
YIELD(GM/KWH)	2.27	2.20	2.14	2.08	2.03	1.97	1.92	1.86	1.81
CONVERSION	0.000	0.017	0.032	0.047	0.061	0.074	0.086	0.098	0.109

SERIES 36

PULSED D.C. PULSE ON TIME 87.0 MICROSECS OFF TIME 1.00* -1SECONDS

RUN NO	POWER PULSE AREA	KWH/PULSE *.10	PULSE BASE LENTGH	ENERGY YIELD (GMS/KWH)	POWER DENSITY (WATTS/CC)	CONVERSION WT PCENT
102	216.7	31.9	12.3	3.87	7.40	0.083
103	270.7	39.8	12.0	3.14	9.48	0.086
104	481.6	28.3	12.1	3.09	6.69	0.060
105	290.9	42.8	12.1	2.92	10.10	0.086
106	273.9	40.3	12.2	3.00	9.43	0.082
107	298.9	44.0	12.1	3.29	10.38	0.099

STATISTICAL ANALYSIS OF RESULTS

LINEAR REGRESSION GIVES LOG(ENERGY YIELD)= 1.402 - 0.026*POWER DENSITY
VARIANCE OF B= 8.50* -4 SIGMA= 9.80* -2

VALUES FROM FITTED REGRESSION LINE

POWER DENSITY	0.0	1.0	2.0	3.0	4.0	5.0	6.0	7.0	8.0
YIELD(GM/KWH)	4.06	3.96	3.86	3.76	3.66	3.57	3.48	3.39	3.30
CONVERSION	0.000	0.011	0.022	0.033	0.043	0.052	0.061	0.069	0.077

SERIES 37

PULSED D.C. PULSE ON TIME 35.0 MICROSECS OFF TIME 1.00* -1SECONDS

RUN NO	POWER PULSE AREA	KWH/PULSE **10	PULSE BASE LENTGH	ENERGY YIELD (GMS/KWH)	POWER DENSITY (WATTS/CC)	CONVERSION WT PCENT
108	242.4	17.8	10.8	5.49	9.43	0.060
109	344.4	10.1	10.5	7.82	5.51	0.050
110	61.9	11.4	10.2	7.44	6.38	0.055
111	73.8	13.6	9.4	6.92	8.24	0.067
112	111.1	8.20	10.8	10.2	4.32	0.052
113	91.7	16.9	10.1	4.37	9.54	0.049

STATISTICAL ANALYSIS OF RESULTS

LINEAR REGRESSION GIVES LOG(ENERGY YIELD)= 2.830 - 0.127*POWER DENSITY
VARIANCE OF B= 5.90* -4 SIGMA= 1.18* -1

VALUES FROM FITTED REGRESSION LINE

POWER DENSITY	0.0	1.0	2.0	3.0	4.0	5.0	6.0	7.0	8.0
YIELD(GM/KWH)	16.9	14.9	13.1	11.6	10.2	8.98	7.91	6.97	6.13
CONVERSION	0.000	0.017	0.031	0.041	0.048	0.052	0.055	0.057	0.057

SERIES 38

PULSED D.C. PULSE ON TIME 13.0 MICROSECS OFF TIME 1.00* -1SECONDS

RUN NO	POWER PULSE AREA	KWH/PULSE *.10	PULSE BASE LENTGH	ENERGY YIELD (GMS/KWH)	POWER DENSITY (WATTS/CC)	CONVERSION WT PCENT
131	226.8	1.67	10.0	28.3	1.91	0.023
132	193.7	2.85	9.8	34.9	3.32	0.050
133	174.9	2.57	10.5	30.0	2.80	0.036
134	243.6	3.58	10.5	22.7	3.90	0.038
135	117.7	0.865	10.5	42.4	0.94	0.017
136	263.8	3.88	10.0	20.6	4.43	0.040

STATISTICAL ANALYSIS OF RESULTS

LINEAR REGRESSION GIVES LOG(ENERGY YIELD)= 3.850 - 0.169*POWER DENSITY
VARIANCE OF B= 3.50* -3 SIGMA= 1.71* -1

VALUES FROM FITTED REGRESSION LINE

POWER DENSITY	0.0	1.0	2.0	3.0	4.0	5.0	6.0	7.0	8.0
YIELD(GM/KWH)	47.0	39.7	33.5	28.3	23.9	20.2	17.0	14.4	12.2
CONVERSION	0.000	0.017	0.029	0.037	0.042	0.044	0.044	0.044	0.042

fig 44.

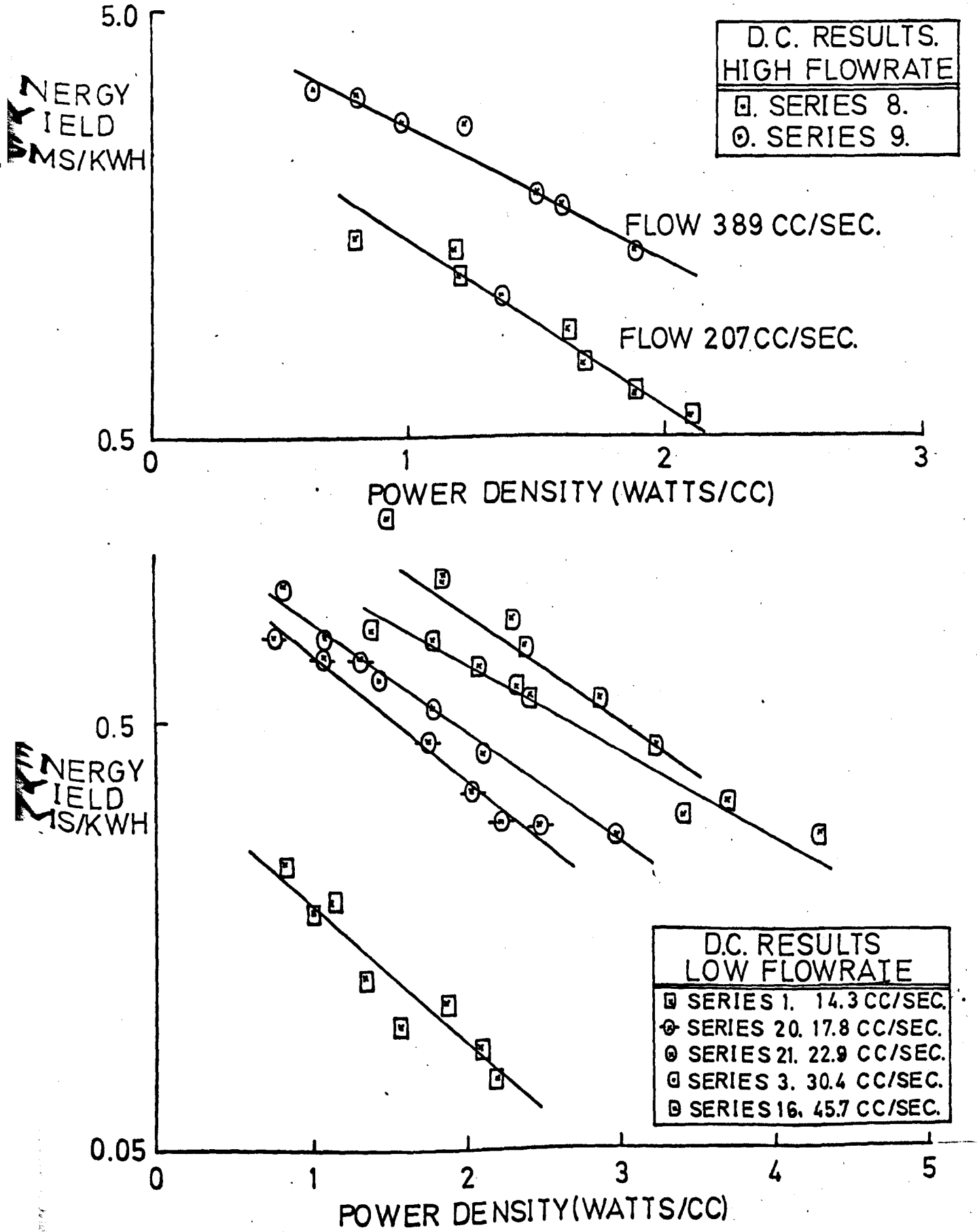
5.0
NERGY
IELD
MS/KWH
0.5
0
1
2
3
POWER DENSITY (WATTS/CC)
D.C. RESULTS.
HIGH FLOWRATE
SERIES 8.
SERIES 9.
FLOW 389 CC/SEC.
FLOW 207 CC/SEC.
0.5
NERGY
IELD
S/KWH
0.05
0
1
2
3
4
5
POWER DENSITY (WATTS/CC)
D.C. RESULTS
LOW FLOWRATE
SERIES 1. 14.3 CC/SEC.
SERIES 20. 17.8 CC/SEC.
SERIES 21. 22.9 CC/SEC.
SERIES 3. 30.4 CC/SEC.
SERIES 16. 45.7 CC/SEC.

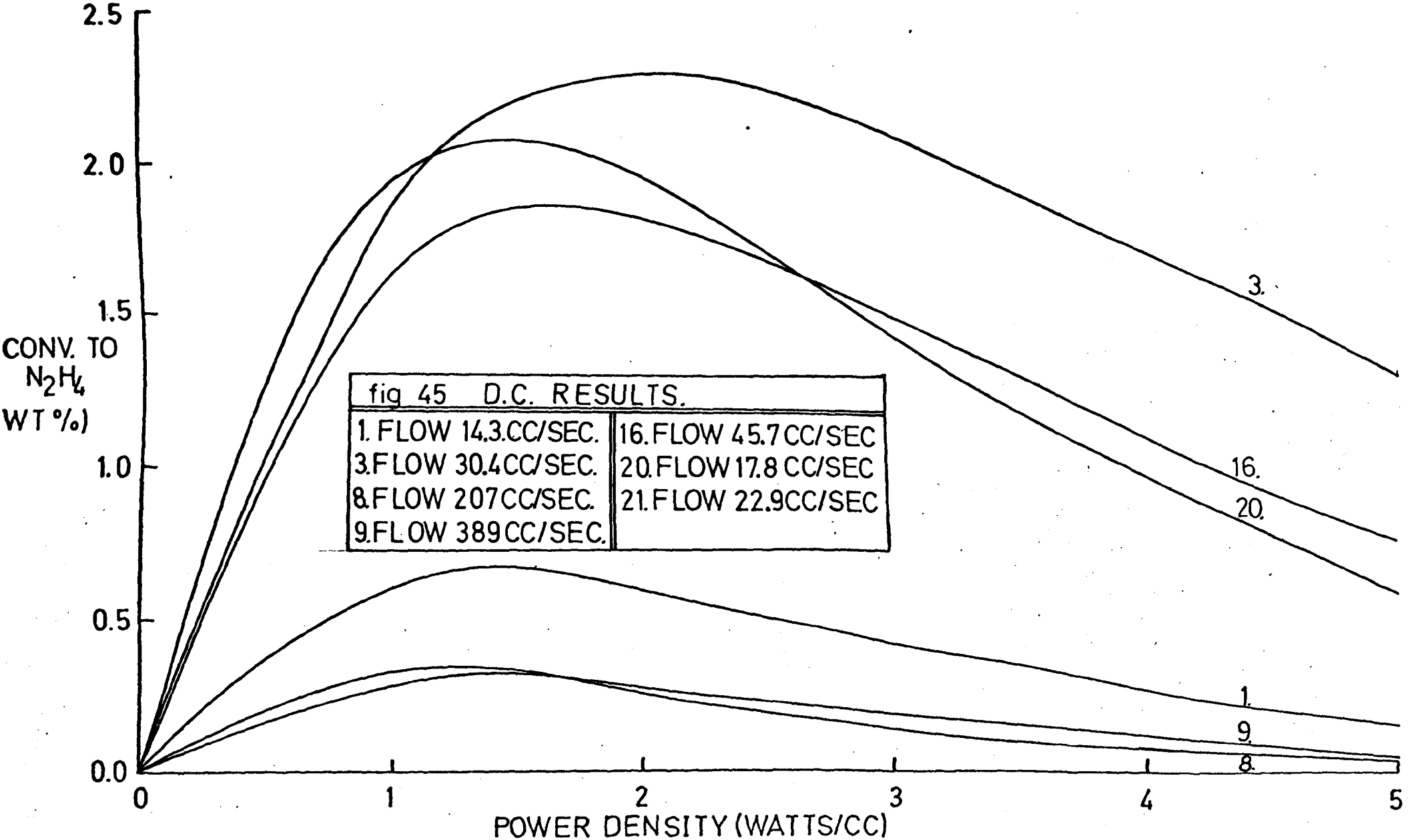
2.5
2.0
1.5
1.0
0.5
0.0
CONV. TO N_2H_4 WT %)
0
1
2
3
4
5
POWER DENSITY (WATTS/CC)
3.
16.
20.
1.
9.
8.
fig 45 D.C. RESULTS.
1. FLOW 14.3 CC/SEC.
3. FLOW 30.4 CC/SEC.
8. FLOW 207 CC/SEC.
9. FLOW 389 CC/SEC.
16. FLOW 45.7 CC/SEC
20. FLOW 17.8 CC/SEC
21. FLOW 22.9 CC/SEC

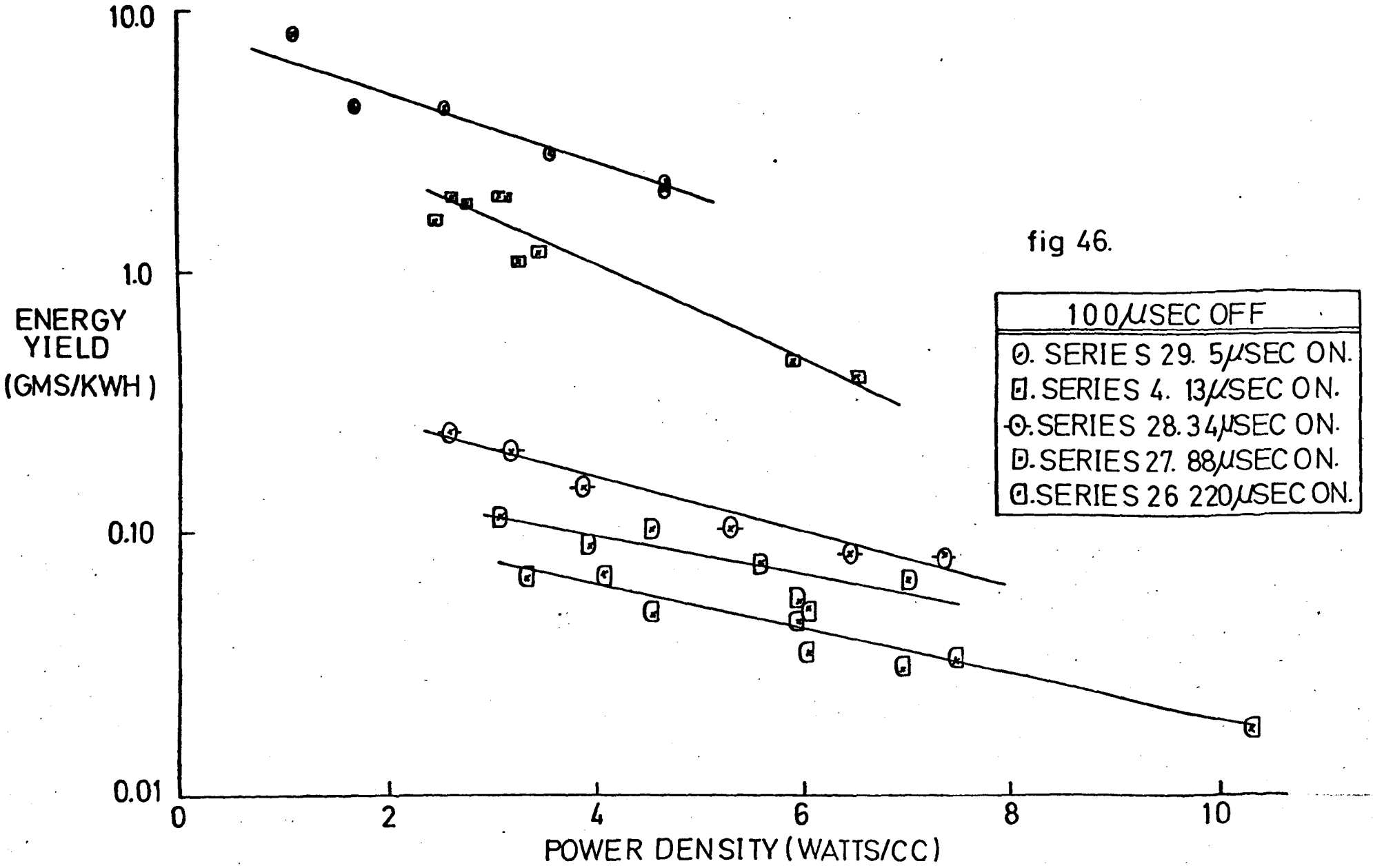
10.0
1.0
0.10
0.01
ENERGY YIELD (GMS/KWH)
0
2
4
6
8
10
POWER DENSITY (WATTS/CC)
100 μSEC OFF
SERIES 29. 5 μSEC ON.
SERIES 4. 13 μSEC ON.
SERIES 28. 34 μSEC ON.
SERIES 27. 88 μSEC ON.
SERIES 26 220 μSEC ON.

fig 46.

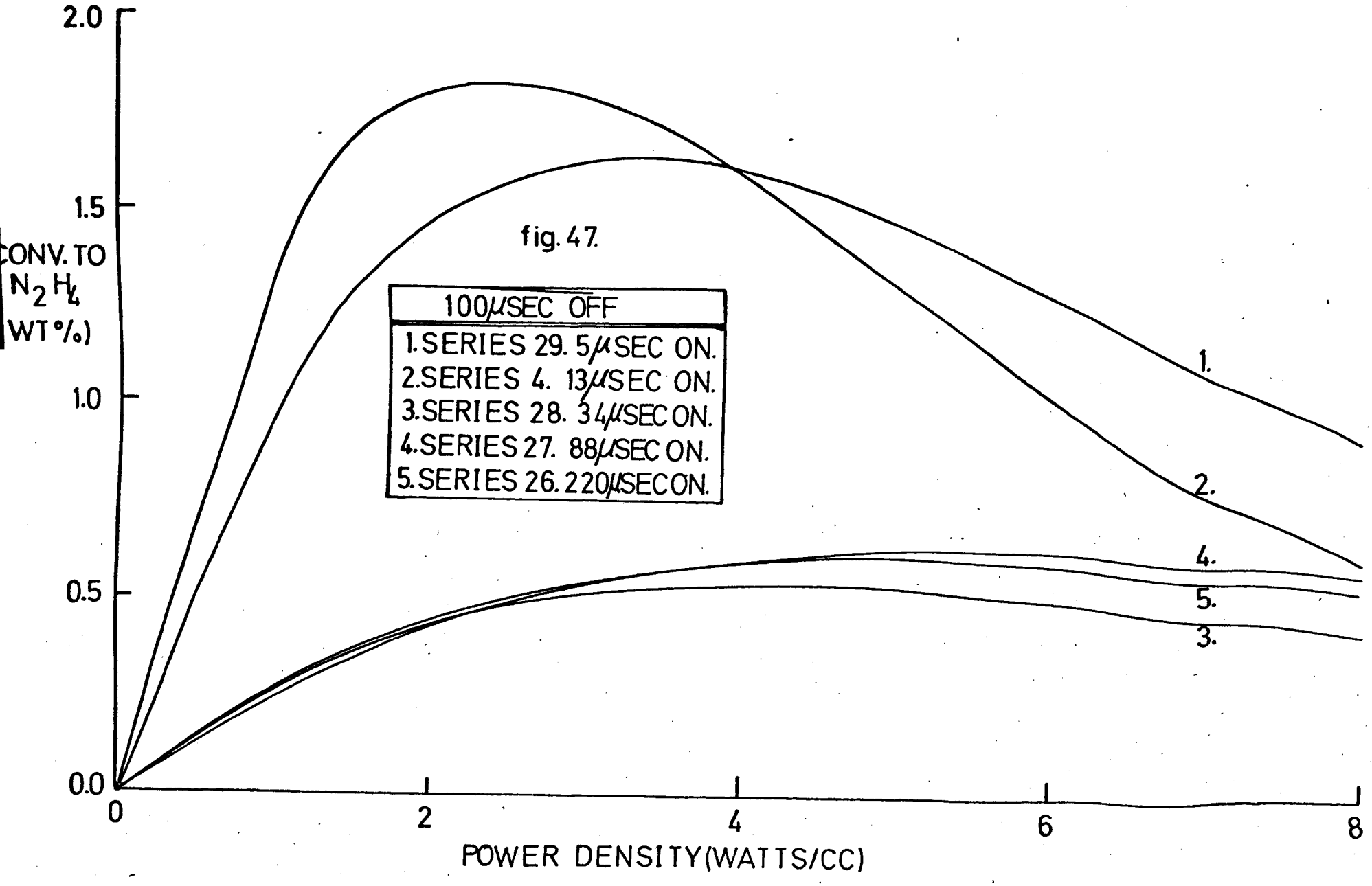
2.0
1.5
1.0
0.5
0.0
CONV. TO N_2H_4 (WT%)
0
2
4
6
8
POWER DENSITY(WATTS/CC)
100μSEC OFF
1. SERIES 29. 5μSEC ON.
2. SERIES 4. 13μSEC ON.
3. SERIES 28. 34μSEC ON.
4. SERIES 27. 88μSEC ON.
5. SERIES 26. 220μSEC ON.
1.
2.
4.
5.
3.

fig. 47.

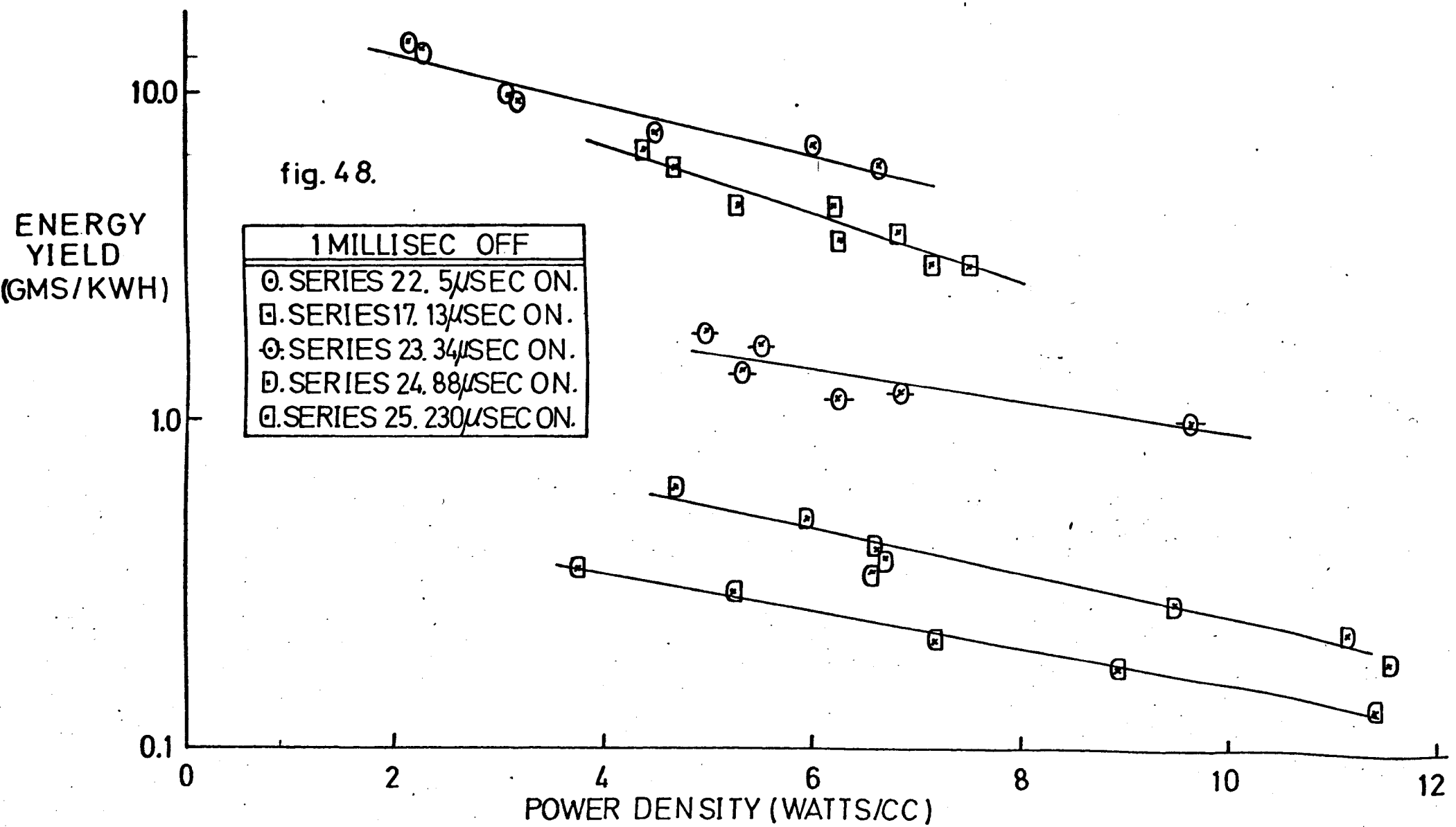
10.0
1.0
0.1
ENERGY YIELD (GMS/KWH)
0
2
4
6
8
10
12
POWER DENSITY (WATTS/CC)
1 MILLISEC OFF
O. SERIES 22. 5μSEC ON.
□. SERIES 17. 13μSEC ON.
⊙. SERIES 23. 34μSEC ON.
D. SERIES 24. 88μSEC ON.
◫. SERIES 25. 230μSEC ON.

fig. 48.

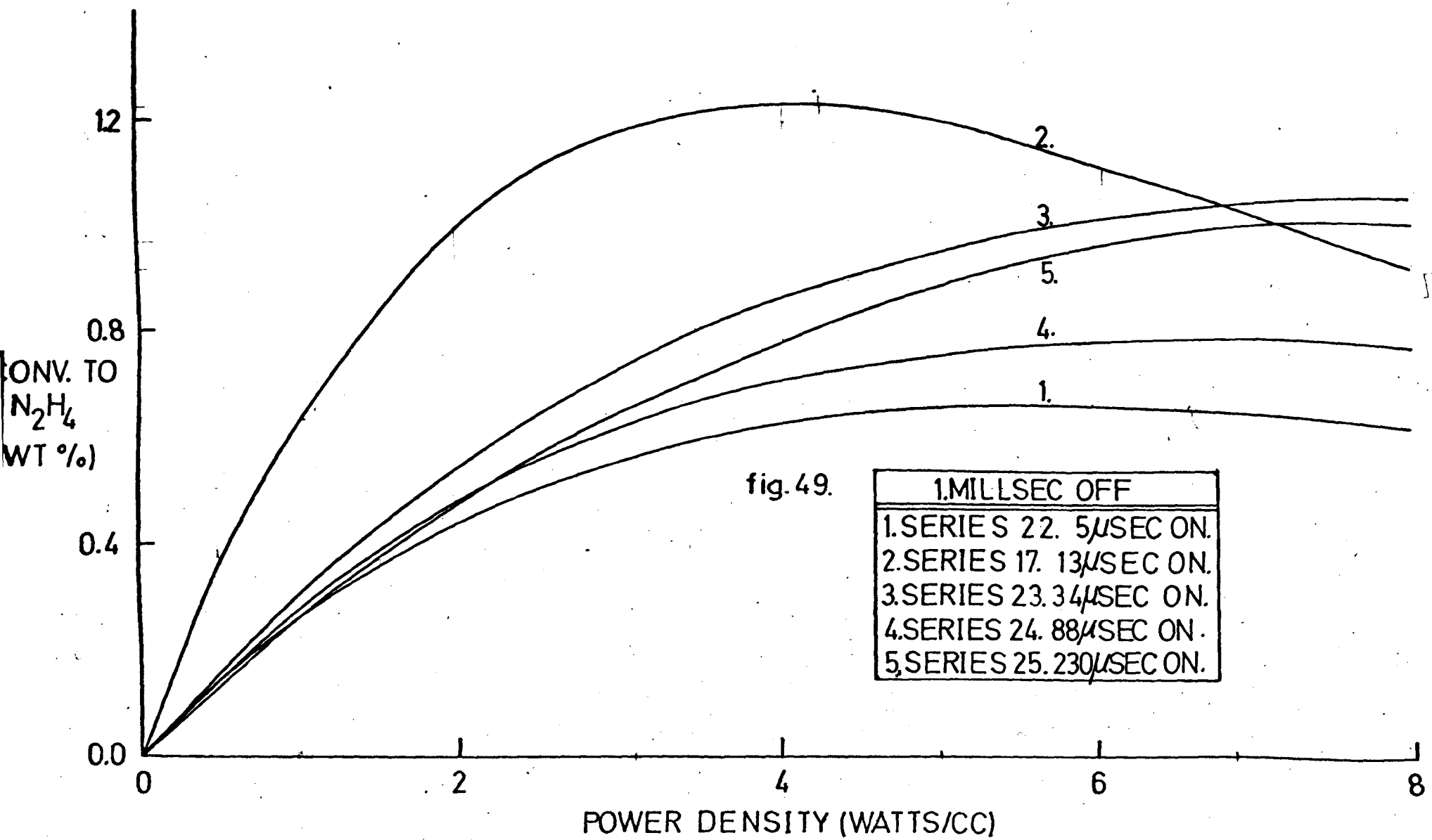
1.2
0.8
0.4
0.0
CONV. TO
N_2H_4
WT %)
0
2
4
6
8
POWER DENSITY (WATTS/CC)
2.
3.
5.
4.
1.
1.MILLSEC OFF
1.SERIES 22. 5μSEC ON.
2.SERIES 17. 13μSEC ON.
3.SERIES 23.34μSEC ON.
4.SERIES 24. 88μSEC ON.
5.SERIES 25. 230μSEC ON.

fig. 49.

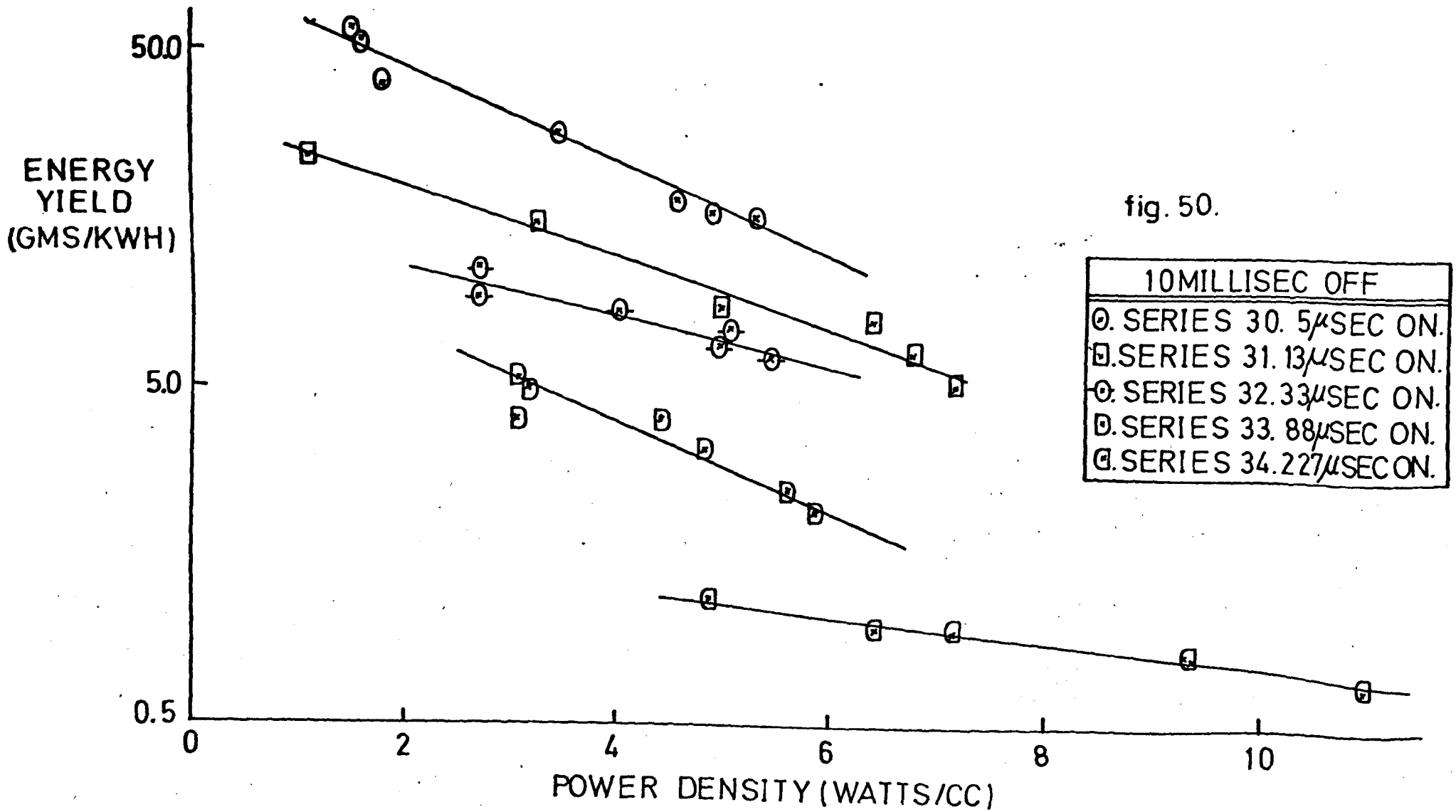
50.0
5.0
0.5
ENERGY YIELD (GMS/KWH)
0
2
4
6
8
10
POWER DENSITY (WATTS/CC)
10 MILLISEC OFF
SERIES 30. 5μSEC ON.
SERIES 31. 13μSEC ON.
SERIES 32. 33μSEC ON.
SERIES 33. 88μSEC ON.
SERIES 34. 227μSEC ON.

fig. 50.

fig. 51

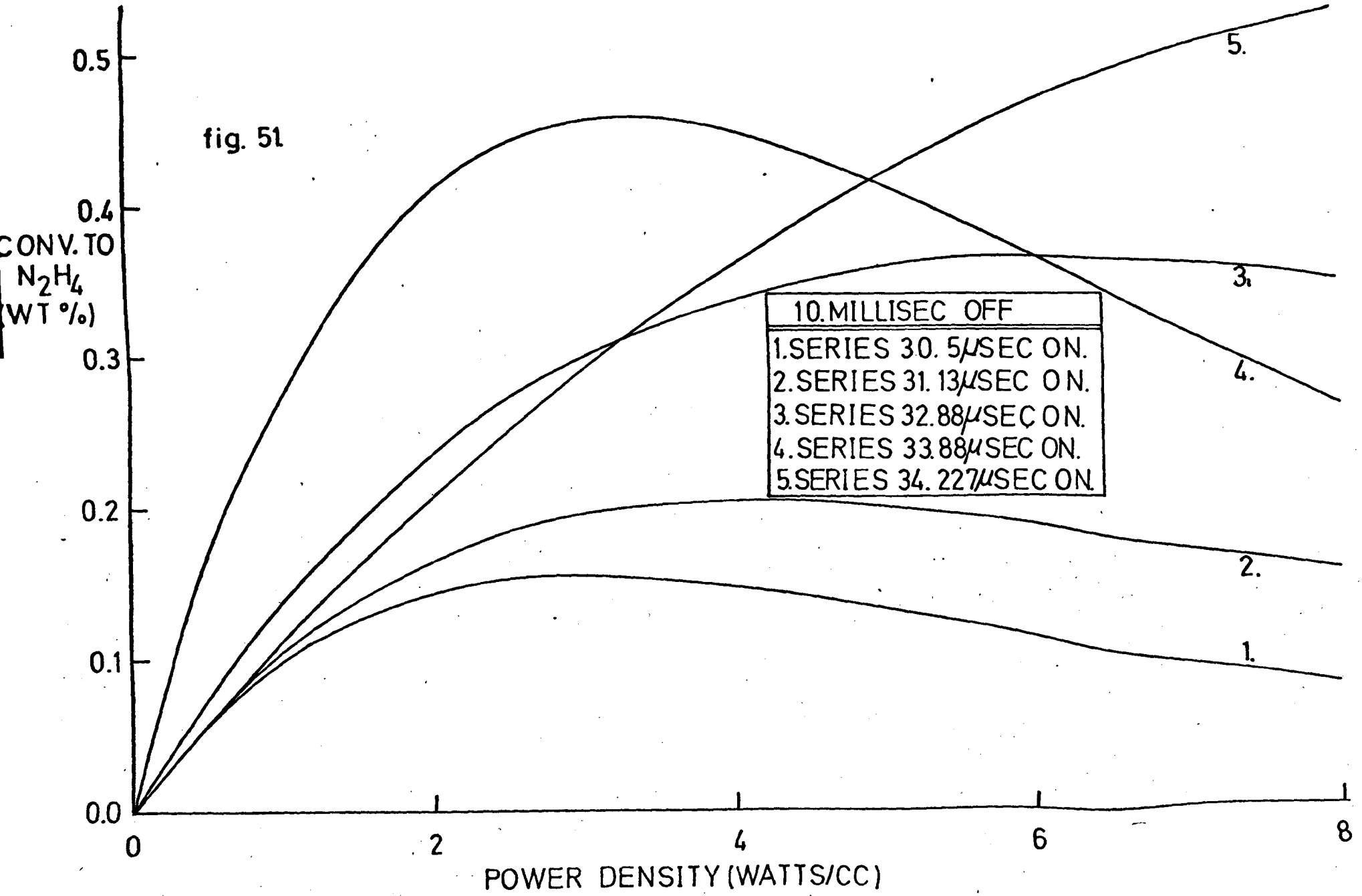
0.5
0.4
CONV. TO
N_2H_4
(WT %)
0.3
0.2
0.1
0.0
0
2
4
6
8
POWER DENSITY (WATTS/CC)
10. MILLISEC OFF
1. SERIES 30. 5μSEC ON.
2. SERIES 31. 13μSEC ON.
3. SERIES 32. 88μSEC ON.
4. SERIES 33. 88μSEC ON.
5. SERIES 34. 227μSEC ON.
1.
2.
3.
4.
5.

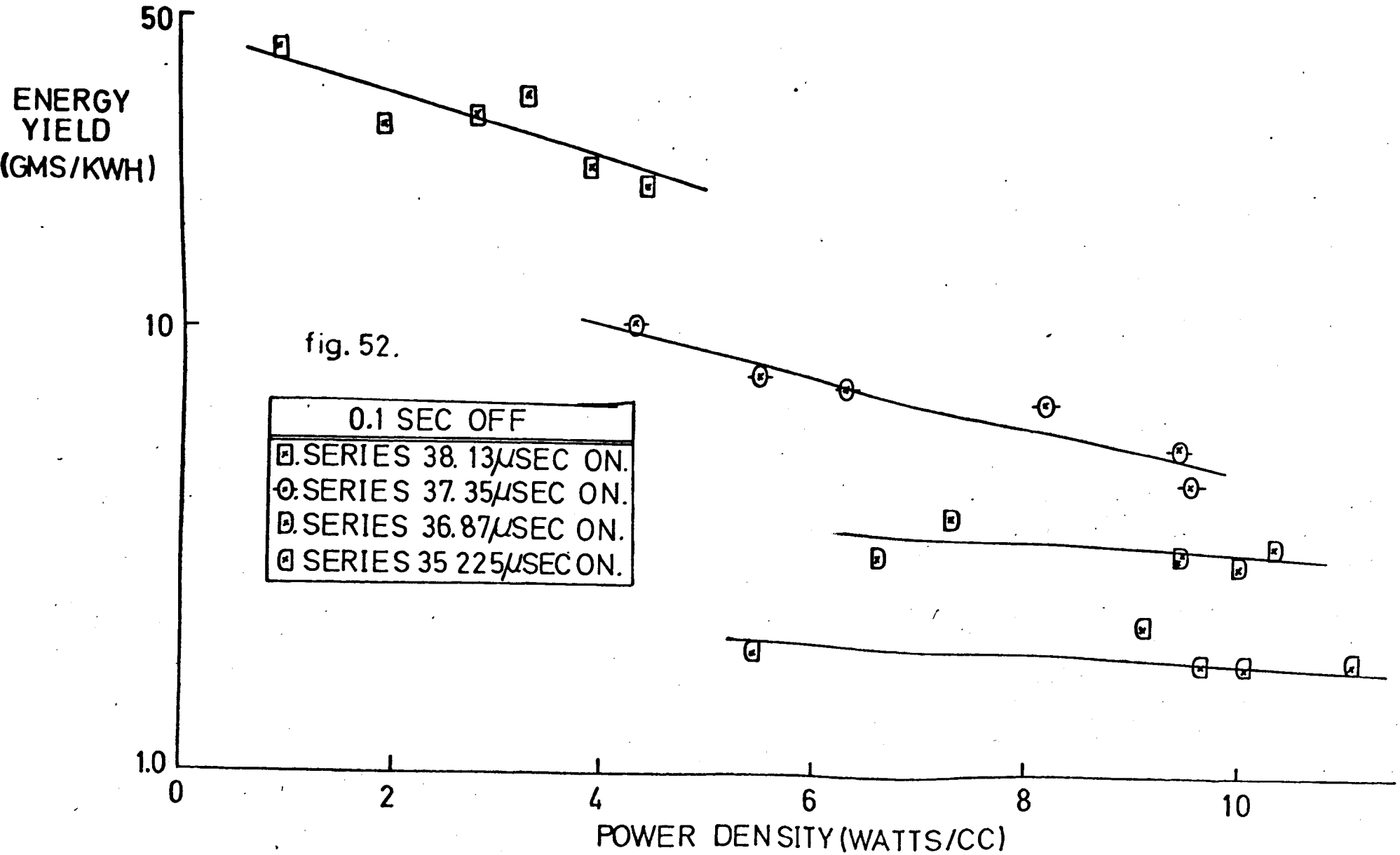
50
10
1.0
ENERGY YIELD (GMS/KWH)
0.1 SEC OFF
SERIES 38.13μSEC ON.
SERIES 37.35μSEC ON.
SERIES 36.87μSEC ON.
SERIES 35.225μSEC ON.
0
2
4
6
8
10
POWER DENSITY (WATTS/CC)

fig. 52.

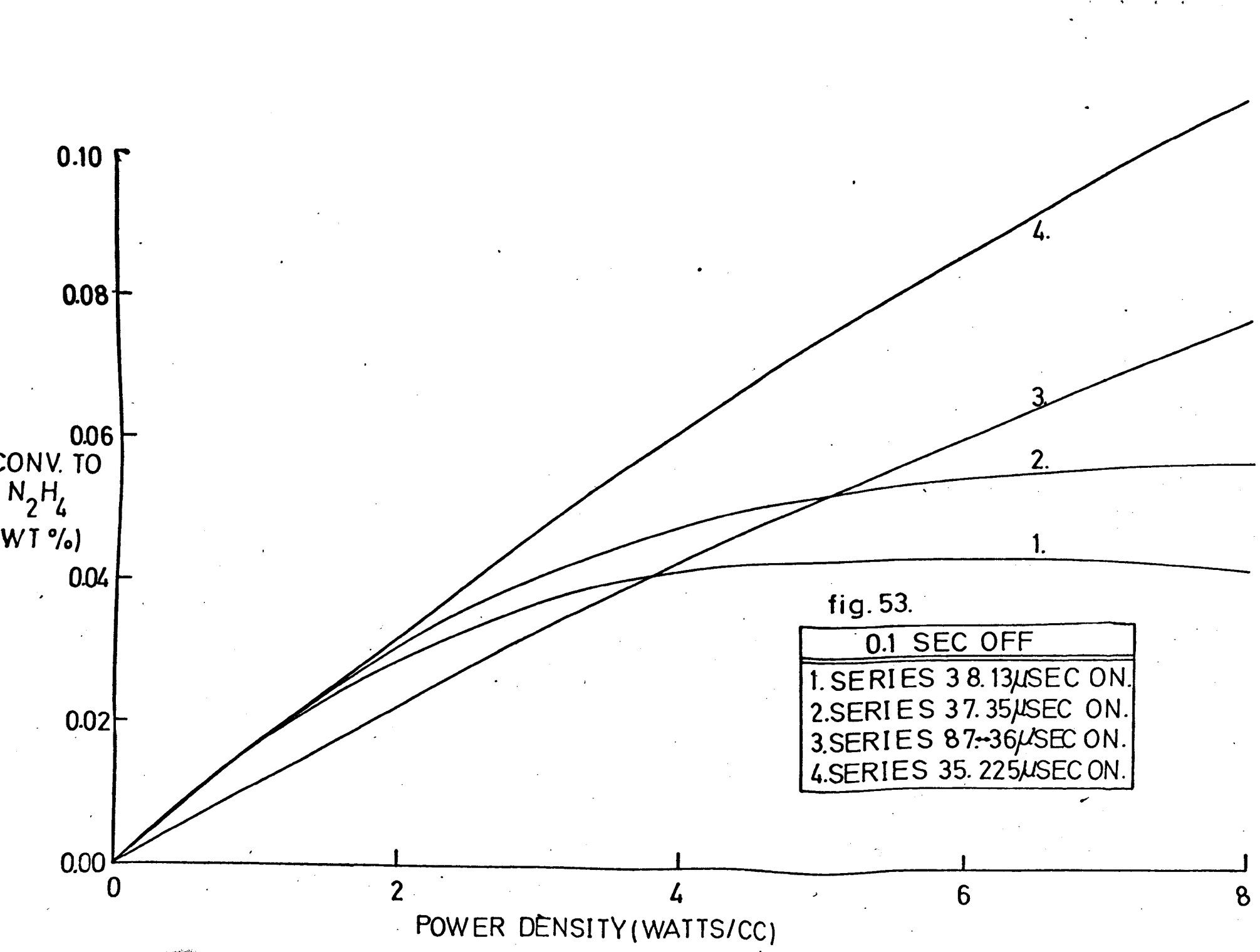

fig. 53.

0.1 SEC OFF
1. SERIES 3 8.13μSEC ON.
2. SERIES 37.35μSEC ON.
3. SERIES 87-36μSEC ON.
4. SERIES 35.225μSEC ON.

fig. 54.

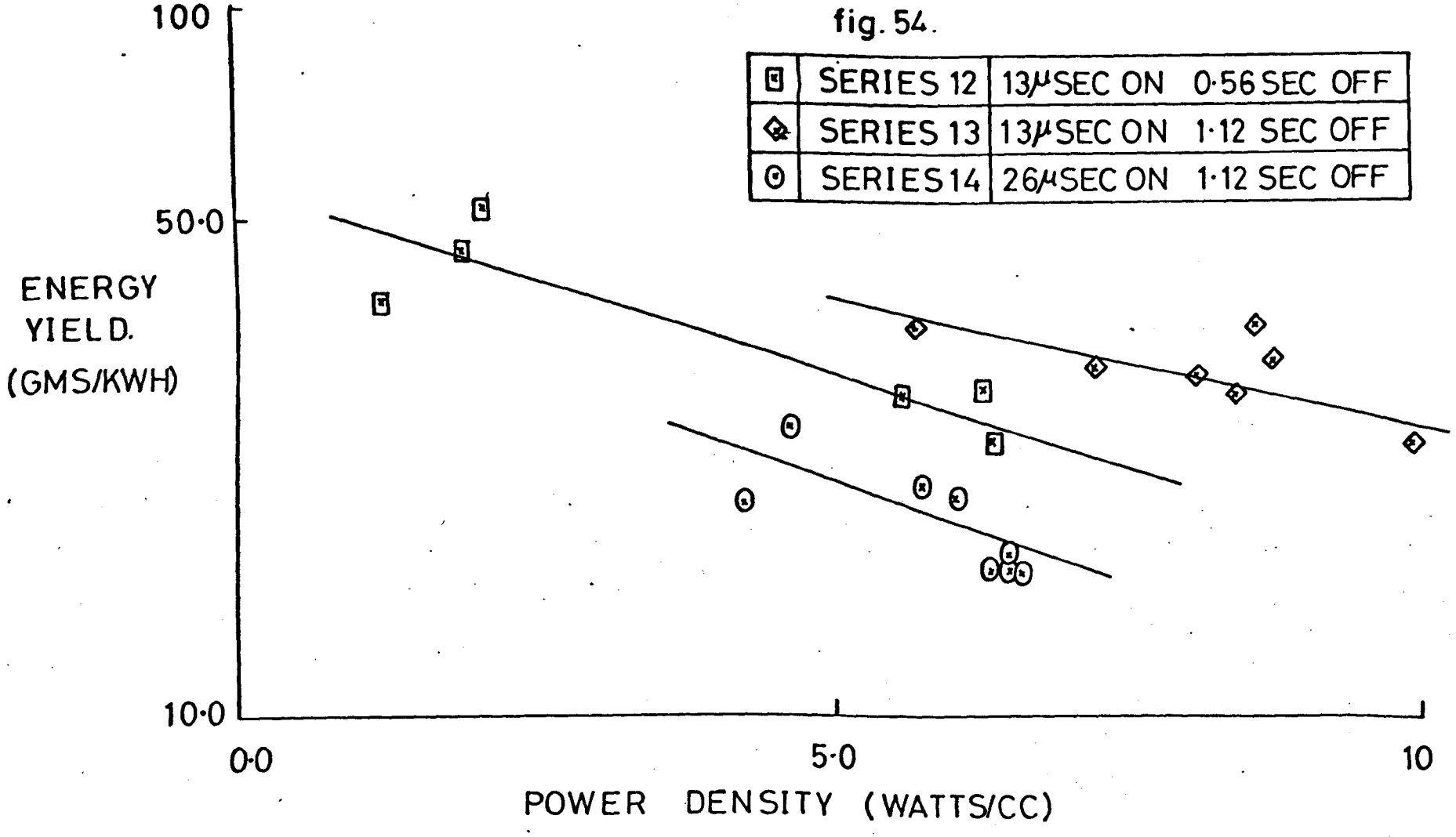
100
50·0
10·0
ENERGY
YIELD.
(GMS/KWH)
0·0
5·0
10
POWER DENSITY (WATTS/CC)
SERIES 12 13μSEC ON 0·56 SEC OFF
SERIES 13 13μSEC ON 1·12 SEC OFF
SERIES 14 26μSEC ON 1·12 SEC OFF

fig.55.

EFFECT OF REACTOR PACKING ON ENERGY YIELD OF HYDRAZINE.

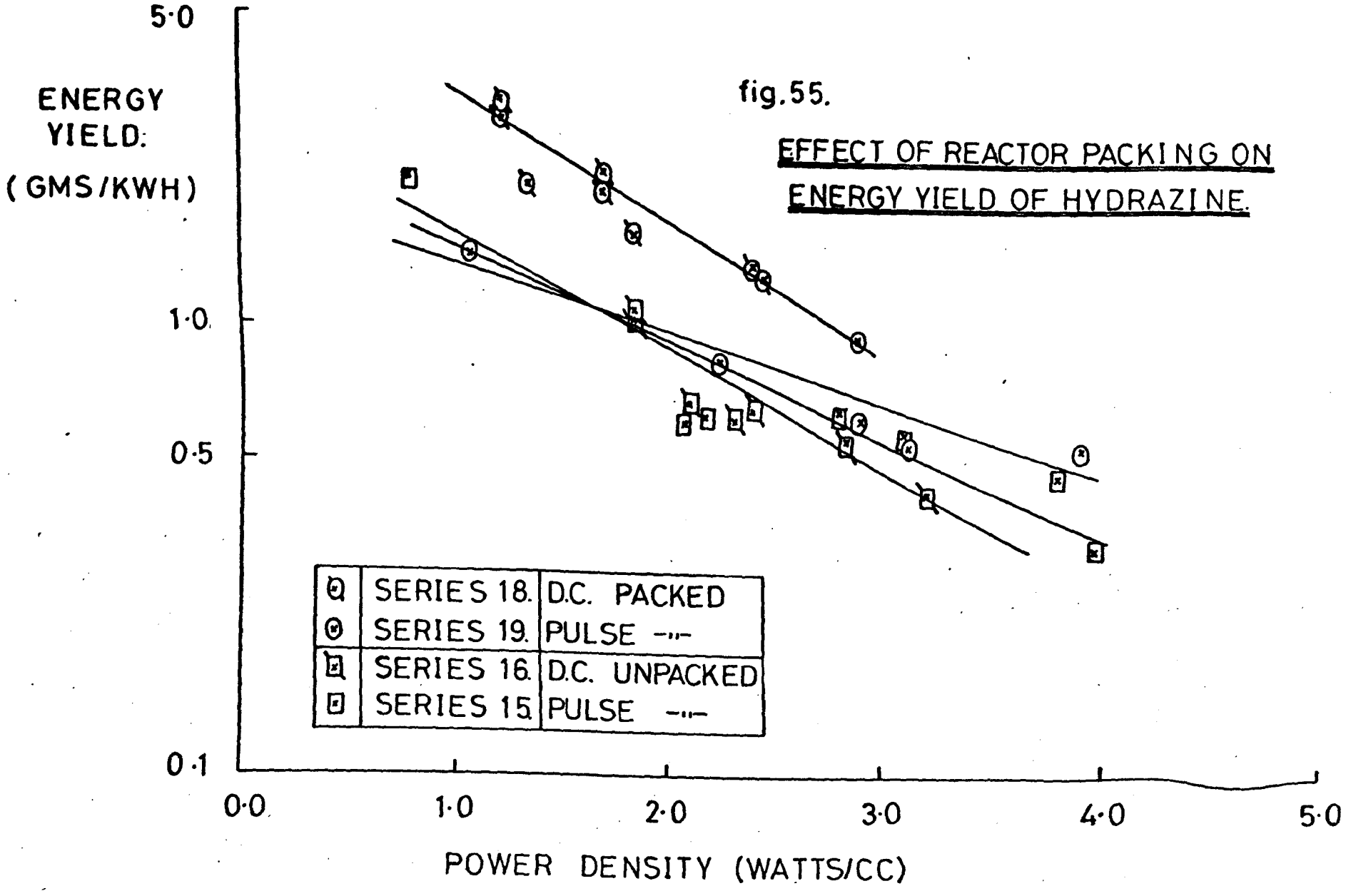

APPENDIX III

PAGE

CALIBRATION CURVE FOR FP 1/8-20-G-5/84.

fig.56.

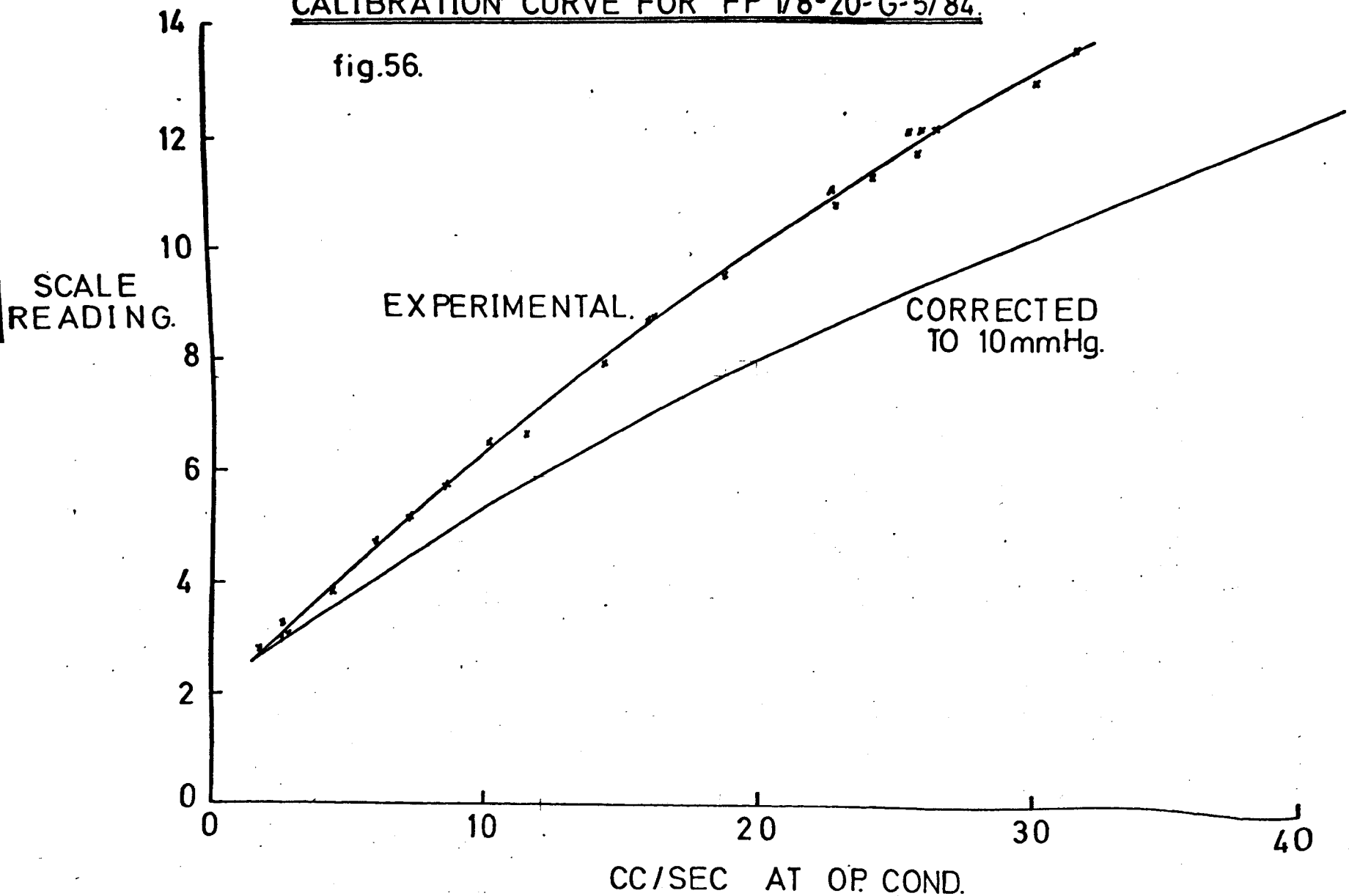

fig.57. CALIBRATION CURVE FOR HYDRAZINE